The Dissertation Committee for Nysha Alana Niela Chaderton Certifies that this is the approved version of the following dissertation:

Sedimentation within the Tobago Forearc Basin with Implications for the Evolutionary History of the Southern Barbados Accretionary Margin

Committee:

Lesli Wood, Supervisor

Ronald Steel

Mark Cloos

William Fisher

Xavier Janson

Sedimentation within the Tobago Forearc Basin with Implications for the Evolutionary History of the Southern Barbados Accretionary Margin

by

Nysha Alana Niela Chaderton, B.Sc.; M.S.

Dissertation

Presented to the Faculty of the Graduate School of

The University of Texas at Austin

in Partial Fulfillment

of the Requirements

for the Degree of

Doctor of Philosophy

The University of Texas at Austin

December, 2009

Dedication

This dissertation is dedicated to my husband, Duane Williams, who has been my unwavering support throughout my PhD program.

Acknowledgements

I would like to thank my dissertation supervisor Dr. Lesli Wood for her ever-present guidance and support. To my committee members, Dr. Mark Cloos, Dr. William Fisher, Dr. Xavier Janson and Dr. Ronald Steel, I would like to express my gratitude for your input which has greatly increased the quality of this research. I must also thank Aysen Ozkan and Dr. Kitty Milliken for their help with my petrographic analysis.

I would like to recognize the assistance of Andre Brathwaite, Jamar White and the staff of the Ministry of Energy of the Government of Barbados, Christopher Mosley and J. Mervyn Gordon of the Barbados National Oil Company Ltd.

My PhD research was generously funded by BHP Billiton and I am especially grateful to Karen Tindale and Kevin Scofield for believing in the value of my research. I am also grateful for additional funding that I received from Chevron, Hess and the Jackson School of Geosciences.

Paula Beard and the entire drafting department of the Bureau of Geosciences must be thanked for their assistance.

Lastly I must express my gratitude to my family, Sean, Risée, Marcia and Timothy Chaderton, my best friend Tanya Greenidge, and my husband Duane Williams, all of whom believed in me even when I did not believe in myself.

Sedimentation within the Tobago Forearc Basin with implications for the evolutionary history of the Southern Barbados Accretionary Margin

Publication No._____

Nysha Alana Niela Chaderton, PhD

The University of Texas at Austin, 2009

Supervisor: Lesli J. Wood

The Scotland Formation onshore Barbados is often called the only example of a successful hydrocarbon producing accretionary prism reservoir. In spite of this, the hydrocarbon system elements of the BAP have nevertheless not been well studied. Seven outcropping locations of the Scotland were examined to document stacking patterns, key surfaces, depositional element geometries, facies occurrences their vertical and lateral extent, and the unit's gamma response. Six facies were identified in outcrop: silty muds; laminated, centimeter-scale sandstones interbedded with silts and muds; cross-stratified sandstones; massive, medium to coarse-grained sandstones; very coarse grained sands with gravel or pebbles; and rare conglomerates. These facies combine to form architectural elements—channels, levees, and depositional lobes. Observations from petrographic, outcrop and seismic data suggest that the Scotland Formation was never deeply buried within the prism proper and was possibly deposited within the much larger proto-Tobago Basin.

Table of Contents

List of Tables

List of Figures

Chapter One: Introduction

The study area of the Barbados Accretionary Prism (BAP), also called the Lesser Antilles Accretionary Prism by some workers, is located in a convergent margin setting near the eastern edge of the Caribbean plate. At this location the Caribbean plate is overriding the westward dipping Atlantic plate, moving eastward at a rate of approximately 20 mm a year, (Mann, 1999; Weber, et al., 2001; Perez, et al., 2001) (Figure 1.1). This plate boundary is marked by the presence of classic convergent margin features such as an accretionary prism (The Barbados Accretionary Prism), a volcanic island arc (The Lesser Antilles Island Arc and an associated forearc basin (The Tobago Basin) and a back arc basin (The Grenada Basin).

The Barbados Accretionary Prism (BAP) is the considered to be the only hydrocarbon producing prism in the world. One of the goals of this research is to examine the petroleum system of the BAP and determine whether the conditions that have made hydrocarbon production possible are unique or whether they exist within similar settings and can be successfully exploited. The following research problems will be investigated.

How has the Southern Barbados Accretionary Prism (BAP) developed through time?

What is the sedimentation history of the Southern BAP and what is the composition and timing of the Tobago Forearc Basin fill?

What is the nature of the petroleum system of the southern BAP?

1. Development history of the southern BAP

Convergent margins can be accretionary, erosive or a combination of the two. Accretionary margins are defined as those which are experiencing net accretion over recent geologic time (Clift and Vannucchi, 2004) (Figure 1.2). Even so at margins experiencing net overall accretion, up to 70 % of the sediment may be being subducted (von Heune and Scholl, 1991; Clift and Vannucchi, 2004).

In the study area sediments which have accumulated on the Atlantic abyssal plain are accreted to the front of the Caribbean plate, as the Atlantic plate is subducted. This has resulted in the growth of an accretionary prism that is greater than 300 km wide and has sediment thicknesses that exceed 18 km (Torrini and Speed, 1989; Westbrook et al., 1973, Moore et al., 1982; Valery et al., 1985; Speed, 1983; Brown and Westbrook, 1987).

Accretionary prisms grow through frontal accretion and underplating. Frontal accretion is the mechanism by which seaward sediments are off-scraped above a basal decollement and incorporated into the growing accretionary prism. In this manner accretionary prisms become wider (Moore and Biju-Duval, 1984, Shipley and others, 1982; DiTullio and Byrne, 1990; Von Heune and Scholl, 1991; Morris et al. 2002). Underplating occurs when off-scraped sediment passes beneath the sediment pile and is added to the base of the prism. This is the mechanism by which prisms thicken (Moore and Biju-Duval, 1984, Shipley et al., 1982; DiTullio and Byrne, 1990; Von Heune and Scholl, 1991; Morris et al. 2002).

The Barbados Accretionary prism has an extraordinarily thick sediment pile- up to 18 km (Speed, 1983; Brown and Westbrook, 1987) that may partially be the result of thickening of the prism by underplating. At 20 mm a year, it also is experiencing one of the slowest rates of convergence recorded at accretionary margins world wide (von Heune and Scholl, 1991). The evolution of the Tobago Basin is recorded by the sedimentary units within it that show its steady decrease in size since the Mid-Miocene (Chaderton, 2005). The existence of a broad proto-Tobago Basin (Speed et al., 1983;

Brown and Westbrook, 1987) has been previously documented however charting the progressive evolution and the sedimentation history of the TFB will allow us to better understand the development history of the Southern BAP.

2. The nature and origin of the sediments in the southern BAP

Four stratigraphic units are identified in the onshore geology of Barbados. They consist of: the Scotland Formation (Lower-Middle Eocene and possibly Oligocene) (Trechmann, 1925, 1933, 1937; Senn 1944), a unit of interbedded sands and muds, the Joes River Formation (post-Miocene), an intrusive unit interpreted to be paleo-mud volcano sediments, the Oceanic Formation (Middle Eocene to Middle Miocene), which are pelagic muds, marls and interbedded volcanic ash beds and Pleistocene Limestones (Trechmann, 1925, 1933, 1937; Senn 1944) which cap the island Barbados.

There is a long standing dispute about the relationship of the Oceanic Formation with the Scotland Formation. The Oceanic Formation is a unit comprised of pelagic muds, marls and interbedded volcanic ash beds (Speed and Torrini, 1989; Torrini and Speed, 1994). It has been described as both an in situ deposit uplifted through the simple rise of the prism (Pudsey, 1982) and as a deposit that has been thrust into place forming nappes (Speed and Torrini, 1989; Torrini and Speed, 1994). The Oceanic Formation that is recognized onshore Barbados has been identified as a unit formed within the Tobago Forearc Basin. The Scotland Formation comprised of sands and muds and has been interpreted as off-scraped abyssal plain or trench deposits that were tectonically incorporated into the accretionary prism (Speed and Larue, 1982; Larue and Speed, 1984; Torrini et al., 1985; Gortner and Larue, 1986).

Pudsey (1982) suggested that the Oceanic Formation is an in situ deposit which has been tectonically uplifted along with the Barbados Ridge. In support of this hypothesis, Poole and Barker's (1980) geological map of Barbados featured a generalized vertical section in which the Oceanic Formation conformably overlies the Scotland

Formation. This interpretation requires the Scotland Formation to be an older unit than the Oceanic Formation; however some age over lap has been noted by some workers.

Speed (1982) contended that the Oceanic Formation was deposited within the Tobago Forearc Basin and has subsequently been thrust more than 20 km eastward to its present position. Speed interpreted the Oceanic Formation as having a lower section which exhibited nappe geometries as a result of its eastward transportation, and an upper section which was a single undisrupted sheet. The timing of the emplacement of this sheet is said to be late Miocene or Pliocene when the sheet was thought to have fully covered the underlying Scotland Formation. This interpretation accounts for the over-lapping age dates of the Scotland and Oceanic Formation but requires significant translation and over thrusting of sediments that is not observed in seismic data.

There are inconsistencies with both of the previously mentioned interpretations and further examination of the Scotland Formation that outcrops onshore Barbados and analysis of the seismic data will allow us to gain an understanding of the depositional environments and location of the Scotland and the Oceanic Formations. Outcrops of the Scotland Formation on the island of Barbados were examined, to determine the lateral continuity and vertical facies associations and architectural elements within the Scotland outcrops, to define an environment of deposition for each described outcrop and to place these disparate outcroppings of the Scotland in a large-scale framework of depositional setting for these units.

3. The nature of the Petroleum System of the southern BAP

Oil and gas is produced from the Woodbourne Oil field in onshore Barbados from what are believed to be structurally segmented Scotland Formation sandstones within a petroleum system where the play elements are poorly understood. The Sandy Lane #1 well drilled offshore Barbados proved significant sands in the sections of interest in offshore basins and recorded gas shows; however no liquid hydrocarbon shows have been

reported. The Scotland reservoir rock outcrops onshore in several localities and has been the subject of preliminary work to understand the sedimentology, depositional environments and reservoir architecture. It is often steeply dipping and highly deformed complicating the details of its nature; however several outcrops do lend themselves to laterally extensive observations of facies distribution and surface relationships.

The fine grained pelagic muds and marls of the Oceanic Formation are considered to be the broad regional seal of the petroleum system. Understanding the regional extent and distribution of the Oceanic Formation across the southern BAP will help us with our understanding of the BAP petroleum system as a whole.

No source rocks are exposed onshore Barbados, nor have they been penetrated by offshore drilling or identified in seismic data. However, geochemical work carried out by geoscientists from the United States Geological Survey (USGS) suggests that Barbados oils are of uniform thermal maturity and originate from a Cretaceous source rock (Hill and Schenk, 2005).

Fluid migration within accretionary prisms occurs along extension fractures, veins faults and also through sediment pores as a result of high fluid pressure created by the reduction of pore volume due to sediment burial (Moore, 2001). Within the BAP, mud volcanoes are associated with thrust faults. Fluid-rich mud that reaches the surface forms expulsion features, suggesting that these structural features are fluid migration pathways.

This dissertation focuses on the defining the characteristics and distribution of the onshore reservoir the Scotland Formation and examining its potential distribution offshore Barbados. In addition the relationship with the Scotland Formation and its equivalents with the Oceanic Formation; which is the regional seal, will be examined. Source rock and migration pathway analysis was not undertaken as part of this study.

DATA AND METHODOLOGY

Extensive work undertaken over the course of four field seasons of varying length offered the opportunity to revisit the previous geoscientists' observations of fault frameworks and structural relationships. The field observations benefited from knowledge of the extensive 2D seismic data surrounding the island (Figures 1.3, 1.4). A number of faults are observed on the island and had to be taken into consideration when mapping stratigraphic relationships. The active tectonic setting has resulted in extensive post depositional modification of the Scotland Formation. The study area is characterized by seismic and outcrop scale thrust faulting and folding. Thrust faults, antiformal and synformal features observed in outcrop all have the NE-SW orientation noted by Speed, (1983).

The lateral continuity of Scotland Formation sands were mapped across outcrops. Several measured sections were made at each large outcrop to analyze the stacking patterns, lateral continuity and geometries of beds. Facies descriptions, and sample collection for petrography was also undertaken in the field.

A total of 44 samples were made into thin sections. The samples were left unpolished and without slip covers and were stained in two separate batches. The Houghton (1980) methodology that stains potassium feldspar yellow and plagioclase feldspar pink. All of the samples were examined under microscope. Ten samples were identified as representative and chosen for more in depth analysis for point counting and measurements. Only 10 samples were chosen for point counting because most were measured at one outcrop location. The selected samples were scattered across and so a smaller number of samples were scattered across the field area.

Existing 2D seismic utilized in previous research (Chaderton, 2005) were available for further analysis and integration with field and subsurface observations. In addition 200 well logs from the Woodbourne oilfield were available for correlation and integration with field and seismic observations.

Chapter 2: The Anatomy of a Coarse Grained Turbidite, Scotland Formation, Barbados West Indies

If production in the BAP hydrocarbon province is to continue in the future, and perhaps increase, then there is an imperative need to improve understanding of the BAP hydrocarbon system and its elements. One of the most important elements of the system is the primary reservoir unit; the Scotland Formation.

The primary producing oil field on the island of Barbados, the Woodbourne oilfield is located in the south of the island and produces from the Eocene-Oligocene age interbedded sandstone and shale succession of the Scotland Formation. Outcrops of the Scotland Formation and other Tertiary units are exposed where the island's Pleistocene limestone cap has been eroded in northeastern Barbados (Figure 2.1, 2.2).

DATA

Twenty-seven measured sections were constructed for seven different outcrop locations across the island of Barbados (Figure 2.3, 2.4). Outcrops were also documented with photomosaics and gamma scans. Rock samples were selected for petrographic analysis and diagenetic history. Each outcrop location varied in terms of the extent of rock exposure, type and intensity of structuring, accessibility and weathering conditions. The number of sections measured at each locality varied from one, at Inner Turners Hall Ridge (ITR) to six at Chalky Mount Ridge (CMR). Photomosaics and walking surfaces for correlation helped document the nature of lateral stratigraphic associations and vertical stacking patterns.

DESCRIPTIVE METHODOLOGY

Each section documented sedimentary structures, degree and type of bioturbation, grain size, bed thickness, paleocurrent indicators and paleocurrent directions. These characteristics were used to define six facies the facies associations and other architectural elements that they comprise. The six facies have also been described based on the spectrum of deposits defined by Lowe (1982) that discusses a full range of sediment gravity flows, including both high and low density flows (Figure 2.5). The six facies identified in the Scotland Formation outcrops include: 1. conglomerates, 2. very coarse grained sands with gravel or pebbles 3. massive, medium- to coarse-grained sandstones; 4. cross-stratified sandstones, 5. laminated centimeter-scale sandstones interbedded with silts and shales, and 6. silty shales with rare sand beds (Figure 2.6, 2.7). These facies combine to make up channel fill, channel-margin/levee, master levee/overbank levee and lobe facies associations.

Channels

A single channel element is the product of a single cycle of channel cutting, filling and avulsion and abandonment (Sprague et al., 2002; Abreu et al., 2003). Channels in the Scotland Formation have large levees but most channels have small levees or are unleveed. Channel fill bodies are composed of the coarsest sediments seen in outcrop, the channel fill axes are comprised of basal conglomerate lag deposits of Facies 1, pebbly sandstones of Facies 2 thick-bedded medium coarse grained sandstones of Facies 3, and thin bedded fine grained turbidites (Facies 5) (Lowe,1982) (Figure 2.7).

Levees

Levee (or inter-channel) deposits are channel marginal wedges formed by the overbanking of flows causing the deposition of thin bedded turbidites of Facies 5. In

ancient systems they include by channel-related overbank deposits, overbank wedges lacking sizeable channel fill units but locally containing discrete meter-thick packages of thin-bedded and fine-grained sandstone or mudstones of Facies 6 that are laterally persistent. These deposits are not commonly recognized in ancient fans and it has been suggested that they are often mistaken for 'distal' turbidites (Stow, Reading and Collinson, 1996) (Figure 2.7).

Where these deposits overlie channel complexes, they record an abandonment phase in space or time of the channel complexes or channel complex set (Schwarz and Arnott, 2007). Levee deposits are characterized by the occurrence of thin bedded turbidites that occur as bundles of up to a few meters thick, with even- and parallel-bedding surfaces and minor lensing and wedging. Levee or inter-channel deposits are distinguished from basin plain deposits by the occurrence of broad and shallow channels that do not occur in basin plain deposits (Mutti, 1977).

Lobes

Lobes occur as roughly tabular, non-channelized bodies, 3 to 25 m thick composed of well-graded to thick-bedded classic turbidites, commonly developed as very small-scale, thinning- and thickening- upward cycles. This facies association is comprised of Facies 3, 4 and 5 of the Scotland Formation outcrops. Erosive bases are not common and have less erosional relief when they do occur than in some other elements of a fan system (Reading, 1991) (Figure 2.7).

Deep Water Hierarchy

Channel fill and channel margin/levee facies associations are comprised of high and low density turbidite deposits. A channel complex is comprised of two or more vertically or laterally stacked channel elements- of similar architectural style (Campion, 2000; Sprague et al., 2002; Abreu et al., 2003) (Figure 2.8).

Two or more channel complexes stack vertically to form a channel complex set The channel complex set is bound at its base by a basinward shift in facies and at its top by a surface of abandonment. Genetically related, stacked channel complex sets form a channel complex system (Campion, 2000; Sprague et al., 2002. Abreu et al. et al., 2003) (Figure 2.9).

Chalky Mount

The Chalky Mount outcrop (CM) is approximately 100 m high at its highest point and has over 400 m of continuous lateral exposure (Figure 2.10). Steep surfaces and the friable nature of the outcrop constrained the location of the measured sections. It is at location 1 in Figures 2.3 and 2.4.

Description

At the Chalky Mount exposure five stratigraphic sections were measured to document the vertical stacking of stratigraphic units and the lateral relationships between beds. The Chalky Mount section is composed of several separate depositional cycles which stack to form an overall fining up stratigraphic succession that is overlain by several meters of fine grained muds and silts (Figure 2.5, 2.6). The stratigraphic section consists of over 90% coarse-grained to granule sized sands. Individual beds at this location are predominantly S_1 and S_3 beds of Facies 2 and 3 that have wavy or scoured bases (Figure 2.11) along with the ripple laminated T_c beds of Facies 4 (Figure 2.12) and the cm scale, interbedded sand, silt and mud T_b, T_d and T_e f beds that comprise Facies 5 (Figure 2.13, 2.14). The coarse grained beds of Facies 2, 3 and 4 comprise the channel axis fill (Sprague et al., 2002; Abreu et al., 2003; Schwarz and Arnott, 2007) (Figures 2.8 and 2.9). The thin bedded turbidites of Facies 5 laterally inter-finger with channel fill associations and are interpreted as the margins or localized levees of the channels (Deptuck, 2003; Schwarz and Arnott, 2007)**.** Up to nine individual channel elements made up of channel fill and margin facies associations are at this location. Channel

element number 6 has the mostly deeply eroded base at this location with approximately 5 m of scour (Figure 2.15). Together the eight stacked channel elements form a channel complex in the sense of Campion (2000) (Figure 2.8 and 2.15). The upper portion of the outcrop is characterized by 10 m of laminated silts, muds and rare sand beds that comprise Facies 6. It is possible that more of this facies existed at one, time but was eroded. Thin bedded turbidite deposits that overlie a channel complex such as those of Facies 6 at this location, record an abandonment of the channel complex in space or time (Schwarz and Arnott, 2007).

Chalky Mount Lower (CML)

This section is located at the base of the prominent Chalky Mount Ridge. Although the contact between the two areas is obscured by thick vegetation, it is thought to be a fault due to the appearance that the entire Chalky Mount Upper package seems to have been thrust into place with beds at the southern end of the outcrop as the beds are almost vertical. The Chalky Mount Upper package is nevertheless still interpreted to overlie the Chalky Mount Lower at this locality. However, one must bear in mind that the upper part has been displaced some unknown distance from its original location of deposition.

Description

The Chalky Mount Lower (CML) section is a large thickness of finer-grained sediments geographically located beneath the Chalky Mount Upper section. However, the exact stratigraphic relationship to the CMU is not known due to separation of the two intervals by a thrust fault.

The CML consists of 50 meters of continuous section characterized at its base by several thicker bedded (20-70 cm), sharp-based, coarse-grained sands (Figure 2.16a-c).

These poorly sorted sands are laterally continuous for the length of the outcrop (approximately 20 m). These sands are coarse grained with some granules.

The bases of these sands are erosive and are locally overlain by a lag of armored mud balls. Sandstone beds become thinner up-section and finer. The finer-grained sands have both planar laminations and climbing ripples. However, ripples are not found up-section as the uppermost sands show only parallel laminations. Dewatering structures related to the loading of sand beds onto finer grained silt and mud beds was also noted. Although there are thin (2-4 cm) sand beds at the top of the section, the majority of the prominent sand beds occur at the base of the section. Some unidentified trace fossils appear in the units.

The lower 10 meters of the section is dominated by interbedded centimeter scale T_e, T_b beds, minor T_c, T_d and rare T_a beds that make up the sands, silts and muds of Facies 6. In this lower 10 m, there are medium grained sands with erosive bases that are absent in the upper portion of the section. Successions of thin bedded turbidite deposits that are 10's of m thick (> 40 m) are interpreted to record an abandonment of the channel complex set in space or time (Campion, 2000; Schwarz and Arnott, 2007). In addition the presence of sand beds with scoured bases confirm that this thick deposit of Facies 6 is not a distal basin plain deposit, but a thick master levee deposit as described by Mutti (1977).

Sleeping Giant Ridge (SGR)

The Sleeping Giant Ridge outcrop (Figure 2.17) is separated from the Chalky Mount by a NE-SW oriented thrust fault (Poole and Barker, 1980; Speed, 1983). Although there is a clear relationship between the two outcrops, the amount of displacement from one outcrop to another is unknown. Therefore, although the Sleeping Giant Ridge outcrops are interpreted as the same depositional "phase" of the system as the Chalky Mount Upper, the beds that have been measured at each locality cannot be traced from one outcrop to the other.

Description

Four stratigraphic sections were measured to document the vertical stacking of stratigraphic units and the lateral relationships between beds at the Sleeping Giant Ridge exposure.

Individual beds at this location are predominantly S_3 beds with $T_{c,}$ and rare S_1 beds (Figure 2.18) that have wavy or scoured bases that comprise the coarse and medium grained sand beds of Facies 2, 3 and 4, (Figure 2.20). In addition T_b, T_d and T_e make up the cm scale, interbedded sand, silt and mud beds that comprise Facies 5 (Figure 2.21). Coarser grained beds of Facies 3 and 4 overlying finer grained beds of Facies 5 load into the finer grained beds resulting in soft sediment deformation features such as flame structures (Figure 2.22). The coarsest grained beds of Facies 2, 3 and 4 comprise the channel axis fill (Schwarz and Arnott, 2007) and the thin bedded turbidites of Facies 5 laterally inter finger with the channel fill facies associations and represent the margins of the channels or local levees (Deptuck, 2003) (Figures 2.7). Up to 6 channel elements as defined by Sprague (2002) comprise Facies 1, 2, 3 and 4 channel fill and Facies 5 channel margin deposits at this location (Figure 2.18). These stacked channel elements form a portion of a channel complex as defined by Sprague (2002).

East Coast Road

Although the East Coast Road outcrop at the East Coast Road cut is not directly accessible when walking from the SGR outcrops, the SGR outcrop is located less than 100 meters from the East Coast Road exposures. Therefore, the stratigraphic relationships between these two outcrops are uncertain, but they are probably related. The lower portion of the outcrop is heavily vegetated and overgrown, nevertheless after a bit of effort, descriptions were made of a continuous 325 m section (Figure 2.9).

Description

This section is the easternmost exposure of Sleeping Giant Ridge and it is identified using the acronym of CRBSGRF. The section that is ~ 325 m long was measured to document the vertical stacking of stratigraphic units and the lateral relationships between beds at the East Coast Road exposure Figure 2.23a-h). Vegetation cover in this area is extensive and several portions are likely now obscured by vegetation cover or rock falls.

At this location $S_{1,}$ S_3 and R_3 beds make up Facies 1, 2 and 3 with the $T_{b,}$ $T_{c,}$ T_d and T_e comprising Facies 4 and 5. Channel fill associations are made up of the combination of Facies 1, 2, 3 and 4 that make up the coarsest grained beds within the system that overlie erosive channel bases. The channel margins are comprised of thin bedded turbidites of Facies 4 and 5 that are interpreted as the margins or localized levees of the channels due to their lateral interfingering relationship with channel-fill facies associations (Deptuck, 2003; Schwarz and Arnott, 2007). Up to 14 individual channel elements make up channel fill and margin facies associations at this location (Figure 2.23a-g). At this location 10 stacked channels form a channel complex (Figure 2.23b-f) that is 167 m thick. This channel complex is overlain by at least 7 m and possibly up to 10 m, of thin-bedded turbidites of Facies 5 that record a localized abandonment phase as discussed by Campion (2000). This channel complex is overlain by four stacked channels that form a

second channel complex (Figure f-g) that is 28 m thick. This channel complex is overlain by at least 79 m of thin-bedded turbidites of Facies 5 and 6 that make up an extensive master levee (after Mutti, 1977).

The stacked channel complexes are bounded below by 31 m of Facies 6 of channel master levee facies (Figure 2.23a) as described by Mutti (1977), Deptuck (2003) and Schwarz and Arnott (2007). They are also bounded above by 79 m of Facies 6 (Figure 2.23h). Two channel complexes can be identified at this location and they are vertically stacked and bound below by 31 m of an extensive master levee sequence and above by 79 m of a master levee sequence that records a more regional abandonment of the system set in space or time (Campion, 2000; Schwarz and Arnott, 2007).

Two or more channel complexes stacked vertically are called a channel complex system. The channel complex system is bound at its base by a basinward shift in facies and at its top by a surface of abandonment (Campion, 2000; Sprague et al., 2002; Abreu et al., 2003). This location has two channel complexes that combine to form a channel complex system set and is bound below by 31 m of a basinward shift in facies and above by a surface of abandonment. The entire 325 m of this outcrop is therefore interpreted as an entire channel complex system set as described by other authors (Campion, 2000; Sprague et al., 2002; Abreu et al., 2003).

Ermy Bourne

The Ermy Bourne (EB) locality is the first package with high sand content that overlies the abandonment facies that cap the Sleeping Giant Ridge section.

Description

The Ermy Bourne (EB) section is exposed in a series of spectacular folds that allow accessibility for closely spaced correlation of beds. Three stratigraphic sections were measured at the locality. The entire upper outcrop is underlain by a thick

succession of interlaminated siltstones and mudstones, with thin interbedded sands; very similar in appearance to those that outcrop at the Walker Ridge locality. These fine-grained units stratigraphically overlie the Sleeping Giant Ridge section, suggesting a second period of sand rich deposition.

S_3 beds with scoured bases (Facies 3) and $T_{c,}$ and T_d beds of Facies 4 and 5 are the most common individual beds identified at this outcrop. Channel fill at this location is made up of the stacked medium to coarse grained sands of Facies 3 and the levee facies association that are comprised of the thin bedded turbidites of Facies 4 and 5 are interpreted to represent the margins or localized levees of the channels due to their lateral interfingering relationship with the channel fill facies association (Deptuck 2003, Schwarz and Arnott, 2007). Only one complete channel that is at least 5 m in height is identified at this location and it overlies 9 m of a Facies 5 levee association (Figure 2.24).

The EB section appears to record a return of the channelized depositional system after abandonment following the deposition of the Sleeping Giant Ridge channel complex set

Walker's Ridge

The Walker's Ridge outcrop (Figures 2.25, 2.26, 2.27) is the most northerly location (Figure 2.3, 2.4) and the stratigraphic relationships with the other locations to the south are unclear.

Description

The Walker's Ridge section is an extensive outcrop of laminated shales and sands (60 + meters) overlain by stacked thick sands separated by silty shale intervals. Three measured sections; WRA, WRB and WRC were correlated across the outcrop and they define a continuous 70 meter thick section. Trace fossils have been identified as *Diplocraterion habichi* (J. MacEachern, pers. comm., 2007). These trace fossils are

common in shallower marine water environments but can also be indicative of a depositional setting near the apex of a fan complex (Figure 2.28). The U-shaped burrow of *Diplocraterion* is indicative of high energy environments which experience erosional and abrupt depositional events (Pemberton and MacEachern, 1995).

Individual beds at this location are predominantly S_3 beds (Facies 3) with $T_{b,}$ $T_{c,}$ T_d (Facies 5) and rare R_3 beds (Facies 1) that overlie scoured bases (Figures 2.29, 2.30, 2.31). Channel-fill associations at this location are dominated by stacked beds of Facies 3 coarse-grained beds within the system that overlie erosive channel bases. The channel margins are comprised of thin bedded turbidites of Facies 5 that are interpreted as the margins or localized levees of the channels due to their lateral interfingering relationship with channel fill facies associations (Deptuck, 2003; Schwarz and Arnott, 2007). Up to 5 individual channel elements make up channel fill and margin facies associations at this location. The five stacked channels form a channel complex (Figure 2.27) that is 40 m thick.

Thick successions of thin bedded turbidite deposits (10's of m thick- > 40 m) are interpreted to record an abandonment of the channel complex set in space or time (Campion, 2000; Schwarz and Arnott, 2007). The presence of sand beds with scoured bases (figure 2.32) confirm that this thick succession of Facies 6 is not a distal basin plain deposit, but a thick master levee deposit as described by Mutti (1977).

The Walker's Ridge lower section is interpreted to have been deposited as outer levees in association with a laterally adjacent large, deep water channel system. These deposits appear to be classic deep water levee deposits as described by Mutti (1977). The Walker's Ridge is expected to be laterally associated with a channel sequence similar to the overlying Walker's Ridge Upper.

Mount All

The beds of the Mount All outcrop are almost vertical and stratigraphic relationships between this and the other study locations are uncertain. Even the stratigraphic relationship between Mount All and Inner Turner's Hall Ridge, located less than 1000 m to the northwest, is unclear.

Description

The Mount All outcrop has been extensively folded and no lateral relationships could be ascertained between individual measured sections. The short measured sections were made at the exposed limb of the anticline (MAA, 8 m thick section) and at the vertical beds adjacent to this anticlinal feature, MAB (20 m thick section). MAA appears to occur stratigraphically higher than MAB.

Very robust and abundant *Thalassinoides* (Figure 2.33) and as well as *Planolites* trace fossils are observed at the Mount All location. *Thalassinoides* is interpreted as a combined feeding and dwelling burrow, but has been observed as a boring geometry in some cases. The probable trace maker was an arthropod. *Planolites* is interpreted as a feeding burrow made by a worm-like animal.

MAA locality

Individual beds at this location are predominantly S_3 beds (Facies 3) along with T_d beds and T_e beds of Facies 5. Channel fill associations at this location are dominated by stacked beds of Facies 3 coarse grained beds within the system that overlie erosive channel bases. The channel margin association at this location is made up of thin bedded turbidites of Facies 5 that are interpreted to represent the margins or localized levees of the channels (Deptuck, 2003; Schwarz and Arnott, 2007) and are overlain by the channel fill deposits (Figure 2.34).

MAB locality

S_3 beds of Facies 3 along with $T_{b,}$ T_c beds and T_e beds of Facies 5 are the most common individual beds observed at this location. Channel fill facies associations are dominated by stacked Facies 3 coarse grained beds within the system that overlie erosive channel bases. The channel margin facies associations are comprised of thin bedded turbidites of Facies 5. Because the beds at this outcrop are almost vertical, lateral relationships cannot be determined. This section is a vertical succession of alternating channel fill and channel margin facies associations (Figure 2.35).

Turner's Hall Ridge

Description

This location consists of ~ 70 m of continuous exposure. Because there appears to be little lateral variation in lithology or bed architecture across the 60 m width of outcrop, only one section was measured to characterize the location (Figure 2.36). Sandstone beds vary from medium-grained (Figure 2.37) to fine-grained and are thickest at the base of the section with a maximum thickness of 420 cm. Sand beds are capped with ripple-laminated, fine-grained sands and silts. Minor loading and planar lamination is observed through out the section. There is no very coarse-grained sand or conglomerate component and no erosive bases were observed.

The first 20 m of the section is dominated by S_3 (Facies 3) beds that are interbedded with $T_{b,}$ T_c and minor T_d beds (Facies 4 and 5). Up section S_3 are rare and T_c and T_d beds make up the bulk of the section. (Figure 2.38 a-e). This section is distinct from the Chalky Mount Shale Ridge and Lower Walker's Ridge sections as it has a higher sand content, but does not show the scoured bases, intermittent very coarse grained sands seen at the other two outcrops.

Lobes are non-channelized bodies, 3 to 25 m thick composed of well-graded to thick-bedded classic turbidites in which erosive bases are uncommon (Stowe, Reading and Collinson, 1996). Based on this description, the ITR succession is interpreted to represent a lobe deposit.

Spa Hill

Description

Two stratigraphic sections were measured to document the vertical stacking of stratigraphic units and the lateral relationships between beds at the Spa Hill Fold (SHF) exposure. The entire outcrop is only 35 m in length.

The SHF section is ~ 13 meters thick and sandstones vary from very coarse grained to medium grained and are massive and blocky with no fining upward trends (Figure 2.39).

DISCUSSION

General Depositional Model

Mixed sand and mud systems submarine systems are defined as those that have sand to mud ratios of 30-70% (Reading, 1991; Richards et al. 1998). This type of submarine fan system is characterized by two main architectural elements; a channel-levee system and down-dip depositional lobes (Normark, 1978; Walker, 1978; Normark et al., 1979; Droz and Bellaiche, 1985). Channel sand bodies are offset stacked and bounded by levee fines. Down dip equivalents are stacked lobate sand bodies made up of mudstones and sandstones (Reading, 1991; Richards et al., 1998). Channel-levee systems form the conduits through which sediment is distributed to the main area of the fan. These systems may become mud-filled if fan abandonment is rapid or can contain a central core of coarse-grained, highly heterogeneous channel fill deposits, flanked by levee siltstones and mudstones if the fan is progradational (Walker, 1978; Winn and Dott, 1979; 1985 Tyler et al., 1984; Mutti et al., 1985a; Weuller and James, 1989; Schuppers, 1992; Richards et al., 1998). Channel facies in these systems vary from sandy conglomerates and pebbly sandstones with thick-bedded, high density turbidites to fine-grained thin bedded turbidites and hemipelagic mudstones (Richards et al., 1998).

The Chalky Mount locality is a good example of this fan architecture. The Chalky Mount Ridge has channel-levee-overbank complex architectural elements. Sandy channel fill within the channel axes are deposits from individual channelized flows within the larger erosionally confined channel complex system. Silty mudstone intervals are out of channel levees, deposited after the individual abandonment of coarse-grained channels (Figure 2.40).

It is believed by the author that this is a mud-rich fan system; however, The sand-mud ratio in the measured sections is skewed toward higher sand percentages by the fact that the thick sandy units are what more prevalently expose themselves for analysis.

Sandy units are the most resistant to weathering and generate poorer soils for the growth of vegetation. The muddier and siltier portions of the outcrop generate good soils for vegetation growth, and usually do not form extensive outcrops. Interpreting this system to be a mud-rich fan system has implications for the distribution of sands in the system. Mud-rich fans can be large systems (up to 1000s of km) dominated by well-developed channel-levee complexes with sand mostly restricted to axial channel fill within the channel levee complexes (Imperato and Nilsen, 1990; Weimer, 1990, 1995; Richards et al., 1998).

Lobes

Constructional lobes form layered sand bodies. The core of the lobe may be dominated by massive thick-bedded high density turbidites (Kleverlaan, 1989; Kulpecz and VanGeuns, 1990, Richards et al., 1998). Some lobes may display more classic turbidites and interbedded hemipelagic shales. Examples are the Stevens Fan, (MacPherson, 1978; Webb, 1981) and the Marenosa-Arenacea Fan, (Ricci-Lucchi and Valmori, 1980; Richards et al., 1998).

Based on this definition of constructional lobes, it is thought that Inner Turners Hall Ridge locality is consistent with channel mouth or depositional lobe development and is interpreted as the most distal feature within the system (Figure 2.40). The Inner Turner's Hall Ridge location has layered sandstone beds that vary from medium-grained to fine-grained and are thickest at the base of the section with a maximum thickness of 420 cm. Sand beds are capped with ripple-laminated, fine-grained sands and silts. Minor loading and planar lamination are observed throughout the section. There is no coarse-grained sand or conglomerate component and no erosive bases.

COMPARISON WITH LARUE'S RADIAL FAN MODEL

In Larue's 1985 paper, five principal units of turbidite successions were described on Barbados and interpreted in the context of the classic "radial fan model" of Mutti and Ricci-Lucchi (1972). Progradational and rejuvenational sequences of the basin plain and lobe, channelized successions of the mid-fan and inner fan; retrogradational and abandonment sequences were identified.

The Breedy's (Walker's Ridge Lower) outcrop was interpreted by Larue (1985) as an extensive abandonment sequence characterized by thick accumulations of basin plain mudstones. In this study, this succession has been reinterpreted as an extensive levee sequence, similar to that described by Mutti (1977), based on the presence of erosive based sand beds. The implication of the latter interpretation is that this sequence and the overlying sand-rich Breedy's outcrop (Walker's Ridge Upper) does not record an abandonment of the system followed by a rejuvenation as proposed by Larue, but is instead a system that experienced lateral shifts in the channel axis through time. The Scotland Formation as a whole does not record up and down system changes from mid-fan to basin plain, but more subtle lateral changes within the mid fan from the axis of the channel complex to the levees of the system. The most distal facies seen in outcrop is the channel mouth complex at Inner Turner's Hall Ridge (Figure 2.36, 2.38a-e). This was the only shift of the system in the dip direction observed in the study area. This outcrop probably records a slight retrogradation of the system.

SUMMARY DEPOSITIONAL SETTING OF THE SCOTLAND FORMATION DEPOSITS

The facies identified in the Scotland Formation outcrops range from conglomerates, coarse-grained sands with gravel and pebbles to laminated silty muds and fine grained sands. The facies and architectural components of the Scotland Formation fit into the mixed sand and mud submarine fan system of Reading (1991). The absence of slump deposits in outcrops, and the sand content of the system suggests a mid-fan depositional location for the Scotland as opposed to either a proximal, slope location or a distal basin plain location.

Trace fossils can be locally well developed in submarine fans, particularly in mid to outer fan settings. *Thalassinoides* and *Planolites* were observed at the Mount All location. These trace fossils were locally abundant on the bases of mudstone beds. A similar assemblage of *Thalassinoides, Scalarituba* and *Planolites* were identified in the Nihoptupu and Tirikohua Formations of New Zealand that are comprised of deep water turbidites deposited in an inter-arc basin of the Northland volcanic arc (MacEachern et al., 2007).

Middle fan environments often contain trace fossils along the soles of sandy turbidites that can suggest “shallow water” deposition (Crimes, 1977; Howell and Normark, 1982). Trace fossils, such as *Diplocraterion habichi,* that are rare in the Scotland Formation are generally shallow-water, high energy indicators ~ 200 m water depth (Pemberton and MacEachern, 1995). This anomalous trace fossil association is the result of the imitation of the high energy neritic environment in a mid fan setting. This occurs because fast flowing depositional currents result in short lived episodes of high oxygenation that, coupled with the slow build-up of organic detritus in the middle fan leads to an imitation of high energy neritic environments (Howell and Normark, 1982).

ANALOGS FOR THE SCOTLAND FORMATION

The Scotland Formation of Barbados shows similarities to the Juniper Ridge Conglomerate (JRC) and the associated Upper and Lower Waltham Shales which are part of the Great Valley Group (GVG) of California. These GVG sediments were deposited in a Cretaceous age forearc basin (Lowe, 2004).

The JRC and associated Upper and Lower Waltham Shales are made up of five lithofacies. Including:

(1) Coarse, cobble and pebble conglomerate channel fill,

(2) Thick bedded sandstone fill,

(3) interbedded sandstone and mudstone levee-deposits flanking the channels,

(4) thick-bedded channel mouth and proximal lobe deposits and

(5) Intervening thick mudstone formations made up of thin fine grained muddy turbidites, recording periods of low coarse clastic-sediment influx. (Lowe, 2004)

Facies 1, 2, 3 and 5 of the Scotland Formation correspond to the JRC channel-levee complex system. Facies 4 corresponds to the JRC channel mouth and proximal lobe sandstone. Facies 6 is the equivalent of the closely associated setting of the Upper and Lower Waltham Shales (Figures 2.6, 2.7, 2.41 and 2.42).

Chapter Three: Petrographic Analysis of the Scotland Formation Sandstones

Eocene-Oligocene sandstones found interbedded with sand and shale in the succession known as the Scotland Formation, onshore Barbados, are the equivalents of the reservoirs that are being produced from in the Woodbourne oilfield in the southern part of the island. Outcrops of this formation are exposed in the northeastern portion of Barbados where the Pleistocene limestone cap has been eroded to expose the underlying Tertiary sediments.

The Scotland Formation sediments have been interpreted as abyssal plain or trench deposits that were tectonically incorporated into the accretionary prism (Speed 1982; Larue and Speed, 1983; Torrini et al., 1985; Gortner and Larue, 1986). Their location onshore Barbados Island means that, if these sediments were originally deposited in a trench setting, they would had to have been tectonized during subduction deformation, transported westward and subsequently uplifted after becoming part of the prism. If this is the case, these deposits were potentially translated > 100 km westward from the trench to the present location through shortening of the prism.

Although none of the previous workers have disputed a trench origin for the Scotland Formation, the results of previous petrographic analyses suggest that the Scotland Formation did not experience such a tectonic history (Larue and Kasper, 1985; and Larue, et al., 1987; Punch, 2004).

PREVIOUS RESEARCH

The source terranes of the Scotland Formation were interpreted by Kasper and Laure (1986) to include the Guyana Shield, the Caribbean Mountain System and possibly the Lesser Antilles or predecessor arc. It is important to note that in 1985, workers wrote that the Eocene sandstones exposed onshore Barbados had not been deeply buried (< 40 km) or exposed to high temperatures (< 60˚C) (Larue et al. 1985; Larue, Gortner and Torrini, 1987), based on extensive petrographic analysis of the Scotland Formation sandstones. Larue and Kasper (1986) and Larue, et al. (1987) further stated that the Scotland Formation was no more diagenetically mature "…than the sediments that lay passively on the floor of the Atlantic Ocean for 40 my…" These authors also interpreted the Scotland to represent abyssal plain or trench deposits that were tectonically incorporated into the accretionary prism. It is hard to reconcile these two observations because sediments deposited so distal in the prism to their current outcropping location would require significant tectonic displacement associated with trench subduction, tectonic burial and subsequent uplift.

In 1986, Baldwin undertook fission track analysis on the sandstones of the Scotland Formation. She reported that the ages of the youngest populations were 20-90 Ma. The results of her study also showed that the maximum temperature that the Scotland Formation sediments underwent was 80˚C (Baldwin, 1986).

Punch (2004) examined 13 samples from the Scotland sandstones onshore Barbados found at the Chalky Mount outcrops and along the East Coast Road outcrops (Previous location Figure 2.3). The analyzed samples ranged from mature quartz arenites to feldspathic sublitharenites, sublitharenites and arkoses. Punch concluded that the sandstones were compositionally mature, but texturally submature and had only been transported a short distance. She observed that formation fluids had caused the dissolution of some but not all of the feldspars. Her conclusion was that the sediments

had not been buried deeply or long enough to result in complete dissolution (Punch 2004).

All of these previous results lead to the questions of 1. How can sediments deposited in a trench setting now be uplifted to the highest point of the prism core with little or no diagenetic imprint on the sediments? and 2. If they have been subducted in this transport process why do they show limited signs of high pressure and temperature history? To address these questions we needed to reexamine the samples of the Scotland and reassess the diagenetic history of the deposits within the context of their depositional setting and within the context of previous work by Chaderton (2005) regarding the history of Tobago Forearc Basin development.

METHODOLOGY

Samples were cut and made into thin sections then impregnated with blue dyed epoxy and left unpolished. The sections were then stained for identification of potassium feldspars (yellow) and calcium plagioclase (pink)

Forty samples were examined for petrographic content and sandstone characteristics. However, the majority (33) of these samples were measured from a single locality (SGRF) therefore, only 10 samples were chosen for detailed analysis and point counting. The goal of this analysis was to investigate possible variations in petrographic character between localities and between facies. In each of the 10 samples 200 grains were point counted and 100 grains were measured in each sample along the long axis. Pore spaces and grains were not counted separately. The intergranular volume (IGV) was calculated based on the results of point counting using the following formula:

IGV= Primary pores + Pore-filling Cements + Matrix

The initial intergranular volume is assumed to be 40-45% (Beard and Weyl,1973; Pryor,1973; Atkins and McBride, 1992; Paxton et al., 2002). The amount of compaction that the rock has undergone can be estimated based on the difference between the IGV and the assumed initial intergranular volume of 40-45%. If cement and depositional matrix are subtracted, the intergranular volume (IGV) is the maximum potential intergranular porosity of the rock (Paxton et al., 2002).

Paxton's IGV curve shows that mechanical compaction in the upper 1500 m of burial corresponds to IGV values of 28-42%. From 1500-2500 m of burial, compaction values range from 26 to 30% IGV and below 2500 m, sandstones reach maximum mechanical compaction that corresponds to an IGV of 26% (Paxton et al., 2002).

FRAMEWORK GRAINS

Quartz

The quartz grains in the samples studied are predominantly monocrystalline with less common polycrystalline quartz. These samples are dominated by common quartz. A few quartz grains do have sutured boundaries and exhibit undulose extinction. Some quartz grains are highly fractured (Figure 3.1).

Previous workers have documented quartz cement in the form of overgrowths. Examination of the samples collected in this study shows that many of the overgrowths in the samples are abraded and there are many grains with distinctive dust rims that allow the overgrowths to be readily identified (Figure 3.2). This evidence suggests that the quartz in these samples is of recycled origin and not part of the cementation history of these rocks.

Feldspars

Calcium Plagioclase Feldspar

Calcium plagioclase feldspar was identified by the distinctive pink color imparted by the staining process (Figure 3.3). Some grains also exhibit polysynthetic twinning. Weathered samples show some dissolution and in some grains a secondary moldic porosity is present.

Potassium Feldspar

Potassium feldspar (K feldspar) was identified by the appears yellow-brown color imparted by the staining process. Both fresh and weathered varieties are present in thin section. Some grains show distinctive microcline (tartan) twinning. Weathered samples show some dissolution and in some cases secondary moldic porosity is present.

Rock Fragments

Lithic rock fragments are not common in these samples but examples of volcanic, sedimentary and metamorphic rock fragments are observed within the thin sections in minor amounts.

Altered Volcanic Rock Fragments

Altered volcanic rock fragments are made up of feldspars that have been altered to clay in association with pyrite. Pyrite is opaque in cross polarized light but has a gold color in reflected light (Figure 3.2, 3.4).

Low Grade Metamorphic Rock Fragments

Low grade metamorphic rock fragments occur as folded micaceous rock fragments that are possibly phyllite.

Argillaceous Rock Fragments

Argillaceous rock fragments appear brown in color in plane polarized light. They are generally deformed and in some cases transformed into pseudomatrix.

Chert

Chert is microcrystalline quartz. Like the other types of quartz, it is transparent in plane polarized light but exhibits a salt and pepper appearance in cross polarized light.

Accessory Minerals

Several accessory minerals occur in minor amount and are identified by the criteria listed below. These include:

Biotite - identified by the distinctive brown to dark brown pleochroism in plane polarized light.

White mica - probably muscovite, exhibits second-order bi-refringence colors in cross-polarized light and is white to transparent in plane polarized light. Grains are thin, platy and elongate. They are often deformed and are more abundant in finer-grained samples.

Chlorite - is present as rare chlorite grains with distinctive green-darker green pleochroism.

Glauconite - is rare, but is distinctive with its green color in plane and cross polarized light and its rounded grain shape.

Authigenic Minerals

Authigenic minerals occur as both pore filling and grain replacements. Various types are described below:

Quartz overgrowth – occurs as a pore-filling authigenic material nucleated as overgrowths in optical continuity with the detrital grain. This type of cement is best identified when there is a dust rim present that delineates the original boundary of the quartz grain.

Kaolinite – also occurs as pore-filling material that appears grey or light brown in plane polarized light. A vermicular appearance (wormlike kaolinite “books”) is visible in cross polarized light.

Chlorite – a pore-filling cement that is pale green in plane polarized light.

Grain Replacement

The most common grain replacement cements in these samples is kaolinite. Its vermicular appearance (wormlike kaolinite “books”) is visible in cross polarized light. In plane polarized light, it can have a bluish grey appearance. Kaolinite commonly takes on the shape of the grain it is replacing, most typically feldspar but also other minerals.

TEXTURE

The samples examined ranged from medium- to coarse-grained sandstones, most are interpreted to have been deposited in mid-fan submarine channels (see Chapter 2 this dissertation). Two of the samples from Inner Turner's Hall Ridge (ITR) are interpreted to have been deposited in slightly more distal channel mouth lobes. The mean grain size of all the samples combined is 3.23 phi and the average standard deviation of the samples is 0.80, moderately sorted. Extremely fractured quartz grains are observed within many of the samples. Some of the fractured quartz grains are still recognizable; however it is likely that some of the smaller grains are actually fractured pieces of larger grains. Much of the apparent moderate to poor sorting may be a result of fracturing due to tectonic activity and may not be the result of source area or burial compaction processes.

Sample: SGRF 1C

This sample was taken from the first bed in the measured section labeled SGRF-Sleeping Giant Ridge; section F (Figure 3.5). This measured section is a part of an overturned 250 m vertical succession that has been exposed by a road cut. The entire succession thickens and coarsens upward although individual beds fine upward. The sample was taken from the upper portion of a 150 cm thick bed from an area of coarse- to medium-grained sand that has been interpreted to be a channel fill deposit. This outcrop has been interpreted to be a stacked channel-levee sequence that has been deposited in a mid-fan depositional setting.

Mineralogy

There is grain-to-grain contact within the sample but a significant amount of pore space remains. There is minor biotite, white mica, rare chlorite grains, chert, and minor

amounts of chlorite and kaolinite cement. Some K feldspar and plagioclase feldspar are present. Some of these grains are altered and a few are being dissolved to produce secondary porosity. Quartz overgrowths are present but broken and no other quartz cementation is observed. A large number of quartz grains are fractured (Figure 3.6).

Sample: SGRF 9C

This sample was taken from bed 9 in the measured section labeled SGRF-Sleeping Giant Ridge; section F (Figure 3.5). This bed has been described in outcrop as 90 m of fine-grained, parallel-laminated sand that fines up to very fine-grained sand and silt with well-developed ripples. This bed is part of a levee facies deposit that is part of the channel-levee sequence described at this location. The sample was taken from the parallel-laminated section of the bed, although in thin section there is no variation in grain size or composition that can be observed.

Mineralogy

Grains are in contact with each other, but there is a great deal of pore space. There is minor biotite, white mica, one pyrite grain, hematite and kaolinite cement. Some K feldspar and minor plagioclase feldspar are present, some of these grains have undergone significant alteration (Figure 3.7). A number of quartz grains are fractured to varying degrees, however most porosity primary.

Sample: SGRF 11B

This sample was taken from bed 11 in the measured section labeled SGRF-Sleeping Giant Ridge, section F (Figure 3.5). This measured section records a portion of an overturned 250 m vertical succession that has been exposed by a road cut. The sample was taken from the upper portion of a 150 cm thick bed from an area of coarse- to medium-grained sand that was interpreted as a channel-fill deposit. This outcrop has been

interpreted to be a stacked channel-levee sequence that has been deposited in a mid-fan depositional setting.

Mineralogy

Grains are in point contact with each other, but there appears to be significant amount of relict pore space present. There is minor biotite, white mica, rare chert and volcanic rock fragments, and minor amounts of hematite and kaolinite cement. Larger amounts of K feldspar and plagioclase feldspar are present. Quartz overgrowths are present but broken. No other quartz cementation is observed (Figure 3.8). A large number of quartz grains are fractured to varying degrees and secondary intragranular fracture porosity is moderate.

Sample: SGRF 19C

This sample was taken from bed 19 in the measured section labeled SGRF-Sleeping Giant Ridge; section F (Figure 3.9). This bed is comprised of a 170 cm of coarse-grained to medium-grained sand that has at least two secondary erosive surfaces within the bed. The sample was taken 10 cm from the top of this bed that has been interpreted to be a channel-fill deposit.

Mineralogy

There is minor biotite, white mica, a single chlorite grain, chert, and minor amounts of chlorite and kaolinite cement. K feldspar and plagioclase feldspar are present, some of these grains are being altered and a few feldspar grains are partly replaced by kaolinite cement. Quartz overgrowths are present but broken. No other quartz cementation is observed (Figure 3.10). A number of quartz grains are fractured to produce secondary intragranular porosity.

Sample: WRA 16

This sample was taken from the bed 16 in the measured section labeled WRA-Walkers Ridge; section A (Figure 3.11). The Walker's Ridge section is an extensive outcrop of laminated shales and sands (60 + meters) overlain by stacked thick sands separated by silty shale intervals. The sample was taken from a coarse-grained sand bed interpreted as a channel fill deposit. Three measured sections; WRA, WRB and WRC were correlated across the outcrop to define a continuous 40 meter thick section at this locality. This outcrop has been interpreted to be a stacked channel-levee sequence that has been deposited in a mid-fan depositional setting.

Mineralogy

This sample is dominated by common quartz. Potassium (K) feldspar and plagioclase feldspar are present in small quantities, kaolinite and hematite cement is rare and no accessory minerals are observed. Quartz grains are extremely fractured and secondary intragranular porosity has been created. It is important to note that while fractured quartz is dominant, no quartz cement has formed on fresh, clean fractured surfaces (Figure 3.12).

Sample: WRB 8

This sample was taken from bed 8 in the measured section labeled WRA-Walkers Ridge, section B (Figure 3.13). This measured section records 12 m of a very a sand-rich succession in which very coarse-grained sands dominate and conglomerate lag deposits are observed overlying erosive channel bases. This sample was taken from a coarse-grained sand bed that was interpreted to be a channel-fill deposit.

Mineralogy

This sample is dominated by common quartz and although K feldspar and plagioclase feldspar are present in small quantities, no accessory minerals are observed. Hematite cement is present in greater quantities than in WRA 16 (Figure 3.11). Quartz grains are extremely fractured and secondary intragranular porosity is a significant portion of overall porosity (Figure 3.14). As in the sample labeled WRA 16, fractured quartz is dominant. No quartz cement has formed on fresh, clean fractured surfaces.

Sample: ITR 9

This sample was taken from bed 9 in the measured section labeled ITR- Inner Turners Hall Ridge (Figure 3.15). The sample was taken from a bed that has been interpreted to be a channel-mouth sand lobe. This measured section records 70 m of continuous exposure. Sandstone beds vary from medium- to fine-grained and are thickest at the base of the section with a maximum thickness of 420 cm. Sand beds are capped with ripple-laminated, fine-grained sands and silts. Minor loading structures and planar lamination is present through out the section. No coarse-grained sand or conglomerate component and no scoured bases were observed. This outcrop was interpreted to be a portion of a channel-mouth lobe.

Mineralogy

The quartz content of this sample is lower and K feldspar and plagioclase feldspar are more abundant (Figure 3.16). A small number of lithic fragments are present and they include altered volcanic rock fragments, argillaceous rock fragments, rare metamorphic rock fragments and chert. Minor amounts of biotite and white mica are present and the most abundant cement is hematite with minor amounts of pore-filling chlorite and kaolinite. Quartz overgrowths are present, but broken. No other quartz

cementation is observed. A number of quartz grains are fractured to produce secondary intragranular porosity.

Sample: ITR 14

This sample was taken from the bed 14 in the measured section labeled ITR-Inner Turners Hall Ridge (Figure 3.15). Bed 14 has been interpreted to be a channel-mouth sand lobe. This measured section records 70 m of continuous exposure. Sandstone beds vary from medium- to fine-grained and are thickest at the base of the section with a maximum thickness of 420 cm.

Mineralogy

The quartz content of this sample is lower and K feldspar and plagioclase feldspar are more abundant. A small number of lithic fragments are present and they include altered volcanic rock fragments, argillaceous rock fragments, rare metamorphic rock fragments and chert. Minor amounts of white mica are present and there are minor amounts of pore-filling chlorite and kaolinite. Hematite cementation has completely occluded porosity in some cases and blocked pore throats in others (Figure 3.17). Quartz overgrowths are present, but broken. No other quartz cementation is observed. Some organic matter is present in this sample.

Sample: CMRA

This sample was taken from the first bed in the measured section labeled CMR-Chalky Mount Ridge section A (Figure 3.18). This measured section records almost 60 m of a stacked channel-levee sequence. The sample was taken from the upper portion of a 3 m thick bed that ranges from gravel overlying an erosive base and fines upward to a medium-grained sand. The sample was taken from the middle of a bed that was interpreted to be a channel-fill deposit

Mineralogy

There is minor biotite, white mica, rare volcanic rock fragments and chlorite and kaolinite cement. K feldspar and plagioclase feldspar are present, some of these grains are altered and a few feldspar grains are replaced by kaolinite cement. There is a significant amount of hematite cement and some siderite (Figure 3.19). Quartz overgrowths are present, but broken. No other quartz cementation is observed. A number of quartz grains are fractured to produce secondary intragranular porosity.

Sample: Breedy's

This sample was taken from a sand bed that overlies an extensive out of channel-mud sequence in a mid-fan depositional system. There was not sufficient exposure to create a measured section. This 1 m sand bed consists of coarse- to medium-grained sand topped by ripple-laminated, fine-grained sands. The sample was taken from a sand that is thought to be an out of channel sand in an overbank levee sequence.

Mineralogy

There is white mica, chert, sedimentary and metamorphic rock fragments and minor amounts of chlorite and hematite cement present in this thin section. K feldspar and plagioclase feldspar are more abundant than in previous samples, and many of the K-feldspar grains are altered. Quartz overgrowths are present, but broken. No other quartz cementation is observed. Fractured quartz grains dominate this sample and secondary intragranular porosity is present. Some organic matter and a rare glauconite grain are also present (Figure 3.20).

COMPARISON WITH PREVIOUS WORK

Punch (2004) and Kasper (1985) classified the Scotland Formation sandstones as moderately-to-poorly sorted. In this study, however, grains that had been completely fractured apart, but appeared to have been part of a single, larger grain were counted as one grain. This approach possibly explains why only two of the samples in my study exhibit poor sorting. Samples WRA 16 and WRB 8 (Figures 12 and 14) have a large number of fractured grains and it is unclear how many grains produced the fragments.

Punch's (2004) samples when plotted on a QFL diagram range from quartz arenites to subarkoses (Figure 3.21). Kasper and Larue's (1986) samples ranged from quartz arenites, to sublitharenites with some sub arkoses (Figure 3.22).

Punch (2004) concluded that formation fluids caused the dissolution of some feldspars in the samples. She determined that burial had not been deep or long enough for dissolution of all of the feldspars to occur. Quartz overgrowths found on clean surfaces void of clay rims were recorded as quartz cement.

Kasper and Larue (1986) noted the abraded quartz overgrowths that are indicative of reworked sedimentary source rocks and recorded that feldspars were rare in the samples they examined. Both Punch's 2004 work and this study (Figure 2.23) observed feldspar in greater amounts.

DISCUSSION

Although many of the samples from this study appear to be poorly sorted when visually inspected in outcrop, thin section examination shows them to actually range from moderately to well sorted. The sorting and measurement of grain sizes is affected by the presence of deformation bands, which can cause larger quartz grains to be broken into smaller fragments. In addition several samples showed fractured quartz grains that were not associated with deformation bands. Where possible, grains that appeared to be part of a larger whole were visually reconstructed and considered a single grain in an effort to maintain the integrity of the grain size measurements.

The Scotland Formation samples range lithologically from quartz arenites to arkoses. The quartz arenites and subarkoses samples were all obtained from the channel-fill sandstones. One subarkose and one arkose sample were obtained from the finer-grained channel mouth sandstone at Inner Turner's Hall Ridge (ITR). The more distal facies at ITR were not only more feldspar rich but also finer grained as one would expect in an unconfined setting. Pudsey (1982) observed that the feldspar content in the Scotland Formation deposits decreased with increasing distance from the Lesser Antilles Island Arc, suggesting that the feldspar was derived from the volcanic island arc. It is possible that there was increased volcanic activity when ITR channel mouth sands were deposited and that resulted in an increased amount of feldspar.

The preservation of K feldspar in these samples suggests that the rocks of the Scotland Formation have <u>not</u> undergone deep burial. K feldspar normally undergoes extensive dissolution during burial diagenesis (Milliken et al., 1989; Harris, 1992; Wilkinson and Haszeldine, 1996; Wilkinson et al., 2001). In rift and passive margin settings, K feldspar preservation is commonly absent in rocks that been buried more than four kilometers. In volcanic arc or strike-slip basins, high K^+/H^+ ratios, high SiO_2 activity or a lack of illite-smectite clay mineral assemblage in the mudrocks may enable

K feldspar preservation to slightly greater depths, perhaps, five kilometers (Wilkinson et al., 2001). These well-established relationships taken in tandem with the field observations suggest that the Scotland Formation exposed on the island of Barbados has never been buried much more than five kilometers and possibly less than four kilometers of burial.

Quartz overgrowths on detrital quartz grains are common in the Scotland Formation sandstones. Studies of the Moogooloo Sandstone, in Western Australia showed that these types of overgrowths increased with thermal maturity and less than 1% of quartz cementation occurred at less than 60˚C (Baker et al., 2000). However, many quartz overgrowths in this study are broken which suggests that the quartz grains are recycled and thus the phase of quartz cementation is not related to the diagenesis of this rock. The lack of quartz cementation that is local to the Scotland Formation suggests that the rocks were not subject to temperatures < 60˚C.

Deformation bands are tabular structures of finite width that are the result of strain localization. These features develop in sand and porous sandstone (Aydin, 1978; Dragantis et al., 2005) and may form during soft sediment deformation or post burial faulting (Fossen et al., 2007). Deformation bands are often classified based on the amount of shear offset that they have undergone. In the thin sections from the Scotland Formation no shear offset has been observed. The deformation features observed in these samples include grain fracturing, a reduction in grain size and in porosity and an apparent reduction of volume within the deformation band. Using the kinematic classification system (Aydin et al., 2006; Fossen et al., 2007), these features would place the Scotland Formation deformation bands within the class of compactional deformation bands. Within the mechanical classification these features would be characterized as cataclastic deformation bands. Cataclastic deformation bands have been found in unconsolidated marine sand buried less than 50 m (Cashman and Cashman, 2000; Fossen et al., 2007).

They are common in accretionary prism settings (Fossen et al., 2007). Deformation bands were observed in 2 of the 10 samples point counted.

There is a reduction in porosity and permeability along deformation bands. However there is thought to be an initial dilation that may aid in fluid flow and lead to preferential cementation along these linear features (Ngwenya et al., 2000; Olgivie and Glover, 2001; Fossen et al., 2007). Fractured quartz grains provide clean sites for nucleation of quartz cements that are so abundant in sand (Walderhaug, 1996, Fossen and Bale, 2007).

Although it is often thought that deformation band zones are baffles to fluid flow, Fossen and Bale (2007) showed that the impact of deformation bands on reservoir performance may be small or negligible.

Within the Scotland Formation samples, no quartz cementation was observed within the deformation bands. This observation further supports the idea that the Scotland Formation did not experience temperatures greater than 60˚C. In addition the observations that cataclastic deformation bands develop at depths of 2.5 km or less and even in sediments buried as shallowly as 50 m also support the concept that the Scotland Formation was never buried very deeply.

Based on the calculations of the IGV of the samples which ranged from a minimum of 27.5% to a maximum of 42 % the rocks of the Scotland Formation appear to have been buried less than 2500 m and possibly only about 1500 m.

CONCLUSIONS

1. No quartz cementation occurs during diagenesis of the Scotland Formation. Quartz cementation as overgrowths is fractured and interpreted to be of recycled origin.
2. Scotland Formation sediments have never been exposed to temperatures greater than ~ 60 C.
3. Scotland Formation sediments have probably been buried less than 2500 m and possibly have never been buried much more deeply than 1500 m.
4. Sandstones within channels, lobes and levee facies have all preserved significant amounts of primary porosity and all of them have an IGV of 27.5% or higher.
5. Cementation is minor and although some samples have kaolinite, chlorite and hematite cements that obstruct pore throats, they are probably not present in large enough quantities to present a major hindrance to fluid flow.
6. The sample from the levee facies sands appears to have been more compacted and this combined with these sands being the thinnest (on the scale of cms) and the least laterally continuous of all the facies, indicate that these sands make the least favorable reservoirs.

Chapter Four: The Evolution of the Tobago Forearc Basin

The objective of this chapter is to define the timing and structural history of the Tobago Basin and its relationship to the larger accretionary prism processes, as well as to interpret the origin of two major stratigraphic units—the Scotland Formation (lower to middle Eocene (possibly Oligocene) and the Oceanic Formation (middle Eocene to middle Miocene)—which fill the basin. The Scotland and the Oceanic Formations comprise known hydrocarbon reservoir and seal units, respectively, in the basin. Understanding their individual depositional and post-depositional histories will in turn enable a better understanding of younger Tertiary units of similar setting in this basin.

The Oceanic Formation

The Oceanic Formation was first recognized in the late 1800's by Jukes-Brown and Harrison (1890), who produced a detailed map of the geology of Barbados and identified the Coral Rock, the Oceanic Series, the Scotland Series, and the Joes River Formation. They interpreted the Oceanic Series as abyssal sediments that had been raised to their current position by tectonic uplift.

Until the late 1970's, because most geological research on Barbados centered on hydrocarbon exploration, the clastic succession of the Scotland Formation had been extensively studied and the Oceanic Formation was largely ignored. This situation changed when Robert Speed began in the early 1980's to investigate the structure and sedimentation of the Barbados Accretionary Prism. Speed described the Oceanic Formation as consisting of calcareous clays and muds and marls with volcanic ash layers (Speed and Torrini, 1989, Speed 1991, 1994). Likewise, micro-paleontologic analysis of the Oceanic units by Saunders et al. (1984) led to the conclusion that these sediments had been deposited in 2,000 to 4,000 m of water.

The highest point of the island, is 336 m above sea level, is located at Mount Hillaby, St. Thomas. At this location there are exposures of the Oceanic Formation. East of this location the Scotland Formation is exposed. According to work carried out on the limestone terraces on Barbados, the island is uplifting in the Quaternary at a rate of 0.44 mm/yr (Taylor and Mann, 1991). Assuming a constant rate of rise of 0.44 mm/yr show that simple uplift could have raised the Oceanic Formation 4,840 m since middle Miocene times. The vertical rise of the Barbados Ridge due to underplating can account for emergence of the Oceanic Formation, with no need for lateral translation by thrust faulting.

This is consistent with the failure to find nappe geometries in seismic reflection profiles in the Forearc Basin sediments (the Oceanic Formation). This observation lends support to the hypothesis that the Oceanic Formation was deposited in situ on top of the accretionary prism sediments.

DATA

The primary data used in this study are a 2D seismic data set measured on 10-km spacing of lines and traces, covering approximately 450 km^2 (Figure 4.1). The data, which image up to 12 seconds of strata, have a good signal-to-noise ratio and are the most complete seismic coverage of an accretionary forearc basin in the world. They were obtained from two industry seismic surveys—one shot in 1979 by Mobil and the other shot in 1999 by ConocoPhillips. Parameters from the 1979 data are not known. The data measured in 1999 were shot using 38-inch air guns as the energy source at a depth of 6 m, with a shot interval of 25 m. The streamer length was 6,000 m, and streamers were towed at a depth of 8 to 9 m below the vessel. The sample rate was 2 milliseconds. Data were acquired predominantly over the Barbados Ridge and the east part of the Tobago Basin (Figure 4.1). Also available for interpretation is a single, long, regional seismic line

that extends 180 km from the Atlantic Abyssal Plain in the east, westward to the east flank of the Lesser Antilles Island Arc High (Figure 4.1). Two additional lines are contained in the data set that trend north-northeast from the north-coast marine area of Trinidad, paralleling the east and west coasts of the island of Tobago, extending northward and paralleling the east and west flanks of the Barbados Ridge. The two additional north-south-oriented, southern regional lines intersect the long east-west-trending regional line. These southern regional lines allow a tie to well data southward in the north-coast marine area of Trinidad (Figure 4.1).

Published age data from wells on the southernmost margin of the Tobago Basin were used for chronostratigraphic control on the younger, Tertiary parts of the stratigraphic section (Robertson and Burke, 1989). However, little information exists in the public domain regarding the age of fill to the north. This lack of data meant that we had to rely on published accounts of stratigraphic ages, as well as personal communication with industry colleagues who had access to proprietary information.

STRATIGRAPHIC FRAMEWORK ONSHORE TO OFFSHORE

The layered Tobago Forearc Basin units (Figure 4.2) are equivalent to the Oceanic Formation recognized in outcrop on the island's eastern side. Although within the TFB it is believed that this unit ranges from Middle Eocene to Upper Miocene in age, onshore units are at youngest Middle Miocene in age (Barker and Poole, 1982) and are believed to have been deposited in water depths between 2000 to 4000 m based on foraminiferal data (Saunders, 1984). The Middle Miocene marks the initiation of TFB closure and the emergence of the Barbados Ridge. Based on onshore analyses, these rocks are interpreted throughout the region as deep marine pelagic clays and marls which are interbedded with volcanic ash deposits (Speed, 1989, 1994). The entire unit thins to the west onto the Lesser Antilles Island Arc high and post Mid-Miocene unconformity sediments thin onto the Barbados Ridge. Sediments below the Mid-Miocene unconformity drape over the Barbados Ridge and extend into the zone of piggyback basins. The seismic character of this unit is that of layered, continuous reflectors with minimal deformation by small-scale normal faulting. This seismic character is expected as the pelagic deposits are interbedded with volcanic ash layers and are locally cut by normal faults in outcrop.

Scotland Formation

The Scotland Formation is dated in outcrop as Lower Eocene in age and includes the oldest rocks exposed on the island. This unit thickens onshore into a thick, (up to 2800 m), succession of sands and clays comprised of very coarse grained turbidites and leveed channels deposits, with a conglomerate lag at the base of some large channels indicating a high energy erosive system. In seismic data, this formation has been equated with the western portion of the Barbados Accretionary Prism sediments and shows up as

highly discontinuous, bright amplitude reflectors. Within the Tobago Forearc Basin, channels and channel fill facies have been identified that suggest that this basin was once a fairway for clastic sediment deposition (Figure 4.3).

Joes River Formation

The Joes River Formation is dark gray to black in color, slickensided, often oil soaked with a distinct bituminous odor. It is comprised of a mélange of structureless clays, sands, and scattered limestone rafts (Poole and Barker, 1980). It has been interpreted to be emplaced as diapiric shales and extrusive muds. Such mobile shale processes are common in accretionary prism settings (Wood, 2004). Mud volcanoes today are most active on the island of Trinidad and its offshore regions (Brooks and others, 2004). Offshore, evidence of continued mud volcano eruption indicates that this is an ongoing process triggered by over-pressurization created by compressional forces within the prism. On the island, this unit is intrusive and post-dates deposition of the Oceanic Formation. The timing of the intrusion of the Joes River Formation is based on observations by Speed (1991) that the Joes River Formation is mushroomed beneath the Oceanic Formation. This phenomenon suggests that although the matrix has been dated with pollen to be Paleocene to Middle Eocene (Speed, 1991) the timing of the deformation and emplacement of the diapirs is after the Oceanic Formation was deposited. The Joes River Formation on Barbados is interpreted as a complex of paleo-mud volcanoes which were extruded in response to the compressional regional setting. They pre-date the localized extensional faulting that characterizes the crest of the Barbados Ridge. Both offshore and onshore, diapiric shale and extrusive muds are isolated pods and more laterally extensive mounds. The unconsolidated nature of the unit makes it prone to mass wasting. These features can be easily identified in seismic reflection profile by the chaotic response of the subsurface material and capped by the spectacular extrusion of mud at the seafloor.

STRUCTURAL FRAMEWORK OF THE BARBADOS ACCRETIONARY PRISM

Convergent margin settings tend to be structurally complex regions of the world, characterized by shortening and local extension or strike-slip tectonics. Deformation involves mud-rich sediments which are tectonized as they dewater, using fluid flow that can cause mud volcanism (Moore, 2001). The Barbados Accretionary Prism (BAP) region is no exception to typical convergent tectonic margins. Although the overall setting of the study area is convergent, as this study documents, there is large-scale, normal faulting that occurs on a sub-regional scale. The west and east margins of the accretionary prism are bounded by thrust faults that dip towards the west and east, respectively (Figure 4.4). The Barbados Ridge, the westernmost high of the prism, is dominated by northwest-southeast-trending normal faults (Figure 4.4, Figure 4.5).

The prism is characterized by five structural regions: the zone of initial accretion, the zone of stabilization, the zone of piggyback basins, the Barbados Ridge, and the Inner Forearc Deformation Front (Figure 4.5) which includes the Tobago Forearc Basin—each having its own unique structural characteristics (Brown and Westbrook, 1987). Data availability did not allow for much analysis of the zone of initial accretion. The remaining regions are summarized in the following section on the basis of observations by Brown and Westbrook (1987), as well as those of the authors.

Zone of Initial Accretion

The zone of initial accretion, composed of an imbricate fan of east-facing thrust faults, marks the youngest phase of deformation in the prism. Because it is the zone where previously undeformed sediments are first accreted to the prism, it is the starting point or *initiation* of accretion. These thrusts all sole into a décollement, below which Atlantic Abyssal Plain sediments are passing relatively undeformed beneath the prism proper, to be ultimately subducted along with the downgoing Atlantic Plate.

Zone of Initial Stabilization

Deformation in the zone of initial stabilization appears less intense than in areas to the east and west. This zone marks a transition in the direction of thrusting in the prism; to the east of this zone, thrusts and thrust sheets dip westward, while to the west of this zone, thrusts and thrust sheets dip eastward (Figure 4.5).

Zone of Piggyback Basins

The zone of piggyback basins is a region in which several asymmetric basins have formed on the eastern side of thrusts that dip toward the west. Huyghe et al. (1999) called this zone “the arcward piggyback basins.” These basins are filled with Holocene sediments derived from the Venezuela-Trinidad margin to the south, as well as from pelagic deposition and sediments transported on offshore currents from regions along the Amazon shelf. Several canyons and channels cut these basins, as well as form linkages across uplifts that separate the basins. Dropcore measured by Faugeres et al., (1993) shows that the most recent fill of the basin is prevalently thin, silty to sandy sequences; however, some thick, sandy sequences are present. The clay portion makes up 10 to 50% of the succession and is primarily illite with minor smectite (Faugeres et al., 1993).

Sandy material is primarily quartz (75–95%) with minor lithic grains, micas, and heavy minerals (Faugeres et al., 1993).

The largest of the prism's many piggyback basins, the Barbados Basin, was the focus of a 2001 exploration well, the Sandy Lane #1 (Figure 4.1). A near-seafloor dredge sample taken from the basin as part of this effort recovered fine-grained quartzose sandstone. These sediments were measured from what was interpreted on the basis of seismic morphology to be a deposit of deep-marine lobate sediments, internally composed of tabular sheet sands (Dolan et al., 2004). These results suggest that even in this confined, tectonically active basin setting, reservoir quality sands are deposited as fans and sheet sands in very deep water.

Barbados Ridge

The Barbados Ridge is the topographically highest part of the accretionary prism and the region along which the island of Barbados is emergent. The island of Barbados is rising at a rate of approximately 0.44 mm/yr (Taylor and Mann (1991). The arcuate ridge, subparallel to the Lesser Antilles Island Arc (Figure 4.1), is formed as accretionary prism material moves westward and interacts with the string basement of the Caribbean Plate, moving up and over the metamorphic basement. In some cases, this material is overriding the lowermost Tobago Forearc Basin sediments, which are deformed by these movements. As a result, the west side of the Barbados Ridge is characterized by large, west-facing thrust faults, while a number of northwest-southeast-striking normal faults dominate the crestal region (Figure 4.6).

The east margin of the Barbados Ridge is characterized by a step-like succession of normal faults. The largest of these, the Barbados Fault, bounds the east coast of the island of Barbados (Figure 4.6). This fault has more than 3 km of down-to-the-east vertical displacement. Underplating of forearc basin and accretionary prism sediments, as well as the presence of basement ridges (Brown

and Westbrook, 1987), are thought to be responsible for the 3,000 m of rise on the prism's interior. Brown and Westbrook (1987) identified the presence of WNW-ESE Atlantic basement ridges beneath the prism using long-range side-scan sonar images and seabeam bathymetry. Their investigations show a correlation between the orientation of these basement ridges and the structural features of the prism. The west- and east-facing thrust faults and associated piggyback basins and sediment ridges are oriented roughly parallel to the deformation front. However, at oblique angles to these roughly north-south features are the NW-SE-trending extensional faults of the Barbados Ridge, which have a similar orientation to that of these basement ridges. Compression and thrust faulting occur on the west side of the Barbados Ridge, where basement ridges act as a buttress to westward movement, causing thrusting and uplift to occur.

Inner Forearc Deformation Front

The Inner Forearc Deformation Front (IFDF) delimits the east margin of the Tobago Forearc Basin and forms the boundary between the highly deformed sediments of the accretionary prism and the relatively undeformed sediments of the Tobago Forearc Basin (Figures 4.4 and 4.6). It is characterized by east dipping thrust faults that are the result of interaction between the downgoing Atlantic Plate and the strong crystalline basement.

Tobago Forearc Basin

The Tobago Forearc Basin, filled with as much as 12 km of sediment, shows little evidence of deformation at its center (Figure 4.6). Several small-scale normal faults along the west and north margins of the basin, confined to the youngest part of the section have very minor throw and appear to terminate at a common shallow horizon. It is not uncommon for normal faults to occur on the stable flanks of forearc basins, and it has been speculated that they form as a

result of extension caused by flexural loading of the crust in response to encroaching fold belts (Harding and Lowell, 1979; Harding and Tuminas, 1989). Dickinson (1995) noted that these faults may act to step the basin downward from the elevated island arc high as localized extension occurs across the forearc belt. The large Barbados Fault (previously discussed) is an example of one of these faults.

TIMING AND PROCESSES IN THE EVOLUTION OF THE TOBAGO BASIN

Observations from Seismic Data

The Tobago Basin is the largest sedimentary accumulation within the basins of Barbados Accretionary Prism system. Nine horizons were mapped across the basin, and six fill units were identified. Isochron maps created on these units show that the basin has evolved from a proto-Tobago Basin that was quite broad, into segments that are the present-day Tobago Forearc Basin (TFB) and more eastward piggyback basins of the Barbados Ridge. Pre-Eocene-age TFB sediments (Unit One of Figure 4.6 and Figure 4.7a) are thickest in the northeast parts of the present-day basin, whereas Eocene to early-Oligocene-age sediments (Unit Two of Figures 4.6 and 4.7b) were deposited within a more central depocenter. This later unit is found south of the older depositional center, suggesting a migration of subsidence to the south part of the basin. During the early Oligocene to early Miocene (Unit Three of Figures 4.6 and 4.7c), sediments were deposited across a broad area, extending as far as the present-day zone of piggyback basins. The thickest sediment deposition at that time was in the southeast part of the basin, adjacent to the present-day Inner Forearc Deformation Front. Sediments deposited after initiation of the closure of the TFB and the emergence of the Barbados Ridge, were confined to a smaller TFB. Isochron

maps of the lower to upper Miocene units (Unit Four of Figures 4.6 and Figure 4.8a) show continued thickening in the southwest part of the TFB, suggesting that subsidence in southwest parts of the basin continued well into late Miocene time.) and increased subsidence and thickening of strata in the southwest part of the basin continued through late Miocene (Unit Five of Figures 4.6 and 4.8b) times until the basin attained the shape that we see represented in the Plio-Pleistocene fill (Unit Six of Figures 4.6 and 4.8c). By Pliocene time, sediments were thickening along a narrow, well-defined TFB, whose east margin is limited by thrusting of the IFDF.

IMPLICATIONS

The concept of a large proto-Tobago Basin is not new. Speed and Torrini (1989) acknowledged that the TFB has experienced shortening over time and noted the shifting depocenter within the basin (Speed and Torrini, 1989; Torrini and Speed, 1989). However, Speed thought that the layered sediments of the TFB (Oceanic Formation) and those of the western BAP (Scotland Formation) were in unconformable contact along thrusted nappes (Speed, 1982, 1983, 1991). Observations from seismic data in this study reveal no such unconformable relationship. We propose, on the other hand, a greater lateral extent of the TFB sediments than previous authors have acknowledged, concurring with Pudsey (1982) and Poole and Barker (1980), who proposed a conformable relationship of TFB sediments and the western BAP sediments versus the allochthonous emplacement of TFB sediments proposed by Speed.

Origin of the Oceanic Formation

The Oceanic Formation is composed of calcareous clays and muds and marls along with volcanic ash layers (Speed and Torrini, 1989; Speed 1991,

1994). The origin of the Oceanic Formation has been debated for more than two decades, and two distinct hypotheses persist that offer opposing explanations.

The first hypothesis, introduced by Speed (1982), puts forward an Oceanic Formation that was deposited within the proto-Tobago Forearc Basin and that has subsequently been thrust more than 20 km eastward to its present position (Figure 4.9). This hypothesis seeks to reconcile the potential age overlap of the Oceanic and Scotland Formations, the latter of which has been dated as young as Oligocene in age (Baldwin, 1986). Speed interpreted the Oceanic Formation as having a lower section that exhibited nappe geometries as a result of eastward transport of the lower section and an upper section that was a single, undisrupted sheet The timing of the emplacement of this upper sheet is said to be late Miocene or Pliocene, when the sheet was thought to have fully covered the underlying Scotland Formation. Speed (1982) used erosion prior to deposition of the Pleistocene reef to explain thinning of the sheet of the Oceanic Formation that occurs over the island of Barbados.

The second hypothesis, proposed by Pudsey (1982), suggests that the Oceanic Formation is an in situ deposit that has been tectonically uplifted along with the Barbados Ridge. Poole and Barker's (1980) geological map of Barbados features a generalized vertical section in which the Oceanic Formation conformably overlies the Scotland Formation of Barbados. These researchers postulated that the Oceanic Formation formed in situ after the rapid submergence of the island and surrounding areas. The Oceanic Formation has been constrained to deposition in 2,000 to 4,000 m of water (Saunders et al., 1984). To accommodate this depth of deposition, Poole and Barker (1982) invoked a subsidence and re-submergence of the island of at least 2,000 m, to allow for deposition of the sediments, followed by a reemergence.

Observations from Seismic Data

In seismic data, these Forearc Basin Sediments show simple onlap relationships with the underlying crystalline basement of the Lesser Antilles Island Arc (Figure 4.5). Time-equivalent units along the east flank of the Tobago Basin show simple onlap relationships onto the accretionary prism sediments. Although there is some deformation of Tobago Forearc Basin units, no nappe geometries or duplex relationships as reported by previous workers (Torrini and Speed, 1989; Speed and Torrini, 1989; Speed and Larue (1982) are observed in the seismic data. The presence of channels, observed on seismic data, within the TFB proper suggests episodes of clastic deposition occurred within the basin (Figure 4.3).

Reconstruction of the Tobago Basin

The closure of the Tobago Basin, as recorded by the sedimentary fill, shows that the basin has steadily decreased in size since the mid-Miocene (Figure 4.10a-e). The earliest stage of development was when Eocene- and possibly Cretaceous-age sediments were deposited into the basin from a southern sediment source, and in lesser amounts from the Lesser Antilles Island Arc (LAIA) (Figure 4.10a). The direction of influx from the LAIA is shown with arrows pointing toward the Tobago Basin. These units fill the deepest part of the basin, immediately west of the thrust front. Sediments are also delivered to the Atlantic Abyssal Plain and are incorporated into the growing accretionary prism at the Outer Deformation Front (ODF). Sediments are accreted adjacent to the basin where the downgoing Atlantic plate (AP) is subducting beneath the Caribbean plate (CCB).

Oligocene-age sediments are deposited over a broadening, deep, Tobago Basin. Sediments of the Barbados Accretionary Prism (BAP) continue to be accreted beneath the Tobago Basin and sediments deposited on the Atlantic Abyssal Plain are thrust beneath older BAP sediments. This latter action causes the prism to broaden and thicken, particularly at the thrust front. During this time, sedimentation within the Tobago Basin keeps pace with the increasing height of the prism, eventually surpassing the prism growth and depositing sediments over the prism (Figure 4.10b). During the Early to middle Miocene, sediments accumulate across the entire area of the very broad Tobago Basin. The most regionally extensive stratigraphic surface, the Mid-Miocene Unconformity, developed in the basin at this time (Figure 4.10c).

Following the extensive erosional event of the Middle Miocene, the BAP continued to thicken through the processes of accretion and underplating. The Barbados Ridge became emergent, uplifted through ongoing accretion of sediments due to increased thrusting and underplating (Figure 4.10d). The Caribbean Plate continued to inhibit the westward movements of the Atlantic Plate prism sediments causing increased offscraping and accretion of sediments, which caused the broad pre-Middle Miocene Tobago Basin to become segmented into several sub-basins.

The Tobago Basin continued to diminish in size to the present, and since the Late Miocene, Tobago Basin sediments have accumulated in a much narrower area than the pre-late Miocene sediments (Figure 4.10e). Today, subduction of the Atlantic plate is ongoing and the Barbados Ridge continues to rise as a result of ongoing underplating. This process has led to extensive crestal faulting along the Barbados Ridge creating steep slopes and resulting instability along the ridge. The largest of these extensional normal faults is the Barbados Fault. This fault,

located off the east coast of the modern island of Barbados see Fig. 4.4), has played a significant role in the emergence of the island.

In Eocene times the proto-Tobago Basin was originally very broad with ill-defined margins. Data from Woodbourne oilfield onshore Barbados support this extended east margin of the Tobago Basin, showing today that the basin deposits extended eastward, well beyond the basin's present margins. However, today this older basin has been segmented into the present-day Tobago Basin and several smaller, more eastwardly located piggyback basins with well-defined margins. The largest of these segmented basins is the Barbados Basin, which lies to the east of the Barbados Ridge. This ridge is composed partly of Tobago Forearc Basin (TFB) sediments, consisting of clastic deep-water sands of the Scotland Formation and the deep pelagic muds that overlie them (Oceanic Formation). It is herein interpreted that the Barbados Ridge was once much deeper than it is today. Data supporting this observation include (1) lower to upper Miocene deep-water units stratigraphically draping the Barbados Ridge and (2) biostratigraphic data on the aforementioned deposits that compose the modern, subaerially exposed Barbados Ridge, which indicate deposition in water depths of 2,000 to 4,000 m (Saunders et al., 1985) (Chaderton, 2005; Chaderton and Wood, 2006). Both observations suggest a significant uplift occurring throughout the Tertiary in the interior of the accretionary prism.

Although two hypotheses have been put forward to explain the occurrence of the Oceanic Formation onshore Barbados, only one of these hypotheses is supported by the data and all of the geological observations contained in this dissertation. Data suggest that the channelized deposits of the Scotland Formation were deposited within the TFB in its present position and the Oceanic Formation was deposited conformably on top.

The observation of channel geometries within the TFB along with the presence of a regional depocenter during Eocene to Oligocene times suggest a clastic sediment fairway within the broader proto-Tobago Forearc Basin. These sediments would then have been incorporated into the present day western BAP on the eastern margin of the TFB. As the TFB closed the sediments on the basin margin became uplifted and deformed. These observations helped us to expand upon the premise of the second hypothesis. Deepwater background sedimentation is pelagic mud and marl such as those that comprise the Oceanic Formation (that appear layered in seismic reflection profiles). Upon initiation of clastic sedimentation within the basin, a mud-rich submarine fan system was deposited within the broader TFB (Scotland Formation). When clastic sedimentation within the Tobago Forearc Basin ceased, pelagic sedimentation dominated once more (Oceanic Formation) (Figure 4.11). Continued closure of the basin and underplating of sediments uplifted the Scotland and Oceanic Members to their present day position onshore Barbados.

Both of these sedimentary packages were later uplifted with the rest of the Barbados Ridge to form the newly defined margin of the shrinking Tobago Basin.

CONCLUSIONS

The Tobago Forearc Basin was broader prior to the Middle Miocene than it is in the present day. It has been segmented into smaller basins with the TFB being the largest.

The Oceanic Formation was deposited in situ and not thrust into place over the Scotland Formation.

Chapter 5: Conclusions

SEDIMENTATION AND HYDROCARBON EXPLORATION WITHIN FOREARC BASINS

The study area is a classic forearc basin depositional setting. Hydrocarbons have been produced economically from some forearc basins such as Cook Inlet, Alaska (Bruhn et al., 2000; Clough et al., 2001), and the ancient Great Valley forearc basin in California (Rentschler, 1985; Vermeesch et al., 2006). In addition to conventional hydrocarbon production, there is thought to be up to 245 tcf of gas available in the unconventional resource of coal bed methane in Cook Inlet, Alaska (Clough et al., 2001; Montgomery and Barker, 2003).

The re-interpretation of the Scotland Formation as a forearc basin deposit has implications for hydrocarbon exploration onshore and offshore Barbados. It has been accepted for several years that the oil and gas production onshore Barbados is the only example of successful hydrocarbon production from true accretionary prism sediments. The new model presented in this research re-defines the depositional setting of the reservoirs and classifies them as forearc basin plays similar to Alaska or California.

Sedimentation within forearc basins is a combination of deposition by turbidity currents travelling parallel to the volcanic arc along the basin axis or travelling perpendicular to the volcanic arc. In the case of island arcs, the sediment sources are usually localized to the volcanic islands (Moore et al., 1980). In the case of the Lesser Antilles volcaniclastic sediments are interbedded with the longitudinal input from the South American continent.

Clastic sediments within the Tobago Forearc Basin (TFB) were transported parallel to the Lesser Antilles Island Arc as evidenced from seismic reflectors prograding from south to north and channels that are visible in the strike (east to west) direction across the basin. Sediment input from the volcanic arc was minor, as evident from the small amounts of volcanic rock fragments that have been identified in thin section.

Pudsey, (1982) interpreted smectite and kaolinite rich clays within the Scotland Formation as ash fall deposits from the volcanic island arc. Punch, (2004) and Kasper and Larue, (1986) also found a minor volcanic input to the Scotland Formation sediments. The source of the clastic Scotland Formation sediments was the proto-Orinoco which drained from northern South America during Eocene to Oligocene times and deposited sediment into d the proto-TFB.

As the Orinoco River shifted eastward, the main source of clastic sedimentation to the TFB ceased and pelagic accumulation became dominant as clastic sedimentation lessened. In the TFB-BAP region, the Oceanic Formation is the unit that is comprised of pelagic muds and marls, with interbedded volcanic ash layers. The reinterpretation of the Scotland Formation means that both the Oceanic Formation and the Scotland Formation are now both interpreted to be forearc basin sediments.

Following deposition in the basin of clastic turbidites of the Scotland Formation, the post-Oligocene Oceanic Formation blanketed the basin. Several researchers have noted some confusion regarding the age of the Oceanic Formation (Speed, 1982; Pudsey, 1982; Poole and Barker, 1982). It is probable that the Scotland and the Oceanic formations have an inter-fingering relationship and thus the reason for the age discrepancies that have puzzled researchers in the region for decades.

The Cook Inlet, a structurally complex forearc basin, is located between the Alaska Range-Aleutian Volcanic Arc to the northwest and the Chugach-Kenai accretionary prism to the south. The basin is bounded by active faults and has a number of tight asymmetrical folds that form hydrocarbon traps. These folds are associated with reverse faults (Montgomery and Barker, 2003). Although the distant sedimentary source of the reservoir rocks in the Barbados study area differentiates the TFB fill from most forearc basins, the active faults in the area may form traps similar to those in the Cook Inlet. In Barbados, similar traps may exist within the BAP region along the Barbados

Ridge high. The traps would be associated with the large thrust faults that create the ridges and mini basins of the Zone of Piggy Back Basins (Figures 4.3 and 4.10).

The implications of the interpretation of the Scotland Formation as a forearc basin are that depositional lobes should be elongated parallel to the major structural highs at the time of deposition. Therefore, it is speculated herein that coarse-grained clastic deep water deposits, similar to those seen in outcrop and in seismic to the south, may exist to along the trend (to the north and south) of the Barbados Ridge and to the west within the Tobago Basin proper. If this is correct, the likelihood of finding deposits similar to or time equivalent to the Scotland formation decreases eastward. It is important to note that within the piggyback basins of the BAP, the Miocene age and younger, sand and shale successions have similar architecture and geometries.

Hydrocarbon exploration of the BAP region must therefore take into account two distinctive play types:

1. The raised forearc basin reservoir plays that are located along the high of the Barbados Ridge and the eastern margin of the present day TFB.
2. The younger piggyback basin reservoir plays that have been deposited within these mini-basins that have formed on the BAP.

The complex structuring of a convergent margin setting creates folds and faults that may give rise to hydrocarbon traps. However active faults may provide permeable pathways that cause leakage (Dolan, et al., 2004). Stratigraphic heterogeneity is complex as the potential reservoirs are highly channelized (Chapter Two, this volume).

The interpretation of the Scotland Formation as a forearc basin-deposited reservoir is a simpler model for the evolution of the BAP-TFB petroleum system. However the entire petroleum system is still poorly understood. The source rock for the hydrocarbons does not outcrop onshore and has not been imaged by seismic reflection profiles. T thermal maturation history is also poorly understood as accretionary prisms are understood to be regions of low heat flow which is not conducive to hydrocarbon maturation. Hydrocarbon exploration within the TFB and BAP region will remain risky until additional wells are drilled, 3D seismic is shot and exploration and development in the region matures.

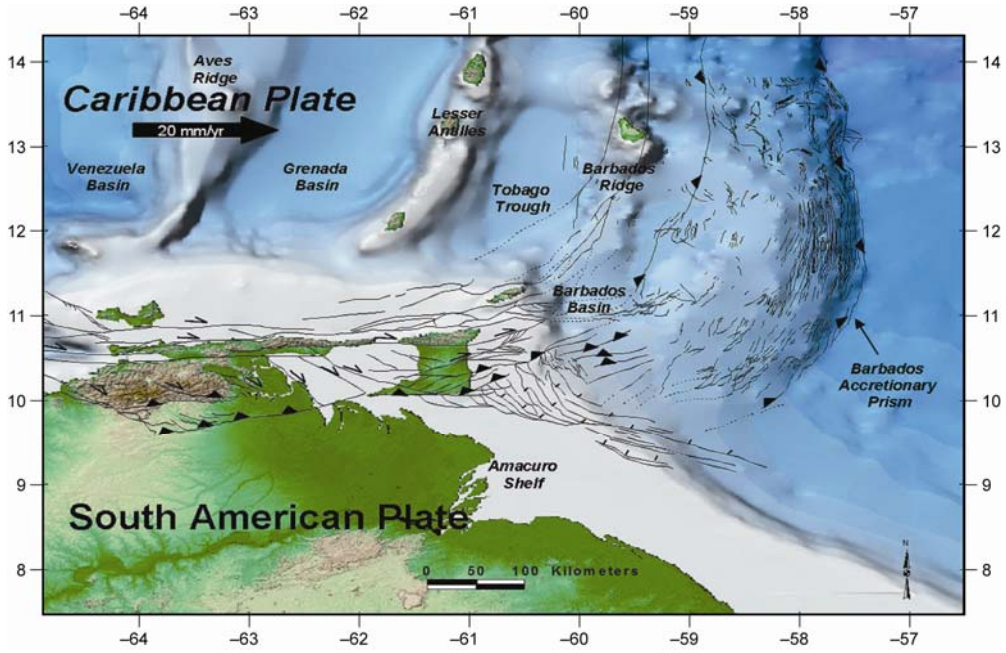

Figure 1.1: Base map showing location of study area within the southeastern margin of the Caribbean Plate BAP. Direction of plate movement based on GPS vectors (Weber 2001). Faults were mapped on seafloor bathymetry based on the work of Brown and Westbrook (1987) and Robertson and Burke (1989).

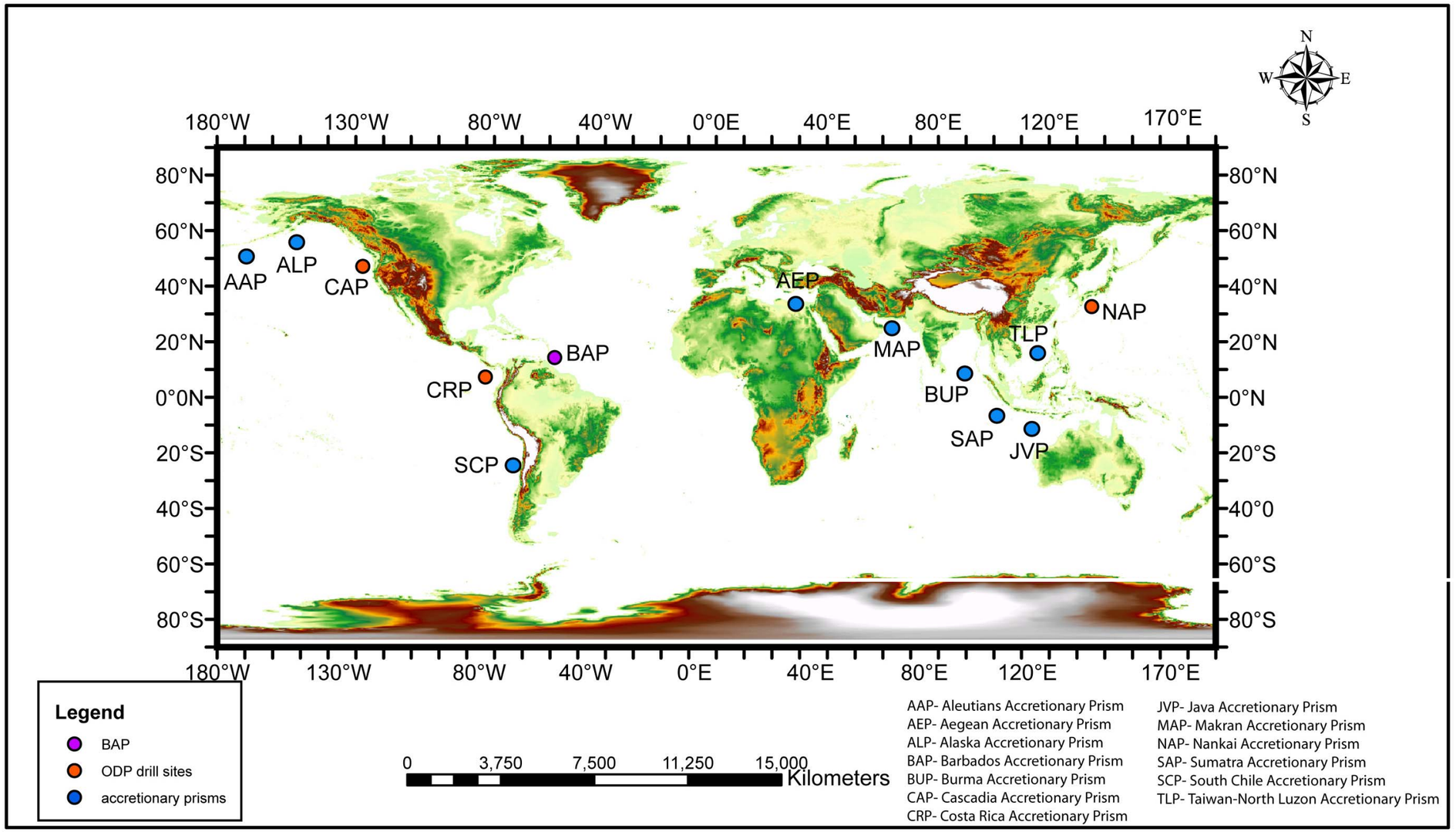

Figure 1.2: Convergent margins around the world that are experiencing net accretion and have an accretionary prism that is currently growing. Oversized Plate (11x17) requires plotter or printer with tabloid printing.

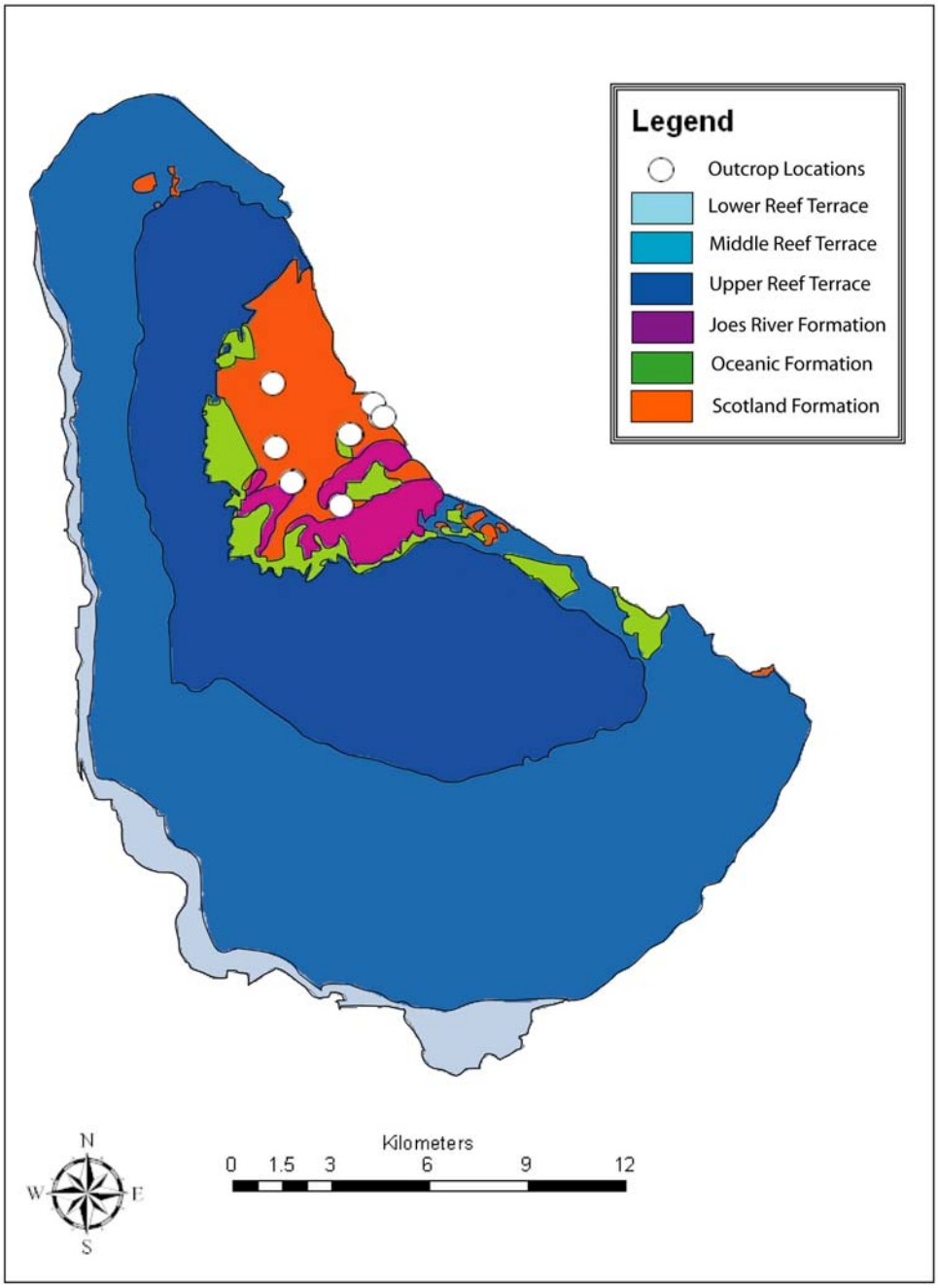

Figure 1.3 Geological Map of Barbados showing the onshore geology and the outcrop locations within the study area. Modified from Poole and Baker (1980).

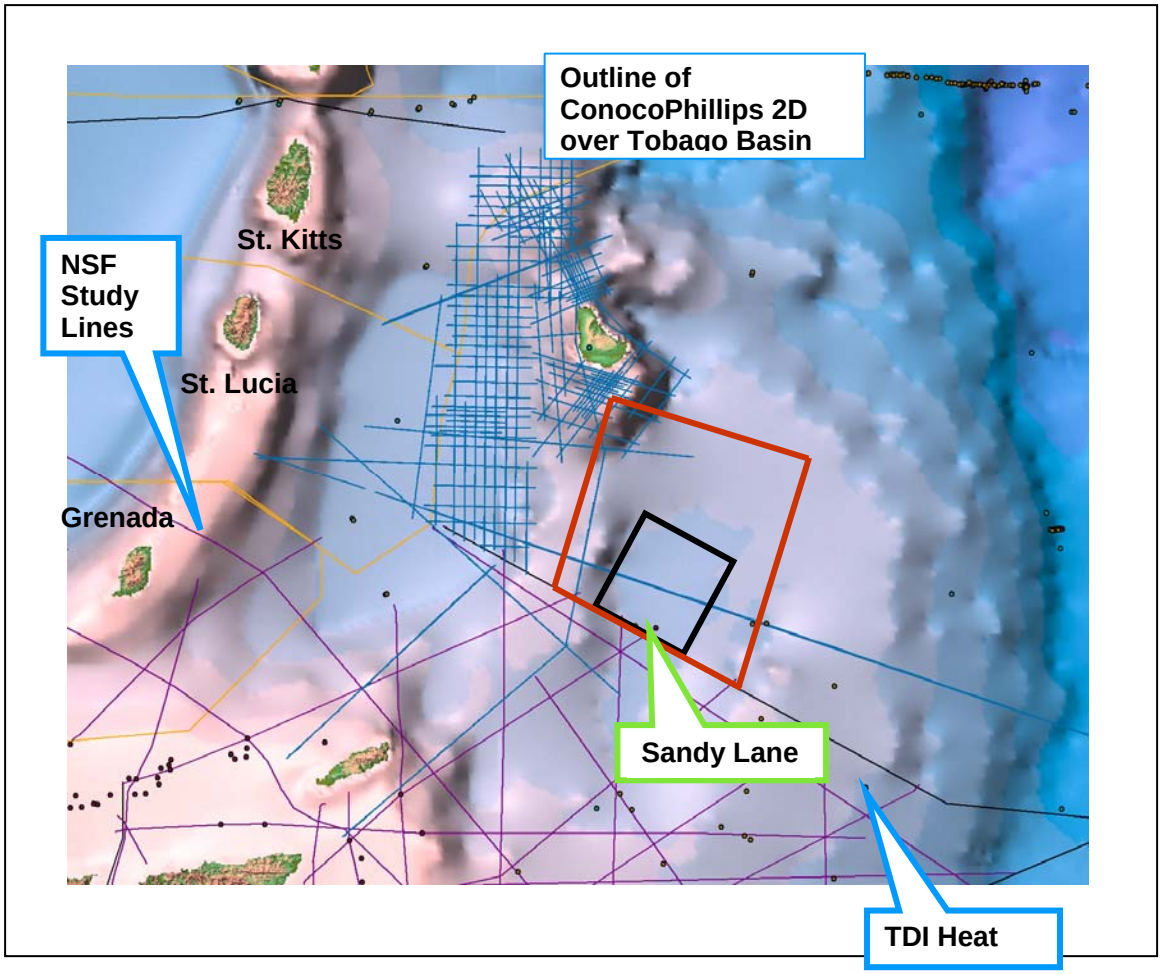

Figure 1.4: Data sets that are located in the southern BAP region. The only data shown on this map that permission has been granted for integration for this study are the blue lines of the ConocoPhilips 2D survey.

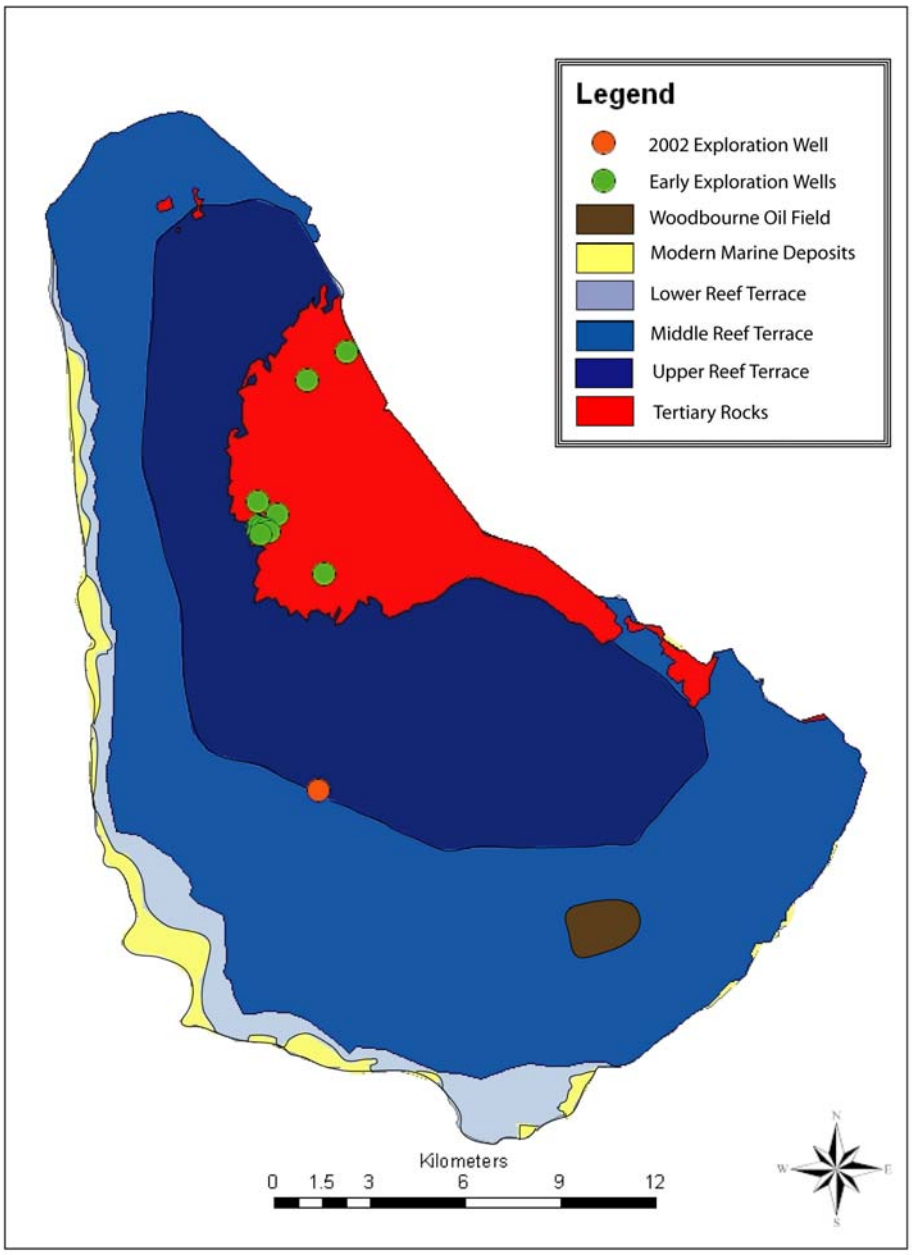

Figure 2.1: Map of Barbados showing the portion of the island (shown in red) where the Pleistocene limestone cap has been eroded to expose the underlying Tertiary sediments Modified from Pool and Barker, (1980).

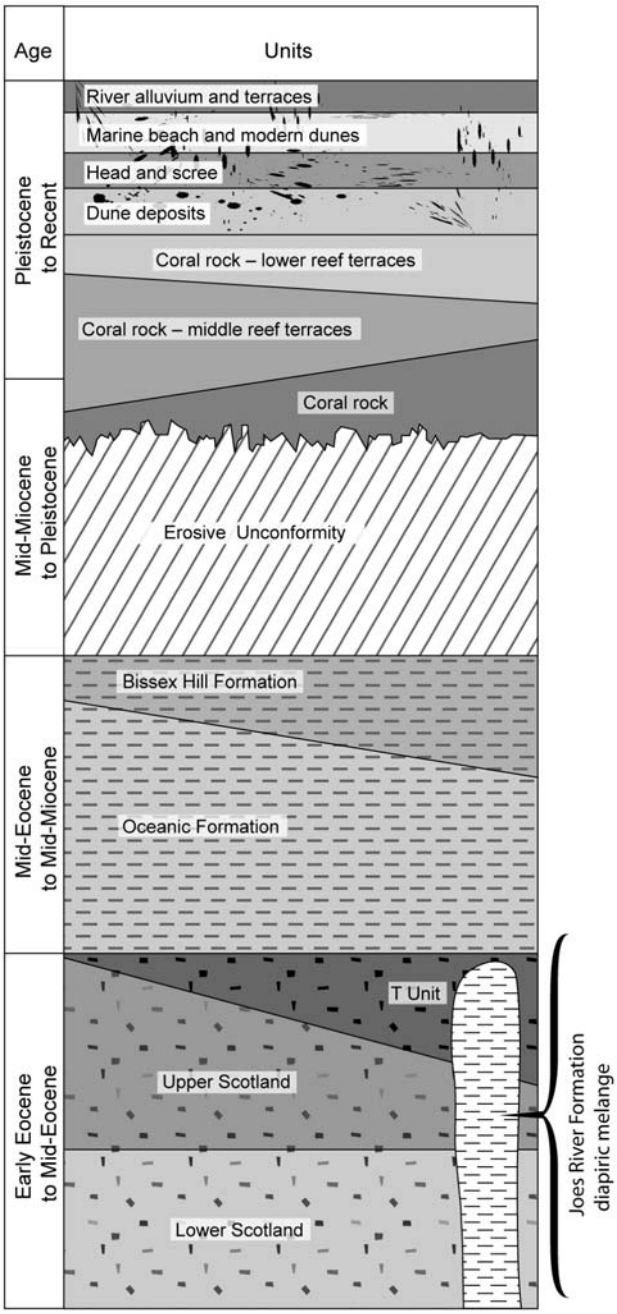

Figure 2.2: Generalized vertical section of the formations identified onshore Barbados after Poole and Barker, 1980.

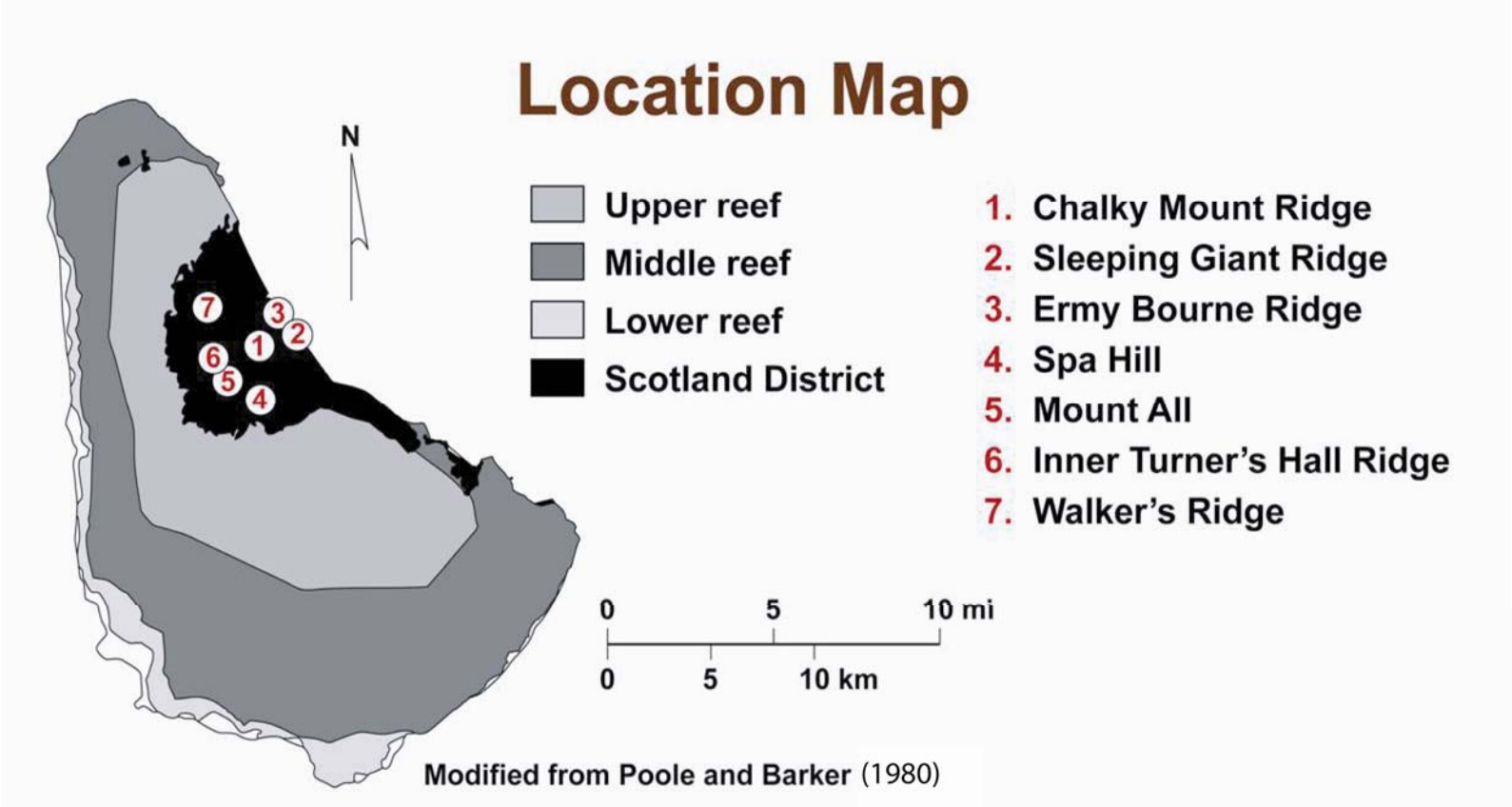

Figure 2.3: Map of Barbados showing the outcrop locations within the study area.

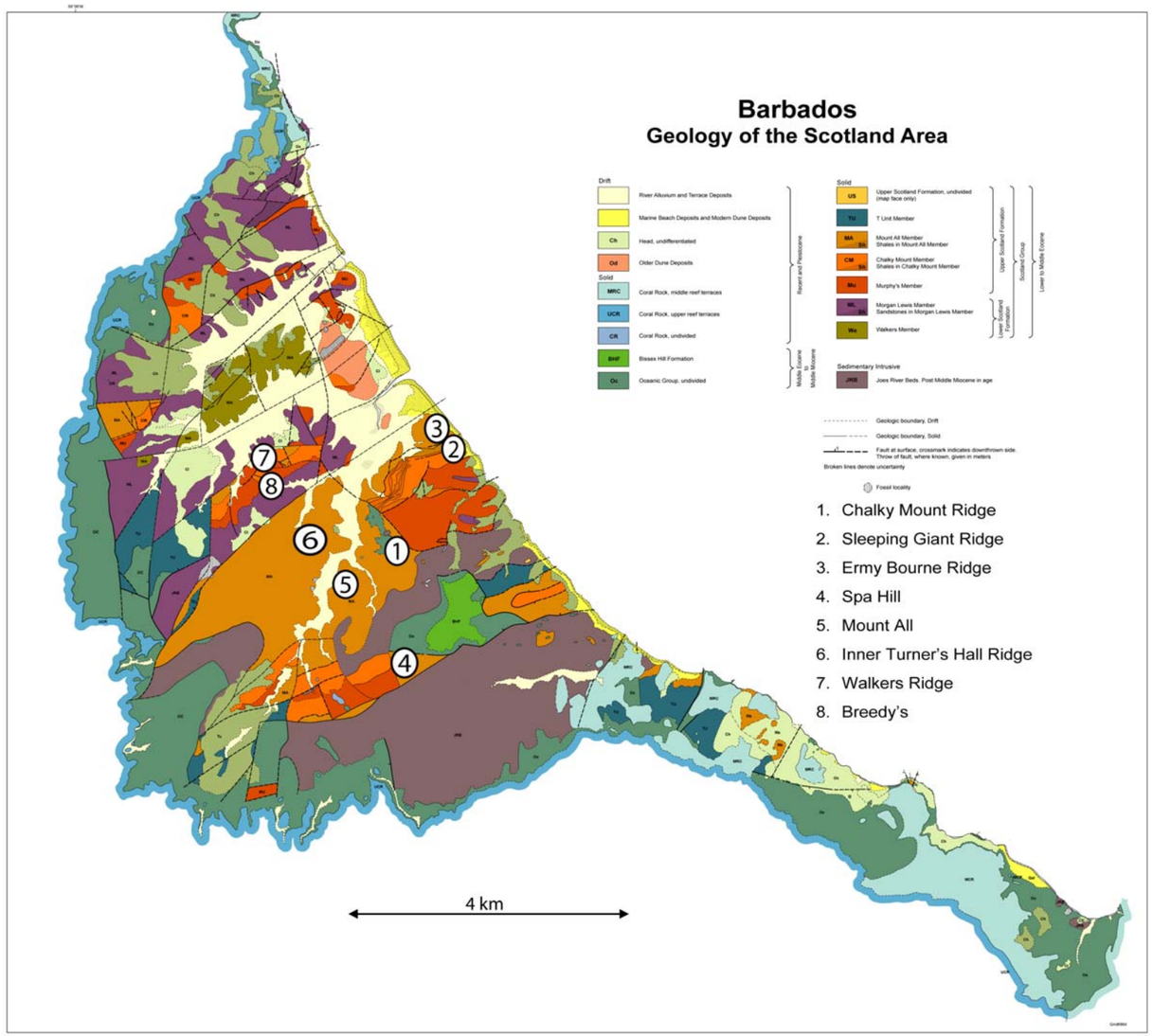

Figure 2.4: Detailed Geological map of the Scotland District. Oversized Plate (11x17) requires plotter or printer with tabloid printing.

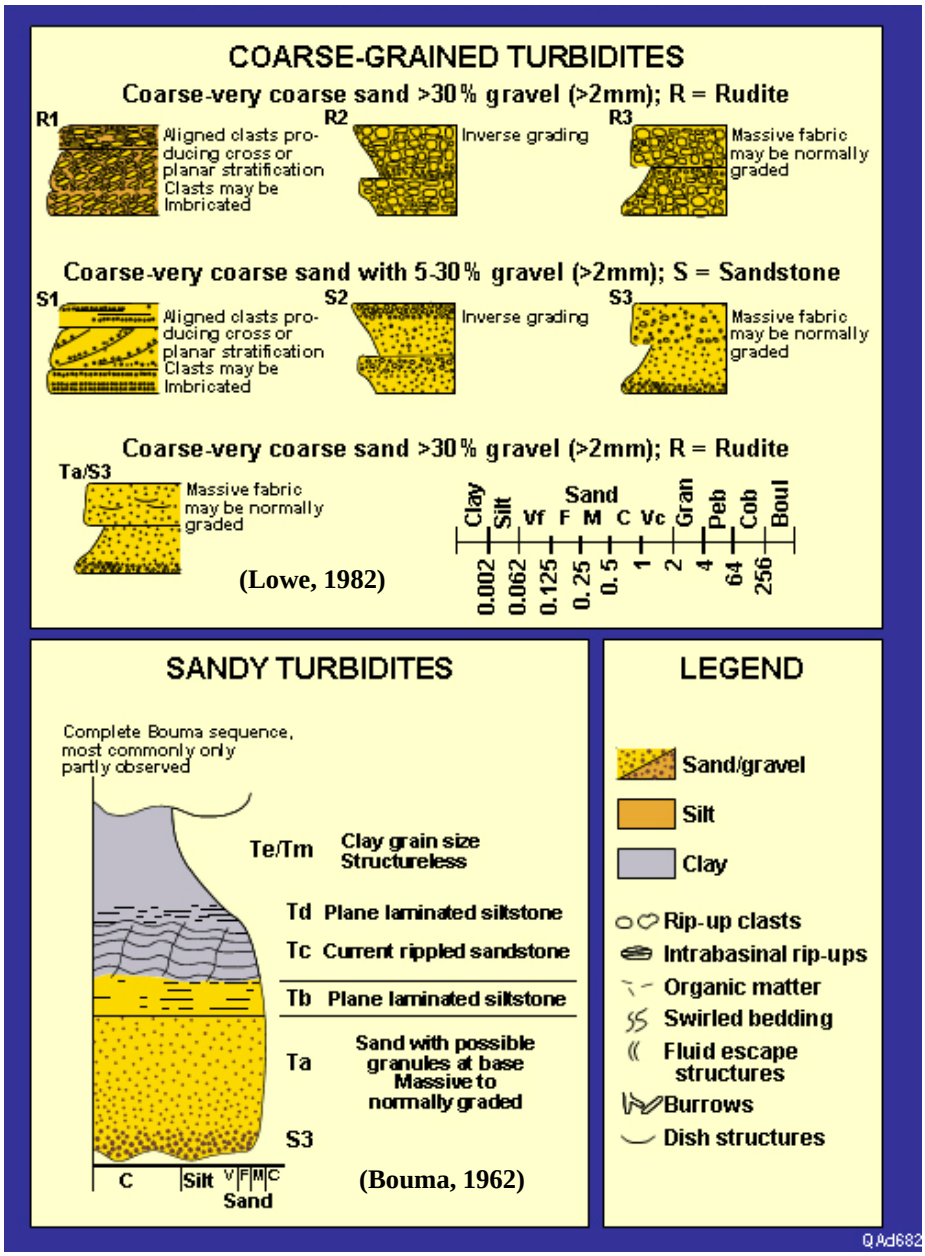

Figure 2.5: Descriptions of high and low density turbidite deposits after Lowe (1982) and Bouma (1962.)

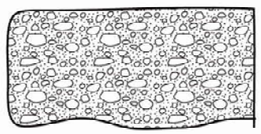

Facies 1 : Conglomerates.
Clast-supported with well-rounded clasts up to 10's of cm in diameter. They don't appear graded and have a minor coarse-grained sand component. Photo taken at Sleeping Giant Ridge.

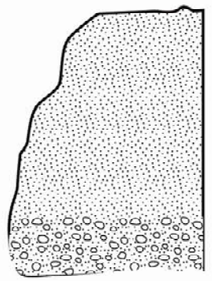

Facies 2 : Very coarse grained sand with gravel and pebbles.
Amalgamated packages composed of both fining upward sequences and massive sequences.Sub-meter to 10 meter scale units. Photo taken at Sleeping Giant Ridge.

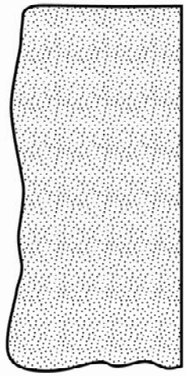

Facies 3 : Massive, medium to coarse-grained sandstones.
Completely lacking any bedding. Photo taken at Chalky Mount Ridge.

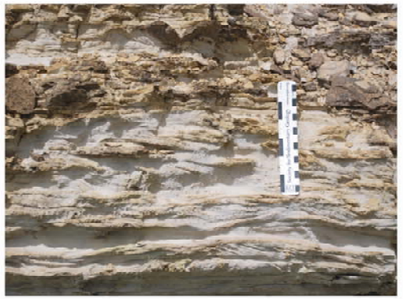

Facies 4 : Cross-stratified sandstones.
Medium-fine grained sands, no coarse grained sand. Photo taken at Chalky Mount Ridge.

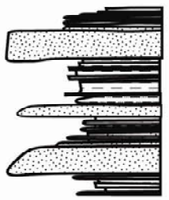

Facies 5 : Laminated, centimeter-scale sandstones. interbedded with silts and shales. Continuous bedding in sands and shales. Wavy bedding, excellent flame structures and other evidence of dewatering. Photo taken at Sleeping Giant Ridge.

Facies 6 : Mm-cm beds of silty shales or muds with rare sand beds. Well laminated up to 70 meter thick packages topping coarser grained cycles.
Minor load structures are observed at some localities. Photo taken at Walkers Ridge.

Figure 2.6: Photographs and illustrations of the six facies identified in outcrops of the Scotland Formation. Oversized Plate (11x17) requires plotter or printer with tabloid printing.

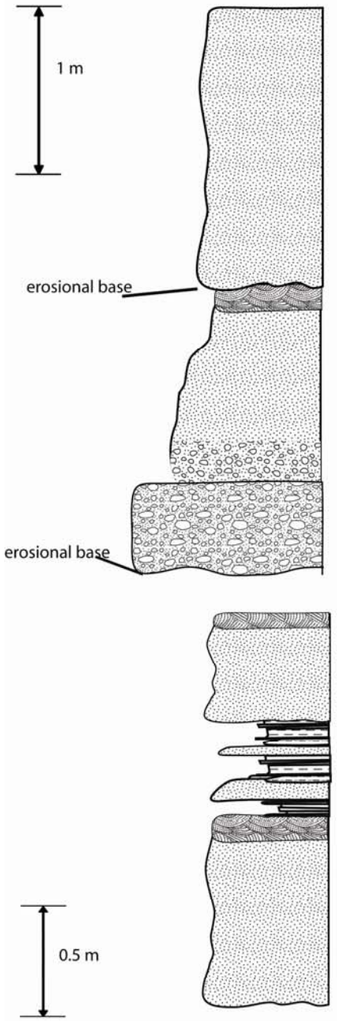

Channel Fill: Facies 1,2 3, and 4 stack to form channel fill elements that are dominated by the coarsest grained facies observed in outcrop. The lowermost channel fill overlie erosive bases.This facies association is seen at the Sleeping Giant Ridge locality.

Lobes: Facies 3, 4 and 5 form non-channelized bodies, normally graded coarse to medium grained sands with minor amounts of fine grained sand and silt and rare mud. This facies association is seen at the Inner Turner's Hall Ridge locality.

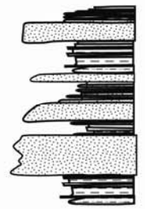

Channel Margins: Facies 5. Laminated, centimeter-scale sandstones interbedded with silts and shales. Continuous bedding in sands and shales. These are low density turbidite deposits that repesent channel margin deposits that together with channel fill deposits comprise individual channels.

This facies association is seen at the Sleeping Giant Ridge locality.

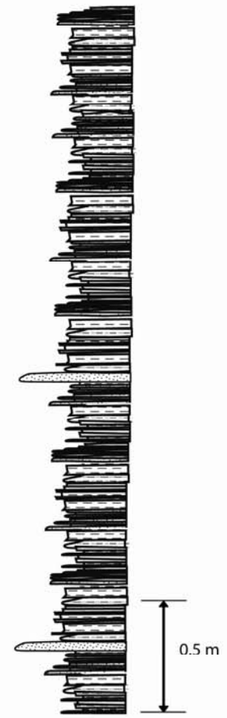

Master Levees : Thick succession of Facies 6. Mm-cm beds of silty shales or muds with rare sand beds. Well laminated up to 70 meter thick packages. Very rare thin bedded but coarse grained sands with erosive bases.

These represent master levees that occur adjacent to channelcomplexes.

This facies association is seen at the Walkers Ridge locality.

Figure 2.7: Illustration of the facies associations identified as comprising the Scotland Formation deposits in outcrop. Oversized Plate (11x17) requires plotter or printer with tabloid printing.

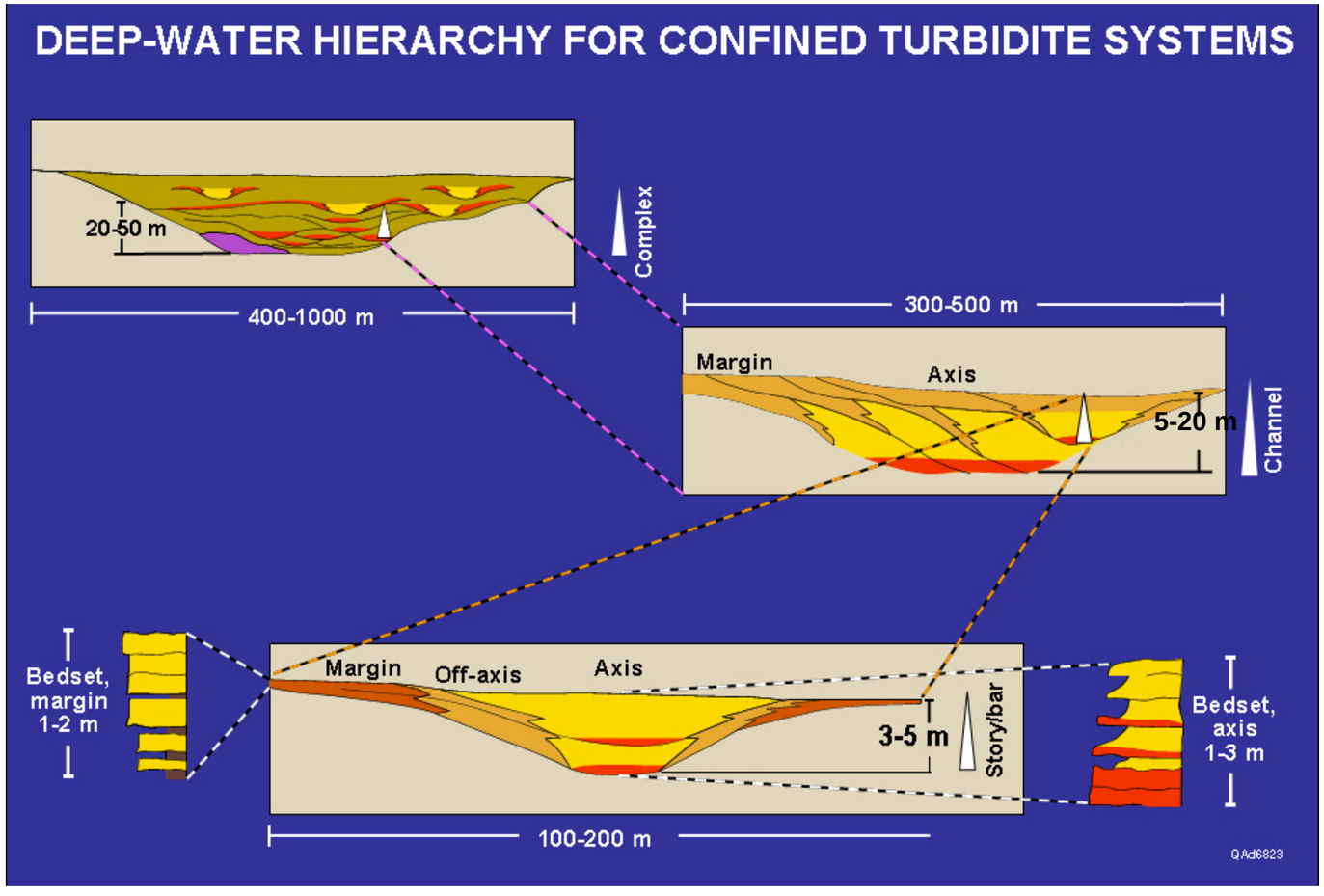

Figure 2.8: Bedsets on the channel margins are made up of thin bedded, finer grained low density/concentration turbidite deposits. Bedsets in the channel axis are made up of coarse grained high density/concentration turbidites. Together these facies associations form an entire channel fill sequence. The channel and channel margin/levee elements form channel complexes and channel complex sets. (Campion, 2000, Sprague et al., 2003; Abreu et al., 2003). Oversized Plate (11x17) requires plotter or printer with tabloid printing.

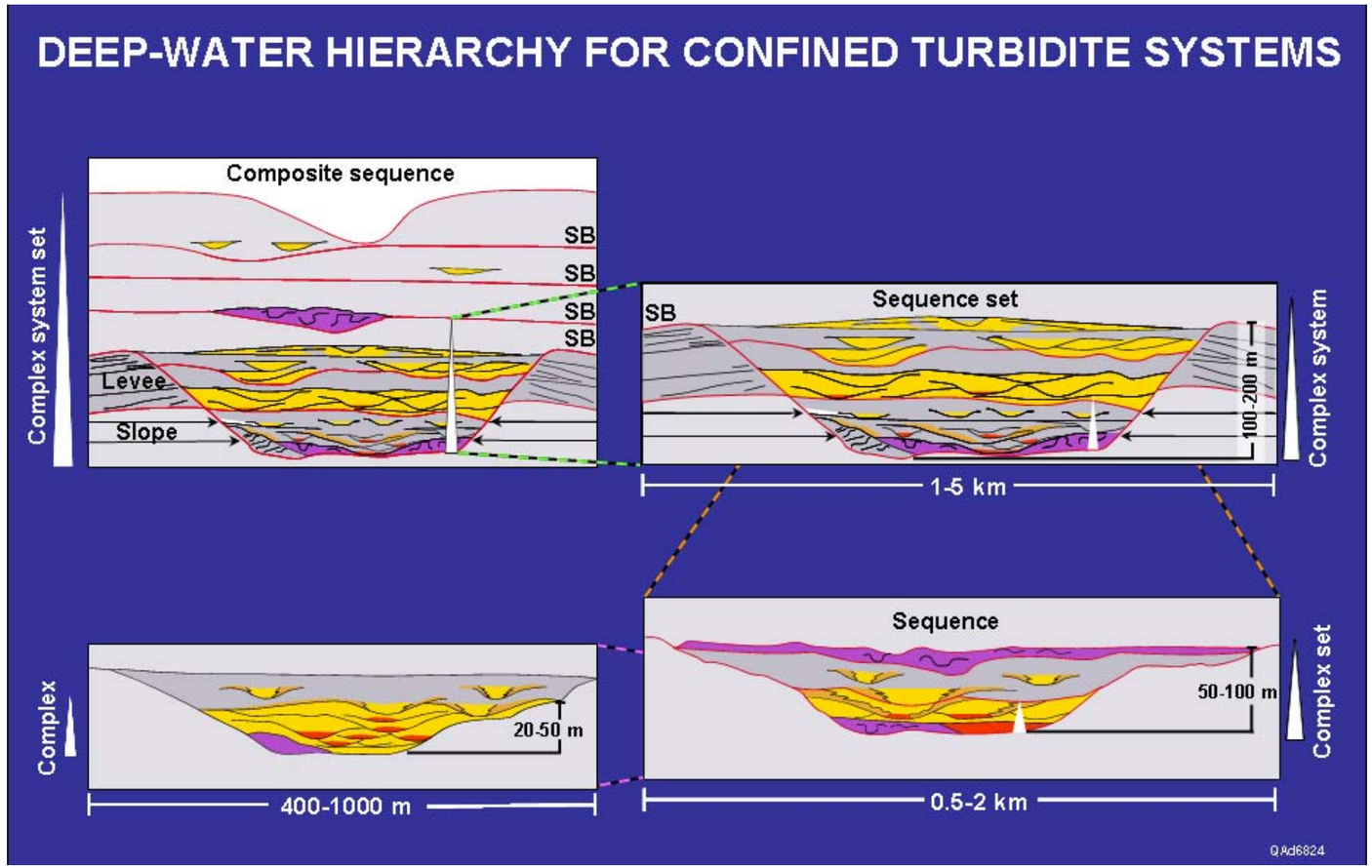

Figure 2.9: Two or more stacked channel elements form a channel complex and two or more stacked channel complexes are called channel complex sets.(Campion, 2000; Sprague et al., 2002; Abreu et al., 2003). Oversized Plate (11x17) requires plotter or printer with tabloid printing.

Figure 2.10: Photo-panorama of Chalky Mount Ridge. View Looking West. Oversized Plate (11x17) requires plotter or printer with tabloid printing.

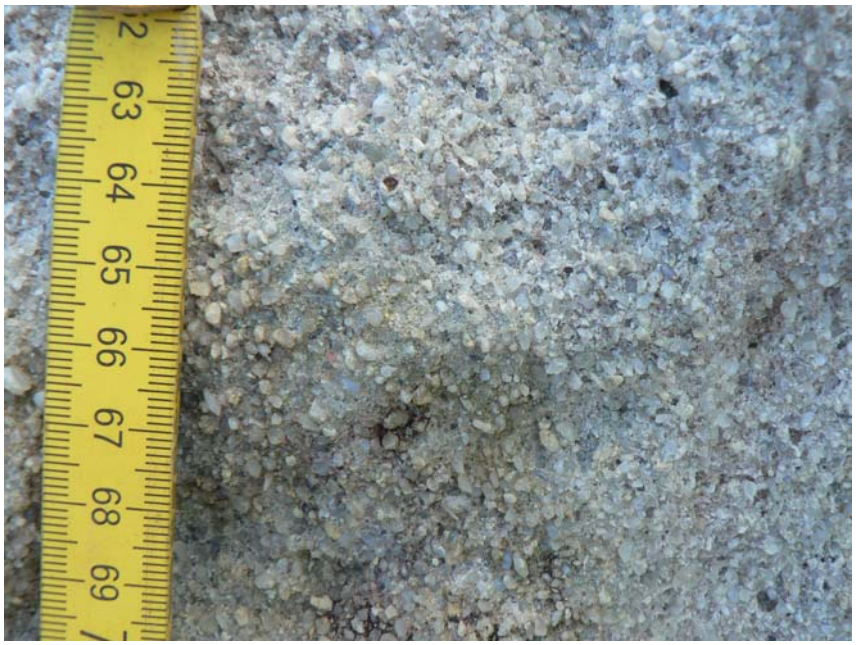

Figure 2.11: Very coarse grained sand at Chalky Mount Ridge. Tape measure is in cm.

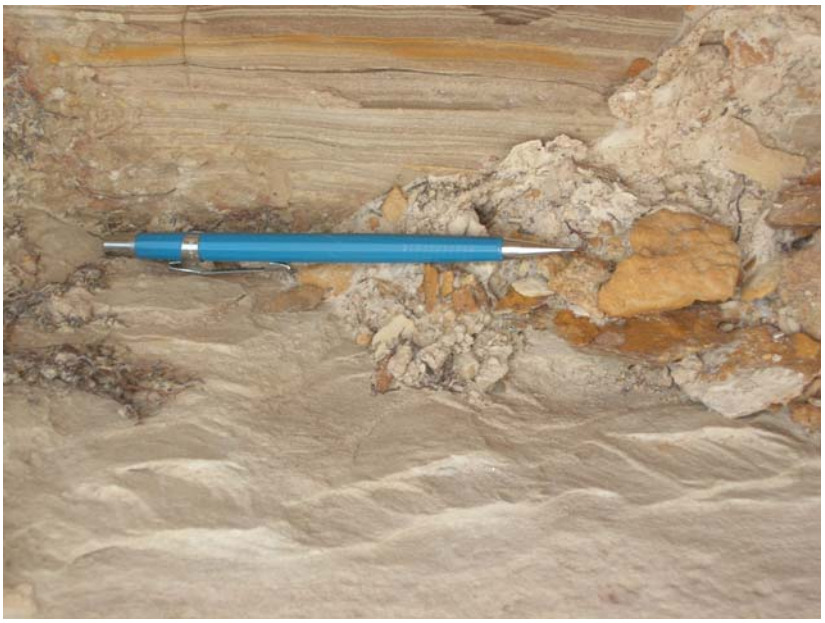

Figure 2.12 : Ripple laminated fine grained sand bed at Chalky Mount Ridge. Overlain by mm scale parallel laminated silts and muds. Pencil shown for scale.

Figure 2.13: Laminated silt and mud overlain by coarse grained sand bed at Chalky Mount Ridge. Pen for scale.

Figure 2.14: Planar parallel laminated silt and fine grained sand at Chalky Mount Ridge. Overlying sand bed is coarse grained and the base of the sand bed is cemented with hematite. Hammer for scale.

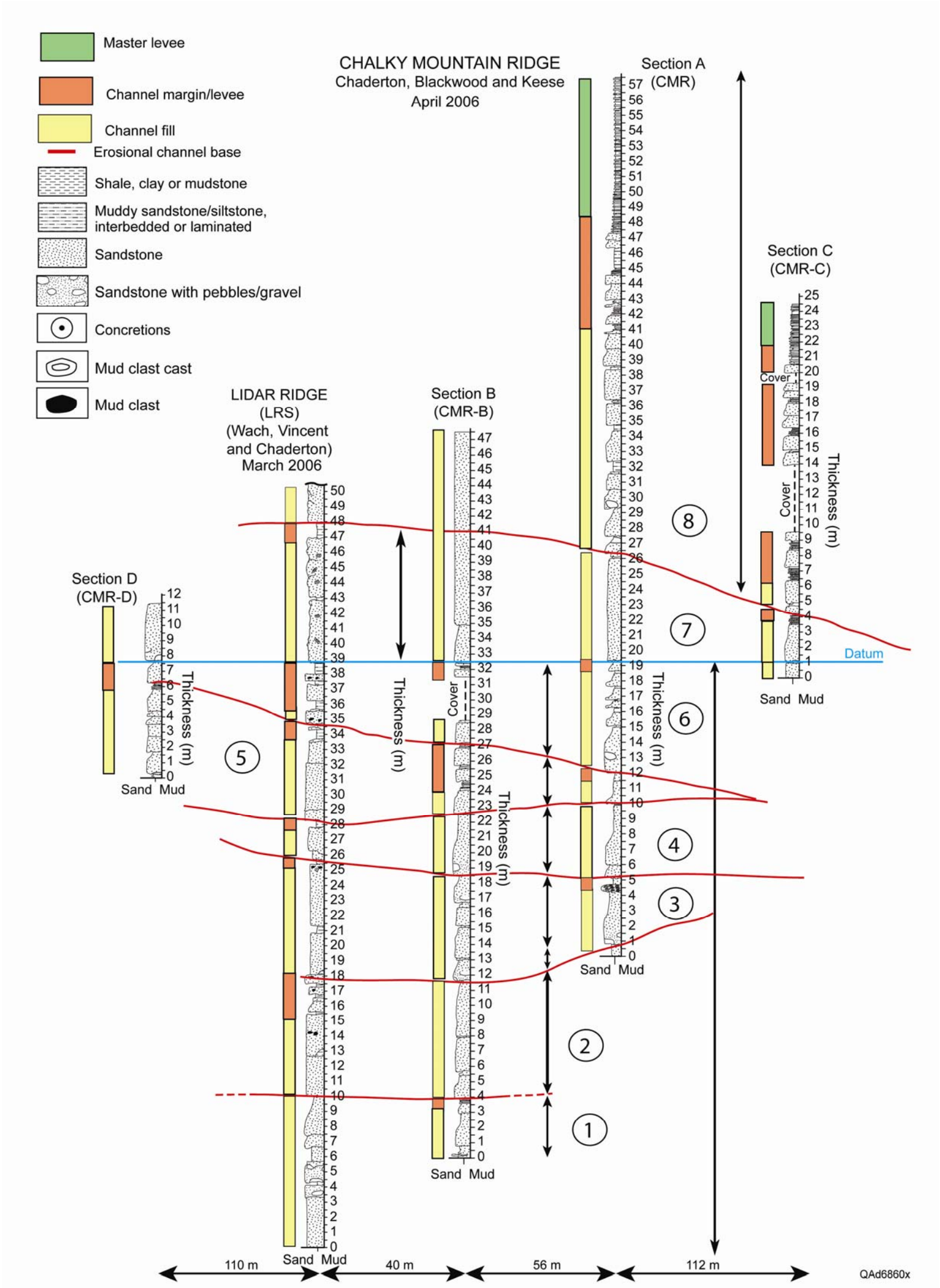

Figure 2.15: Correlation of sections measured at Chalky Mount Ridge showing stacking patterns of channel elements. Contacts were walked in the field where possible. Oversized Plate (11x17) requires plotter or printer with tabloid printing.

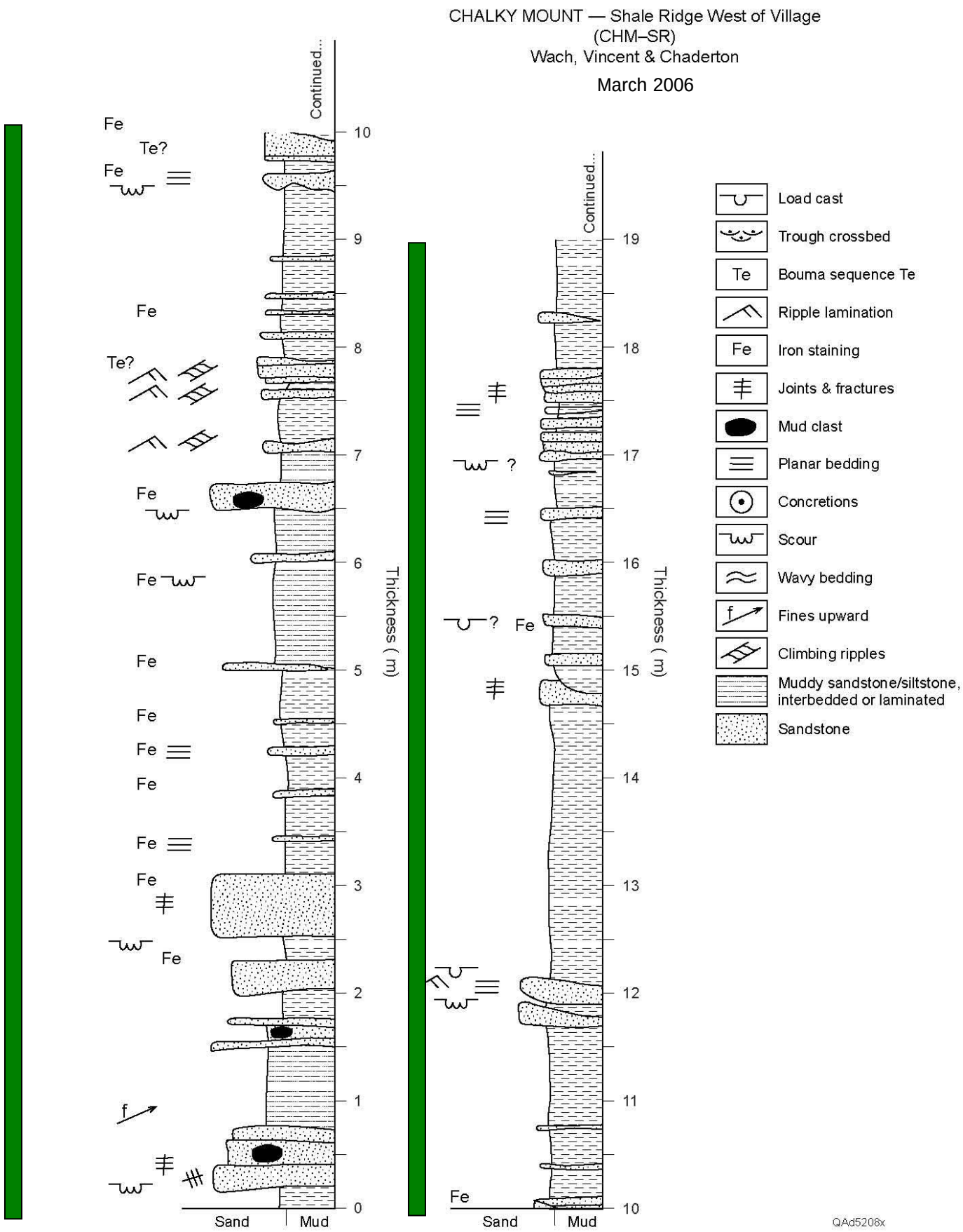

Figure 2.16a: Measured section at Chalky Mount Ridge Lower showing the thick overbank/ master levee deposit. Oversized Plate (11x17) requires plotter or printer with tabloid printing.

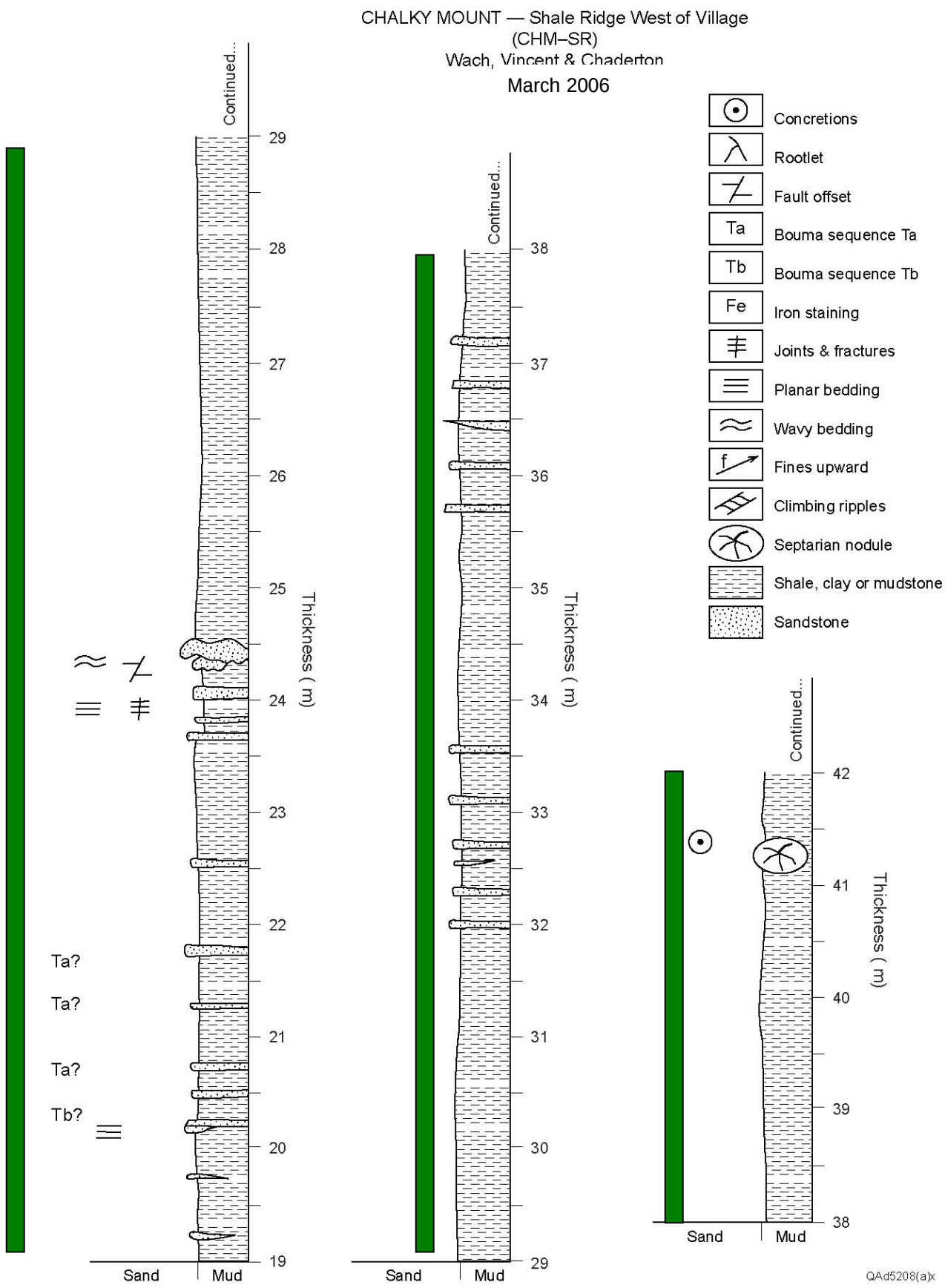

Figure 2.16b: Measured section taken at Chalky Mount Ridge Lower showing the thick overbank/ master levee deposit. Oversized Plate (11x17) requires plotter or printer with tabloid printing.

.

CHALKY MOUNT — Shale Ridge West of Village
(CHM–SR)
Wach, Vincent & Chaderton

March 2006

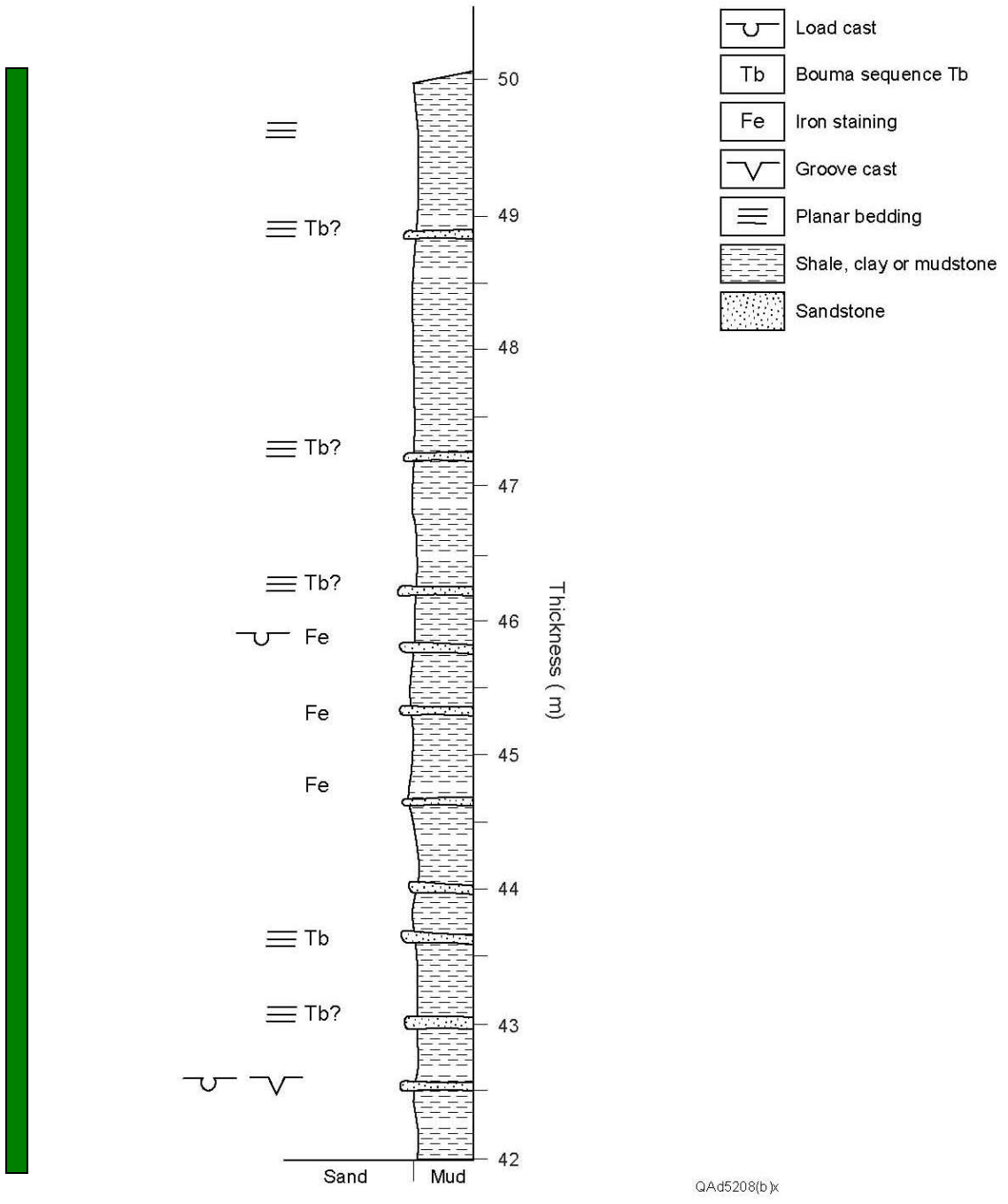

Figure 2.16c: Measured section at Chalky Mount Ridge Lower showing the thick overbank/ master levee deposit. Oversized Plate (11x17) requires plotter or printer with tabloid printing.

Figure 2.17: Sleeping Giant Ridge outcrop. View looking north. Oversized Plate (11x17) requires plotter or printer with tabloid printing.

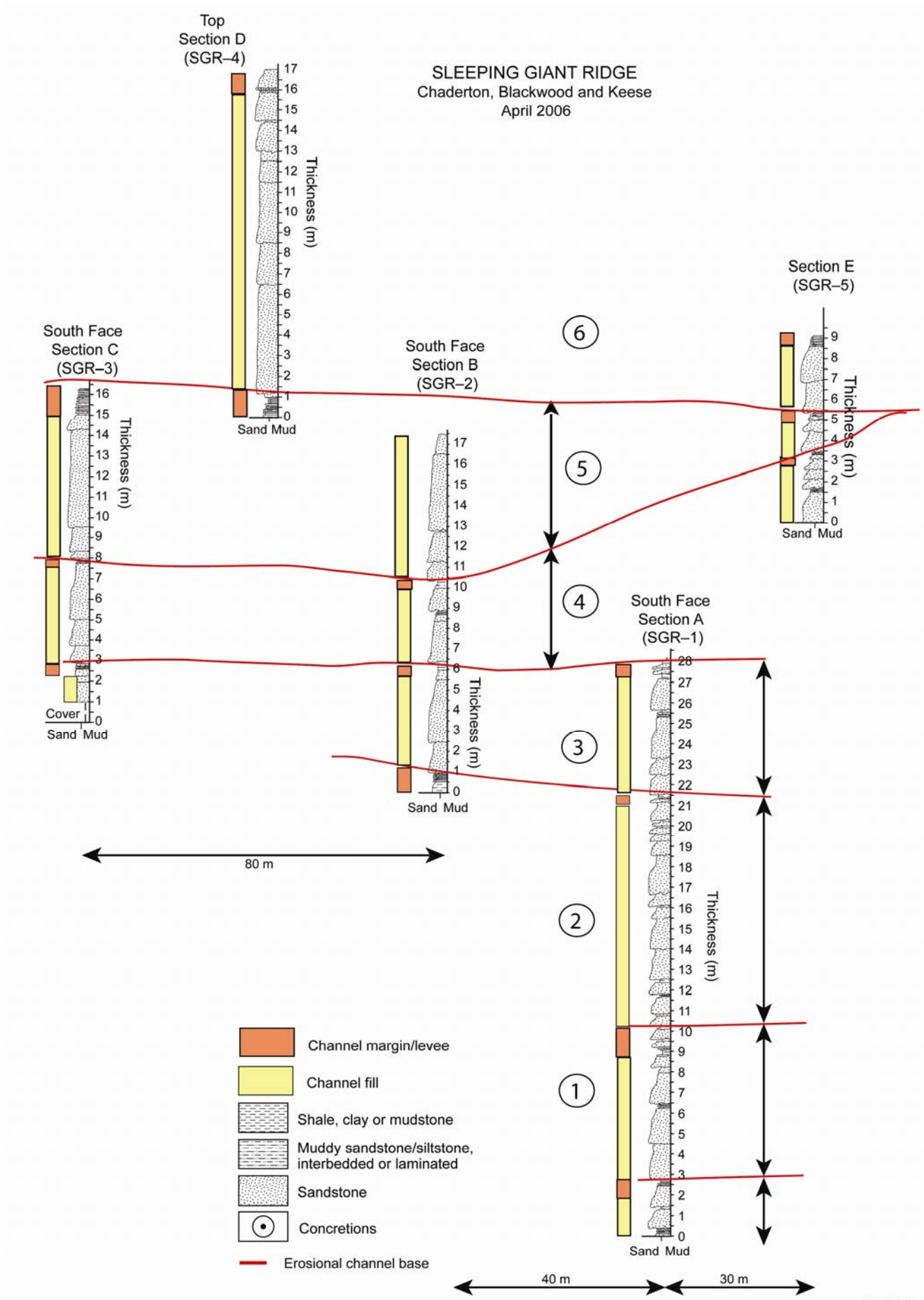

Figure 2.18: Correlation of sections measured at Sleeping Giant Ridge showing stacking of the six channel elements identified at this location. Oversized Plate (11x17) requires plotter or printer with tabloid printing.

Figure 2.19: Conglomerate bed observed at CRBSGRF section with pencil shown for scale. Clasts are well rounded and comprised of iron-rich clasts (red and orange) and white lithified mud clasts.

Figure 2.20: Very coarse grained quartz rich sand bed at Sleeping Giant Ridge. Orange-red hematite cement is only a surface feature- fresh faces do not show this cement. Mechanical pencil point for scale.

Figure 2.21: Parallel laminated silt and mud overlying wavy beds of silt and mud at Sleeping Giant Ridge. Pencil for scale.

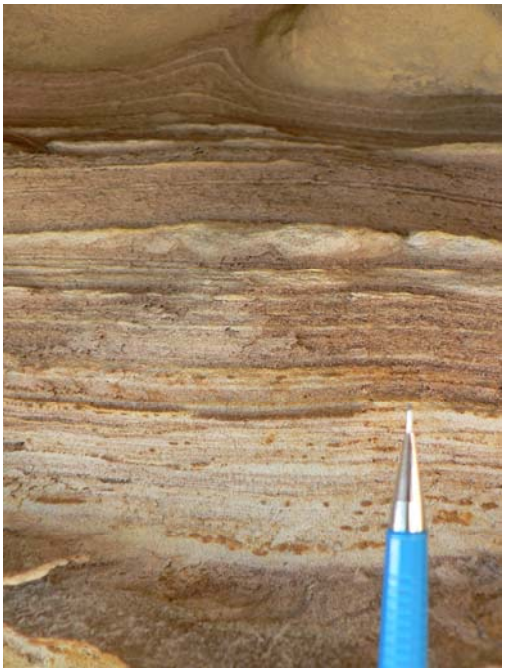

Figure 2.22: Parallel laminated silt and mud overlain by a coarser grained sand bed that is loading into the underlying finer grained bed at Sleeping Giant Ridge. Flame structures have developed. Pencil for scale.

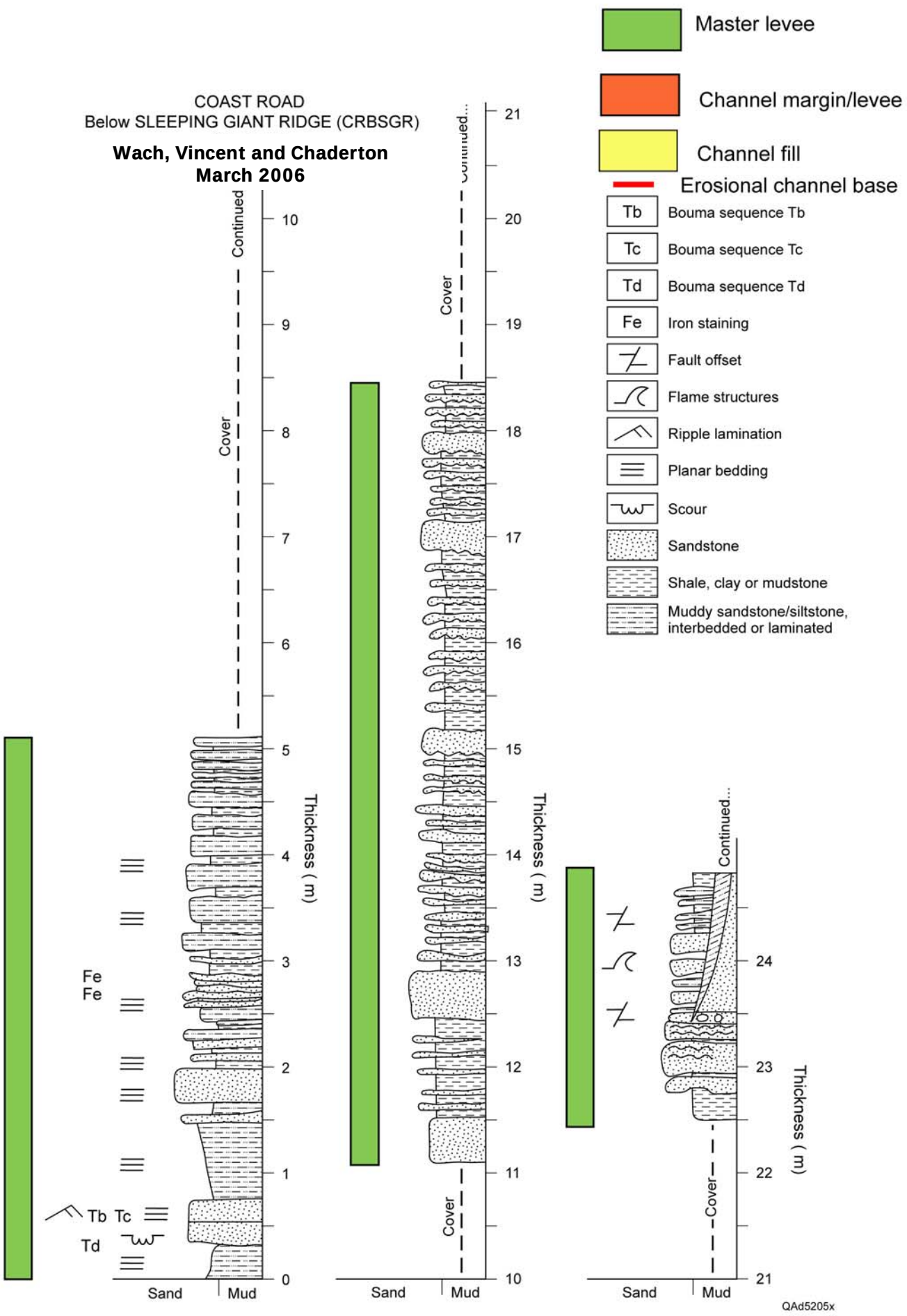

Figure 2.23a: Measured section at the East Coast Road Beneath Sleeping Giant Ridge showing a thick master levee package. Oversized Plate (11x17) requires plotter or printer with tabloid printing.

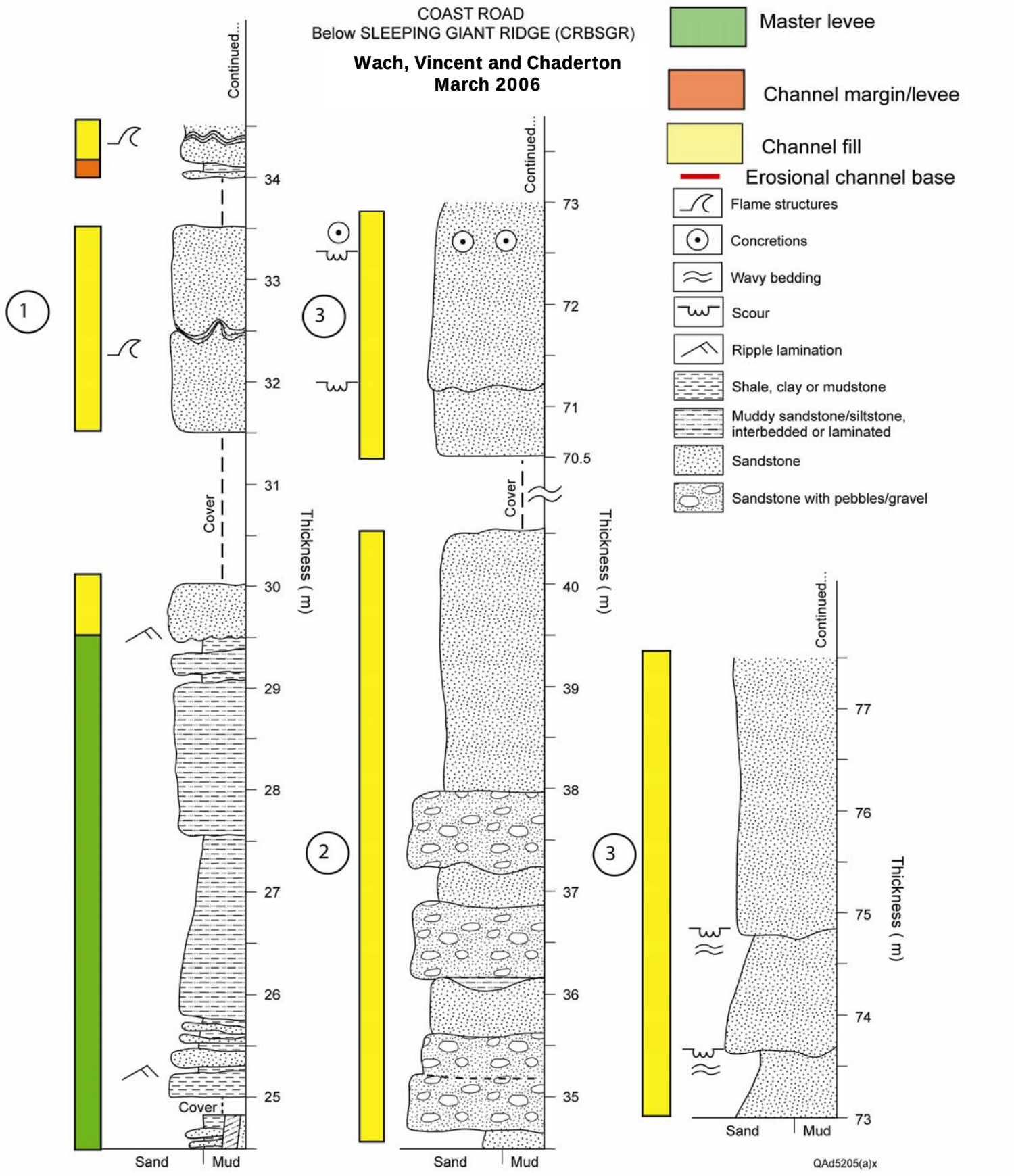

Figure 2.23b: Measured section at the East Coast Road Beneath Sleeping Giant Ridge showing a master levee package overlain by stacked channel fill packages. Oversized Plate (11x17) requires plotter or printer with tabloid printing.

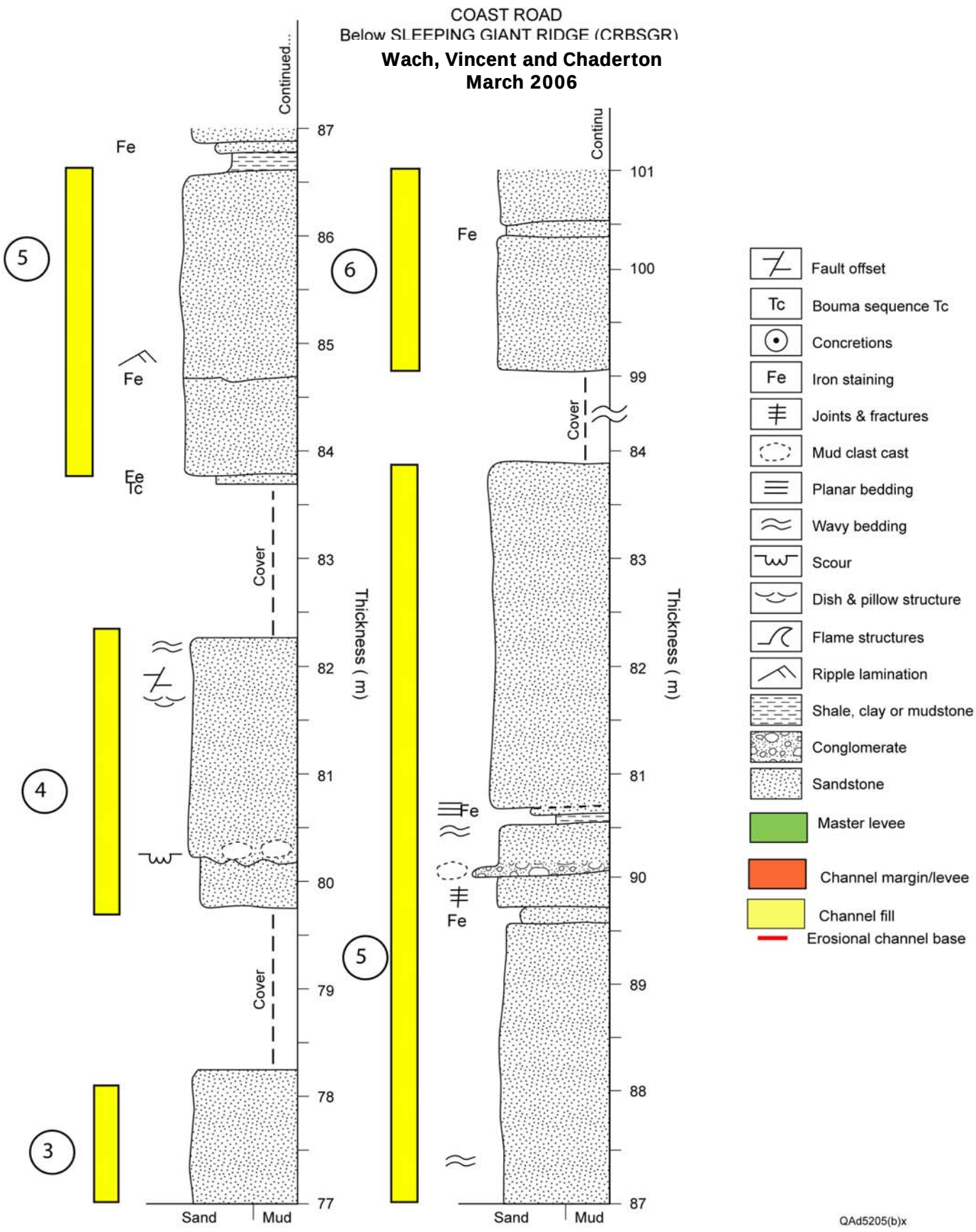

Figure 2.23c: Measured section at the East Coast Road Beneath Sleeping Giant Ridge showing a master levee package overlain by stacked channel fill packages. Oversized Plate (11x17) requires plotter or printer with tabloid printing.

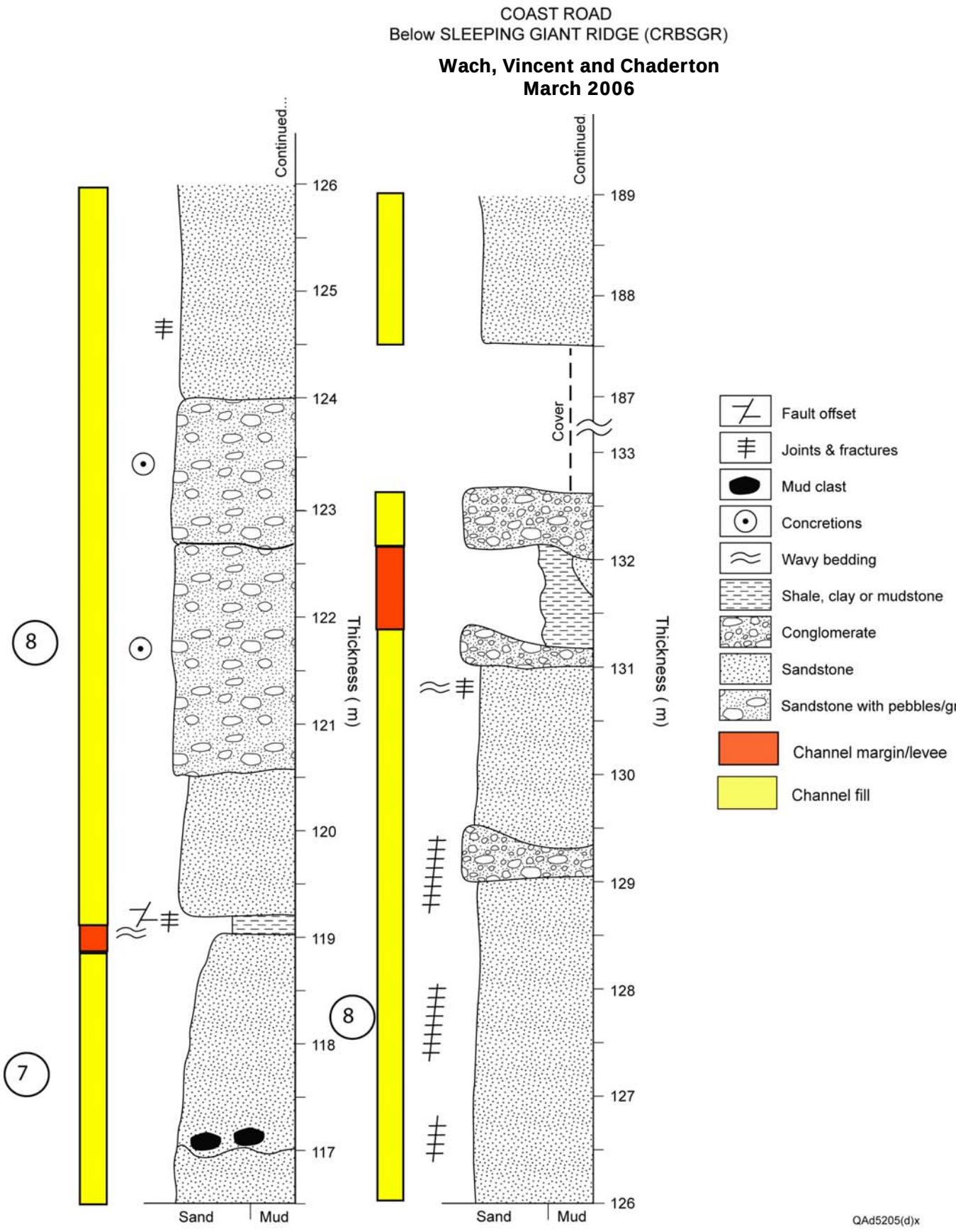

Figure 2.23d: Measured section at the East Coast Road Beneath Sleeping Giant Ridge showing a master levee package overlain by stacked channel fill packages. Oversized Plate (11x17) requires plotter or printer with tabloid printing.

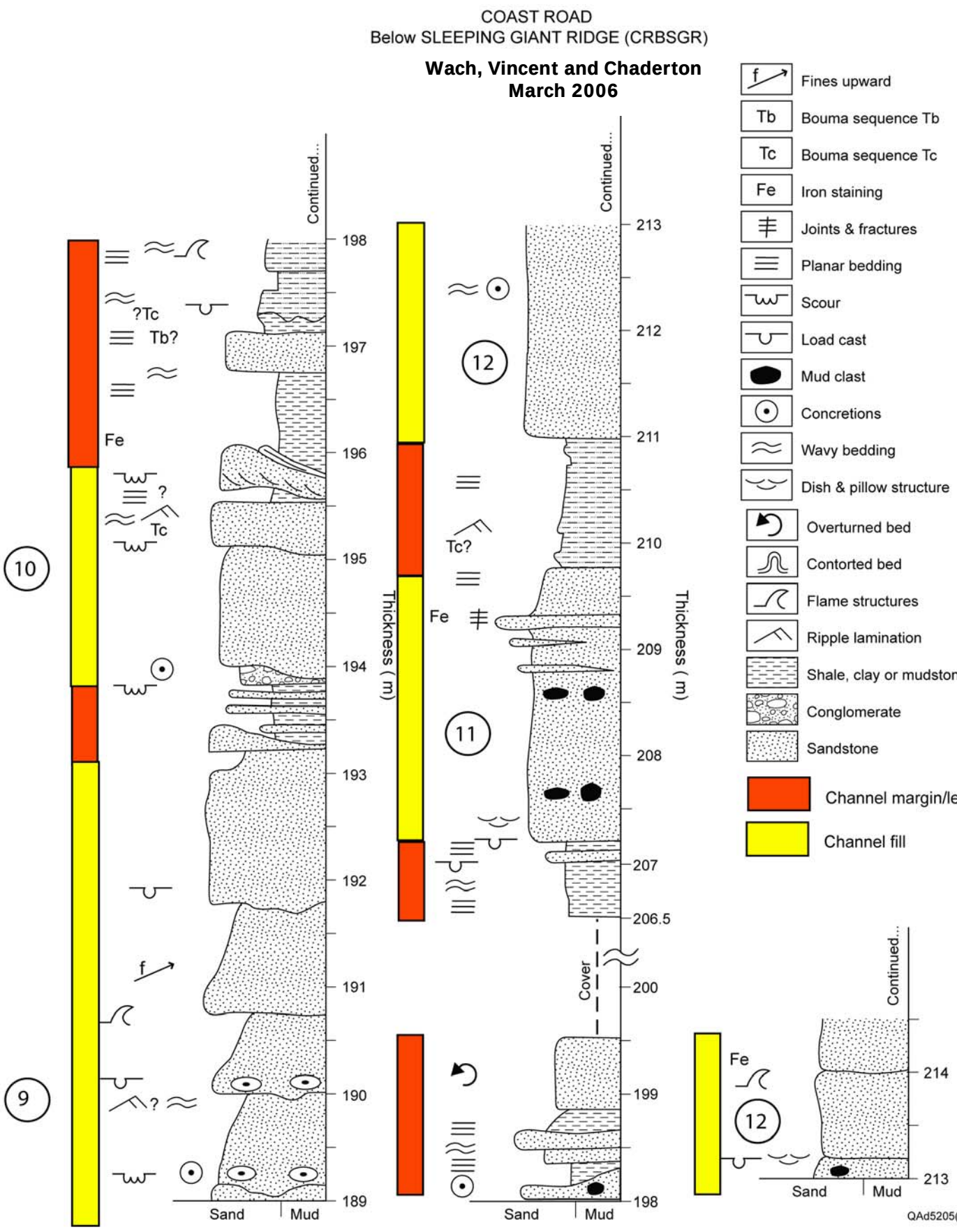

Figure 2.23e: Measured section at the East Coast Road Beneath Sleeping Giant Ridge showing stacked channel fill packages interbedded with channel margin packages. Oversized Plate (11x17) requires plotter or printer with tabloid printing.

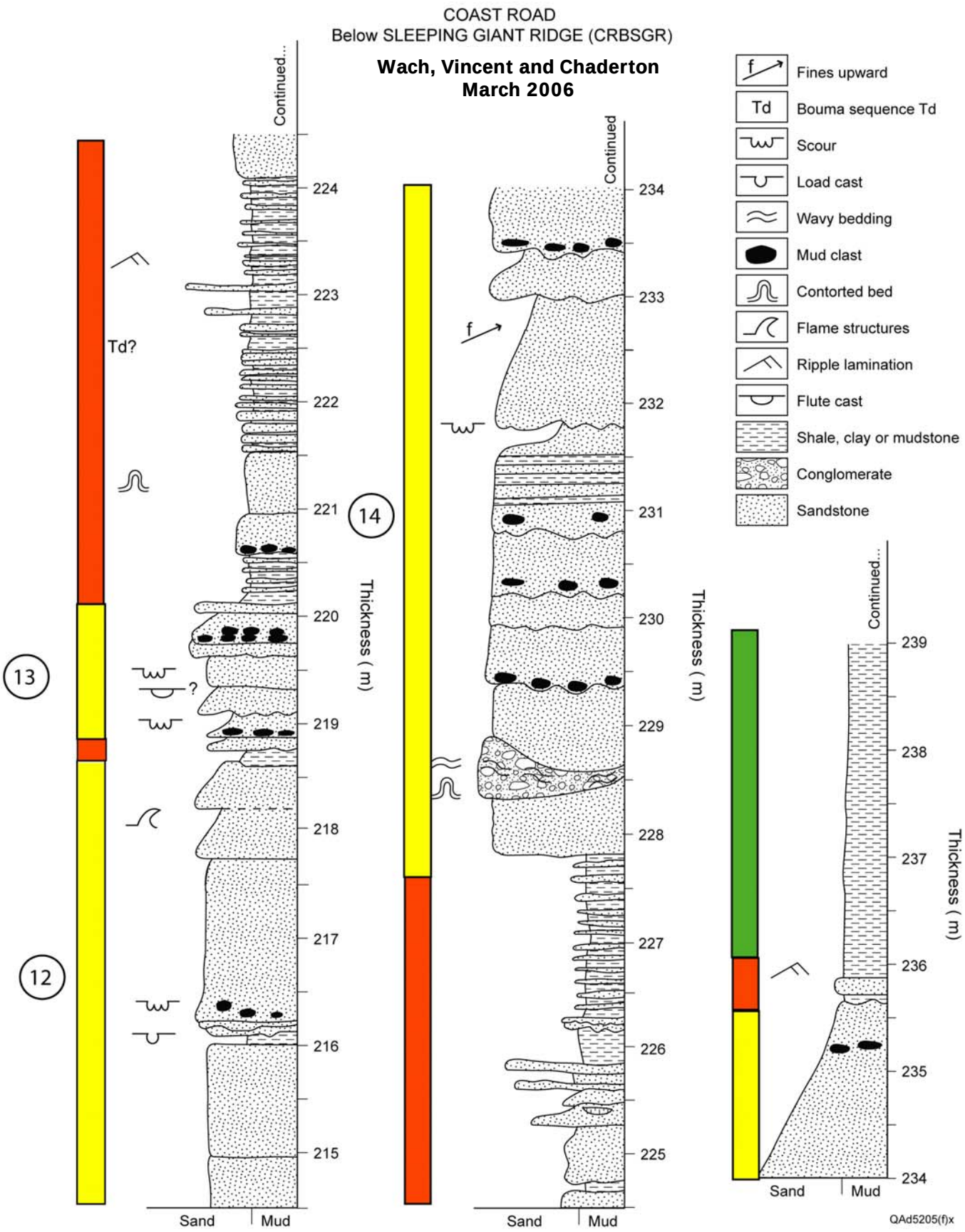

Figure 2.23f: Measured section at the East Coast Road Beneath Sleeping Giant Ridge showing stacked channel fill packages interbedded with channel margin packages. Oversized Plate (11x17) requires plotter or printer with tabloid printing.

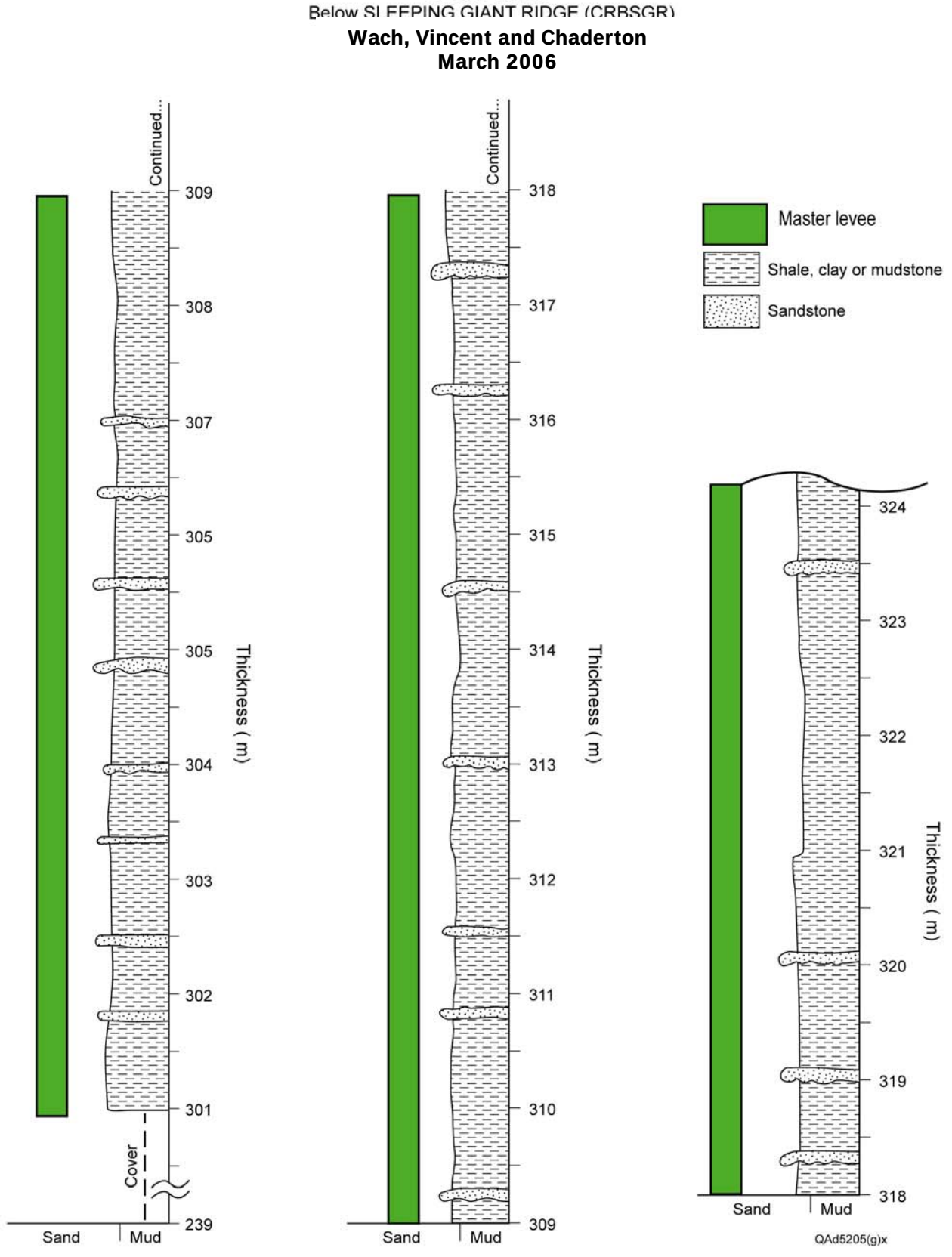

Figure 2.23g: Measured section at the East Coast Road Beneath Sleeping Giant Ridge showing a master levee package that overlies stacked channel fill packages. Oversized Plate (11x17) requires plotter or printer with tabloid printing.

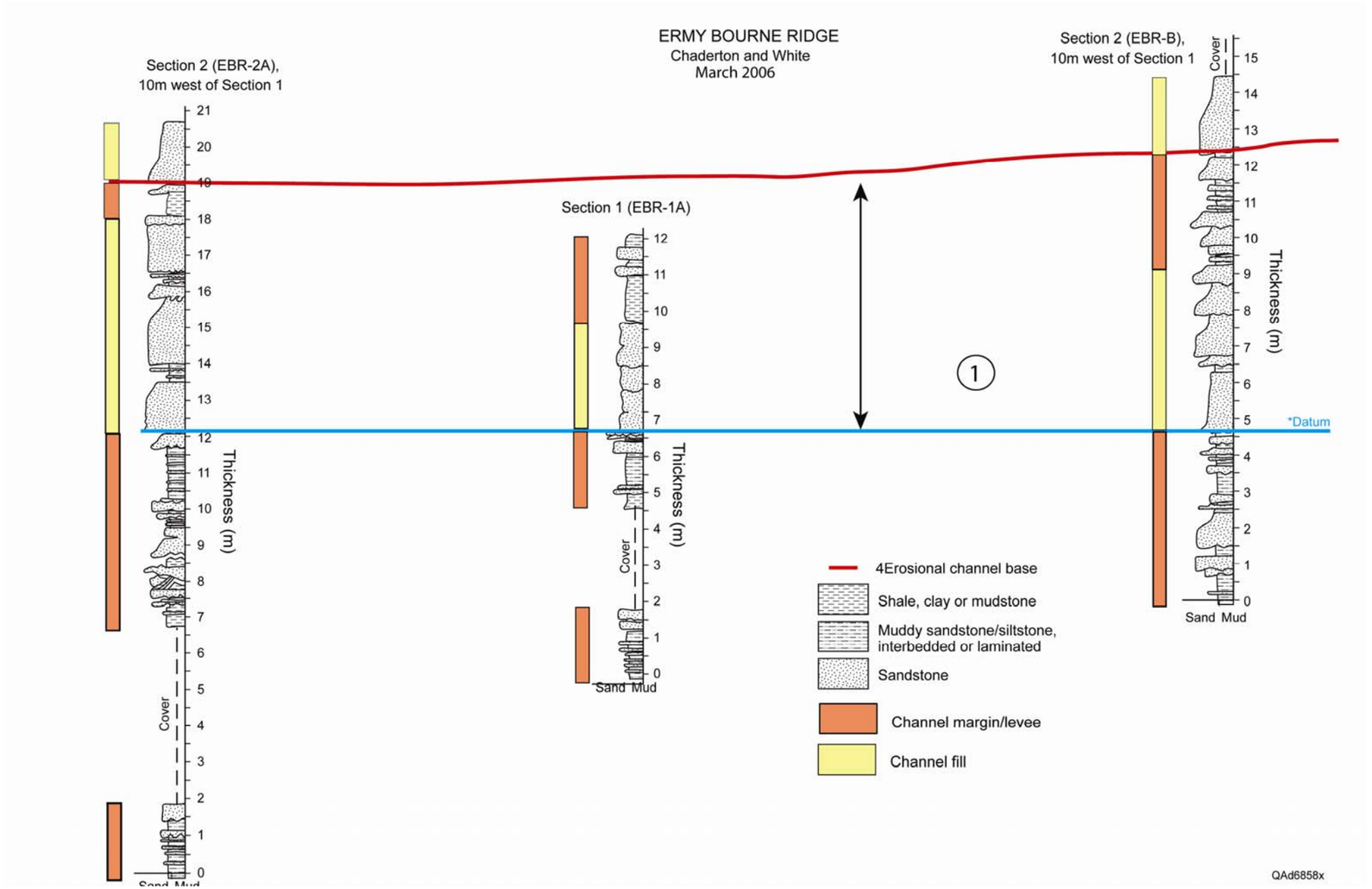

Figure 2.24: Channel element identified at the Ermy Bourne Ridge. Oversized Plate (11x17) requires plotter or printer with tabloid printing.

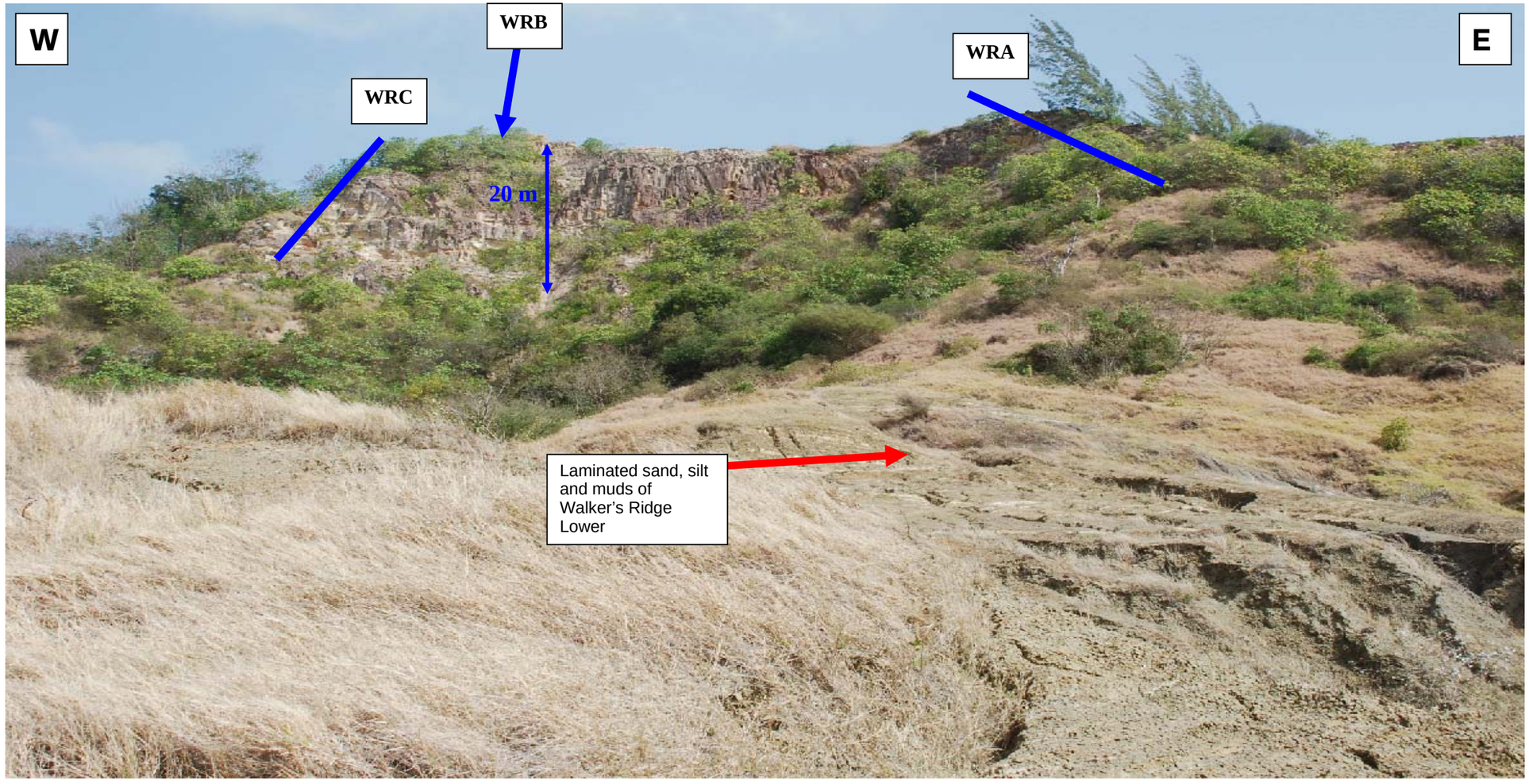

Figure 2.25: Photograph of Walker's Ridge showing the channelized sands overlying an extensive overbank levee sequence. Blue lines show the location of the measured sections. View looking north. Oversized Plate (11x17) requires plotter or printer with tabloid printing.

Figure 2.26: Photograph of Walker’s Ridge showing the location of the measured section WRB and shows a dip section view of the outcrop. View looking West. Oversized Plate (11x17) requires plotter or printer with tabloid printing.

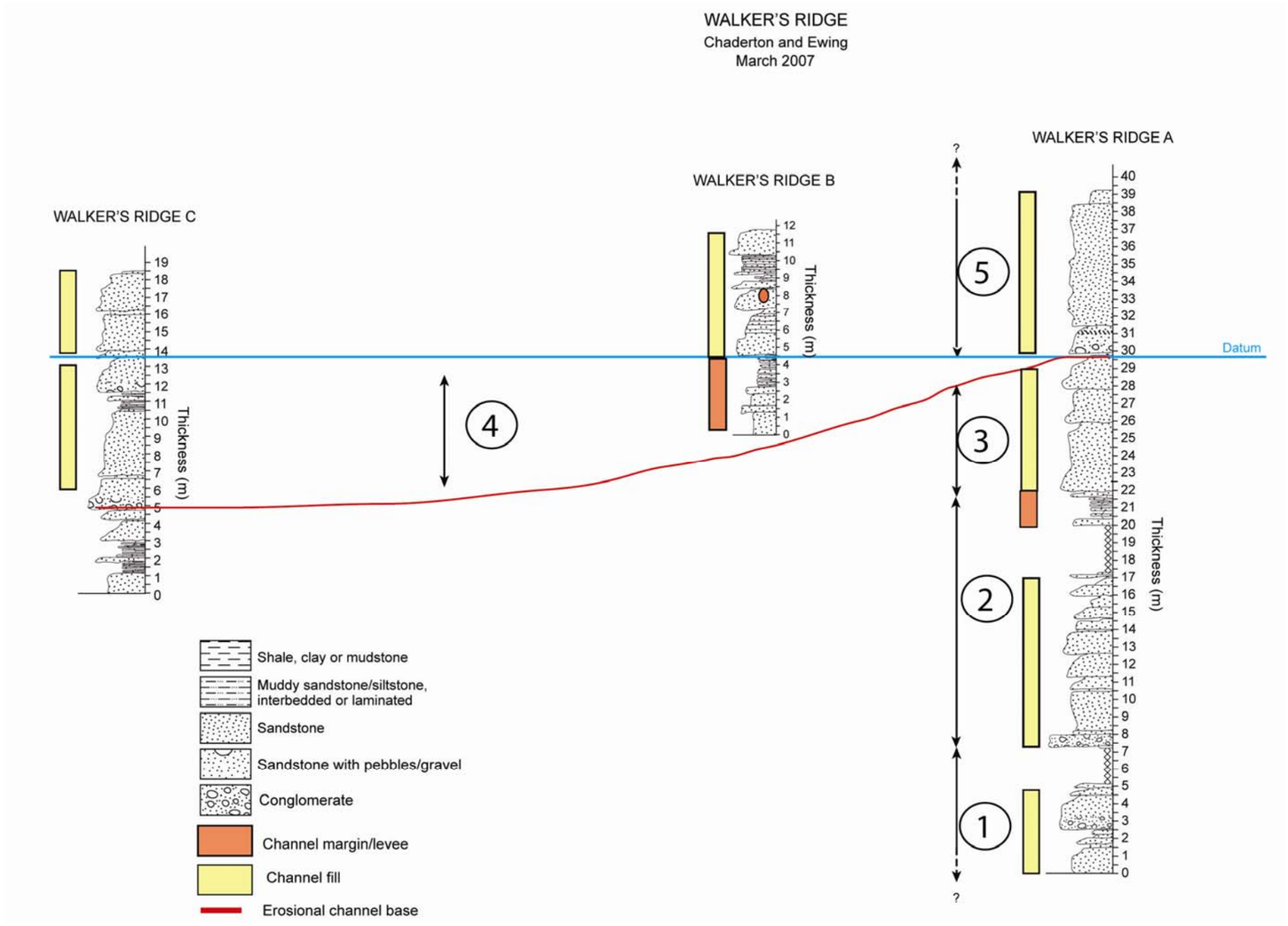

Figure 2.27: Correlation of sections measured at Walker's Ridge Upper showing the stacking patterns observed at this location. Orange dot on WRRB section identifies the location that Photographs A and B were taken. Oversized Plate (11x17) requires plotter or printer with tabloid printing.

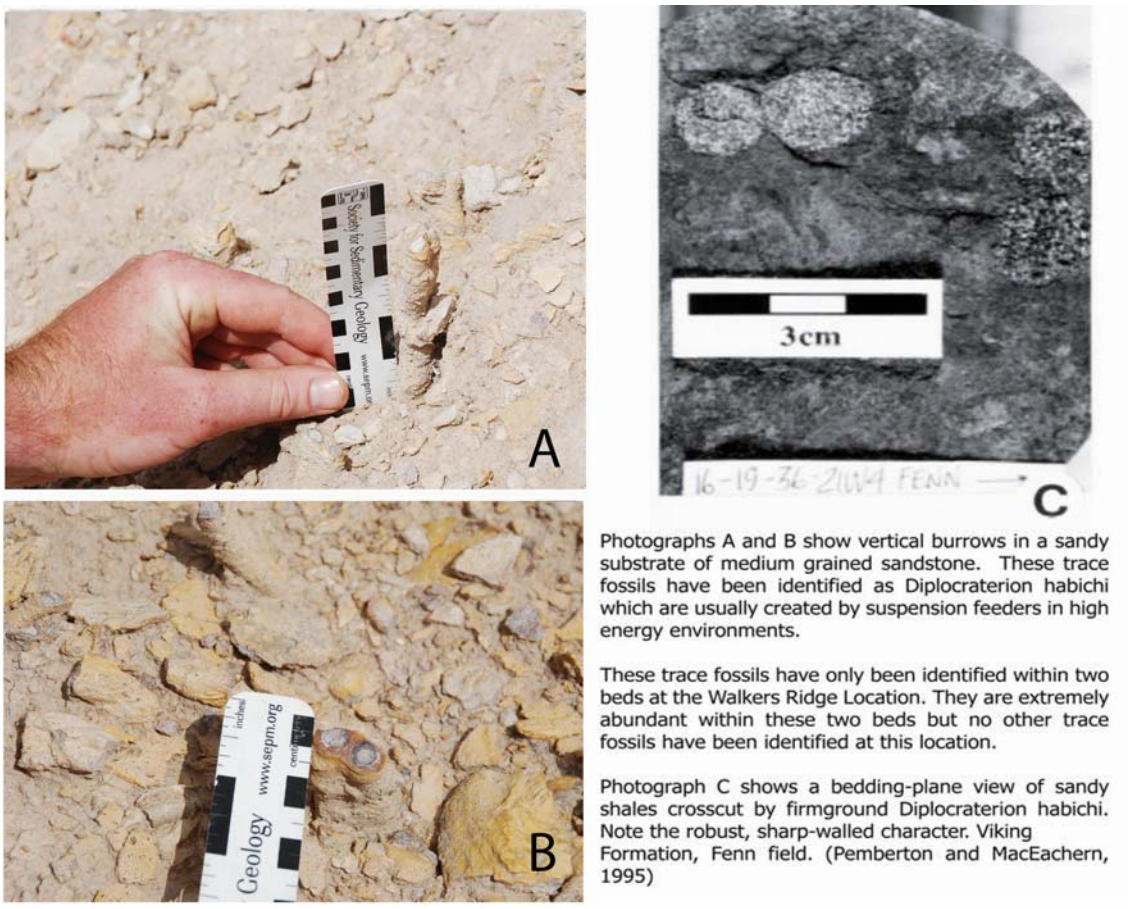

Figure 2.28: Photograph of Diplocraterion habichi found at Walker's Ridge and comparison to example from literature.

Figure 2.29 : Sharp based coarse gained sand bed overlying finer grained silt and mud at Walker's Ridge. Marker for scale.

Figure 2.30: Ripple laminations within a fine-grained sand bed at Walker's Ridge. Marker for scale.

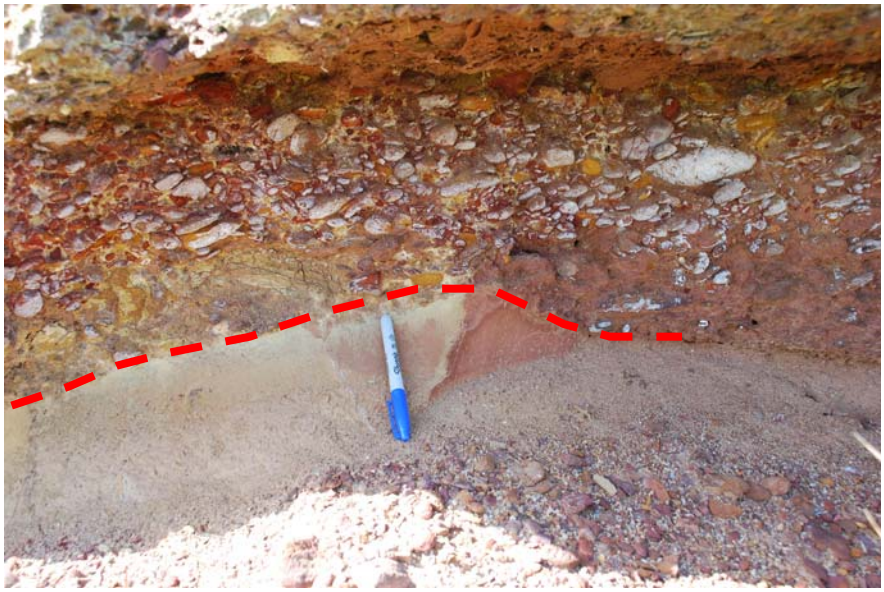

Figure 2.31: Conglomerate with erosive base that overlies fine grained sand bed at Walkers Ridge. Marker for scale.

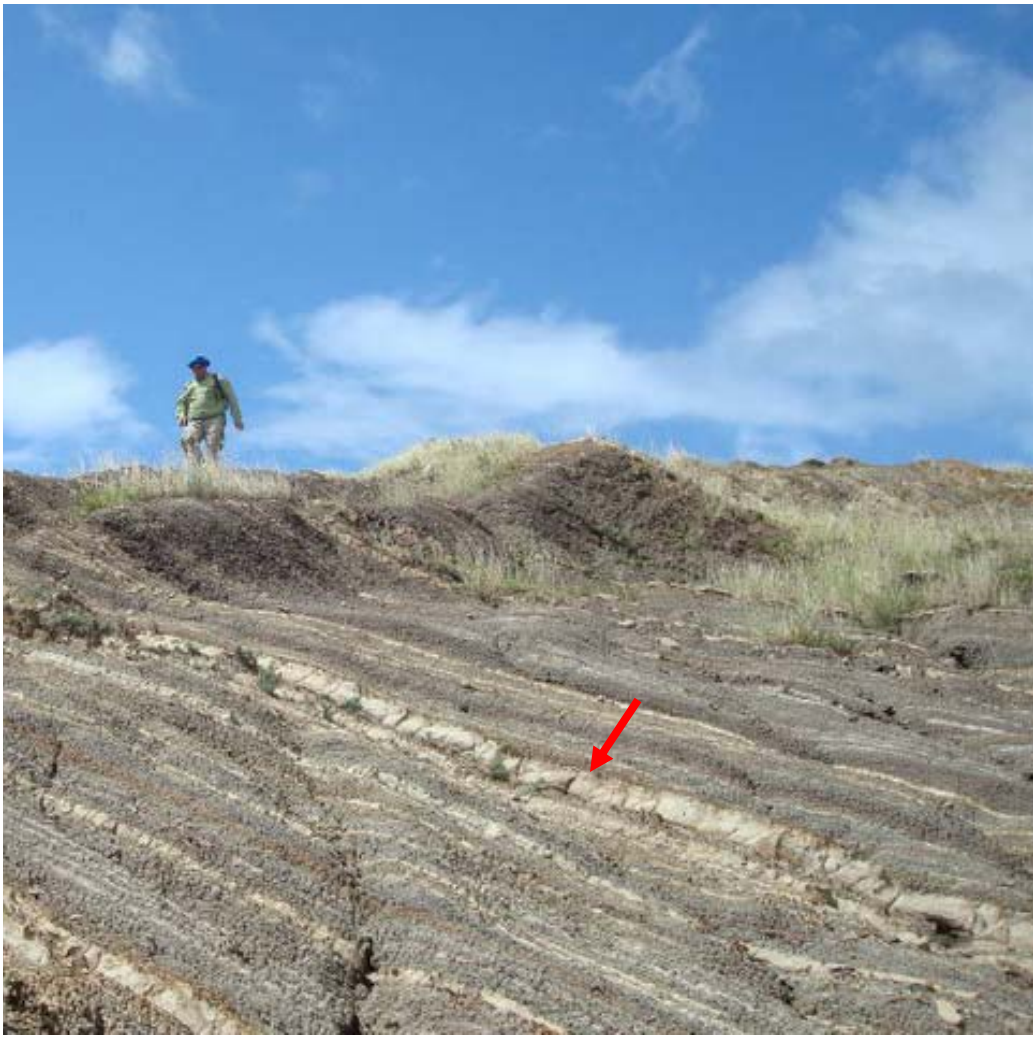

Figure 2.32: Laminated sand, silt and muds of Walker's Ridge Lower. Lighter colored laminae are thin sand beds. Red arrow points to 20 cm thick coarse grained sand bed with an erosive base. View looking northwest.

Figure 2.33: Thalassinoides trace fossil observed at Mount All. Pencil for scale.

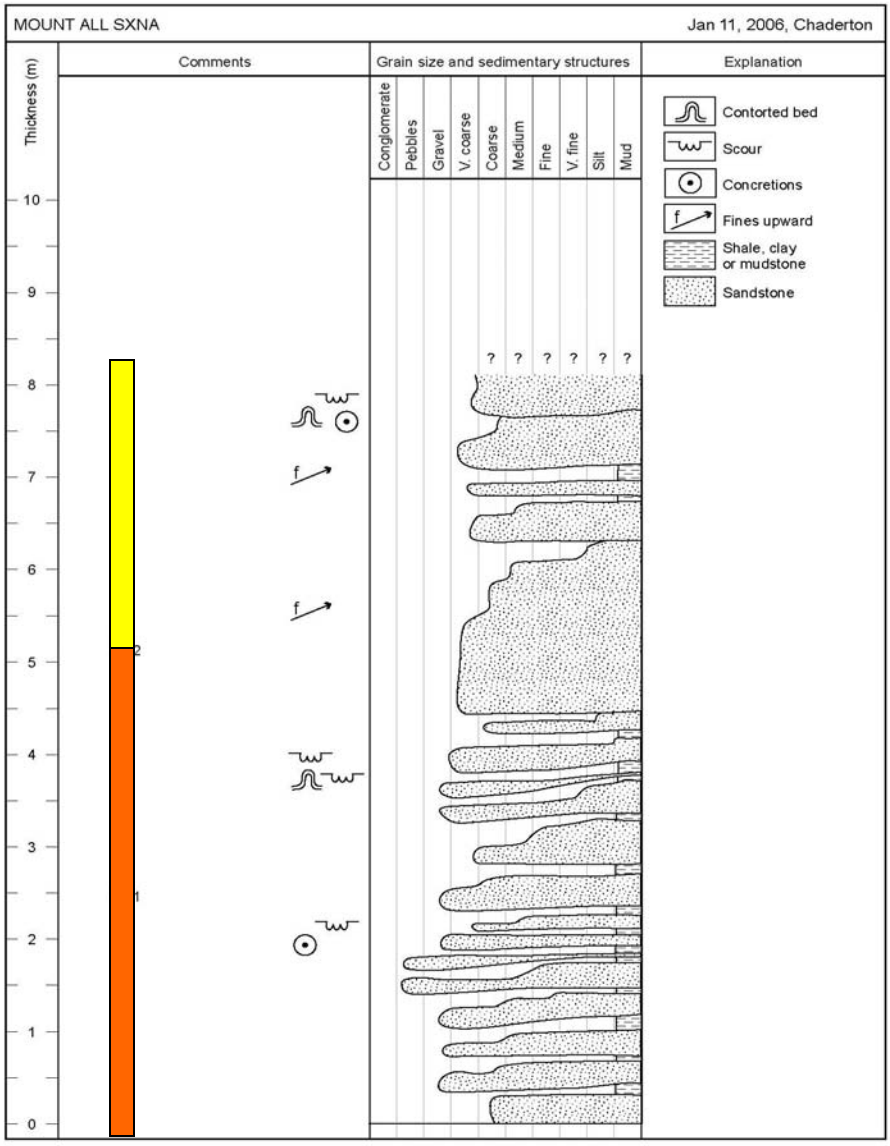

Figure 2.34: Mount All measured stratigraphic section A.

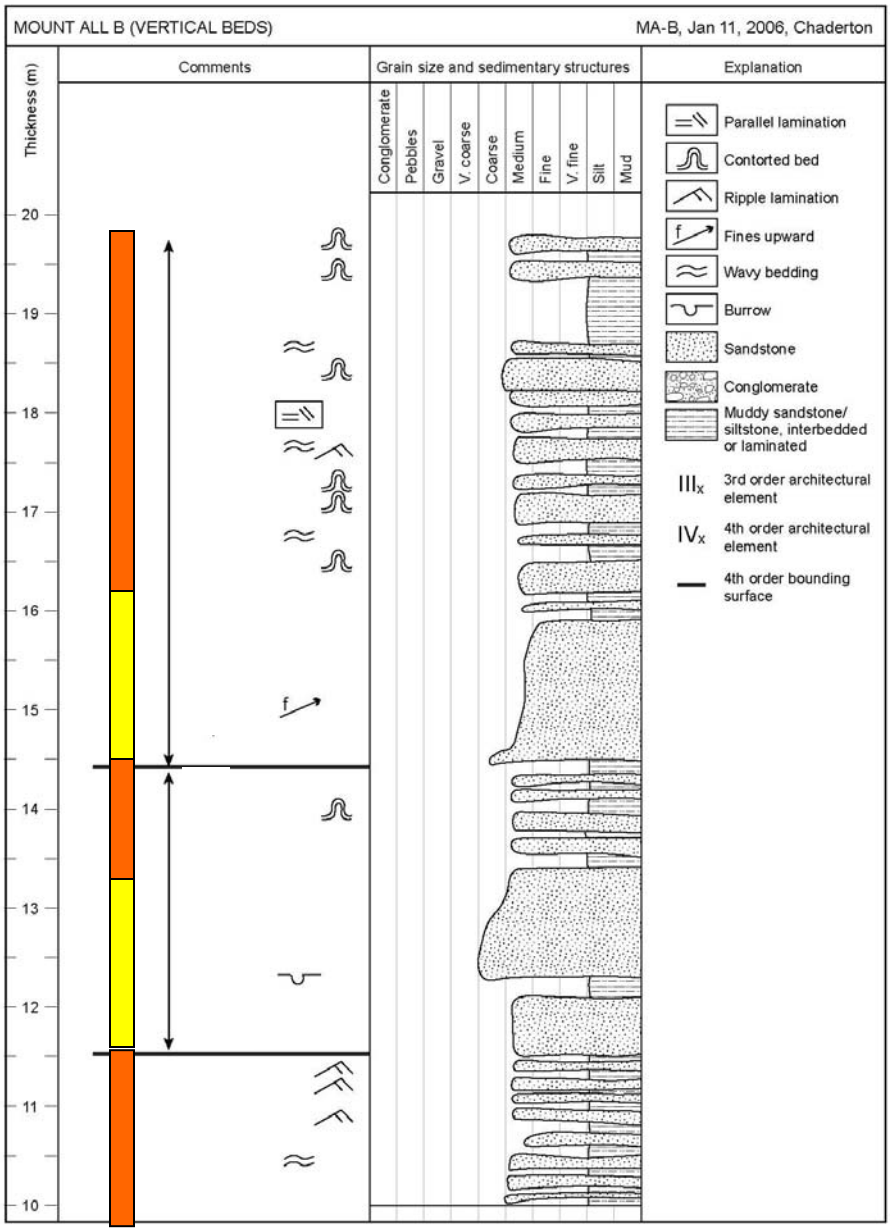

Figure 2.35: Mount All measured stratigraphic section B.

Figure 2.36: Inner Turner's Hall Ridge (ITR). Blue arrow shows location of measured section.

Figure 2.37: Medium grained sand bed at ITR outcrop. Marker for scale.

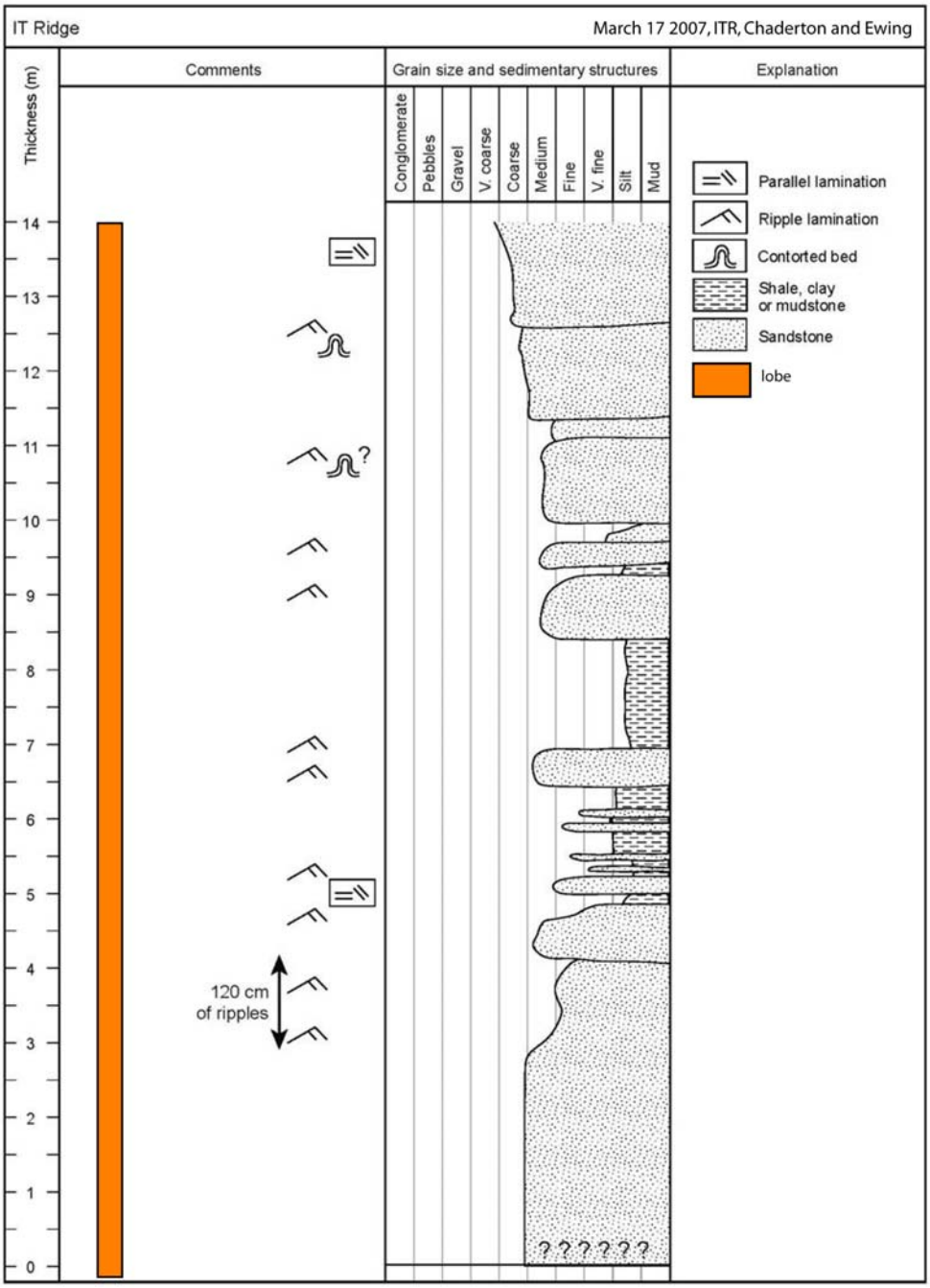

Figure 2.38a: Inner Turner's Hall Ridge measured stratigraphic section, interpreted as deposits of a deep water fan depositional lobe.

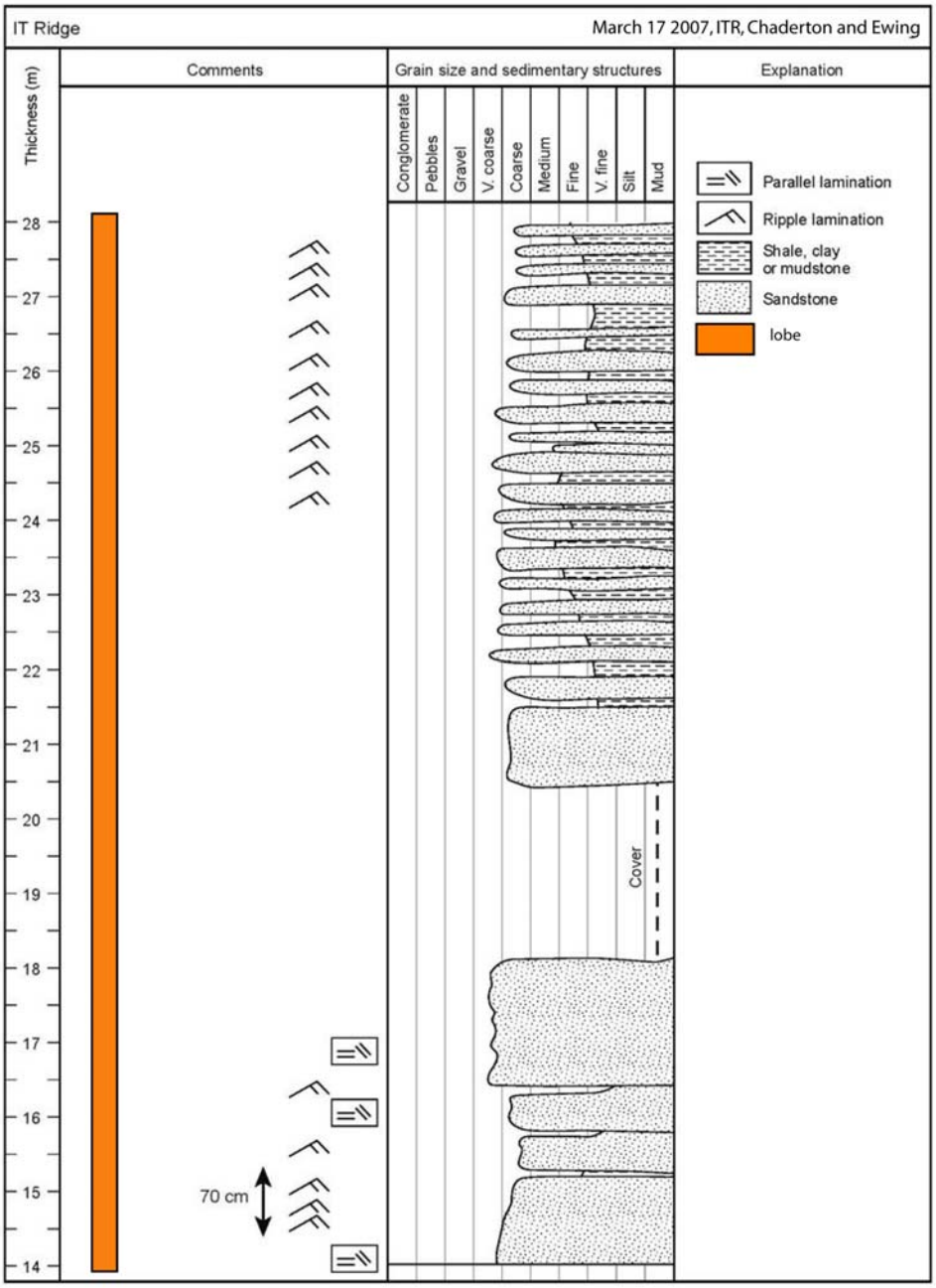

Figure 2.38b: Inner Turner's Hall Ridge measured stratigraphic section interpreted as deposits of a deep water fan depositional lobe.

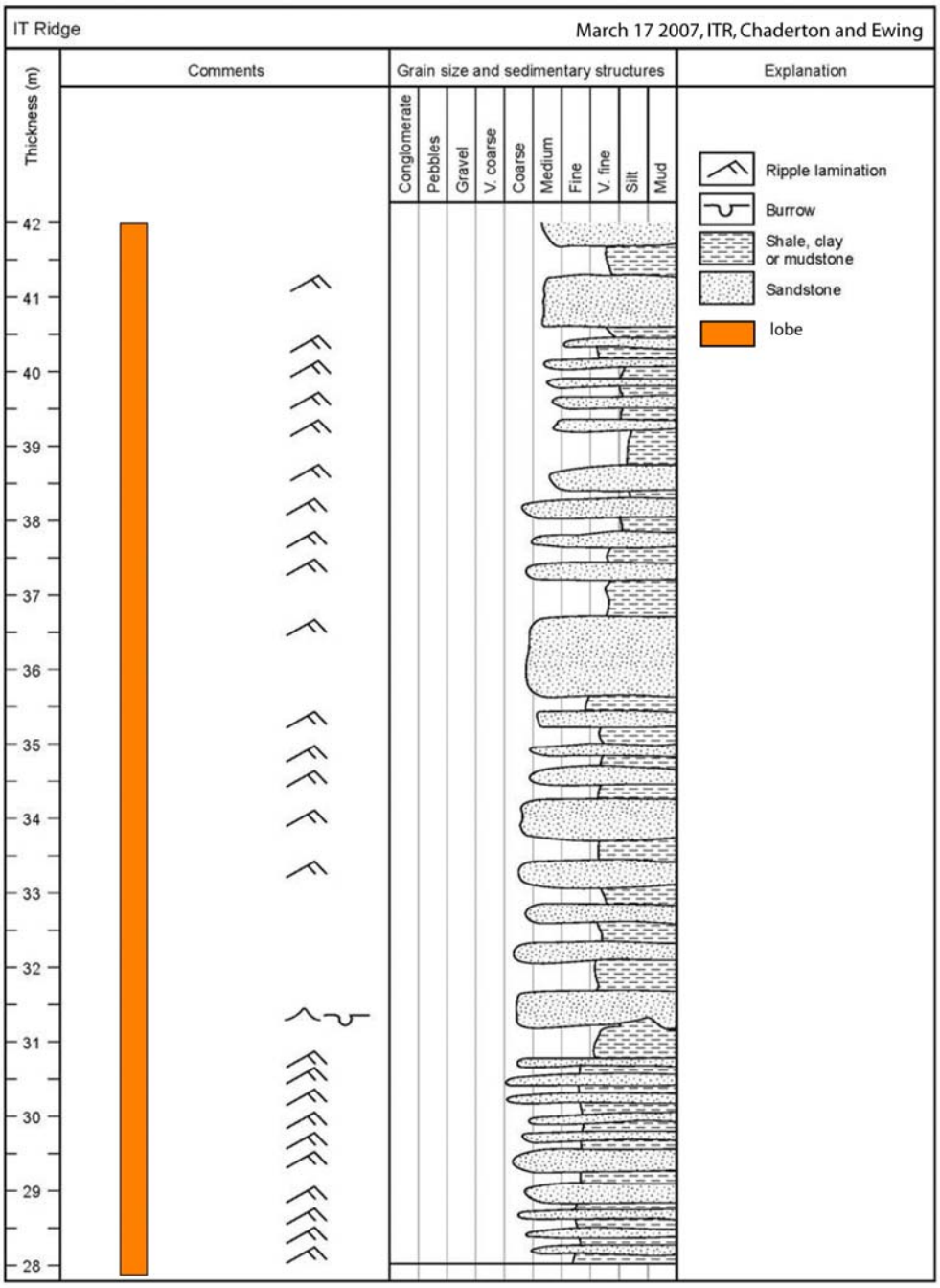

Figure 2.38c: Inner Turner's Hall Ridge measured stratigraphic section interpreted as deposits of a deep water fan depositional lobe.

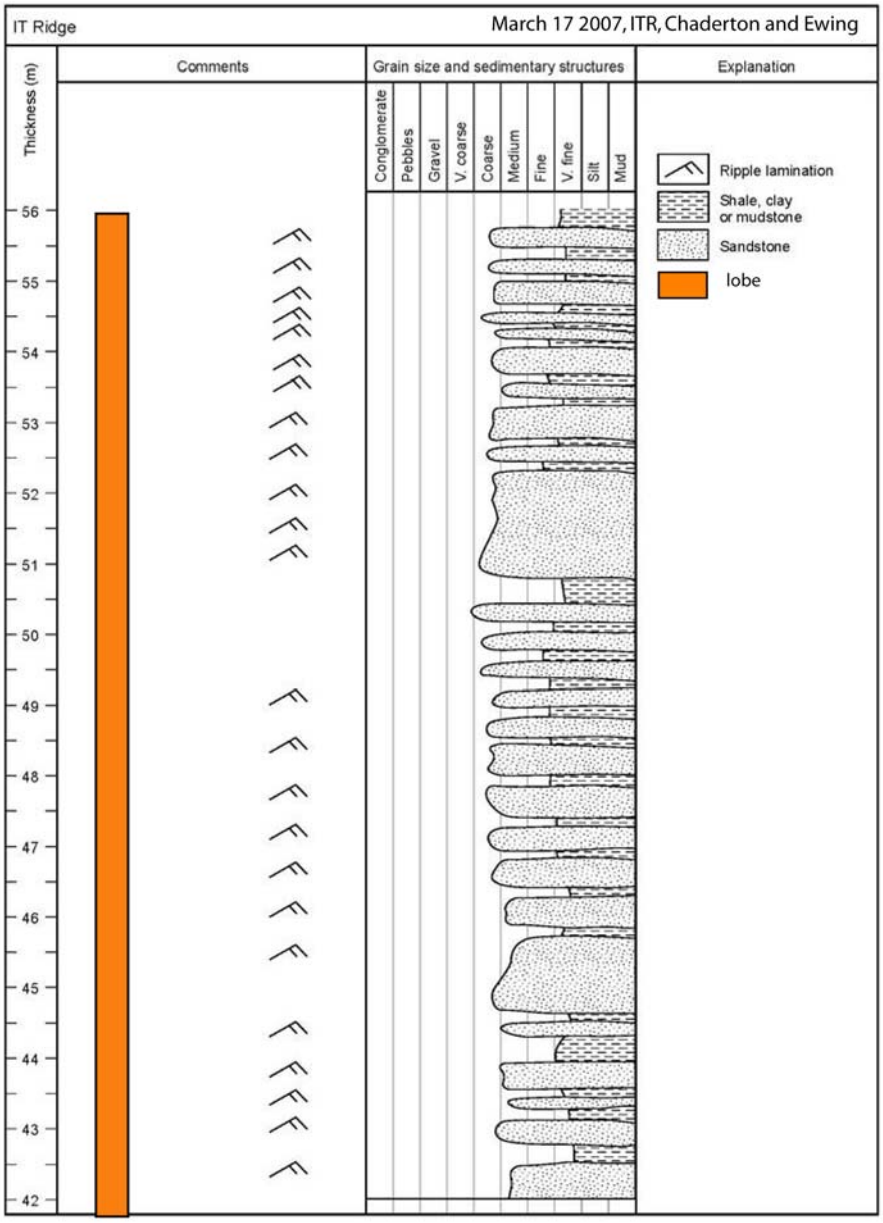

Figure 2.38d: Inner Turner's Hall Ridge measured stratigraphic section interpreted as deposits of a deep water fan depositional lobe.

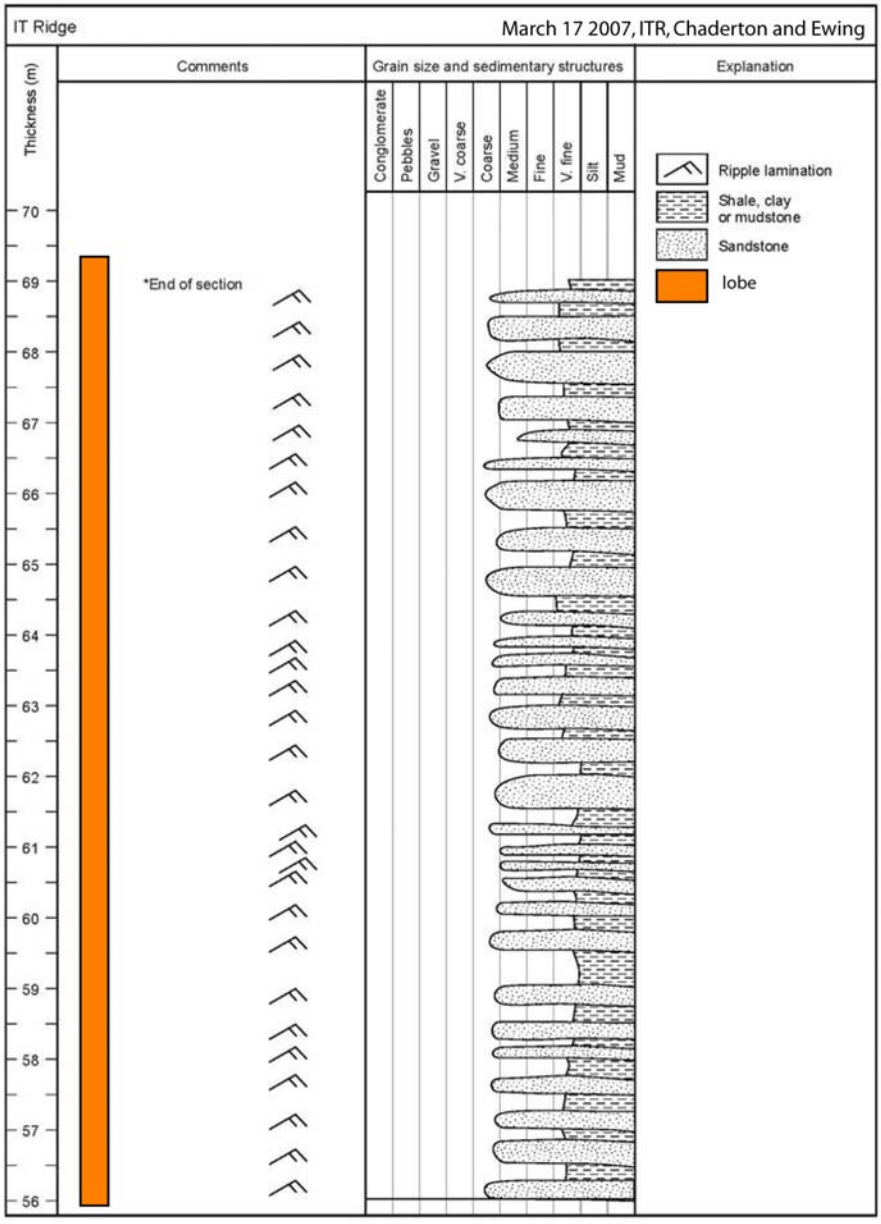

Figure 2.38e: Inner Turner's Hall Ridge measured stratigraphic section interpreted as deposits of a deep water fan depositional lobe.

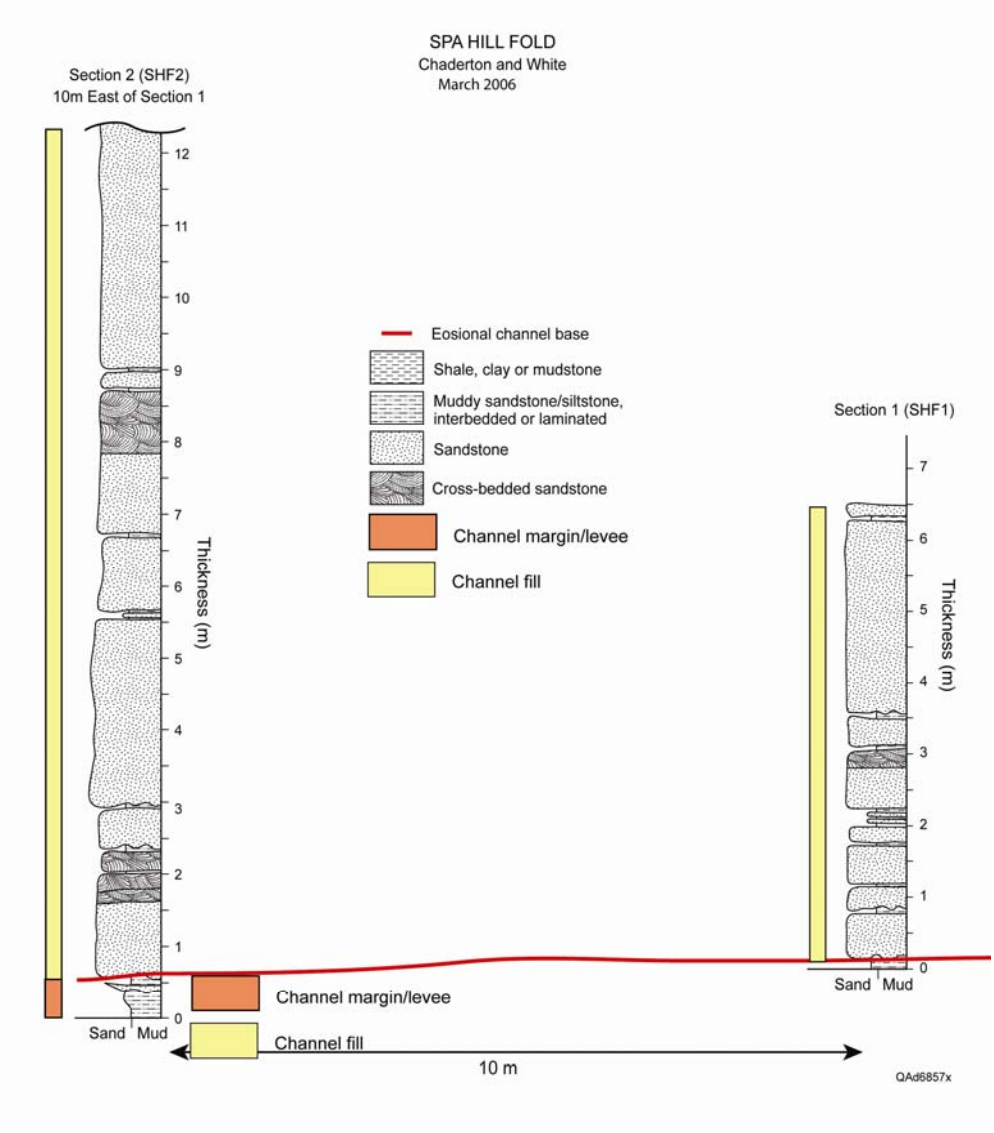

Figure 2.39: Spa Hill measured stratigraphic sections and correlation panel. The section is interpreted as deep water channel and channel margin elements.

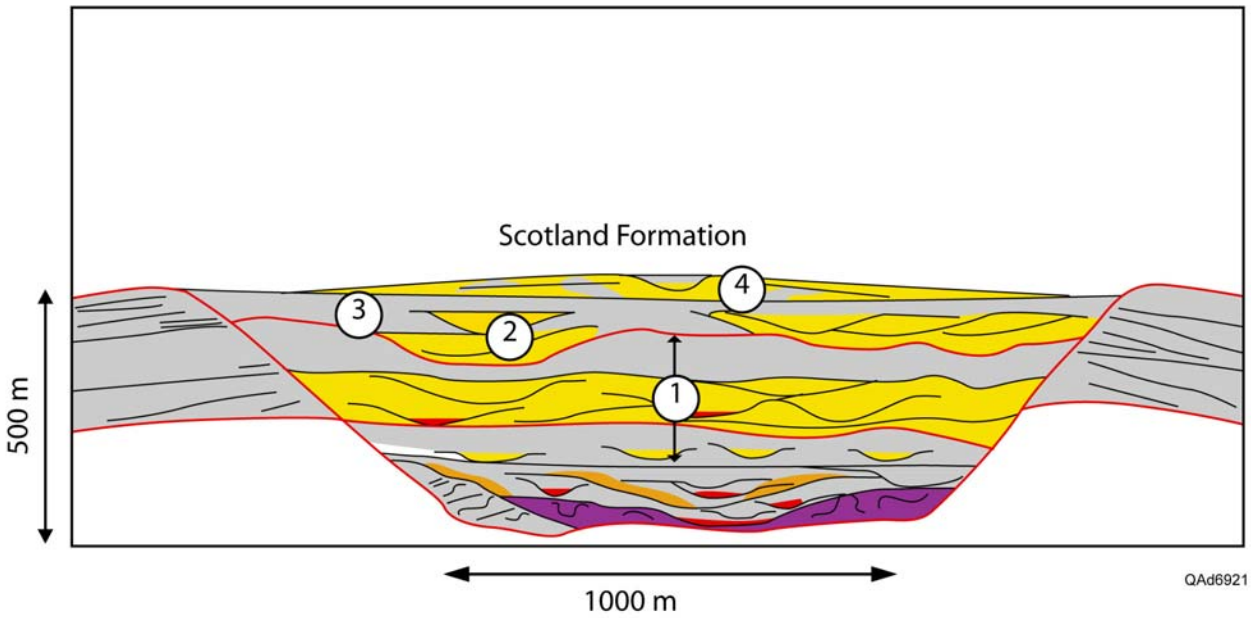

1. Sand rich- Channel complex system set- Chalky Mount Ridge, Sleeping Giant Ridge type deposit

2. Sand rich Channel Complex- Walker's Ridge type deposit

3. Mud rich Master Levees- Chalky Mount Lower, Walker's Ridge Lower type deposit.

4. Sand Rich- more distal lobe facies- Inner Turner's Hall Ridge deposits

Figure 2.40: Depositional Model for Scotland Formation deposits

Juniper Ridge, California **Scotland Formation, Barbados**

Figure 2.41: Interbedded sandstone and mudstone levee-deposits flanking the channels within the JRC on the left, Facies 5 of the Scotland Formation on the right (photo taken at the Ermy Bourne Ridge). Photo on the left is from Lowe (2004).

Juniper Ridge, California **Scotland Formation, Barbados**

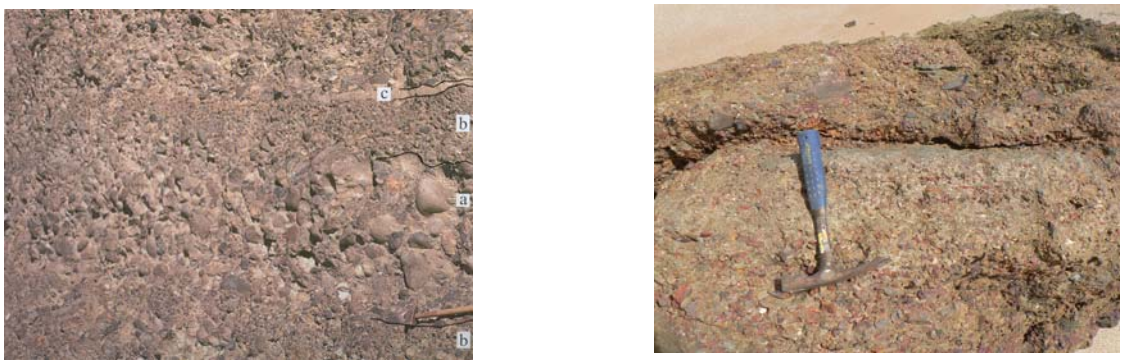

Figure 2.42: Coarse, cobble and pebble conglomerate channel fill of the Juniper Ridge Conglomerate on the left photo from Lowe, (2004). The Scotland Formation is on the right. Photo taken at conglomerate bed exposed n the beach, about 100 m east of the East Coast Road outcrop.

Location Name	Latitude	Longitude
Chalky Mount Ridge	13°14'18.88"N	59°33'18.14"W
Ermy Bourne Ridge	13°14'42.19"N	59°33'3.73"W
Sleeping Giant Ridge	13°14'27.33"N	59°33'4.13"W
Sleeping Giant Ridge/ East Coast Rd	13°14'23.74"N	59°32'46.76"W
Spa Hill	13°12'40.27"N	59°33'53.76"W
Mount All	13°13'22.84"N	59°34'21.33"W
Inner Turner's Hall Ridge	13°13'35.54"N	59°34'36.08"W
Walker's Ridge	13°15'32.09"N	59°34'59.10"W

Table 2.1: Latitudes and Longitudes of outcrop locations where data was collected for this study.

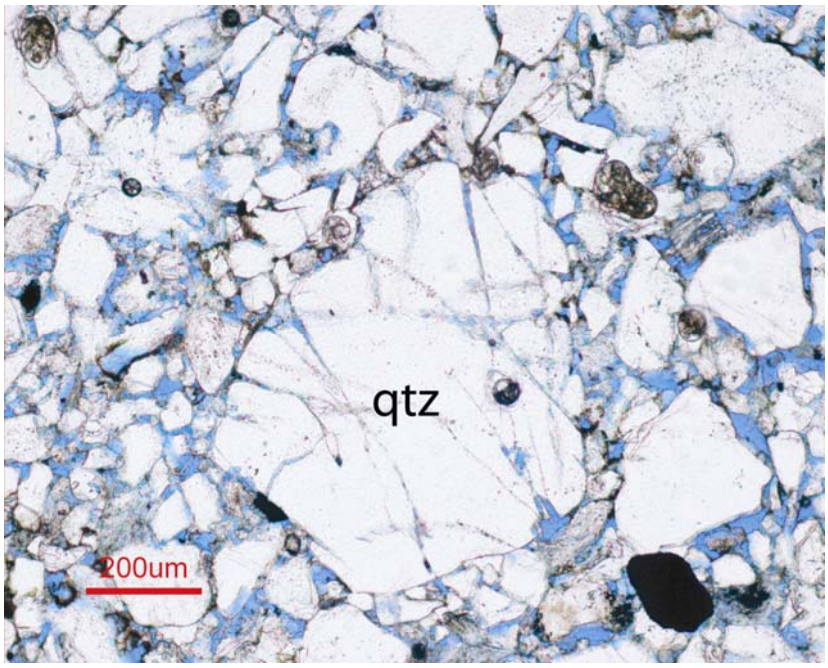

Figure 3.1: Fractured quartz grain (**qtz**). Secondary porosity is created within factures. Also note that no quartz cement has precipitated within fractures.

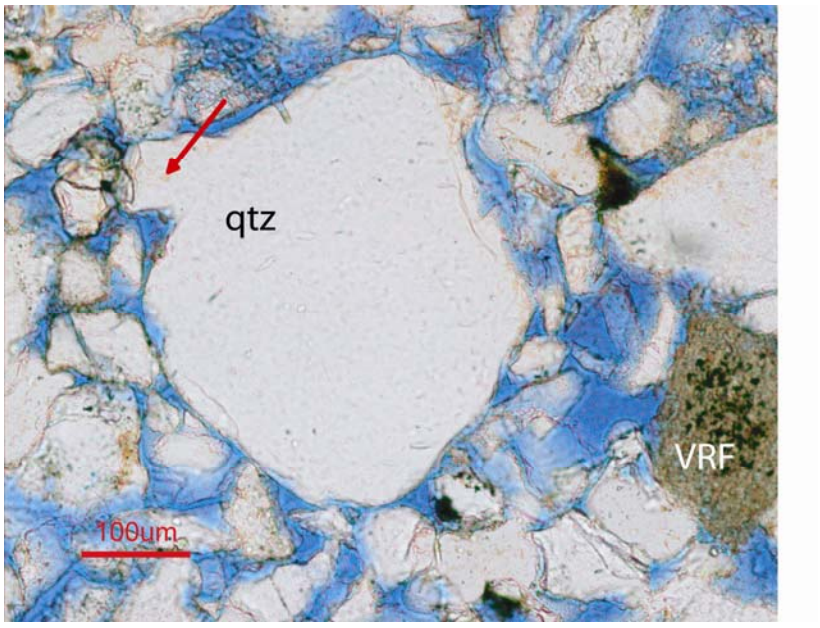

Figure 3.2: Recycled quartz grain. Red arrow shows broken overgrowth. Volcanic rock fragment comprised of weathered feldspars and pyrite is labeled VRF.

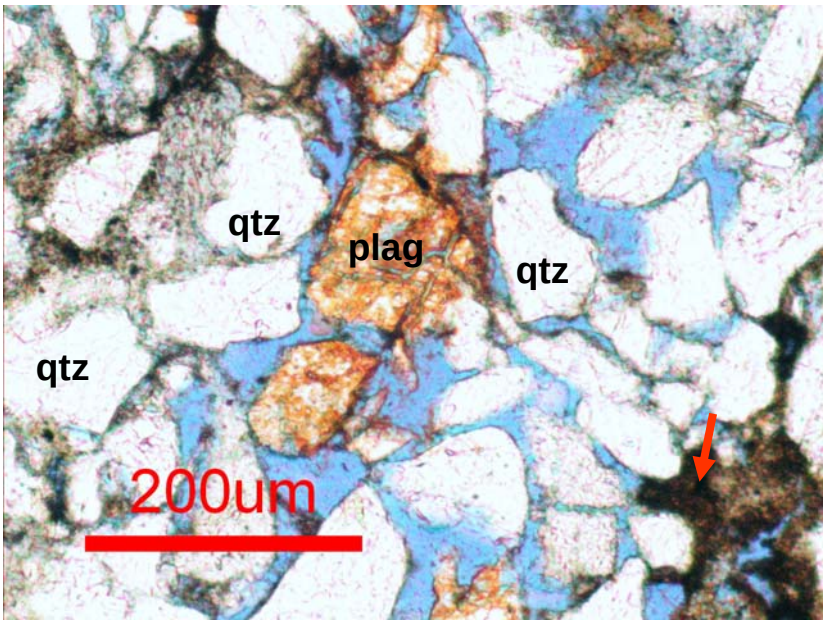

Figure 3.3: Pink stained Ca-plagioclase (plag) that is being weathered. Red arrow shows late stage hematite cement and clay that are filling pore spaces. Quartz grain are labeled with qtz.

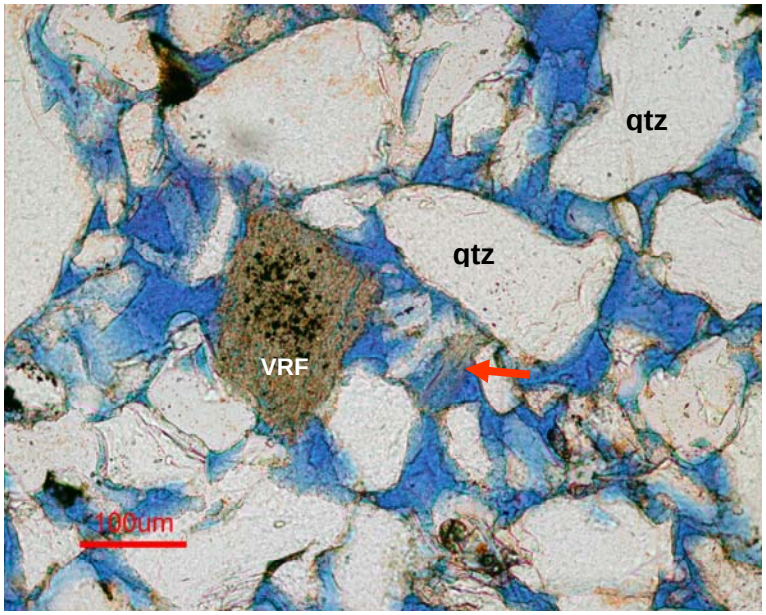

Figure 3.4: Volcanic rock fragment (**VRF**) surrounded by recycled quartz (**qtz**). Black dots within the VRF grain are pyrite. Red arrow shows a K-feldspar grain that has been almost completely dissolved by formation fluids.

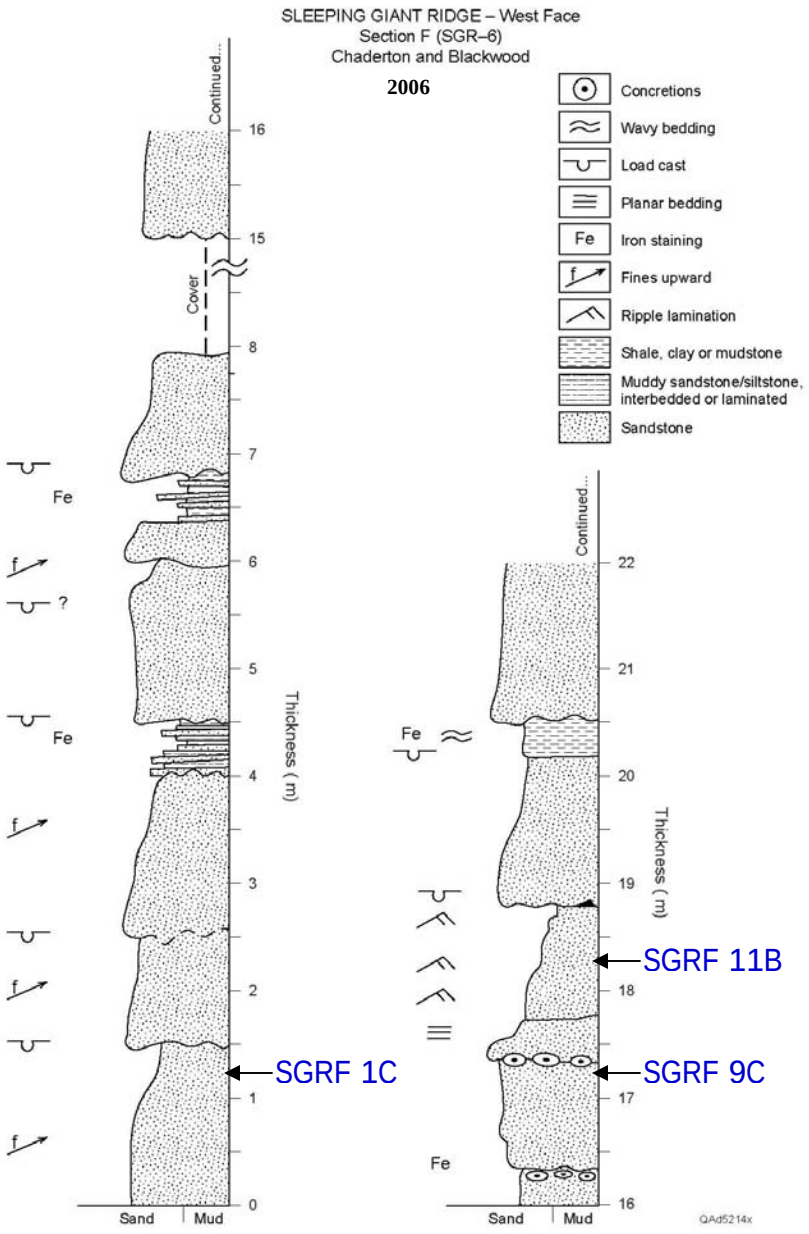

Figure 3.5: Measured Section of outcrop SGRF showing the beds where samples SGRF 1C, SGRF 9C, SGRF 11B were collected.

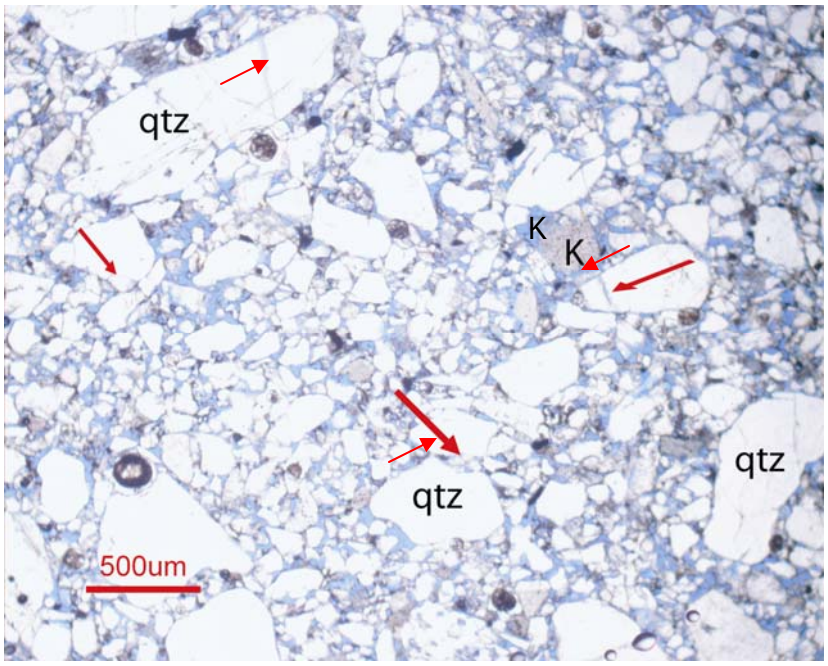

Figure 3.6: Photo of sample SGRF 1C showing fractured quartz grains (red arrows) and the lack of fine-grained matrix. K feldspar is identified with a K.

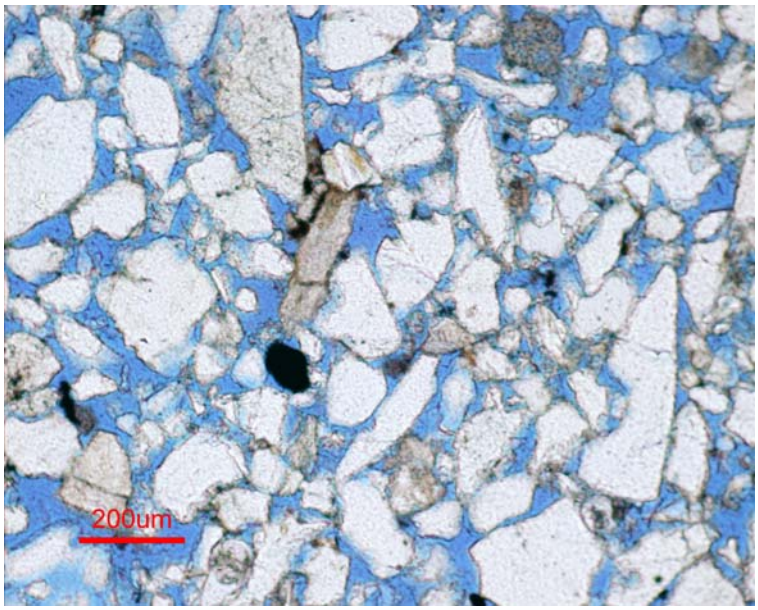

Figure 3.7: Photo of sample SGRF 9C showing grain-to-grain contact. Note the fractured grains and the lack of fine-grained matrix and cement.

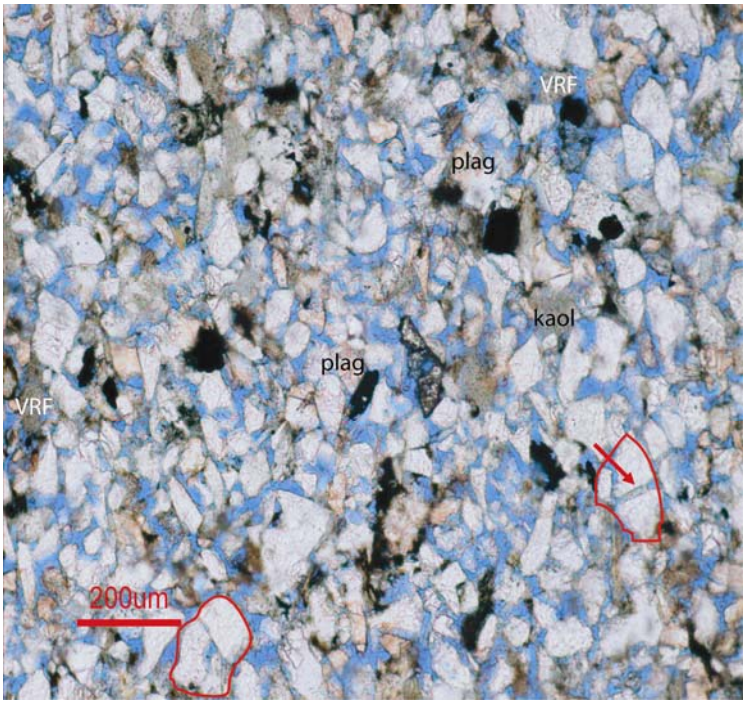

Figure 3.8: Photo of sample SGRF 11B showing fractured grains outlined in red plagioclase feldspar (plag), pore filling kaolinite (kao) and a volcanic rock fragment (VRF).

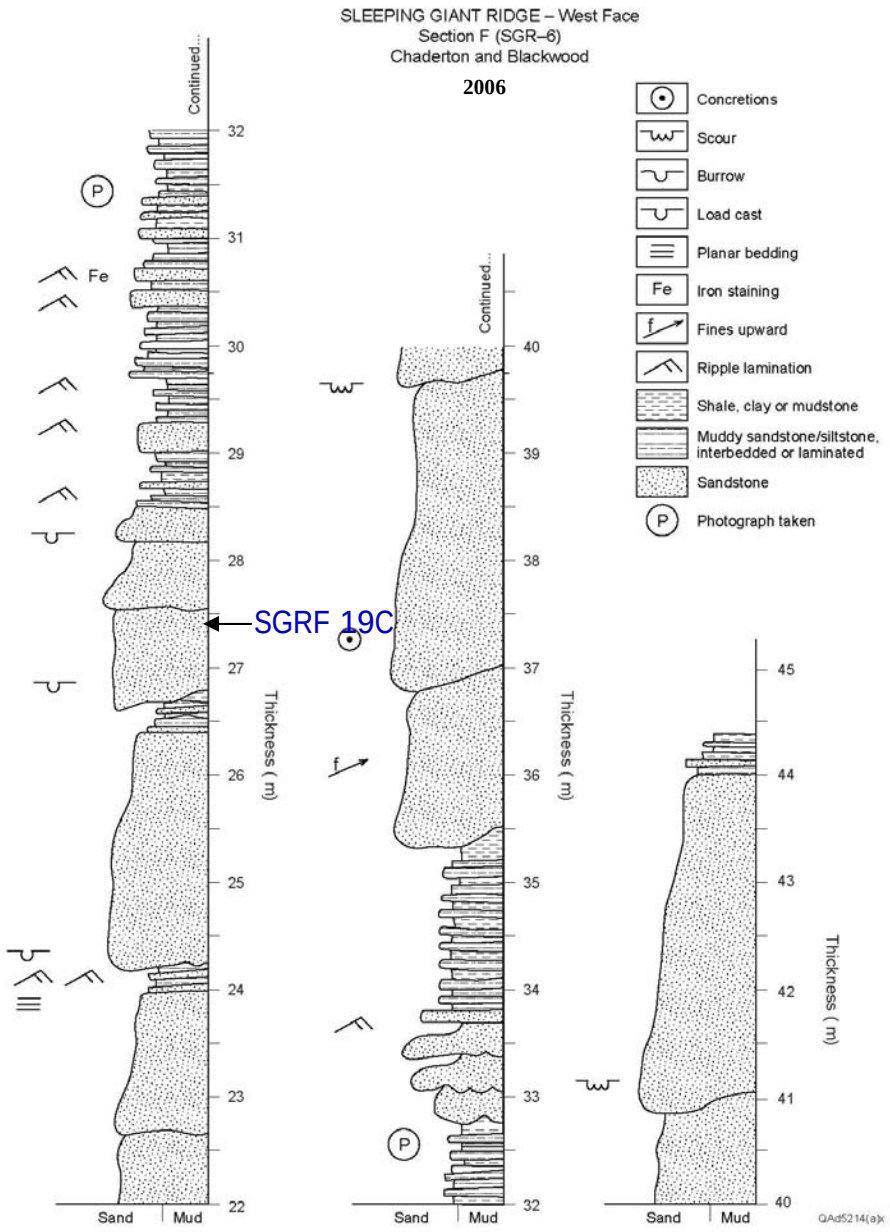

Figure 3.9: Measured Section of outcrop SGRF showing the bed where sample SGRF 19C was collected.

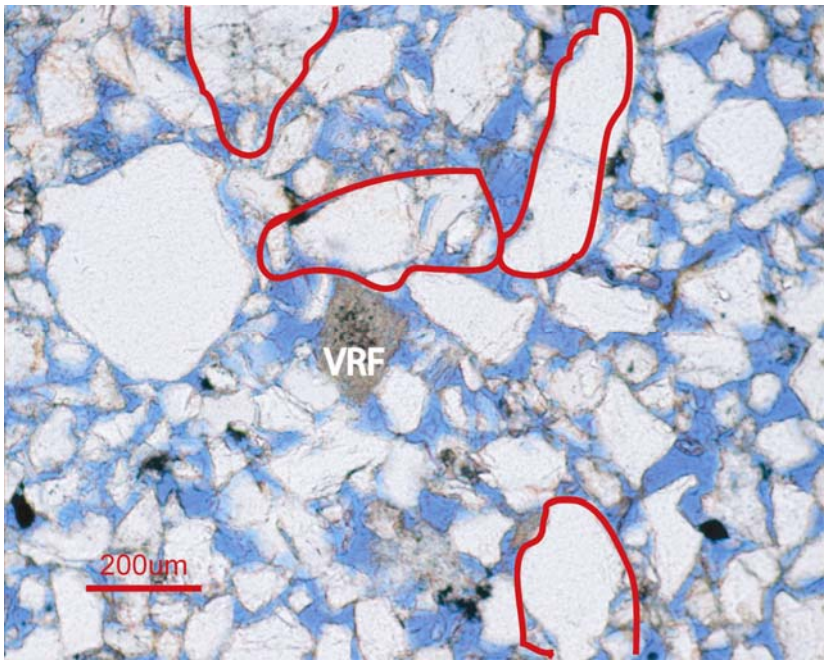

Figure 3.10: Photo of sample SGRF 19C showing grain to grain contact. Note the fractured grains outlined in red and the lack of cement, lack of fine-grained matrix and a volcanic rock fragment (VRF).

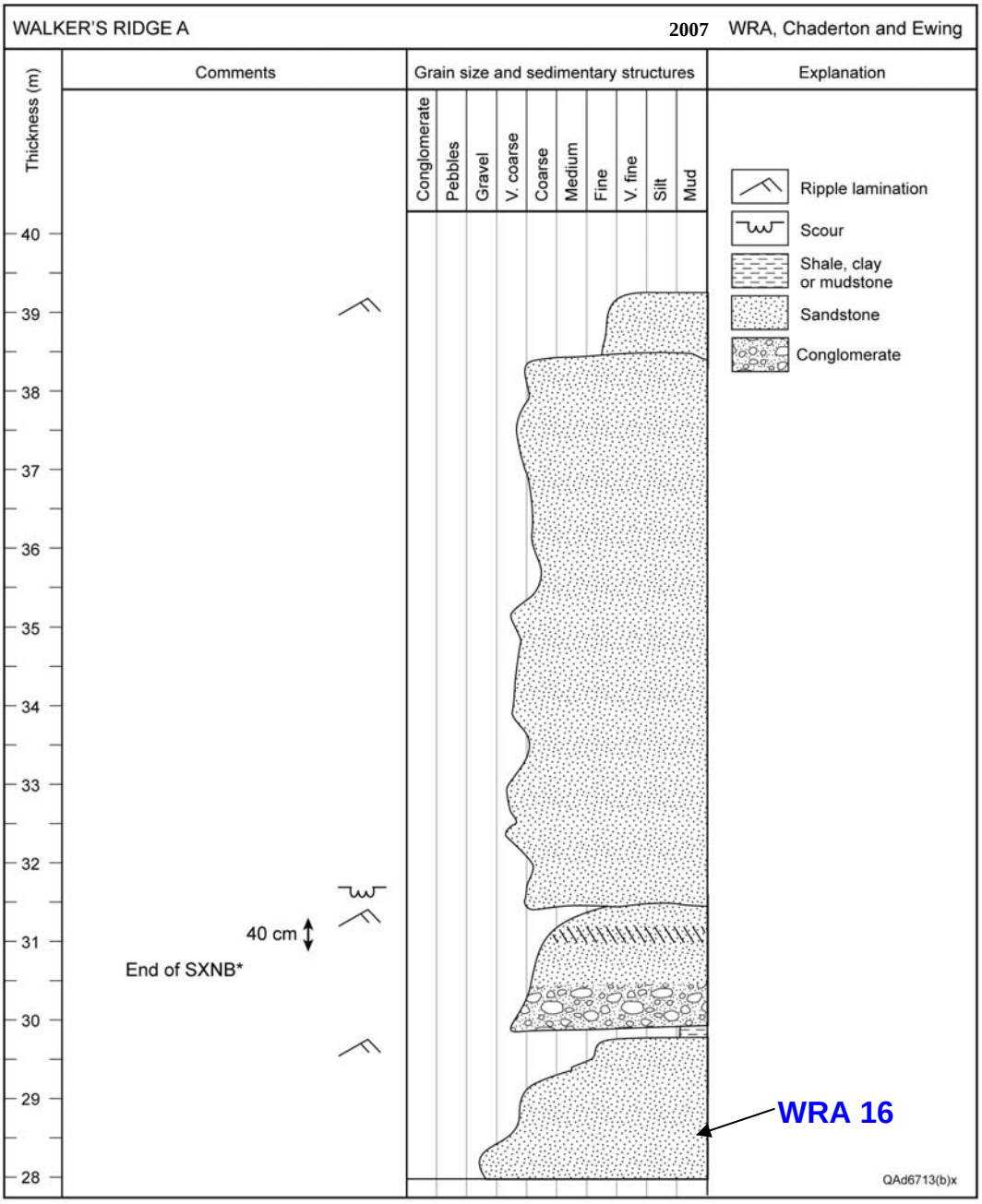

Figure 3.11: Measured Section of outcrop WRA showing the bed where sample WRA 16 was collected.

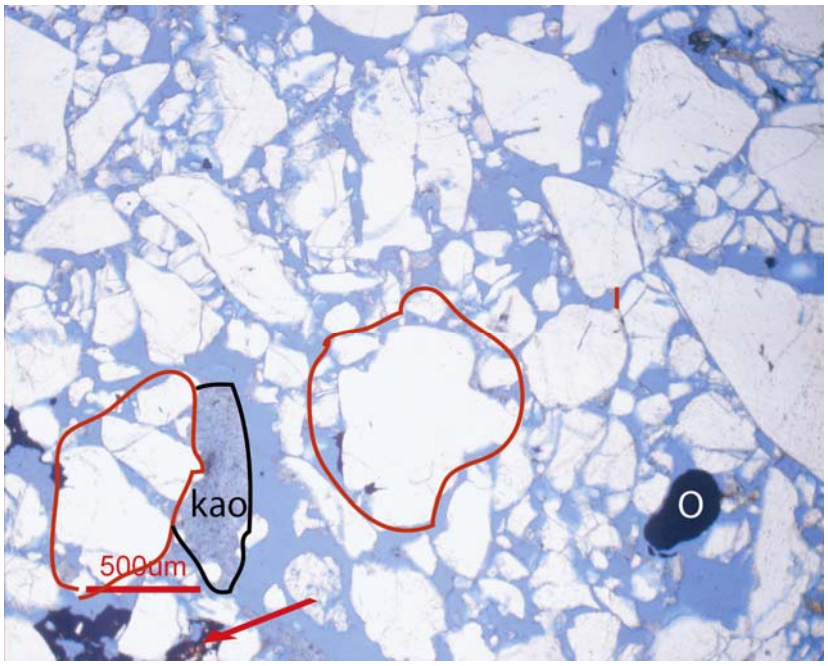

Figure 3.12: Photo of sample WRA 16 showing fractured quartz grains, some of which are outlined in red, organic (O) matter and one feldspar grain that has been replaced by kaolinite (kao). Red arrow points to hematite cement.

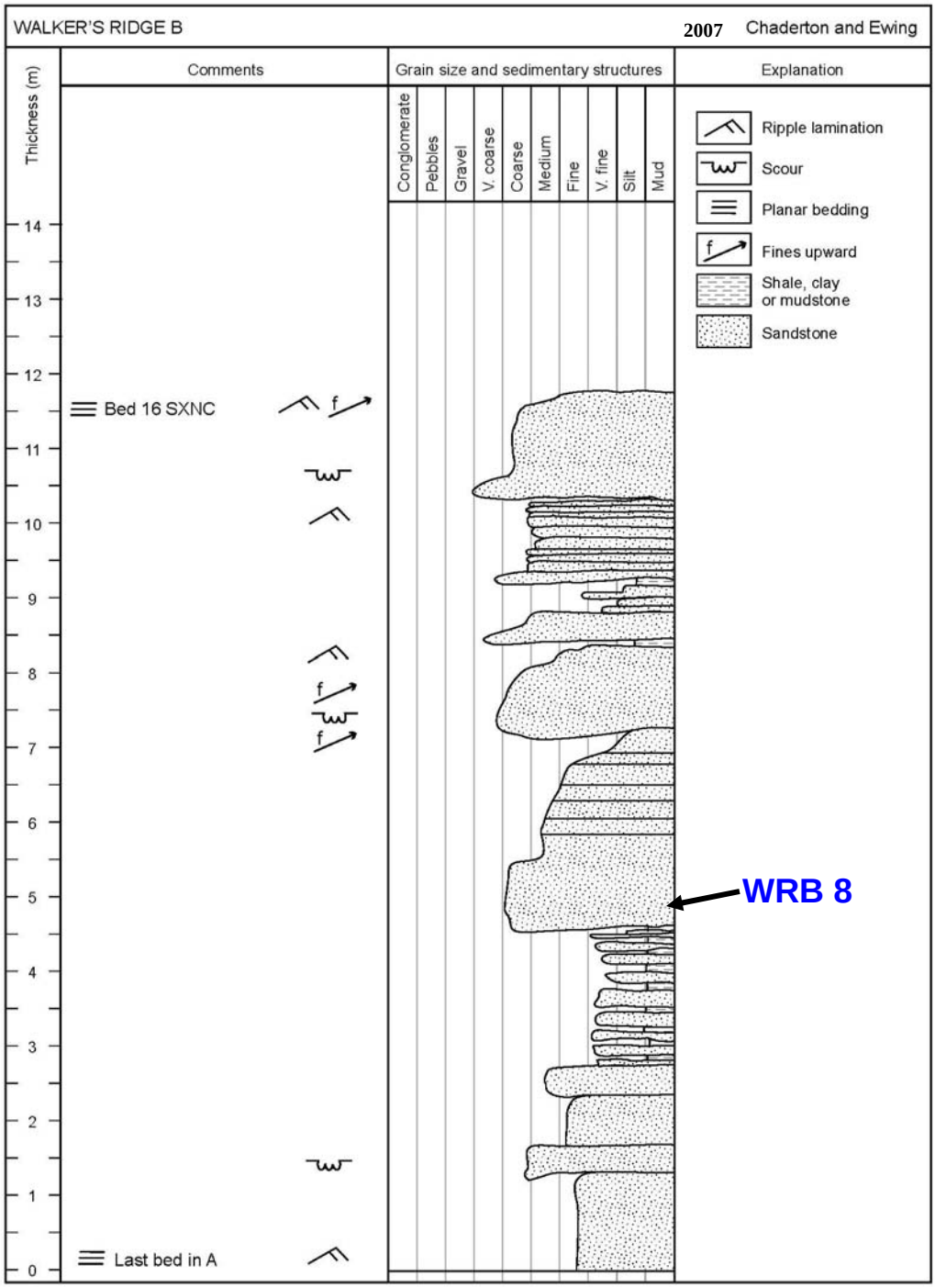

Figure 3.13: Measured Section of outcrop WRB showing the bed where sample WRB 8 was collected.

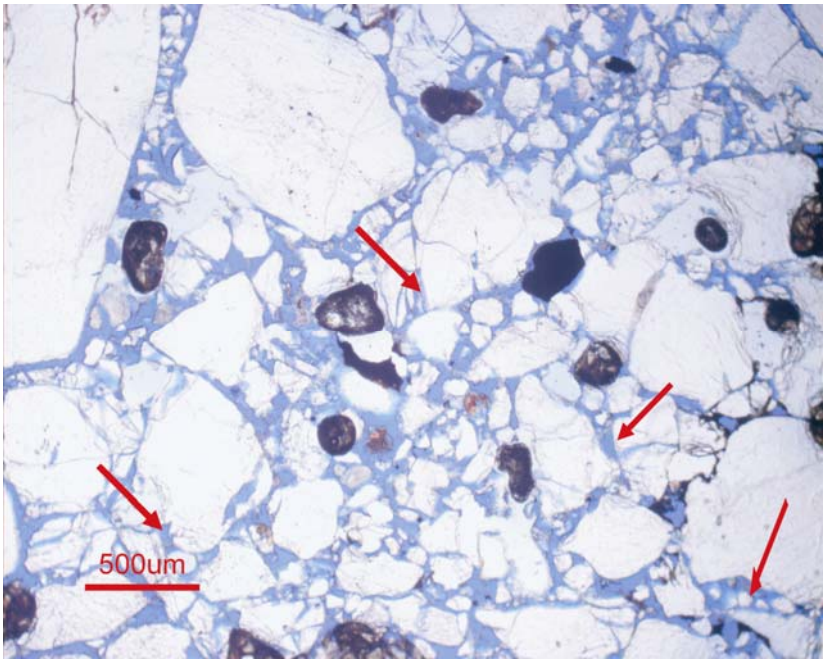

Figure 3.14: Photo of sample WRB 8 showing fractures in quartz grains (red arrows).

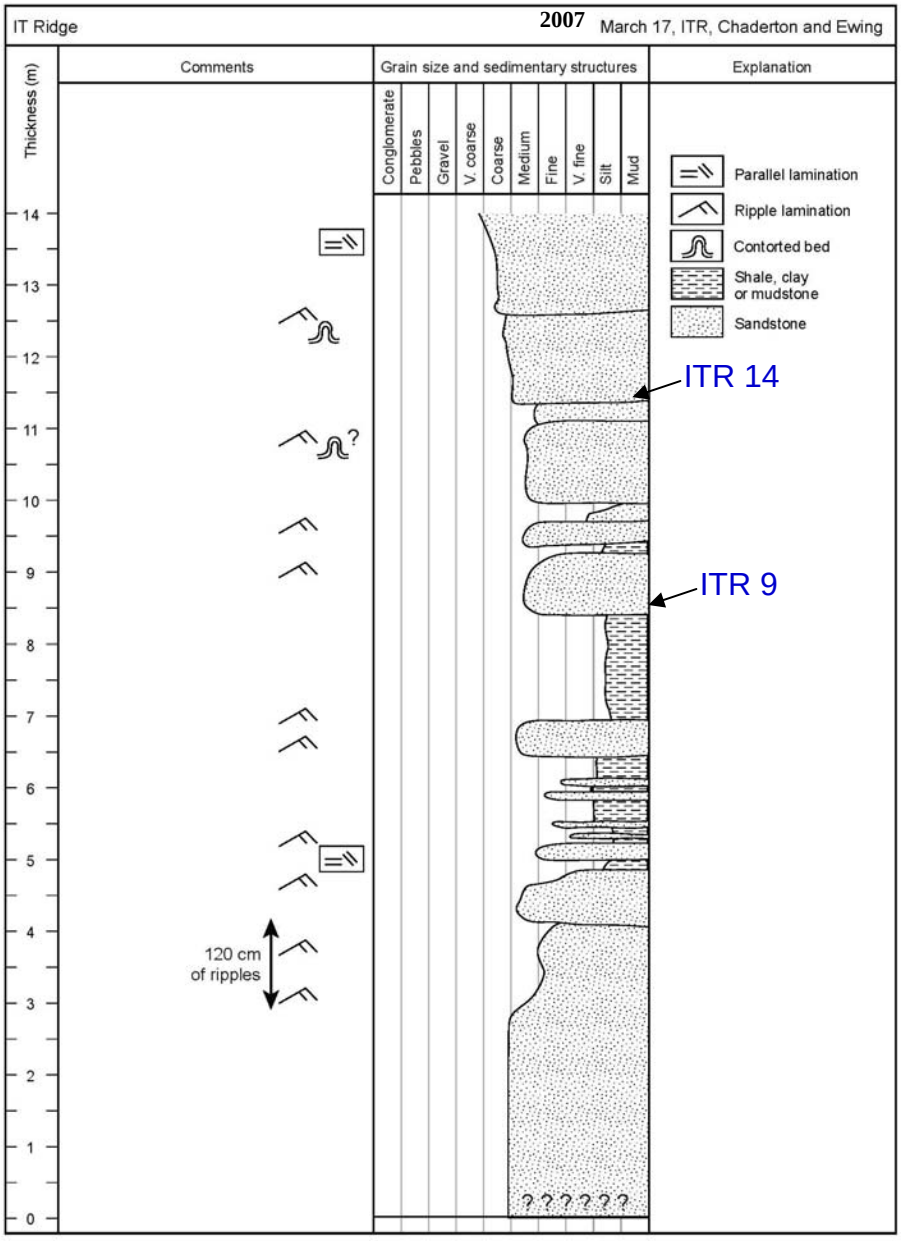

Figure 3.15: Measured Section of outcrop ITR showing the beds where samples ITR 9 and ITR 14 were collected.

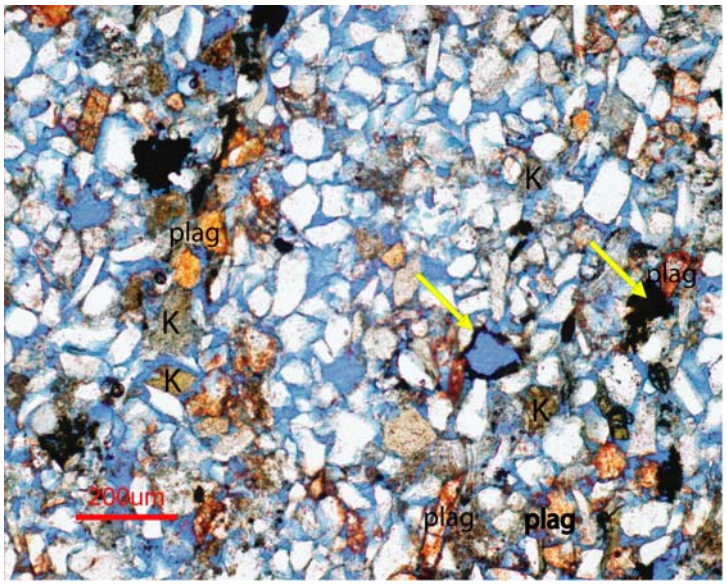

Figure 3.16: Photo of sample ITR 9 showing increased plagioclase (pink) labeled plag and K-feldspar (light brown and yellowish) content labeled K. Hematite cement (black/opaque) is present within pore spaces and is in some areas occluding pore throats (yellow arrows).

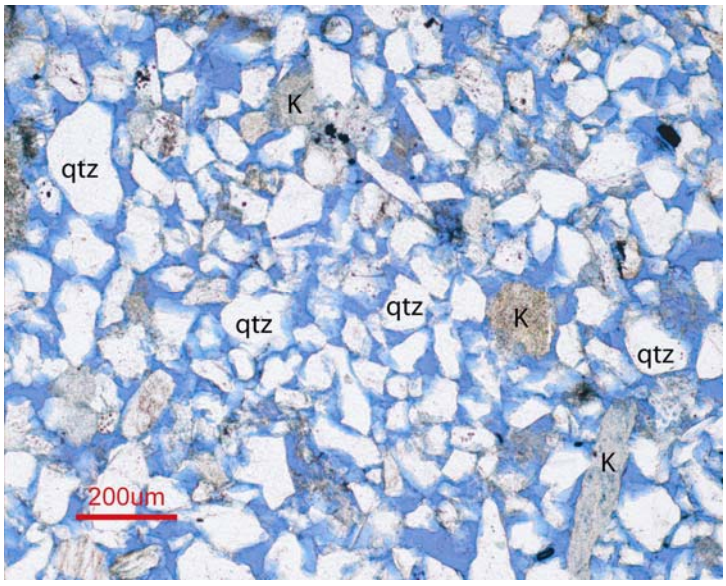

Figure 3.17: Photo of sample ITR 14 showing decreased plagioclase (pink) content. K feldspar (light brown and yellowish) and quartz grains are more abundant in this sample.

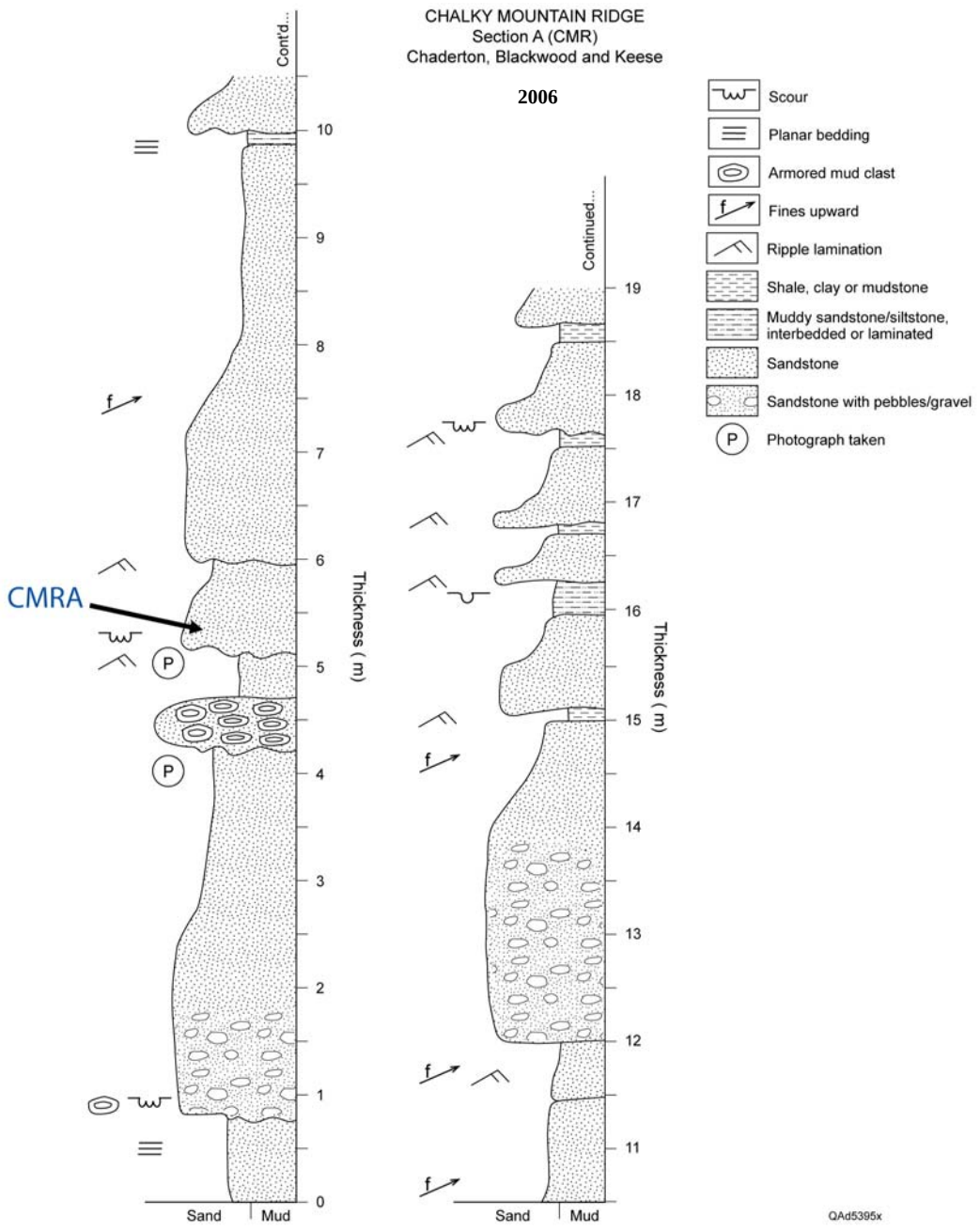

Figure 3.18: Measured Section of outcrop CMRA showing the beds where sample CMRA was collected.

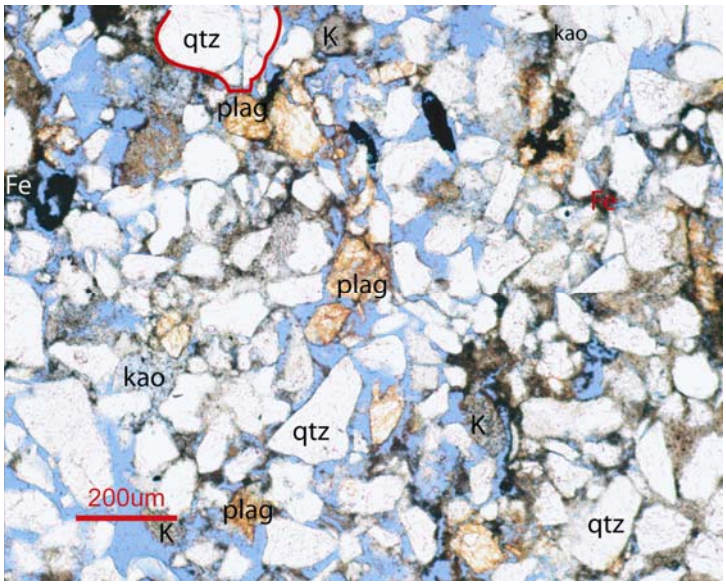

Figure 3.19: Photo of sample CMRA showing plagioclase (pink) and K-feldspar (light brown and yellowish) along with recycled quartz grains. Pore spaces are partially filled with grayish-brownish kaolinite cement

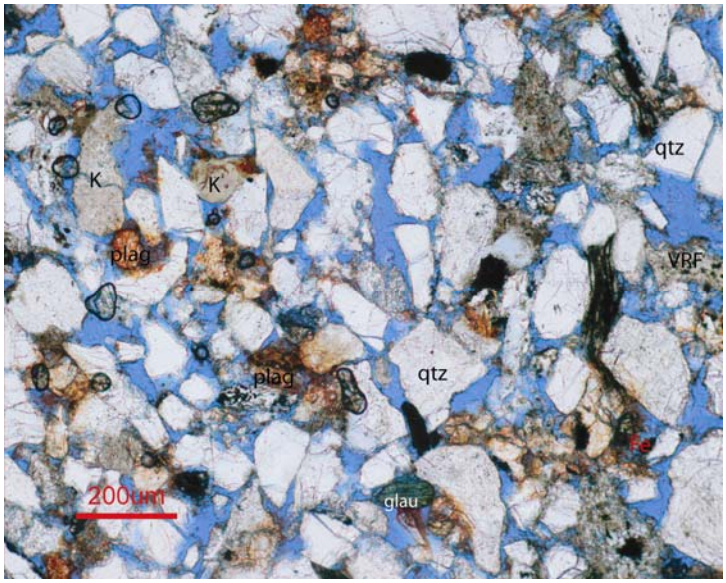

Figure 3.20: Photo of sample from Breedy's location (see Figure 2.8) showing plagioclase (pink) labeled plag, and K-feldspar (light brown and yellowish) labeled K.. In the lower part of the photo there is a rounded, dark green grain that is a glauconite grain. Volcanic rock fragments (VRF) are also present.

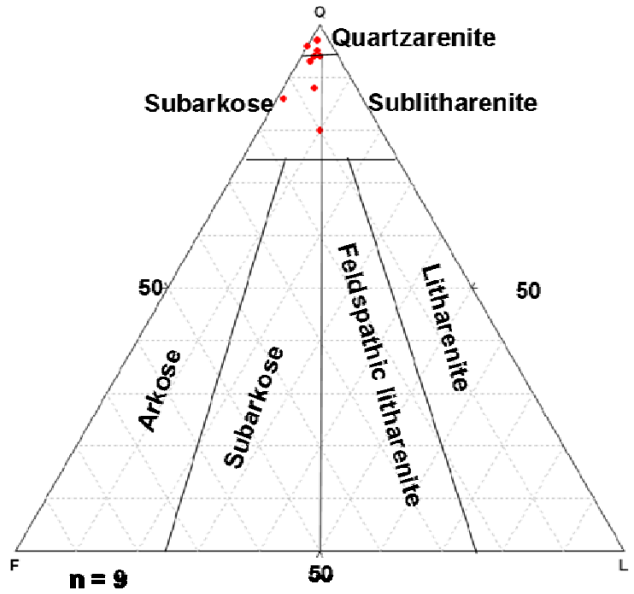

Figure 3.21: Composition of Scotland Formation samples point counted by Punch (2004), plotted on a QFR diagram.

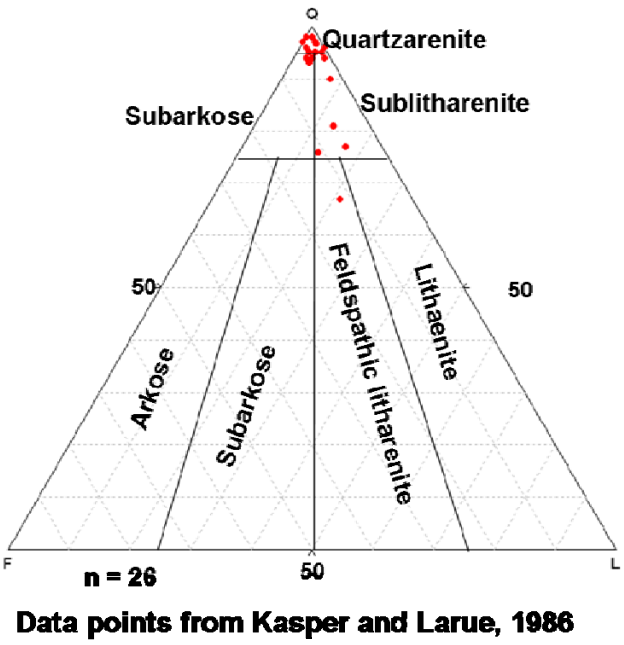

Figure 3.22: Composition of Scotland Formation samples point counted by Kasper and Larue, (1986) plotted on a QFR diagram.

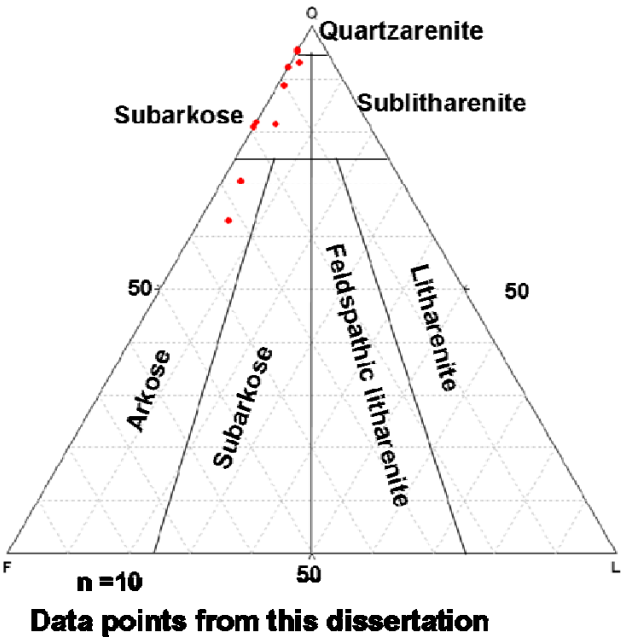

Figure 3. 23: Composition of Scotland Formation samples point counted in this study plotted on a QFR diagram.

Sample	Facies	IGV	Fracture Porosity	Deformation Bands	Sorting	Mean Phi Grain size	Classification
Breedy's	?	41.0%	6.0%	No	moderate	3.29	subarkose
CMRA	channel	42.0%	3.5%	Yes	moderate	3.39	subarkose
ITR 9	lobe	38.0%	5.0%	No	moderate	3.66	arkose
ITR 14	lobe	41.0%	3.5%	No	moderate	3.72	arkose
SGRF 1C	channel	32.5%	2.5%	Yes	moderate	3.56	subarkose
SGRF 9C	levee	28.5%	6.0%	No	moderate	3.7	subarkose
SGRF 11B	channel	32.5%	2.5%	No	moderate	3.56	subarkose
SGRF 19C	channel	32.5%	10.5%	No	moderate	2.97	subarkose
WRA 16	channel	28.0%	5.0%	No	poor	1.99	quartz arenite
WRB 8	channel	29.0%	7.5%	No	poor	2.18	quartz arenite

Table 3.1: Table showing a compilation of some of the results of point counting the thin sections.

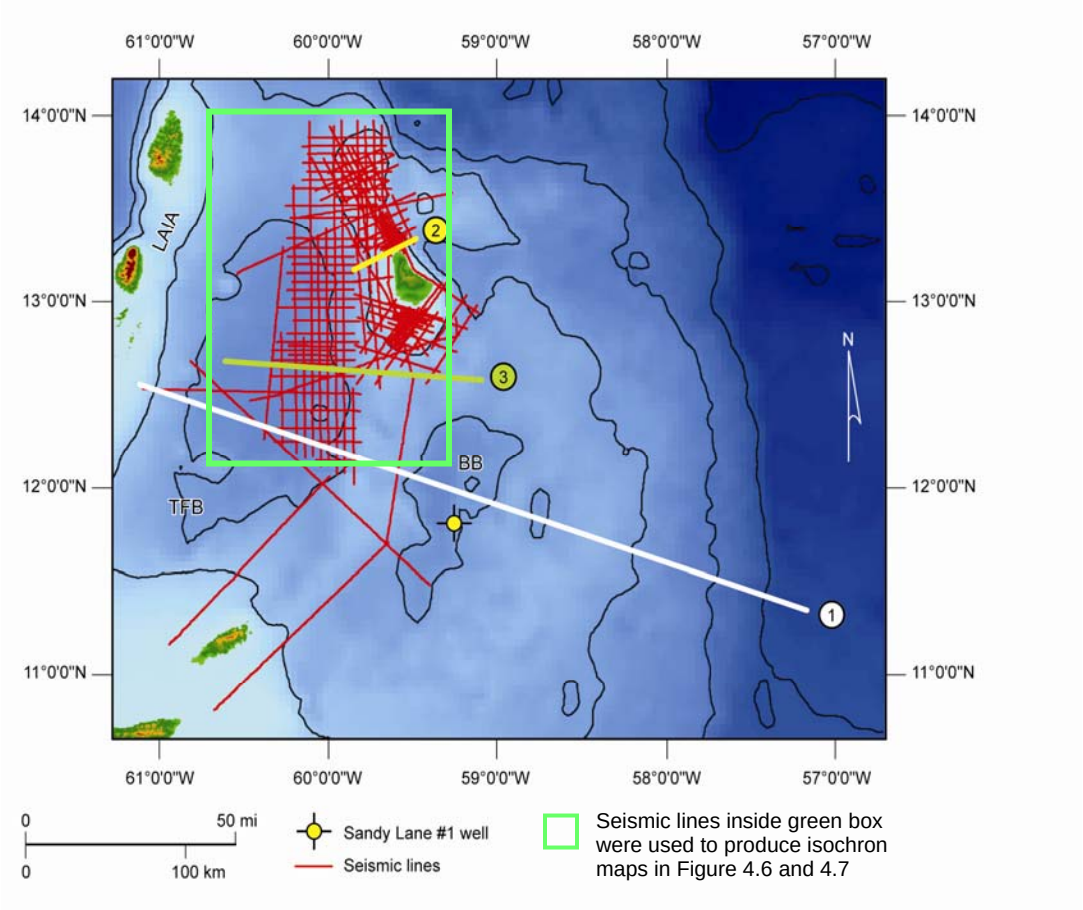

Figure 4.1: Base map showing seismic line survey and location of seismic lines used for interpretation in this study. Numbers indicate lines shown in this paper. BB- Barbados Basin TFB- Tobago Forearc Basin, LAIA- Lesser Antilles Island Arc.

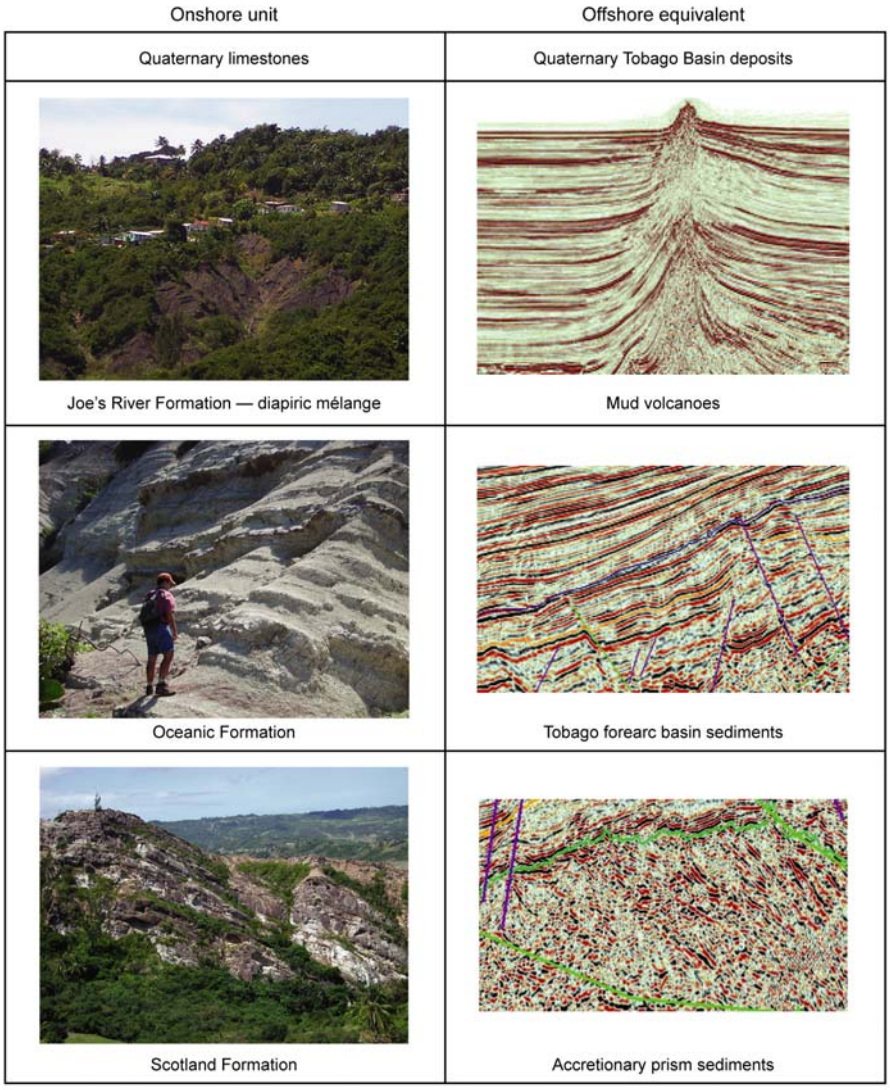

Figure 4.2: Sedimentary units in outcrop and the seismic response of their offshore equivalents

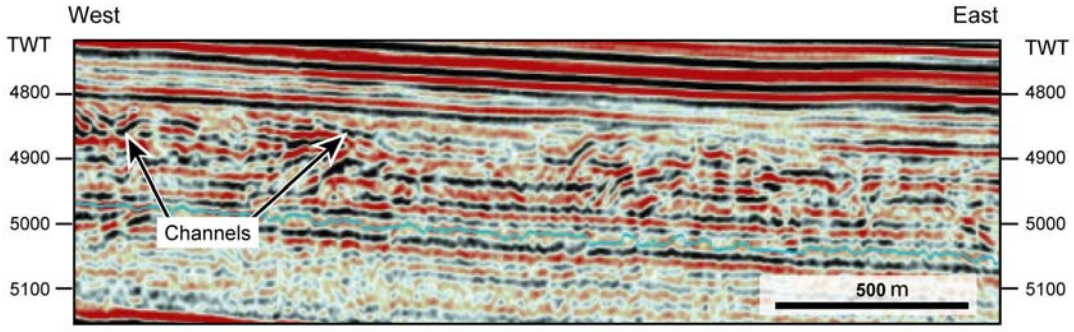

Figure 4.3: Channels within Unit Five. The light blue horizon is the Middle Miocene unconformity that bounds the top of Unit Four.

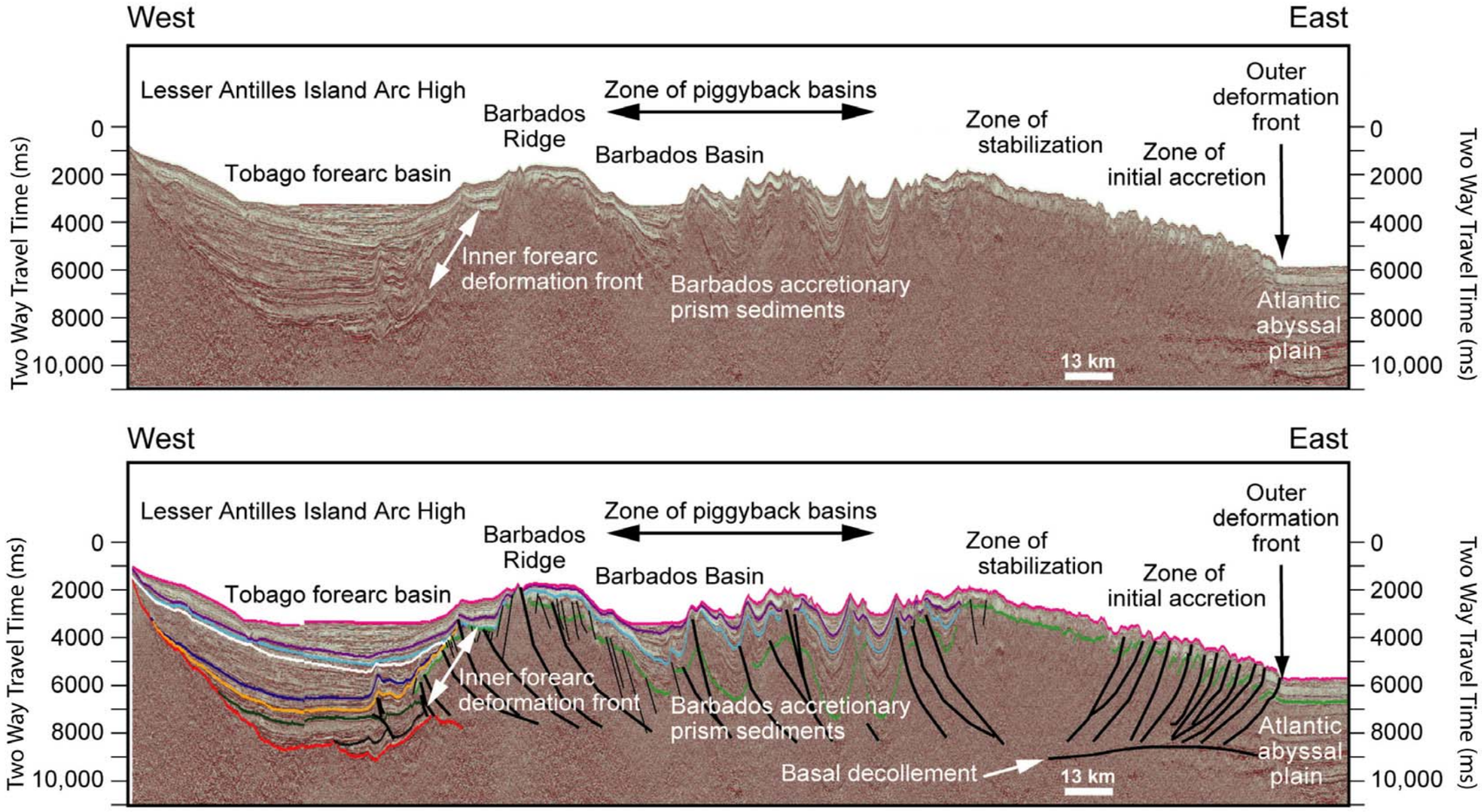

Figure 4.4: East-west seismic reflection profile showing the structural provinces within the study area. The location of the seismic line is shown as line 1 in Figure 4.1. The Lesser Antilles Island Arc High bounds the western margin of the Tobago Forearc Basin (TFB) that has up to 12 km of sediment fill in its deepest part. The Inner Forearc Deformation Front marks the boundary between the highly deformed Barbados Accretionary Prism sediments and the less deformed TFB sediments. The Barbados Ridge is the highest part of the accretionary prism and is characterized by extensive crestal normal faulting. The Barbados Basin is the largest of several piggyback basins that have formed on the eastern slopes of west-facing thrusts. The Zone of Stabilization is a region of less intensely deformed sediment that is a transition zone between the Zone of Initial Accretion and the Zone of Piggyback Basins. The Zone of Initial Accretion is made up of an imbricate fan of east-facing thrust faults (shown as dark blue lines) and marks the youngest phase of deformation in the prism, thus it is the zone where previously undeformed sediments of the Atlantic Abyssal Plain are offscraped and accreted to the prism. The Outer deformation Front marks the boundary between the imbricate fan and the undeformed sediments of the Atlantic Abyssal Plain. Oversized Plate (11x17) requires plotter or printer with tabloid printing.

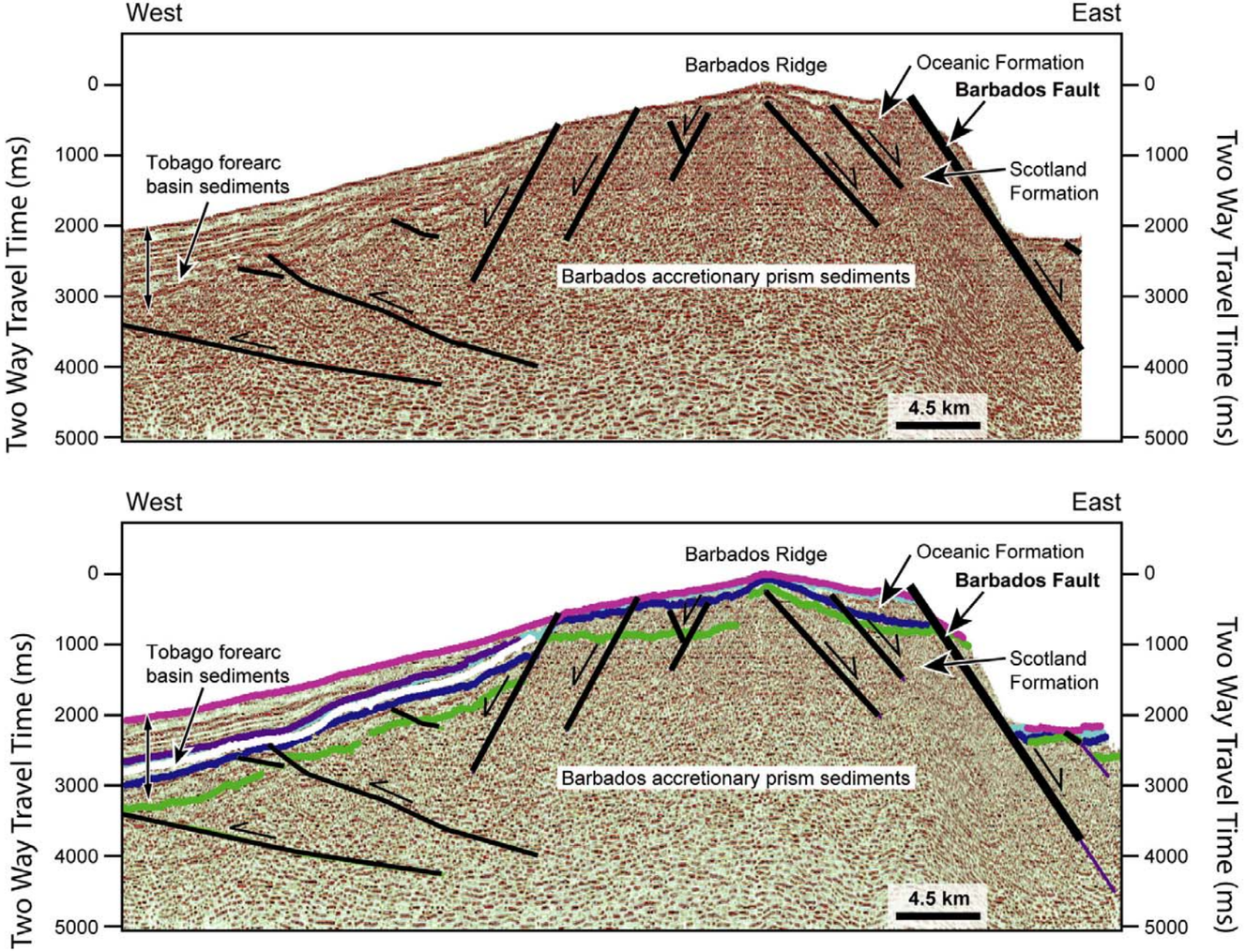

Figure 4.5: Seismic reflection profile across the Barbados Ridge which shows the Barbados Fault to the east and the Tobago Forearc Basin sediments that onlap the Barbados Accretionary Prism sediments to the west. The location of this seismic line is shown as line 2 in Figure 4.1. Oversized Plate (11x17) requires plotter or printer with tabloid printing.

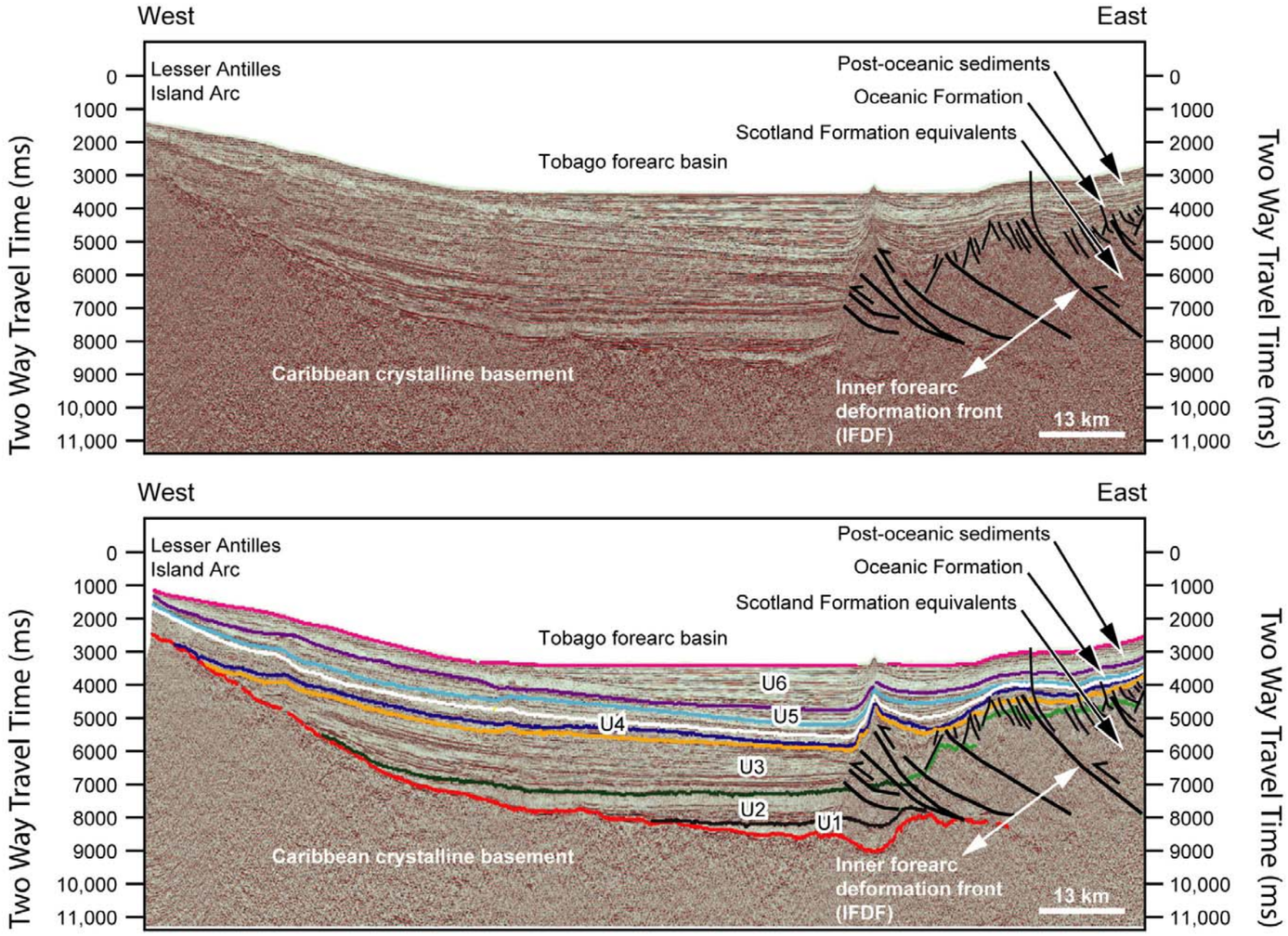

Figure 4.6: East-west reflection seismic profile, shown as line 3 in Figure 4.1, showing 9 horizons mapped across the study area. The Tobago Basin fill is bounded by the crystalline Caribbean Basement and the sea floor. Surfaces shown in the figure are as follows: Bright red- top of the crystalline Caribbean basement; Black- top of Unit One/ Pre-Eocene (no definitive age data exists on this surface but it is thought to be Cretaceous) Dark green, top of Unit Two/ Lower Eocene-Lower Oligocene; Gold -top of Unit Three/ Lower Oligocene to Lower Miocene; Dark blue, top of sub-unit A; White-top of sub-unit B. Light blue- top of sub-unit C/Unit Four/ Lower-Middle Miocene; Purple-top of Unit Five/ Upper Miocene unit; Pink top of Unit Six/seafloor/ Pliocene-Pleistocene ; Bright Green- top of sediments. Oversized Plate (11x17) requires plotter or printer with tabloid printing.

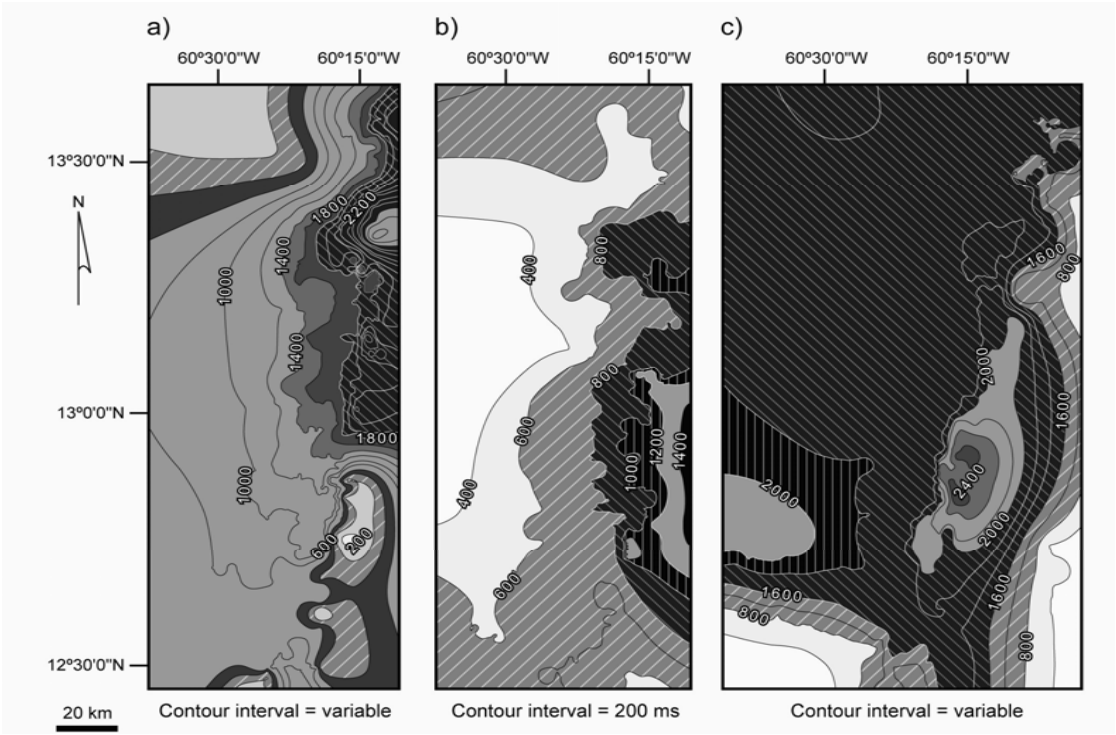

Figure 4.7 Isochron maps of the oldest units of the Tobago Forearc Basin (TFB) fill. A. Pre-Eocene which is confined to a narrow geographic area has a depocenter to the northeastern portion of the TFB. B. Eocene to Lower Oligocene fill is a thinner unit than the previous, older sediments. The depocenter has shifted to the south and is now more centrally located. C. Lower Oligocene to Lower Miocene fill with a depocenter located just west of the present day Inner Forearc Deformation Front. Note that this unit covers a broader geographic area than the previous units and sediment accumulated in the central part of the basin located within an ever broader region to the east of the depocenter. Seismic lines used to produce these isochron maps are shown inside the green box in Figure 4.1.

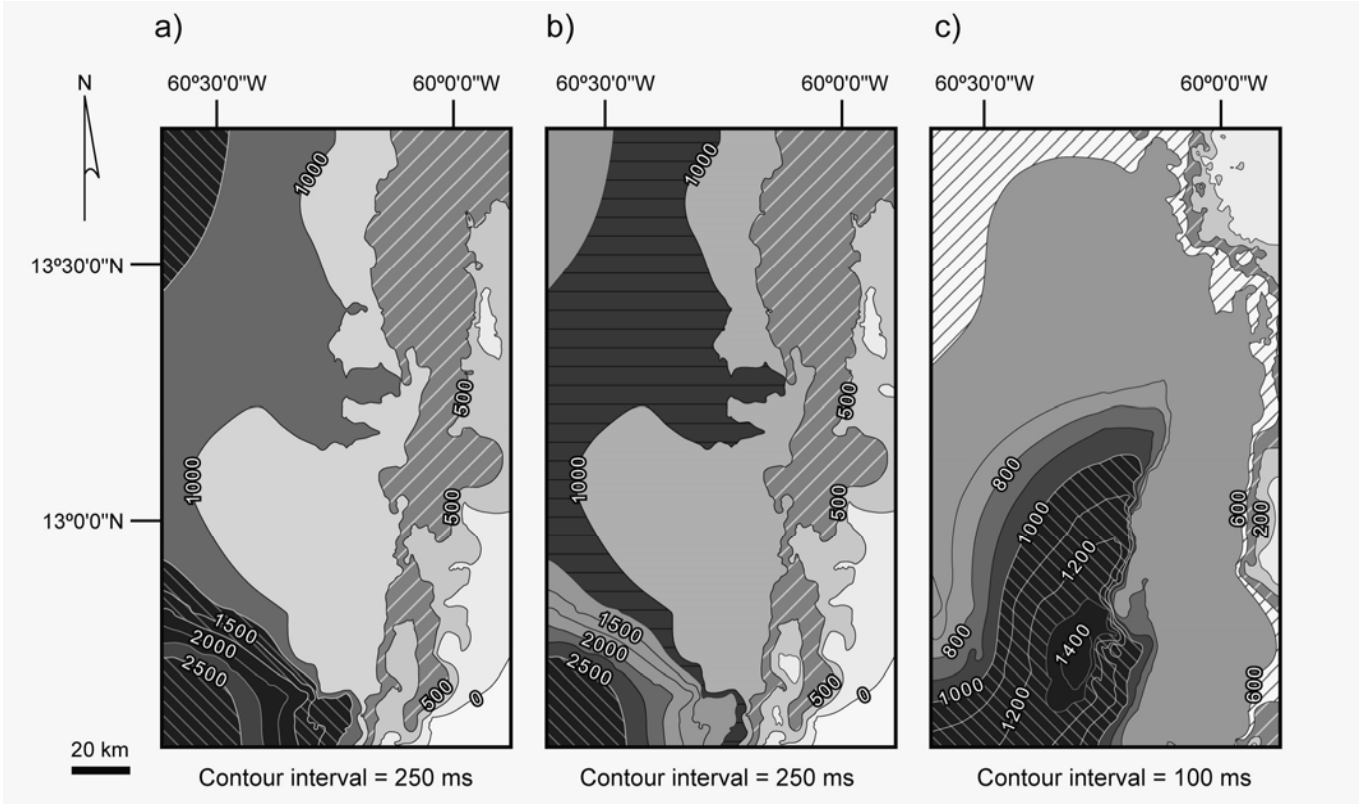

Figure 4.8: Isochron maps of the Lower Miocene to Plio-Pleistocene Tobago Basin fill. A. The Lower Miocene to Middle Miocene TFB fill is relatively thin. The thickest portion is preserved in the southwestern corner of the TFB. B. The Upper Miocene fill is almost identical in morphology to the underlying unit. The Pliocene to Pleistocene fill is concentrated in a narrow depocenter in the southwestern portion of the basin. The depocenter is constrained on its eastern margin by the Inner Forearc Deformation Front that is shown in Figures 4.3 and 4.5. Seismic reflection profiles used to produce these isochron maps are located inside the green box in Figure 4.1.

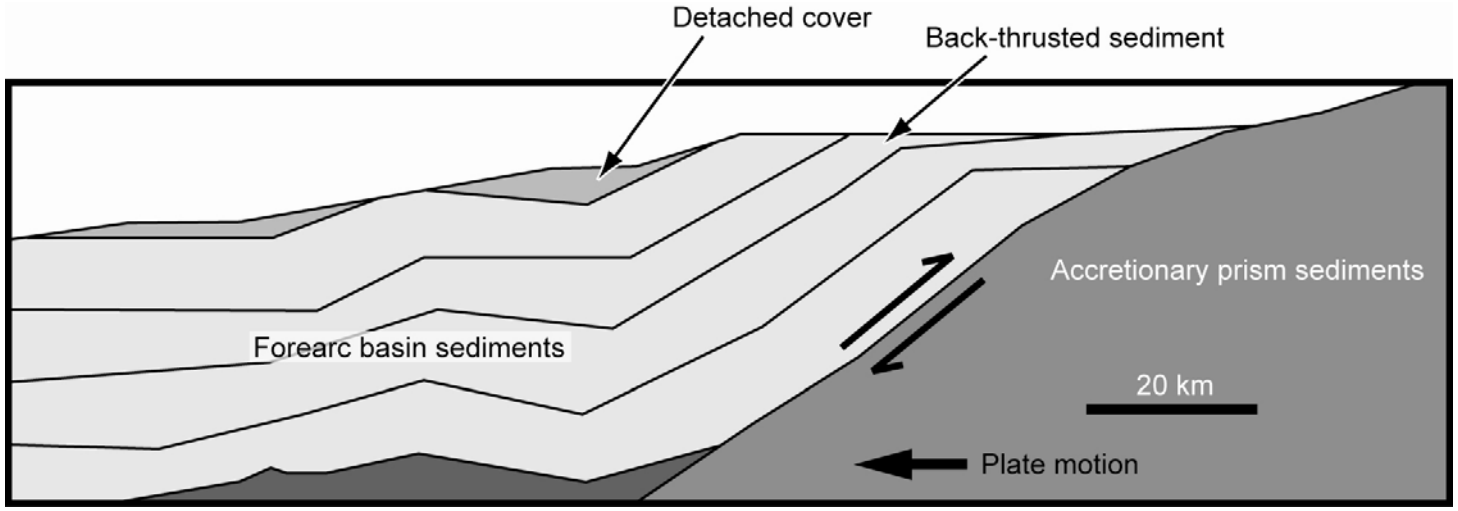

Figure 4.9: Illustration of the Speed model of tectonic emplacement of the Oceanic Formation (Tobago Forearc Basin sediments) onto accretionary prism sediments.

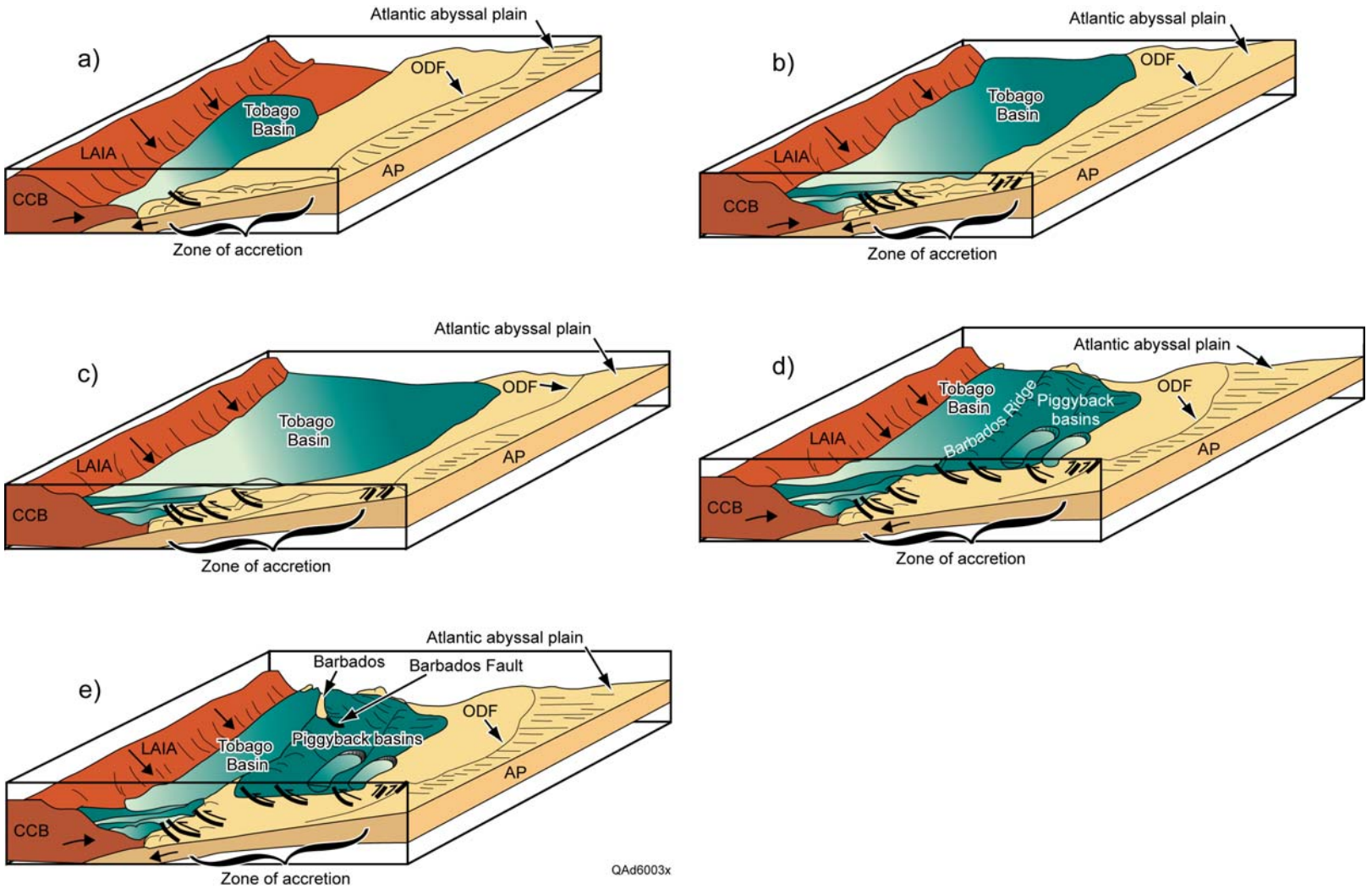

Figure 4.10: A series of schematic drawings that illustrates the evolution of the Tobago Forearc Basin.

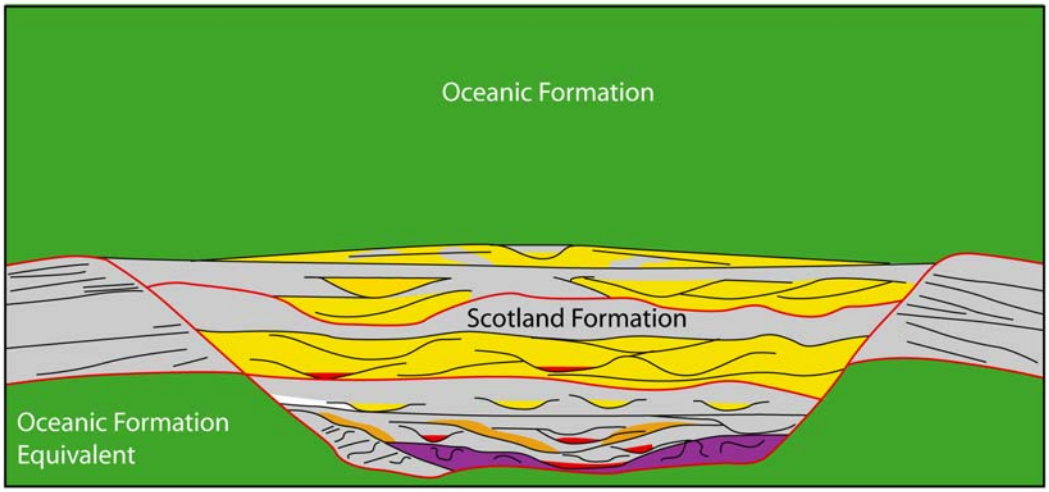

Figure 4.11: Illustration of Hypothesis 2- early pelagic sedimentation (Oceanic Equivalents) followed by clastic basin fill (Scotland Formation) and a return to pelagic sedimentation (Oceanic Formation) that is deposited conformably on the clastic basin fill.

Appendix

DIRECTIONS TO OUTCROPS

1. Chalky Mount Ridge

From Bridgetown take the Spring Garden Highway NW to the roundabout at the bottom University Hill. Turn right up University Hill and this road becomes the ABC highway. At Warrens roundabout take the second left exit to travel east and stay on the ABC highway until you reach the Jackson Roundabout. Take the first left exit towards Jackson and onto Highway 2. Stay on Highway 2 (for about 4 km) until you reach Haggatts. At the intersection follow Chalky Mount sign that points East and up a hill. At the top of this Hill there will be a blue and yellow rum shop on the right and a Chalky Mount Primary School on the left. Turn left at the school and follow the road until it ends. Park vehicle on Eastern side of the road, do not park in the clearing because quite large buses turn around there. Chalky Mount Ridge should be visible to the West across a valley. Hike West to Chalky Mount Ridge. Portions of Chalky Mount outcrop are also accessible on the Eastern side of the valley.

2. Sleeping Giant Ridge

This ridge can be reached by hiking approximately 1km North East from where the Chalky Mount Village road ends. This route is dangerous as a result of the friable nature of the outcrops. A safer route is to follow directions above and stay on Highway 2 until you reach BellePlaine. At BellePlaine turn right (onto the Ermy Bourne Highway- also locally called “The East Coast Road) and stop just north of Barclays Park. This will take you to the “East Coast Road “ outcrop which is the eastern face of Sleeping Giant Ridge. The upper portions of the ridge can be reached from hiking up and over the eastern face in a westerly direction.

3. Ermy Bourne Ridge

Approximately 500 m north of the Eastern face of Sleeping Giant Ridge. Outcrop marked by a sign in rock with a short write up about “Ermy Bourne”.

4. Spa Hill

From Mount All, drive East to junction at the bottom of Mount All. Turn right (south). Take left at Fruitful Hill and follow the road until it ends. Park vehicle and hike past ruins of old house (Spa House) in a northeasterly direction. You will reach a thicket with trees and a great deal of brush- it may be fenced in some areas. A cutlass (machete) is

necessary to clear a path. Keep to a northeasterly path for about 300 m, outcrop will be visible when brush clears.

5. Mount All

From Bridgetown take the Spring Garden Highway NW to the roundabout at the bottom University Hill. Turn right up University Hill becomes the ABC highway. At Warrens roundabout take the second left exit to travel East and stay on the ABC highway. The next roundabout is Jackson Roundabout. Take the first left exit towards Jackson onto Highway 2. Stay on Highway 2 until you reach Mount All. Outcrop is located on a dirt track on the north side of the road ~ 750 m from the top of Mount All. Track is often over-grown and it is best to park at the crest of Mount All and walk down to track. Wear reflective clothing if possible and keep an eye out for swift moving cars and buses.

6. Inner Turner's Hall Ridge

From Mount All continue on Highway 2. Turn left (West) at Belle Hill and follow the road until it ends. Park vehicle and hike west into woods. About 100 m into the woods take path on the left, in a southerly direction. Hike South for about 250 m until you reach the Inner Turner's Hall Ridge Outcrop.

7. Walker's Ridge

From Mount All follow Highway 2. Highway 2 will travel east and at BellePlaine it curves towards the West. Stay on Highway 2 past Shorey Village to Breedy's. Stop at Greenland Clay Tile Factory, located in Breedy's. Park on grass in front of factory offices and ask at office for permission to hike up the hill. Walk behind clay factory proper and veer slightly westward to find the Walker's Ridge Lower section. Walker's Ridge Upper section is located immediately North of Walker's Ridge Lower.

7.b Breedy's

The entrance to the road is 100 m South of the clay tile factory entrance. Turn left and follow dirt road into Breedy's Shale Quarry. Sandstone beds are visible at the Southern end of the quarry. Be very careful and do not visit this location when it is or has been raining as there is a danger of falling rock and of getting vehicles stuck.

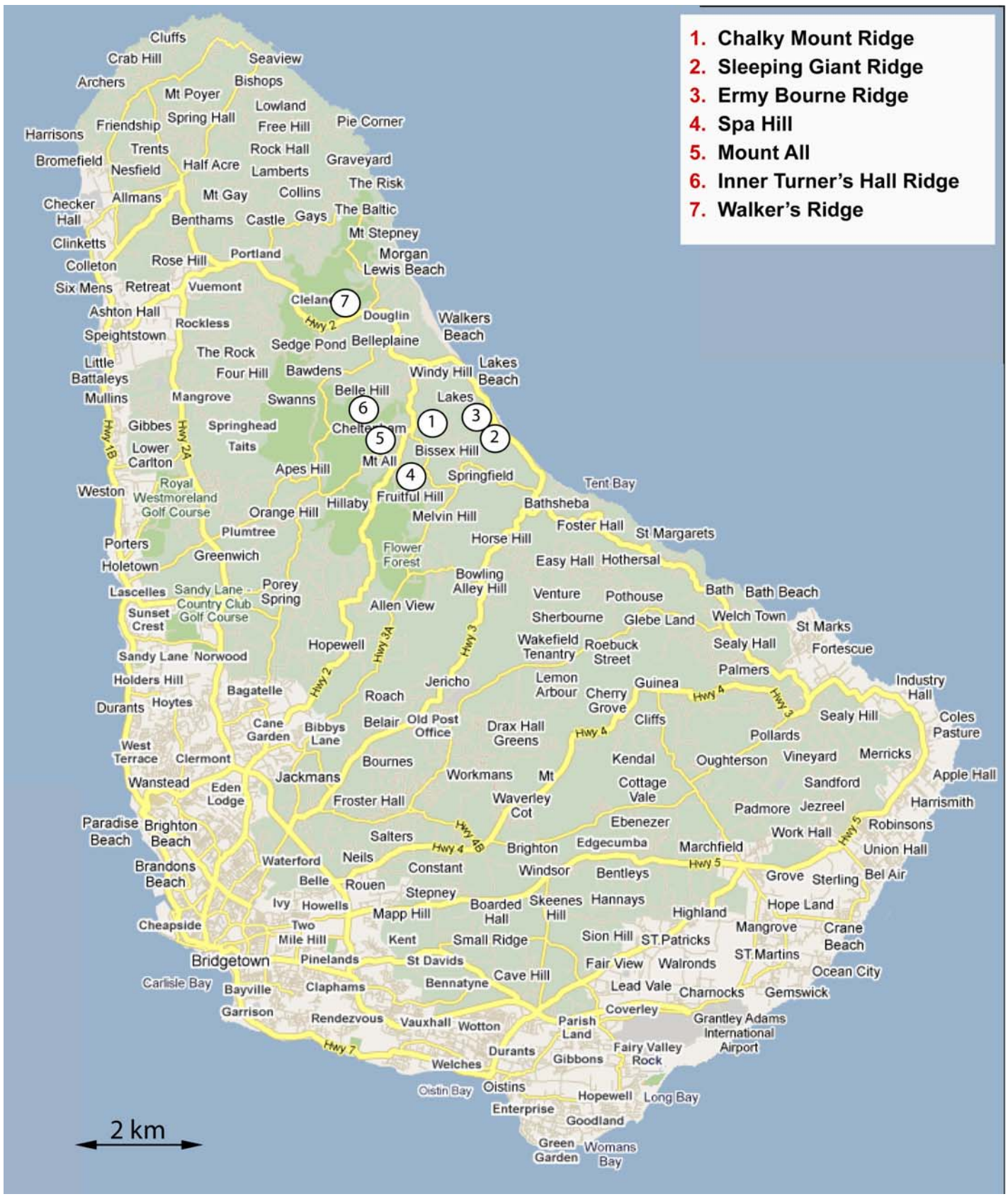

Figure A.1: Location map showing Scotland District Outcrops. Oversized Plate (11x17) requires plotter or printer with tabloid printing.

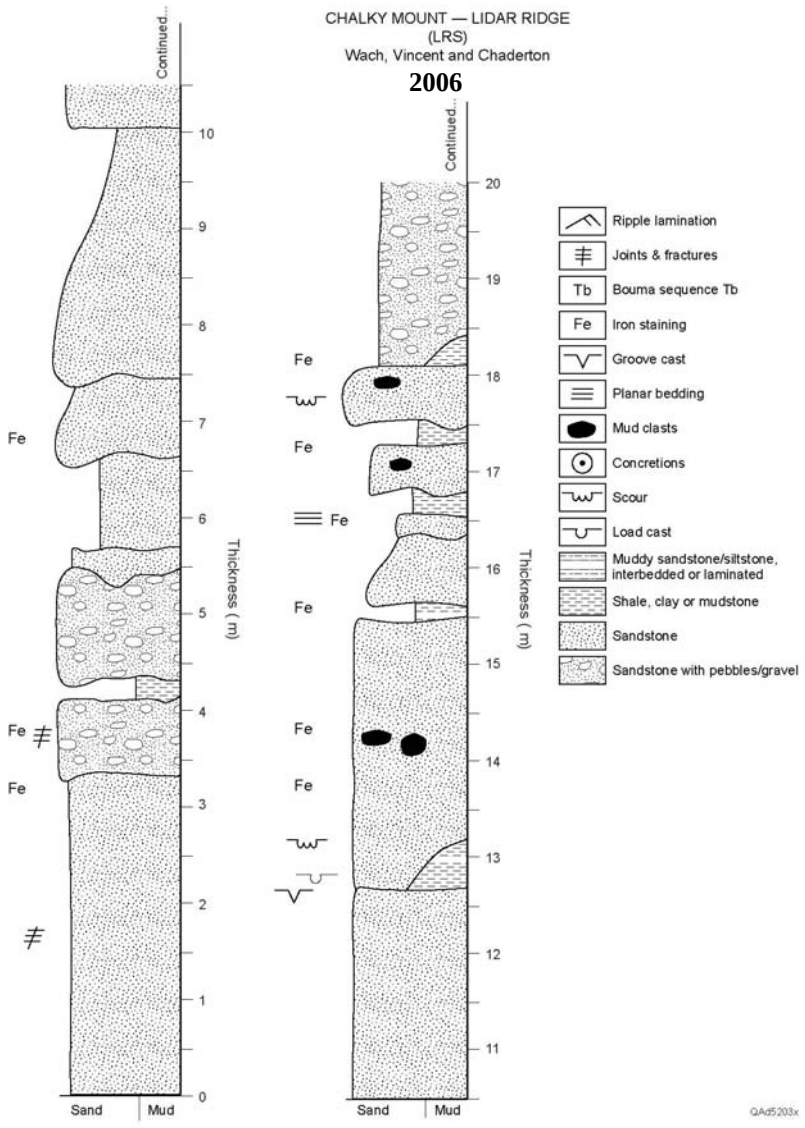

Figure A.2a: Lidar Ridge measured section.

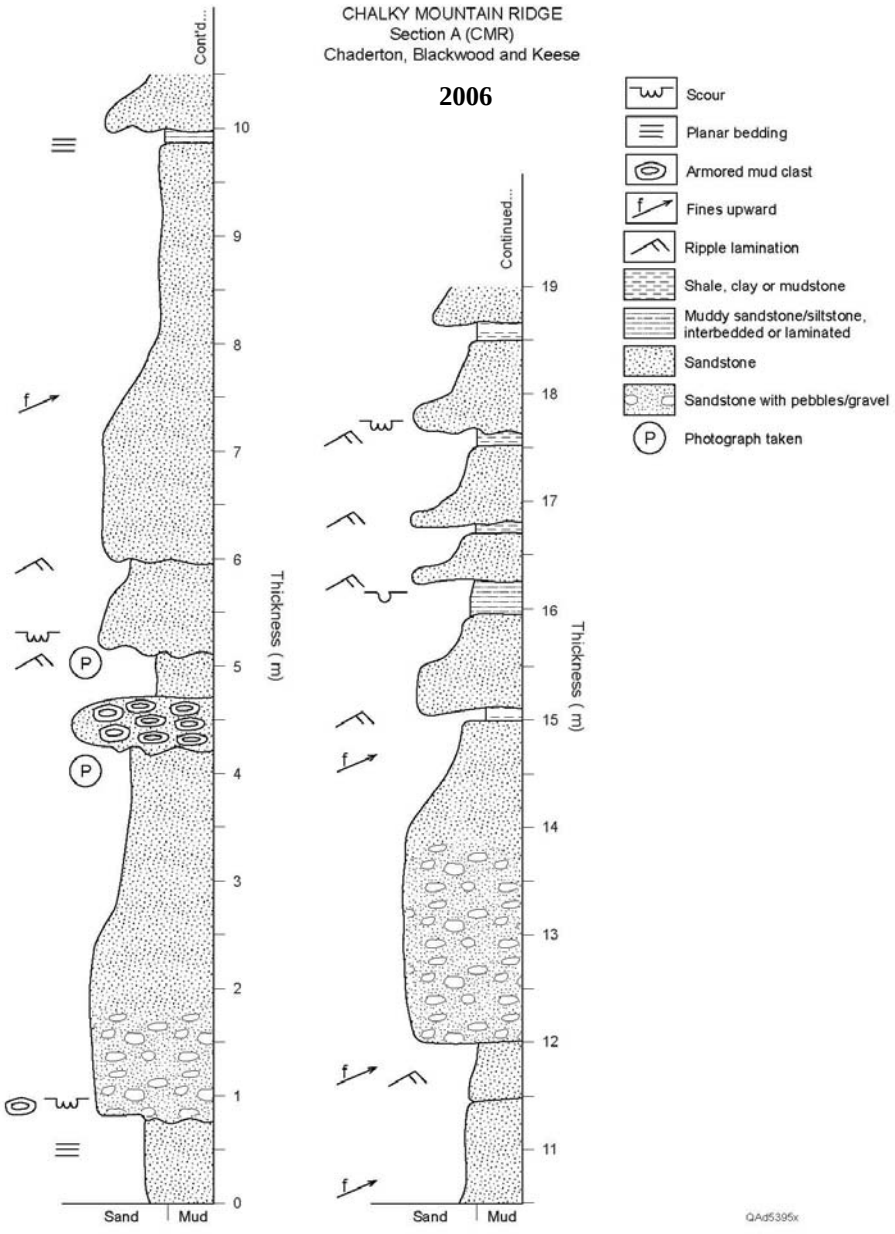

Figure A.3a: Chalky Mount Ridge measured section A.

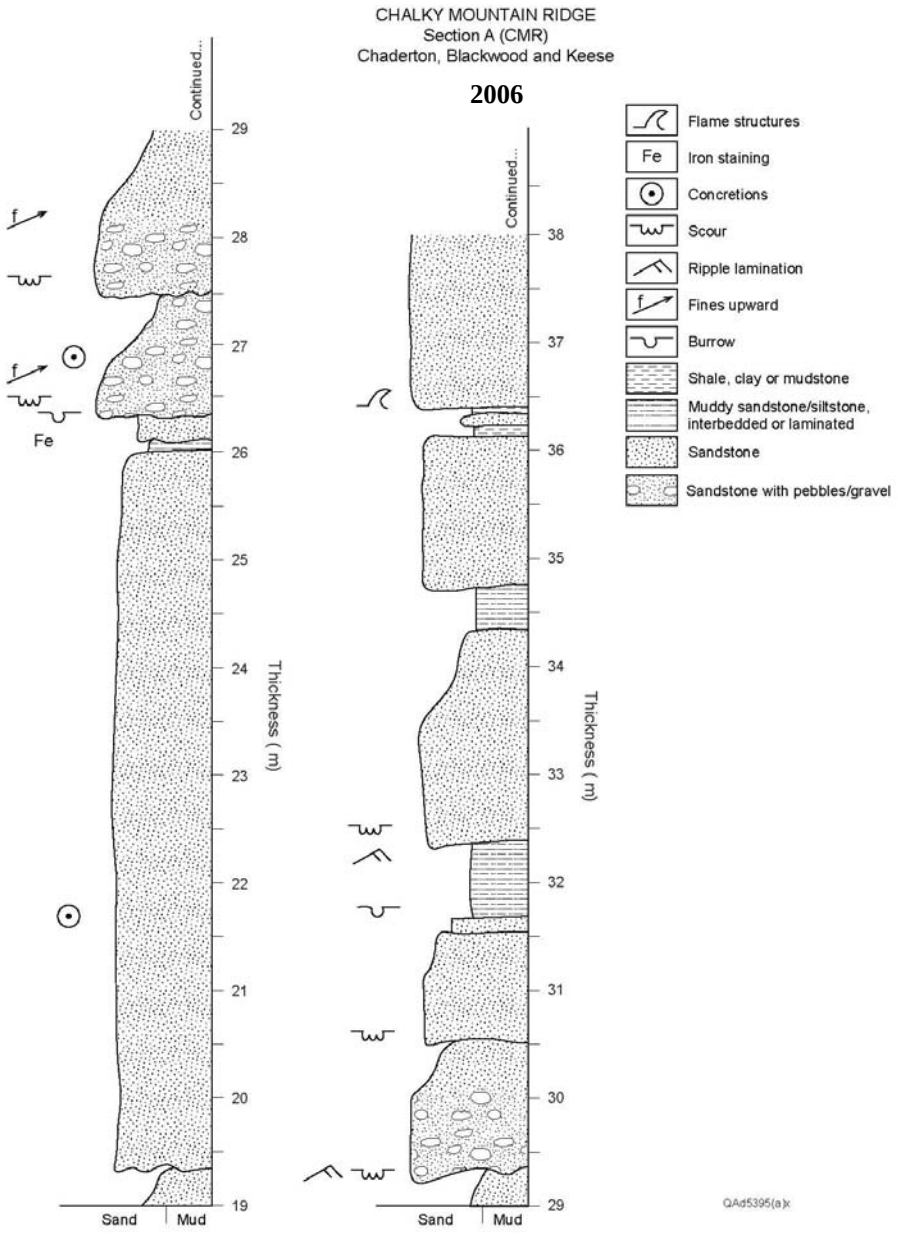

Figure A.3b: Chalky Mount Ridge measured section A.

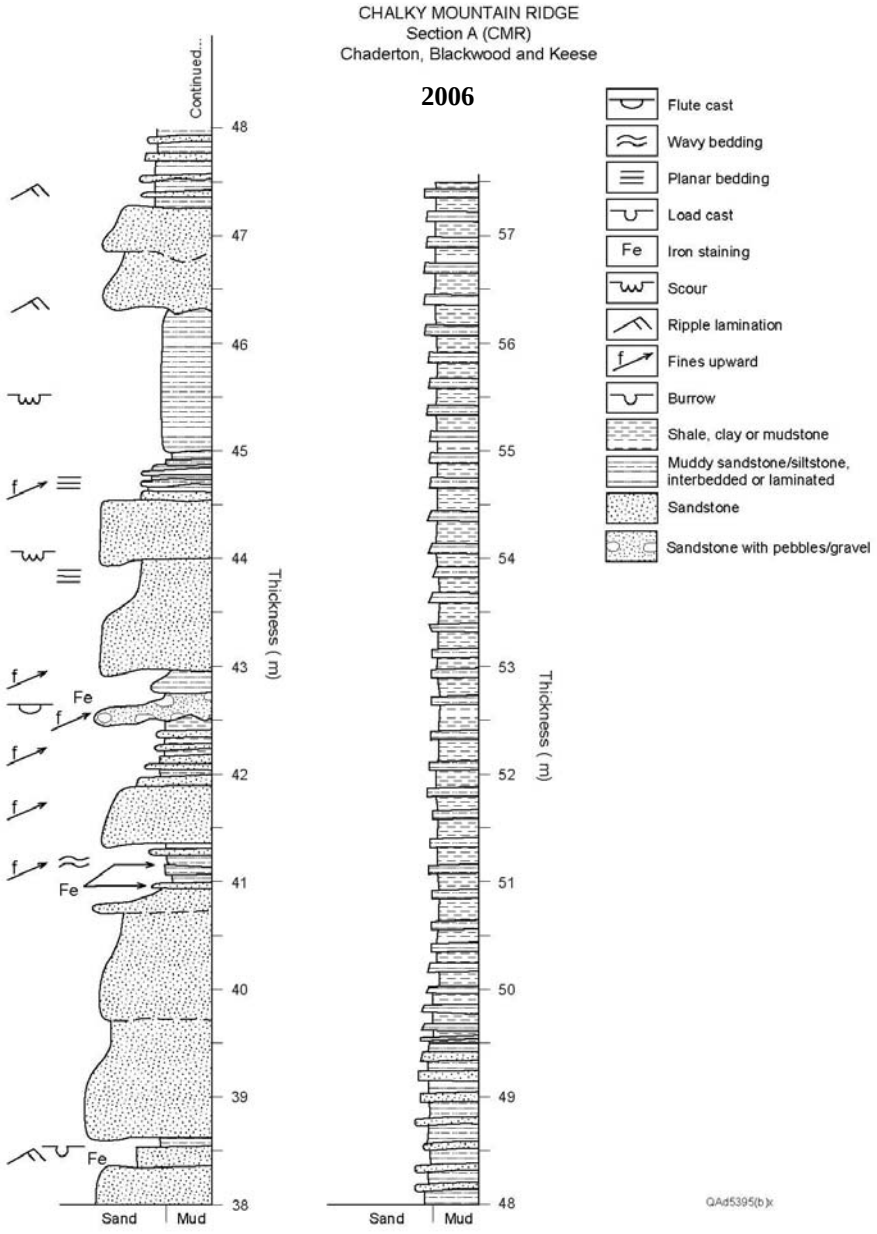

Figure A.3c: Chalky Mount Ridge measured section A

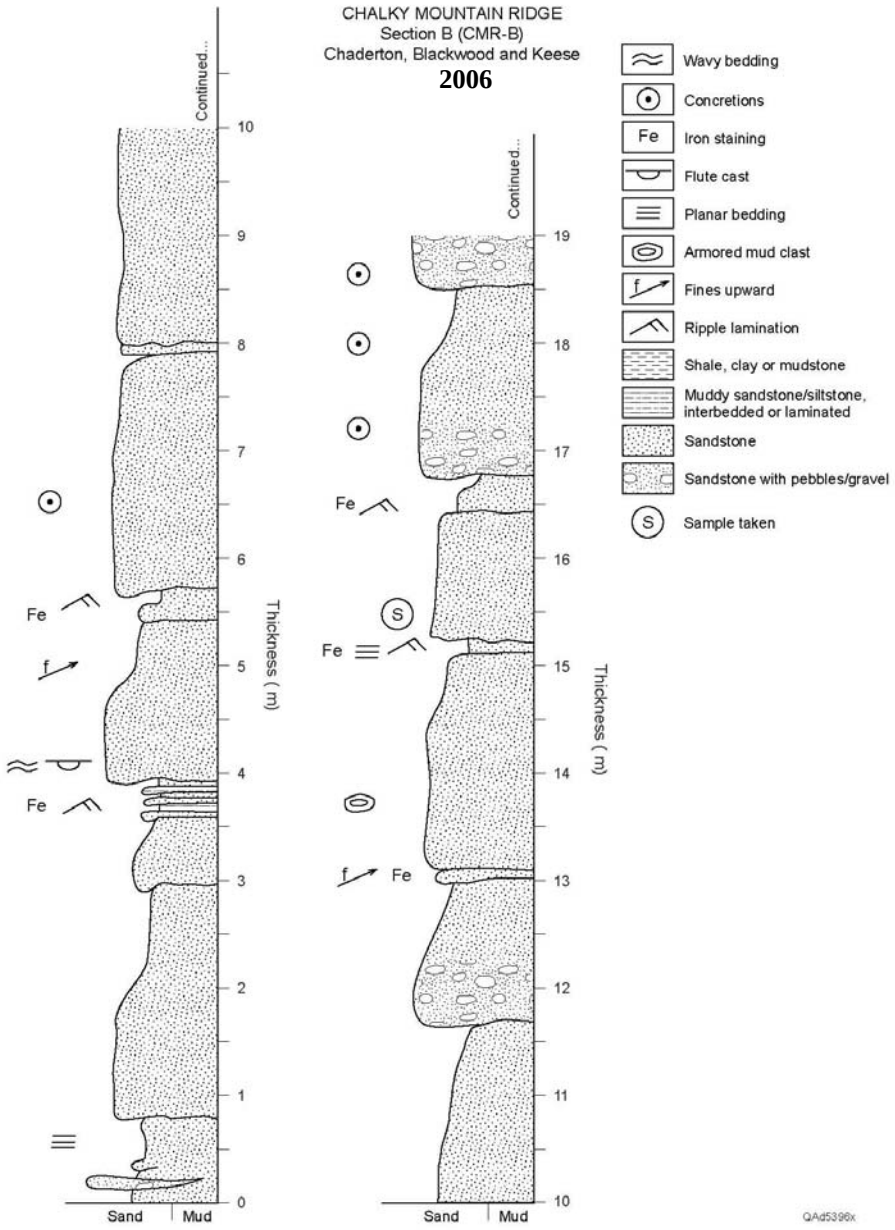

Figure A.4a: Chalky Mount Ridge measured section B.

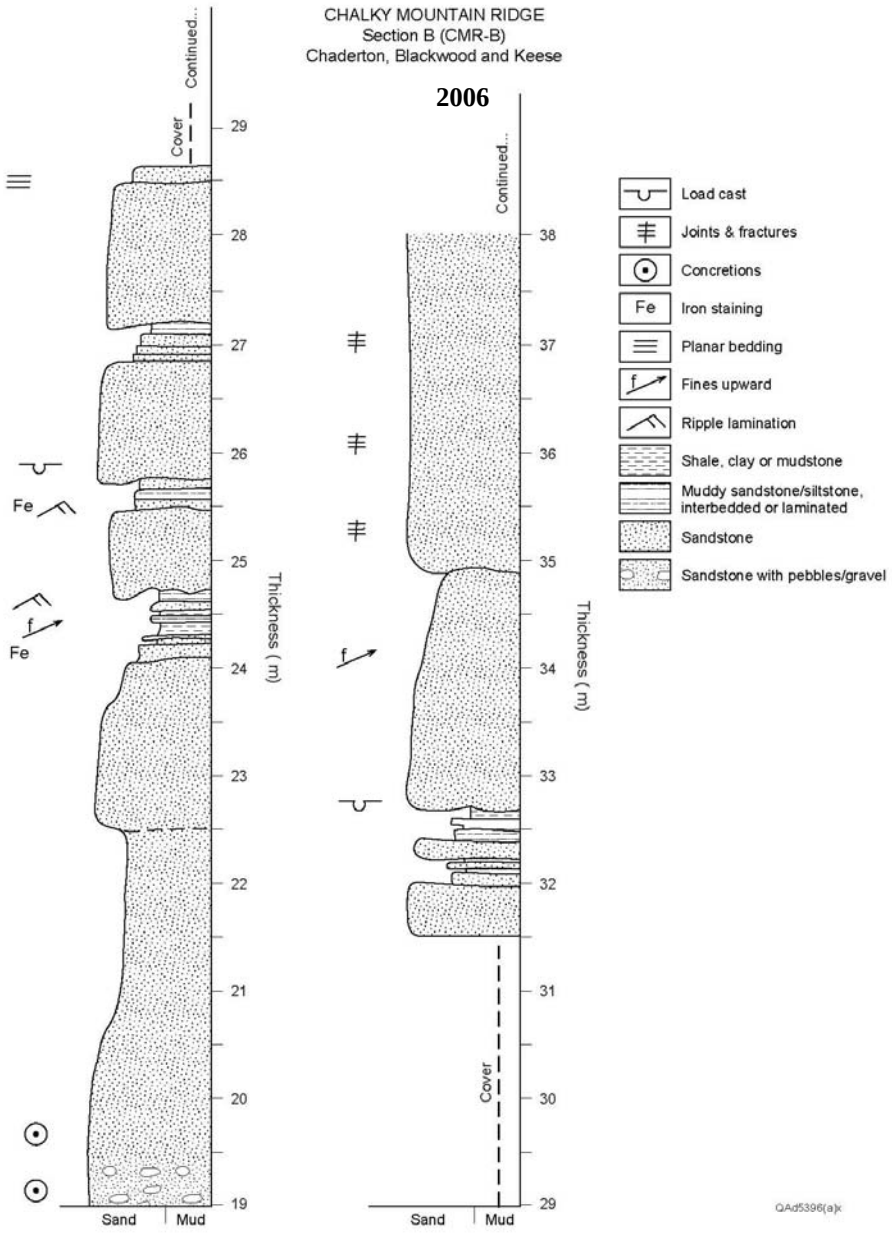

Figure A.4b: Chalky Mount Ridge measured section B.

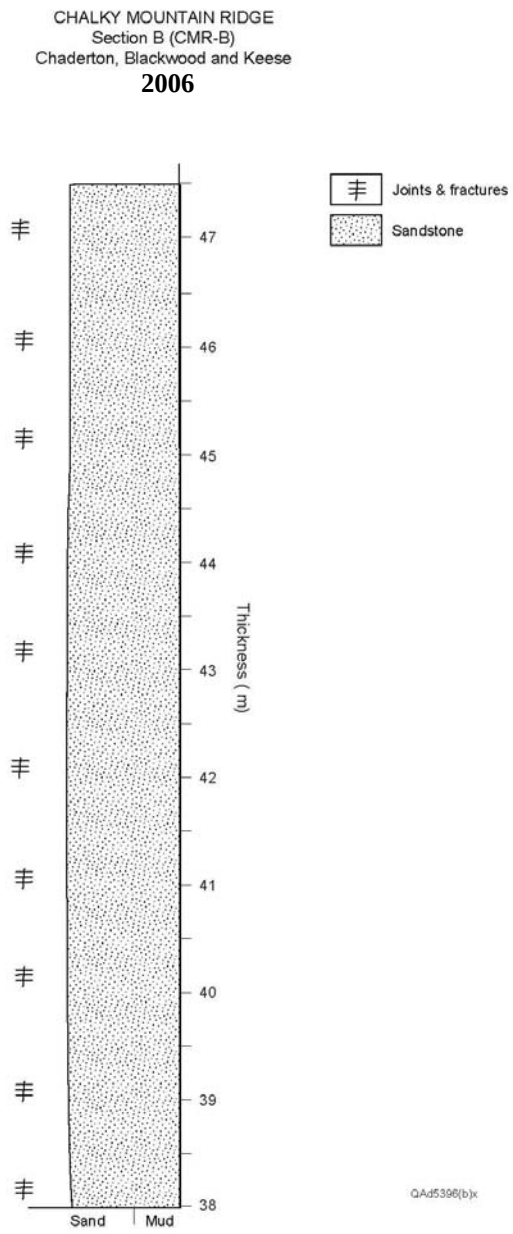

Figure A.4c: Chalky Mount Ridge measured section B.

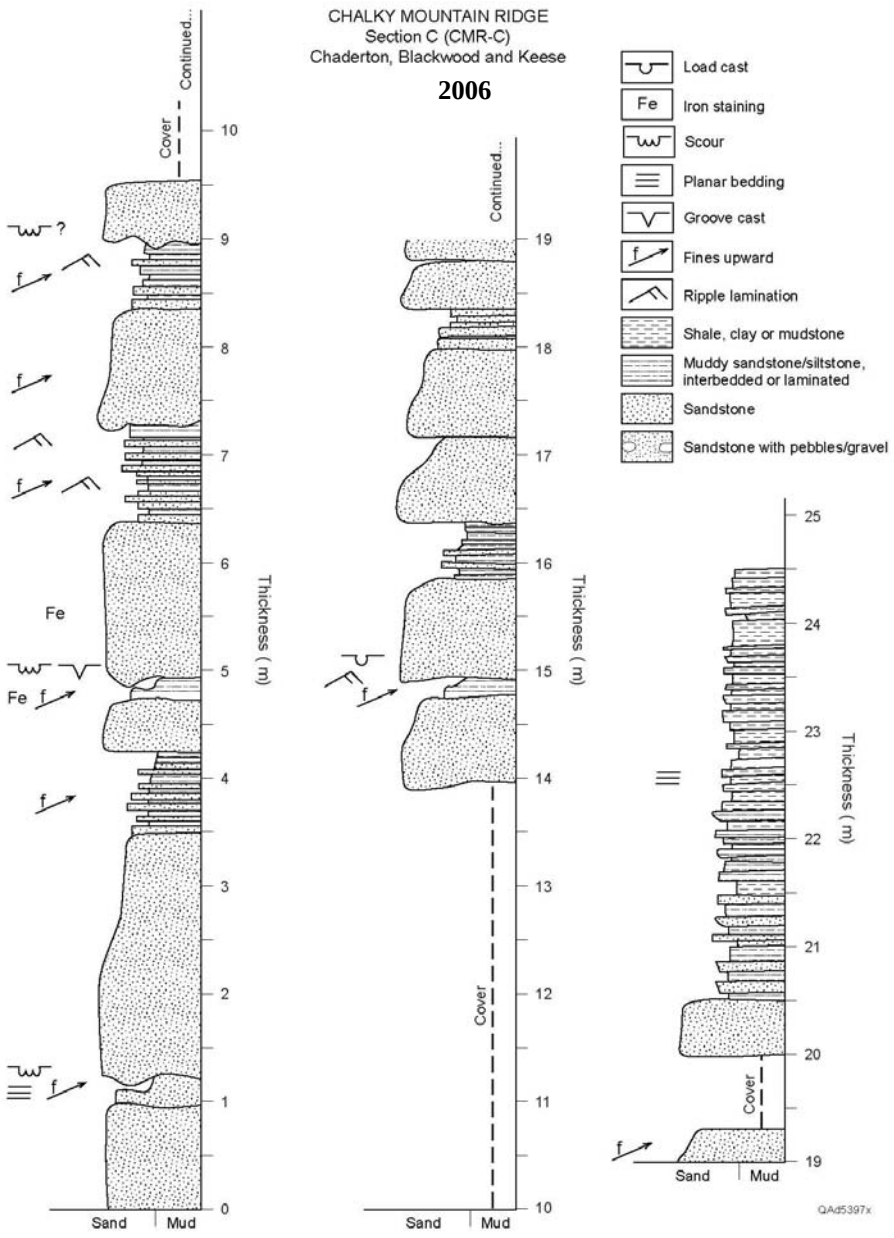

Figure A.5: Chalky Mount Ridge measured section C.

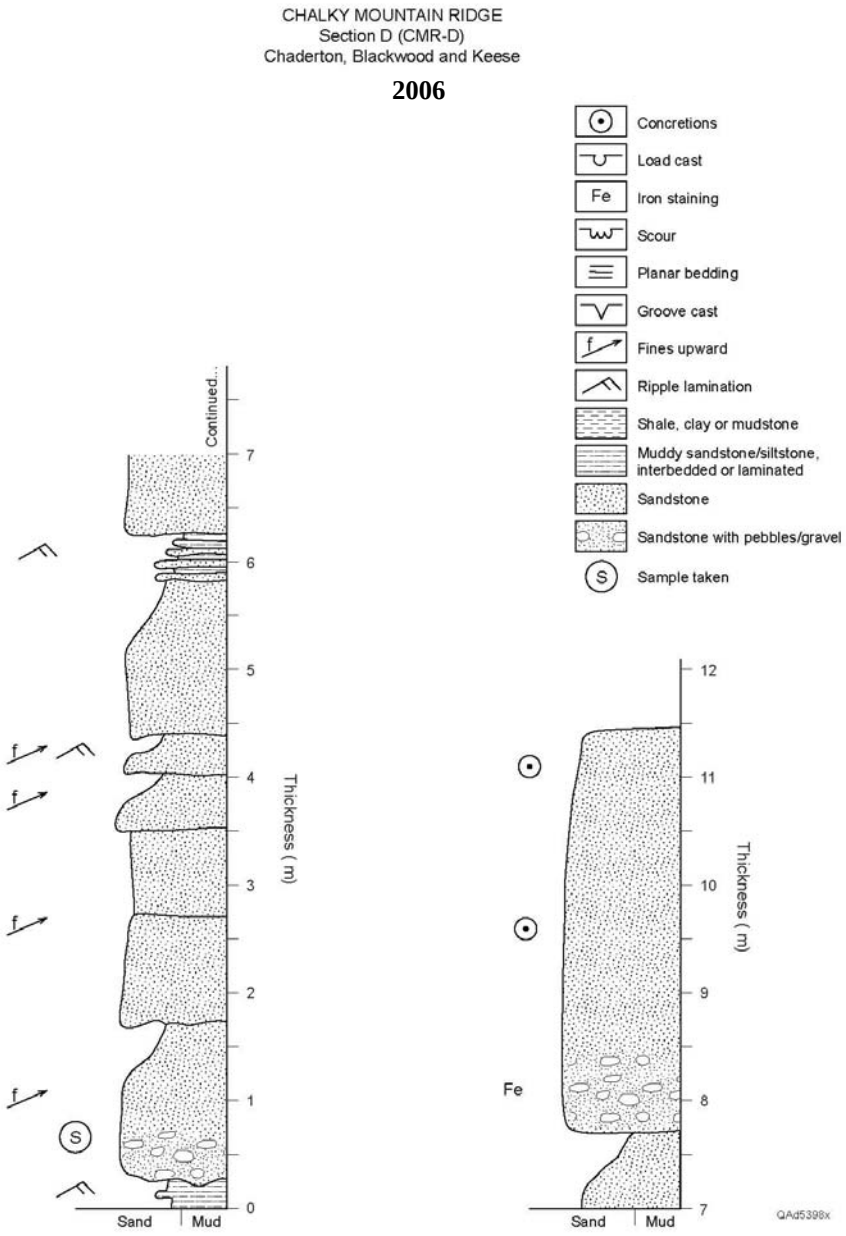

Figure A.6: Chalky Mount Ridge measured section D.

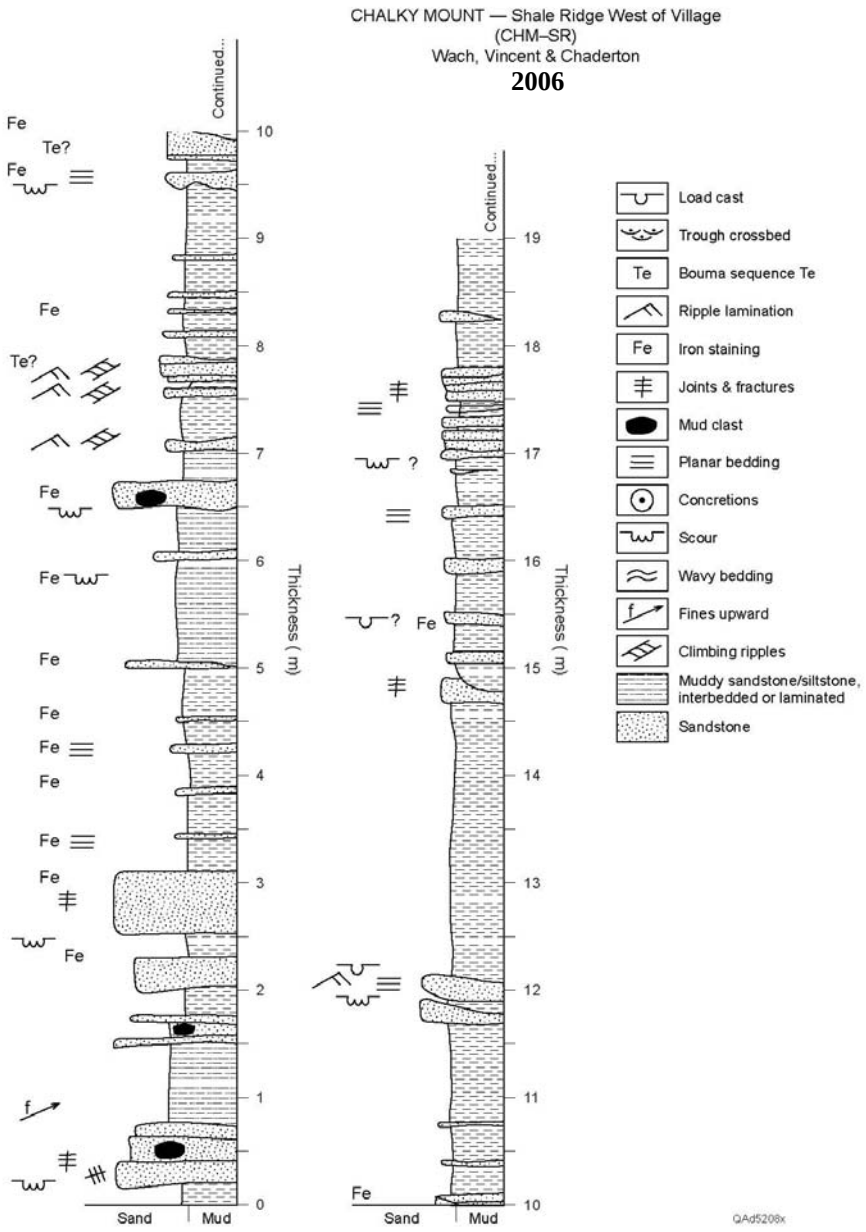

Figure A.7a: Measured Section of Chalky Mount Shale Ridge.

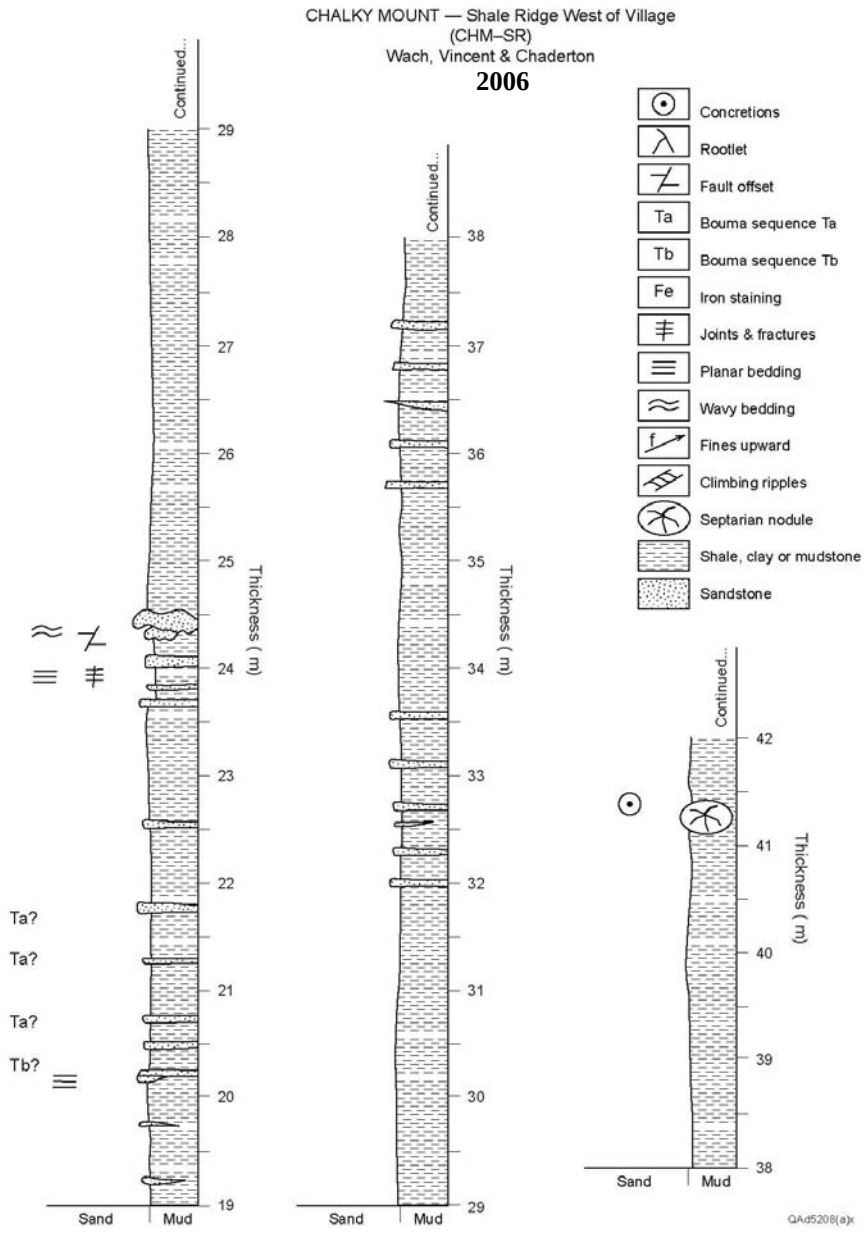

Figure A.7b: Measured Section of Chalky Mount Shale Ridge.

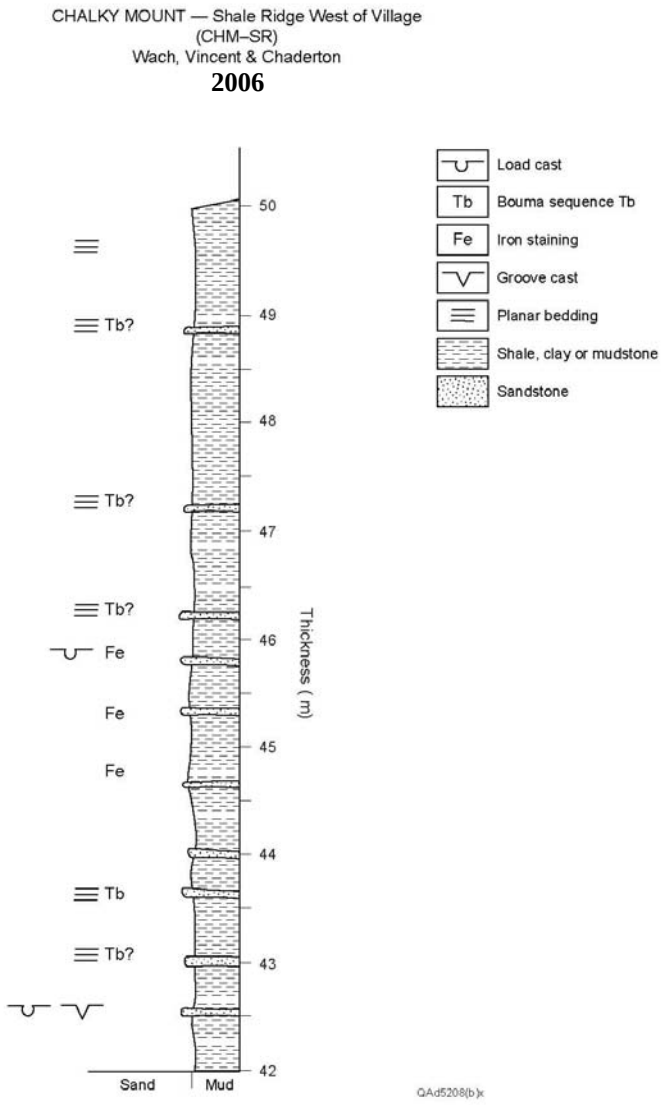

Figure A.7c: Measured Section of Chalky Mount Shale Ridge.

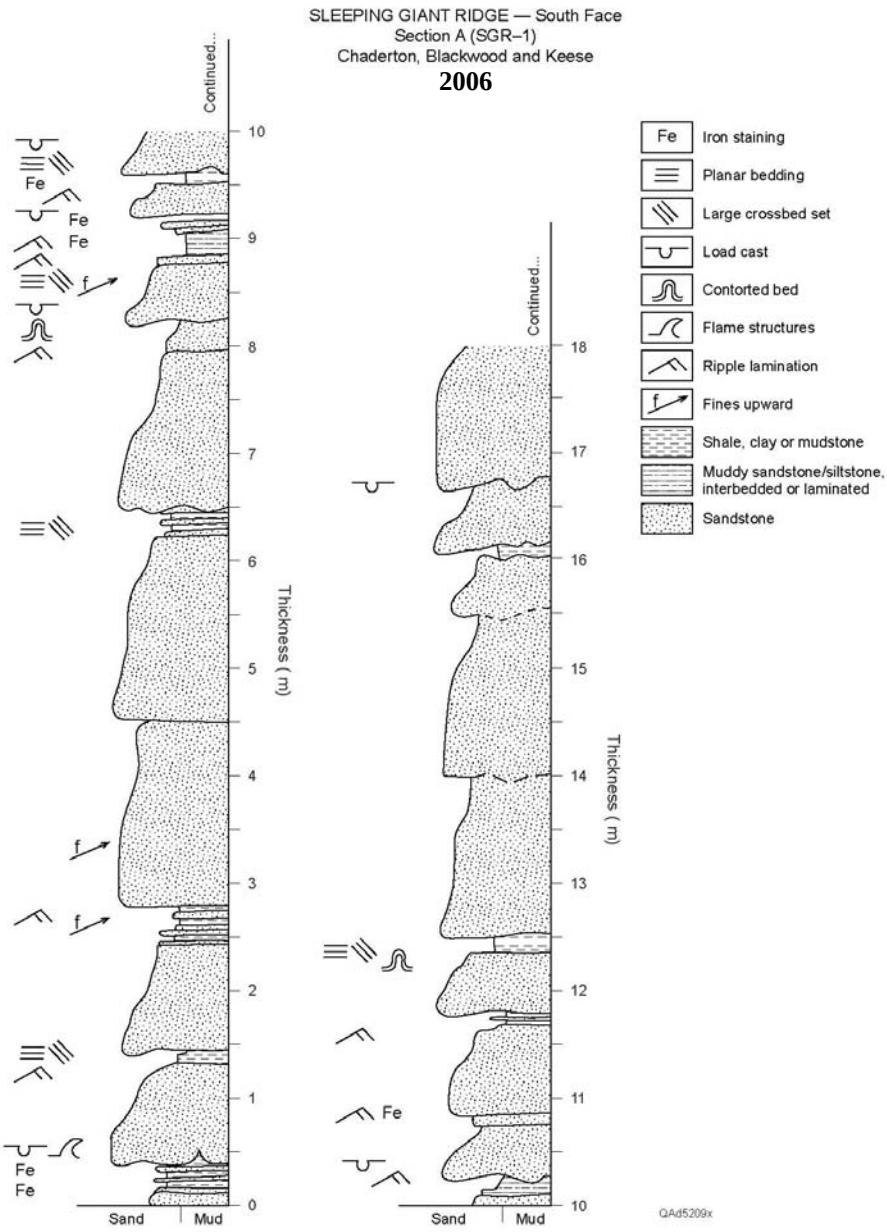

Figure A.8a: Sleeping Giant Ridge Measured Section A.

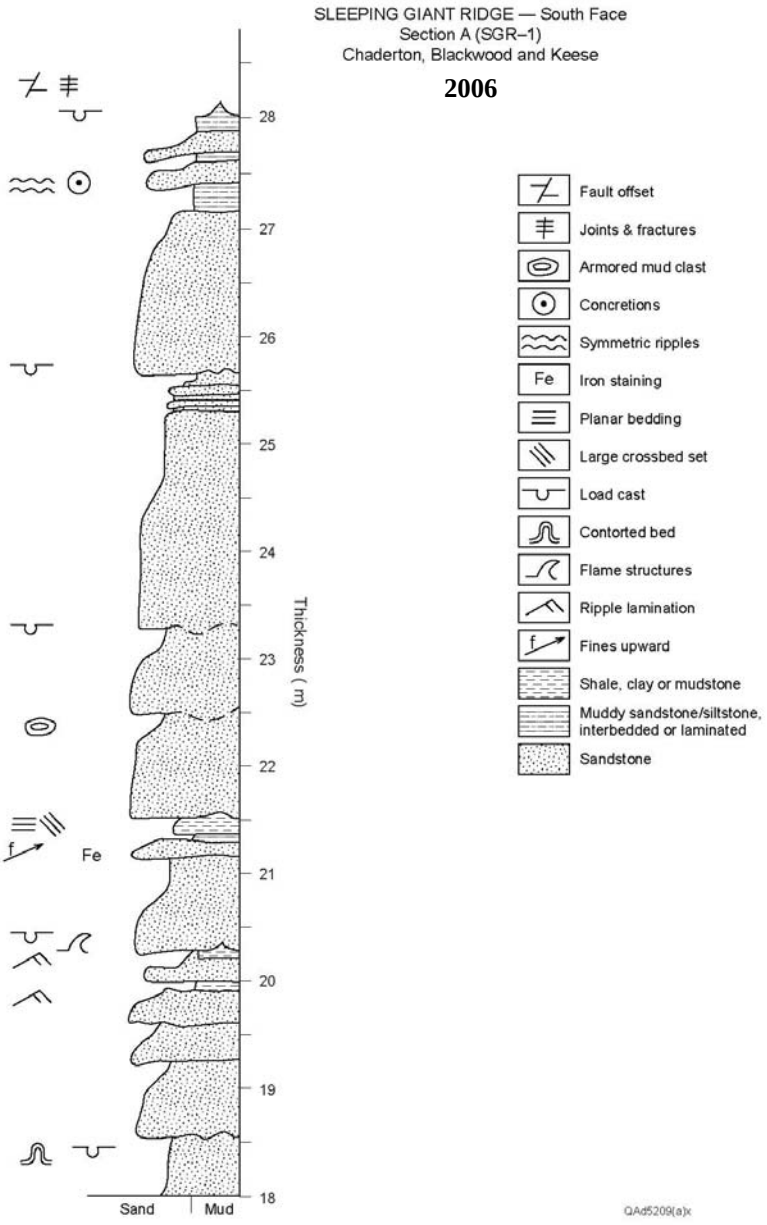

Figure A.8b: Sleeping Giant Ridge Measured Section A.

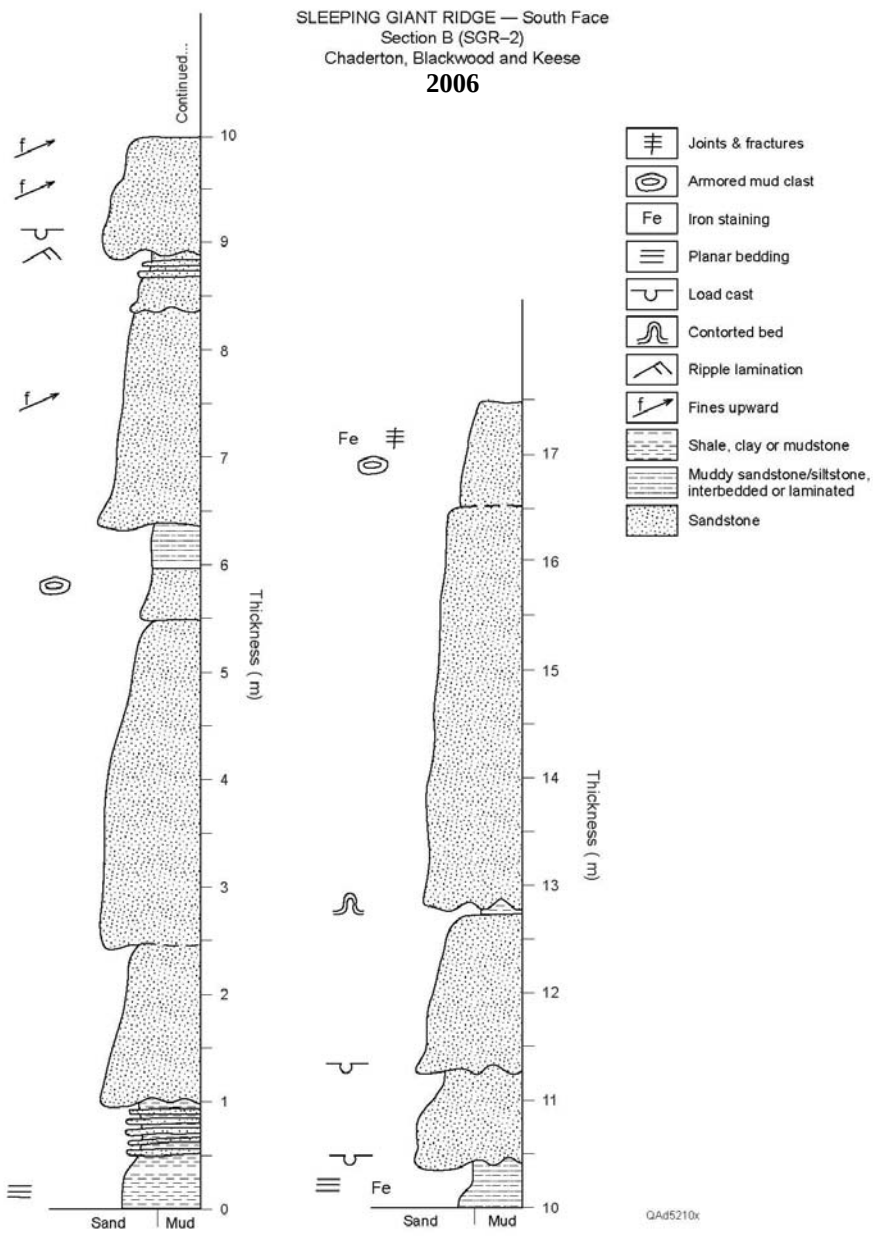

Figure A.9: Sleeping Giant Ridge Measured Section B.

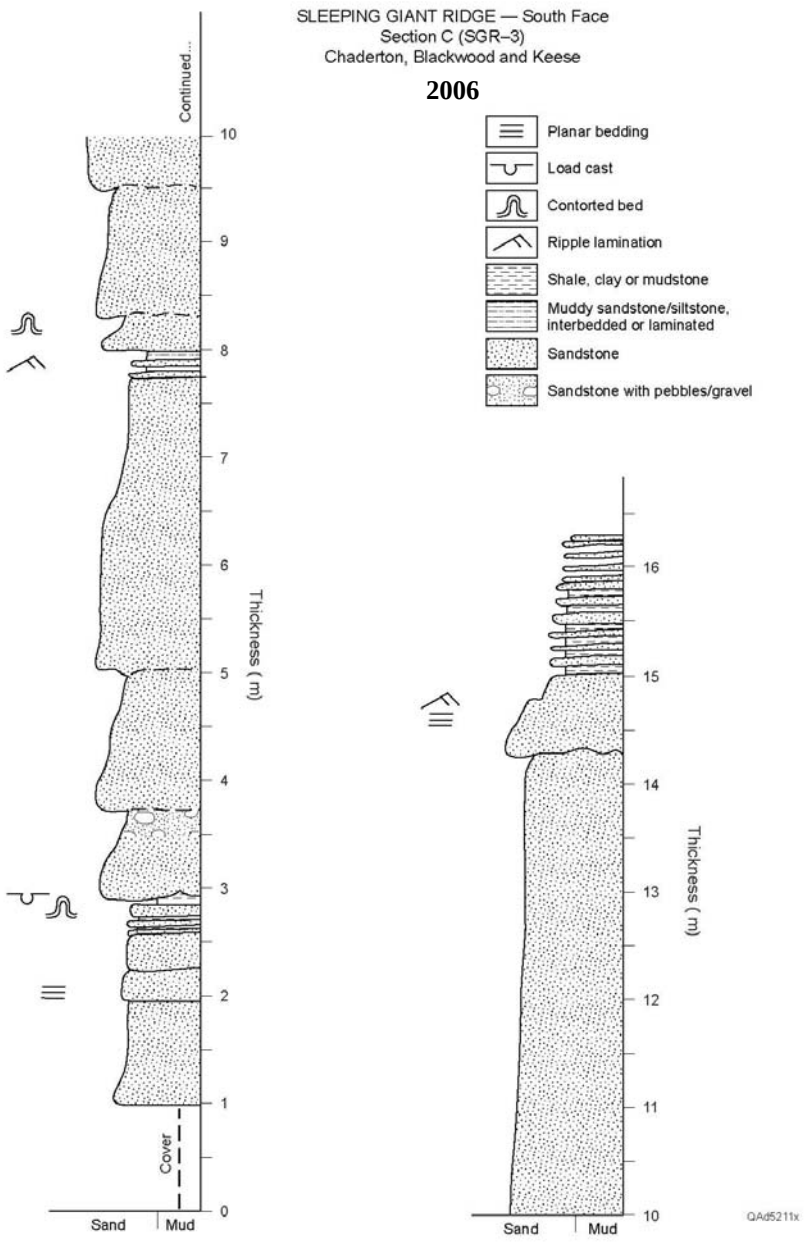

Figure A.10: Sleeping Giant Ridge Measured Section C.

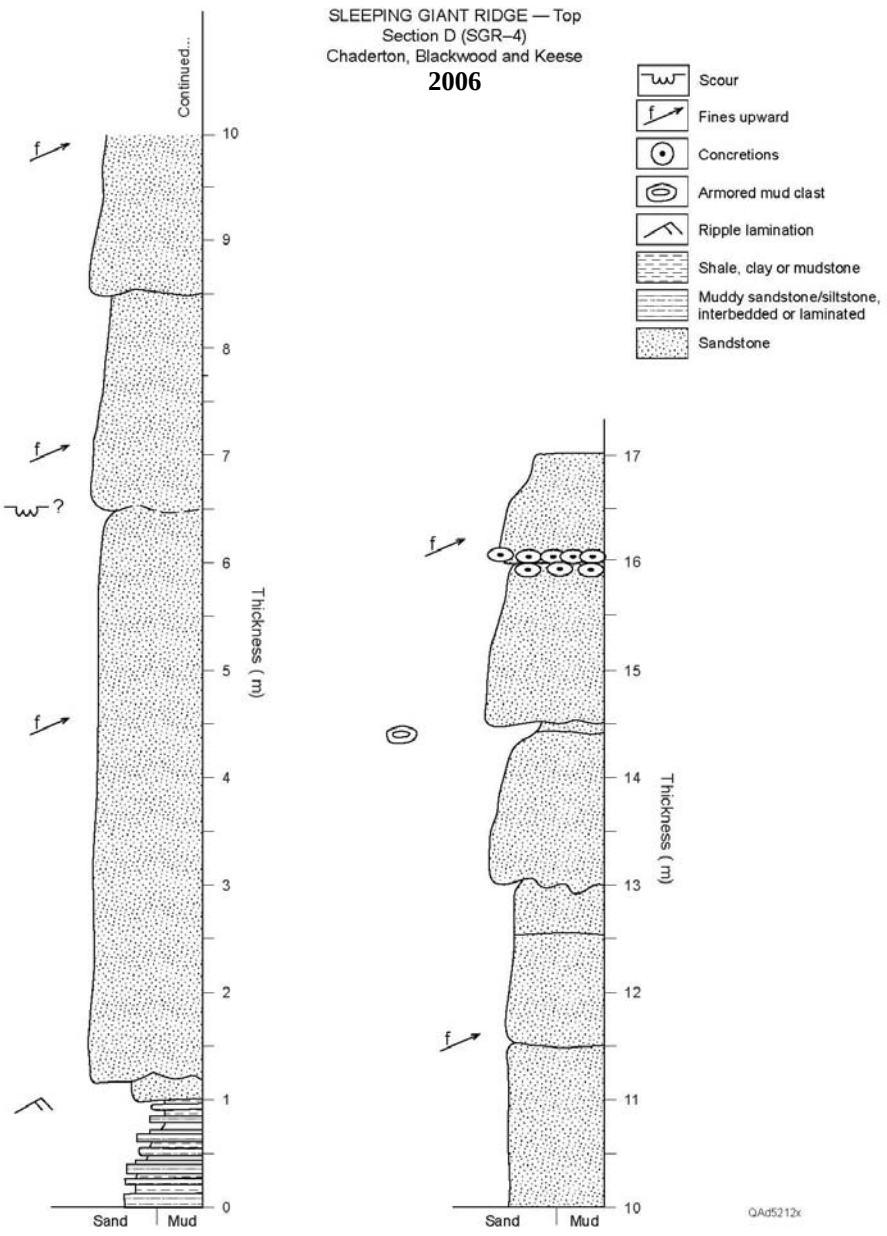

Figure A.11: Sleeping Giant Ridge Measured Section D.

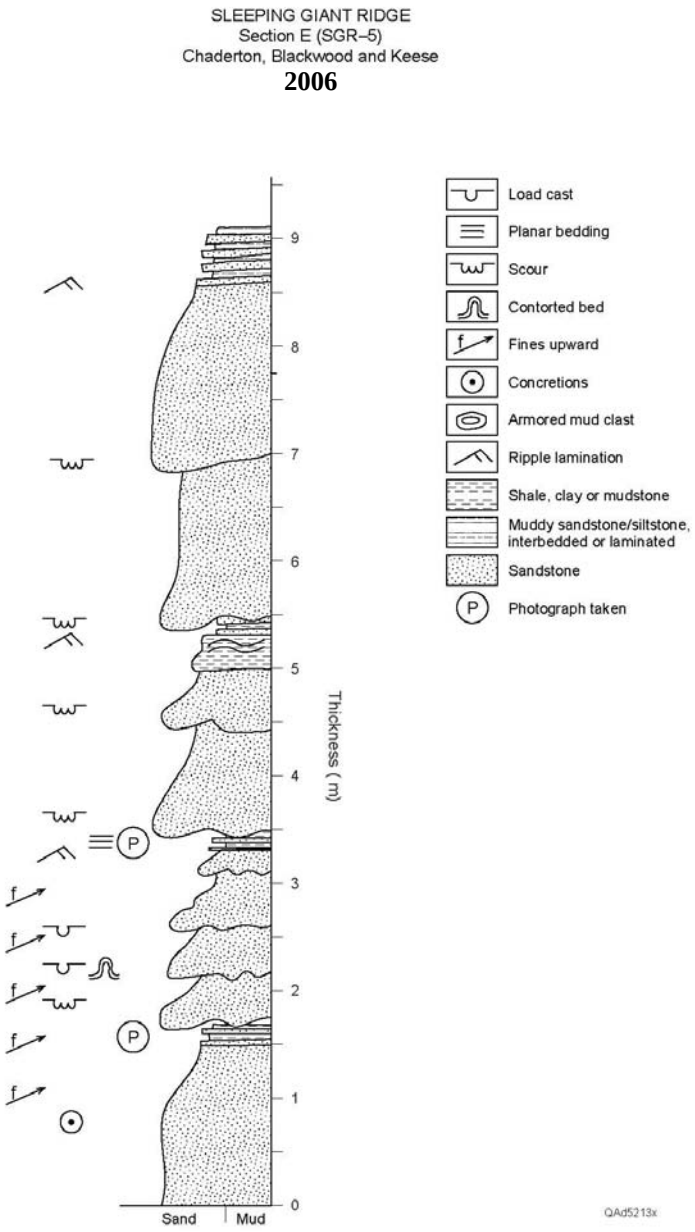

Figure A.12: Sleeping Giant Ridge Measured Section E.

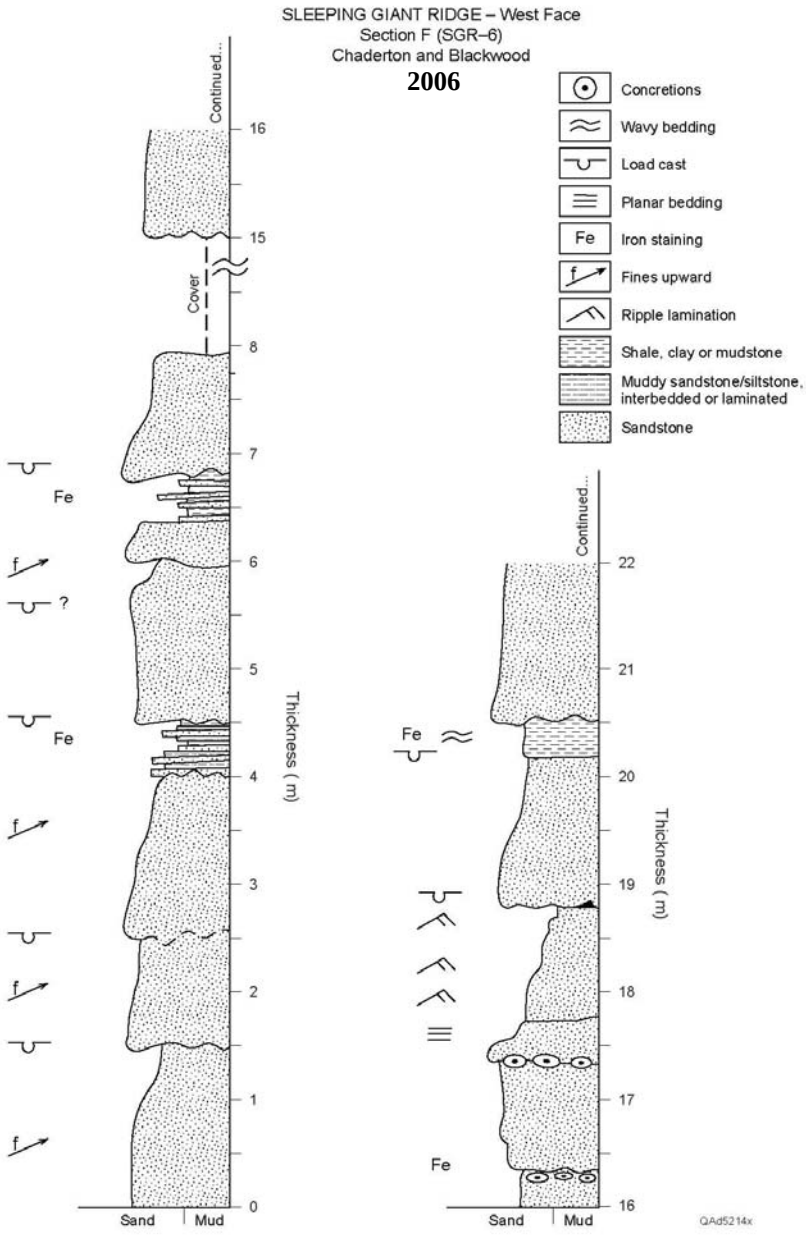

Figure A.13a: Sleeping Giant Ridge Measured Section F.

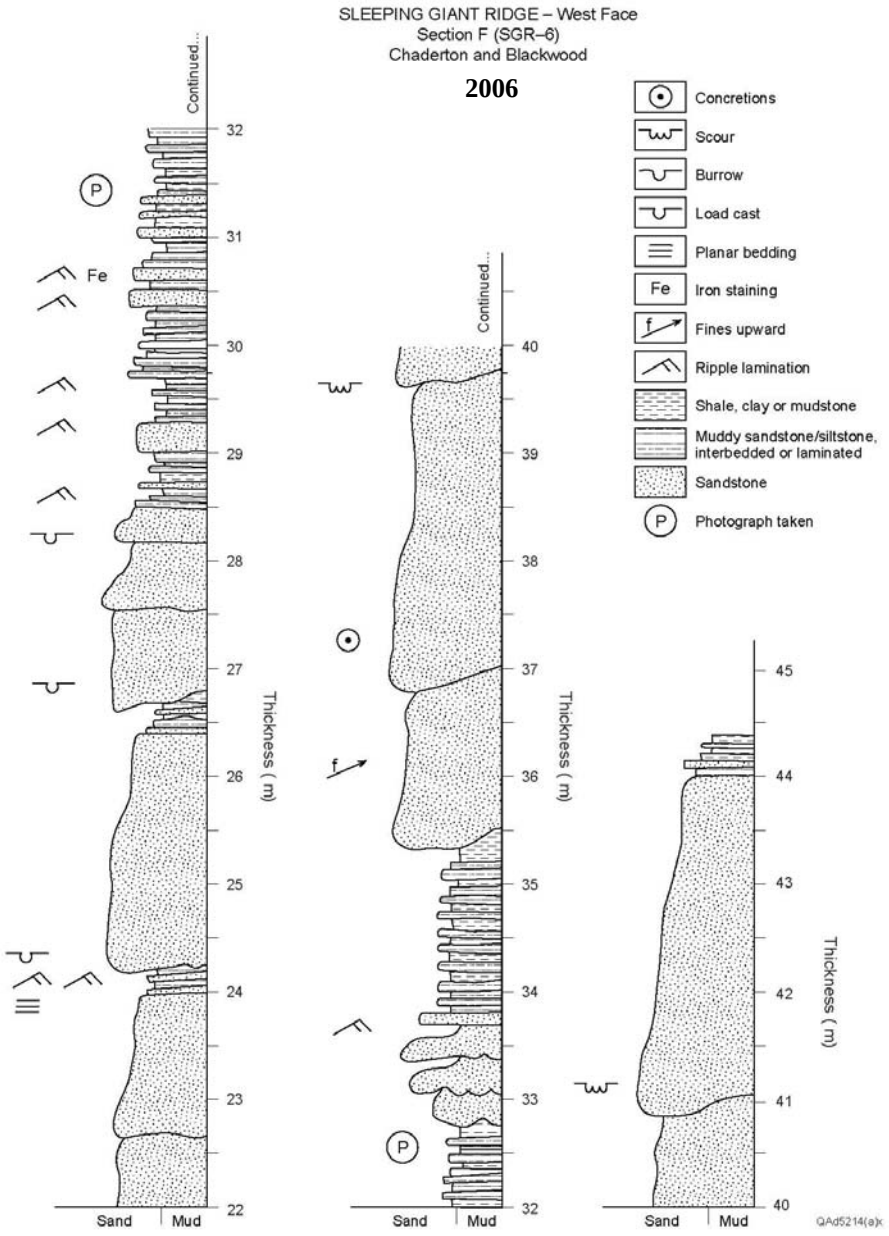

Figure A.13b: Sleeping Giant Ridge Measured Section F.

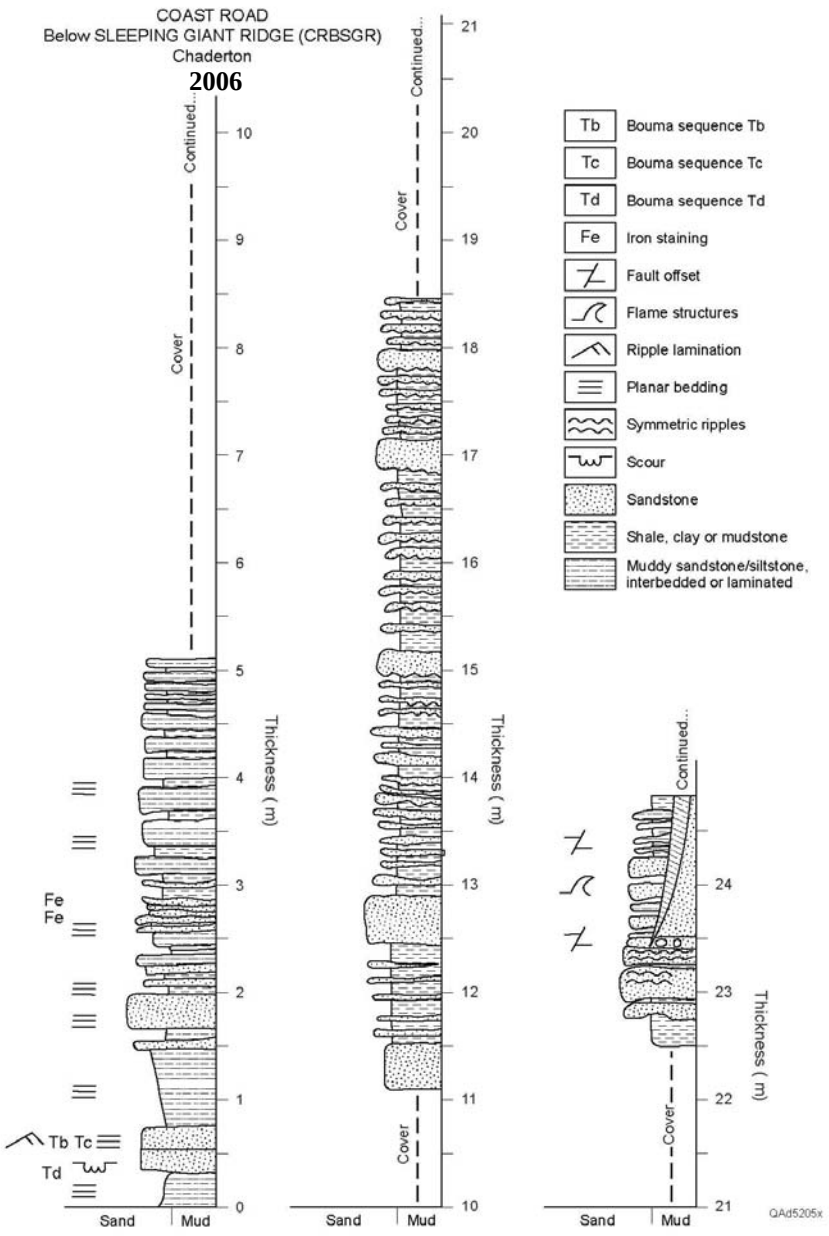

Figure A.14a: Coast Road Below Sleeping Giant Ridge Measured Section.

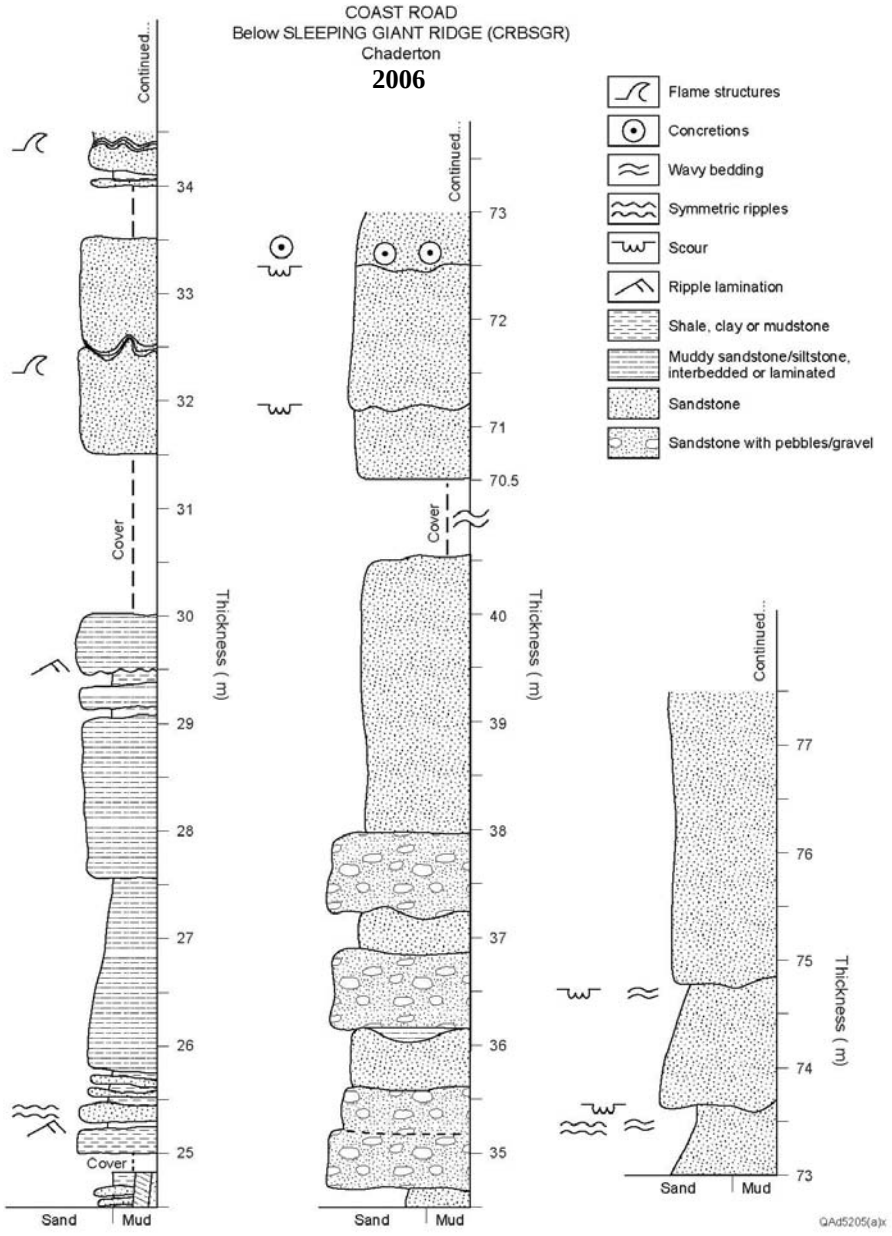

Figure A.14b: Coast Road Below Sleeping Giant Ridge Measured Section.

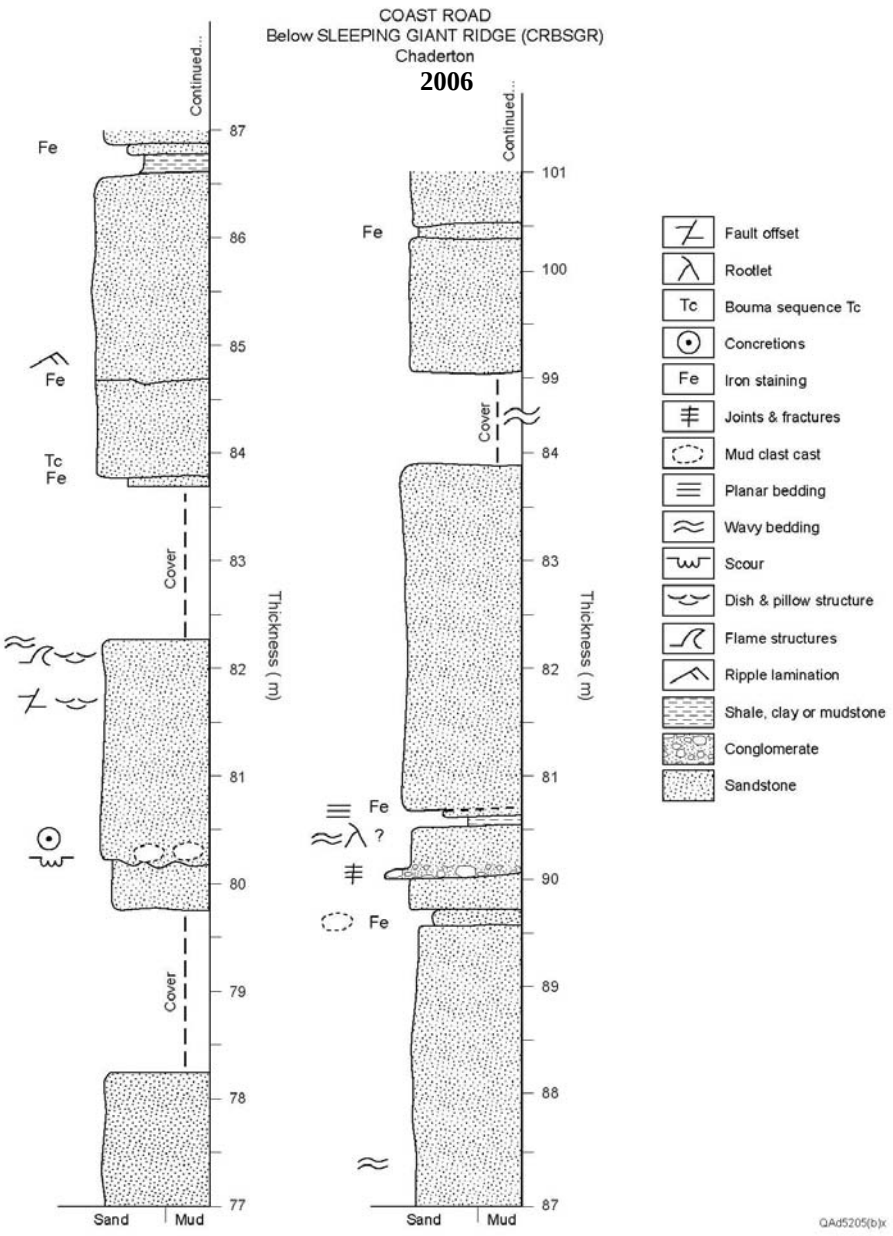

Figure A.14c: Coast Road Below Sleeping Giant Ridge Measured Section.

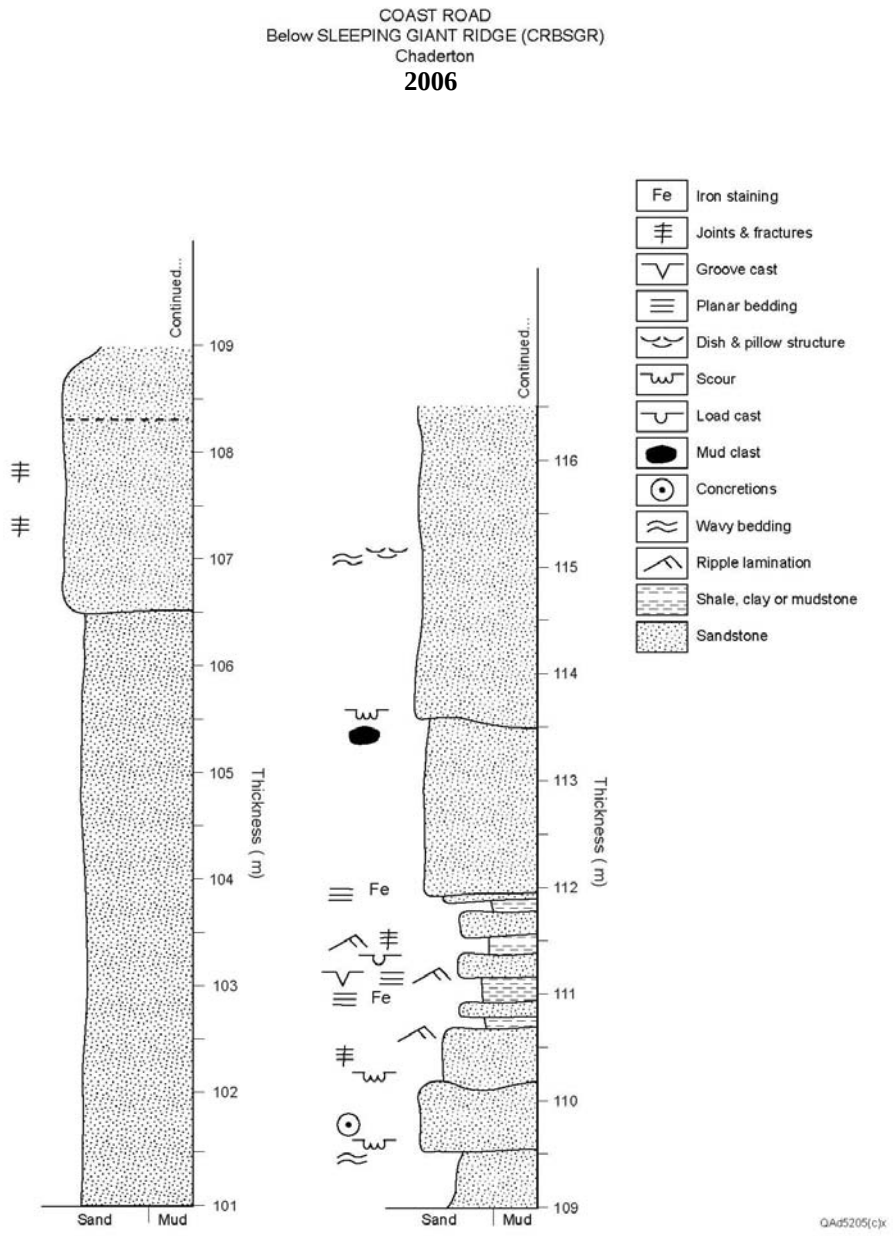

Figure A.14d: Coast Road Below Sleeping Giant Ridge Measured Section.

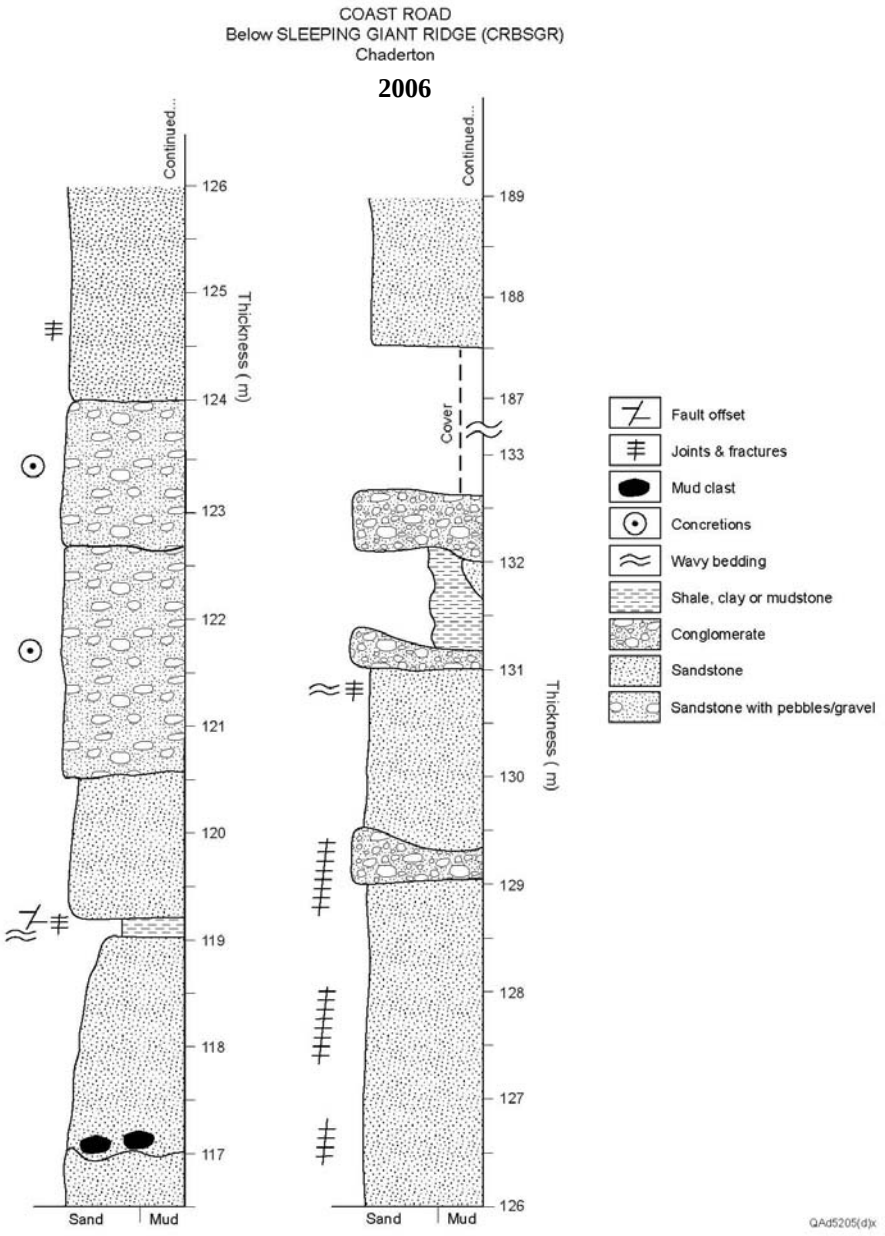

Figure A.14e: Coast Road Below Sleeping Giant Ridge Measured Section.

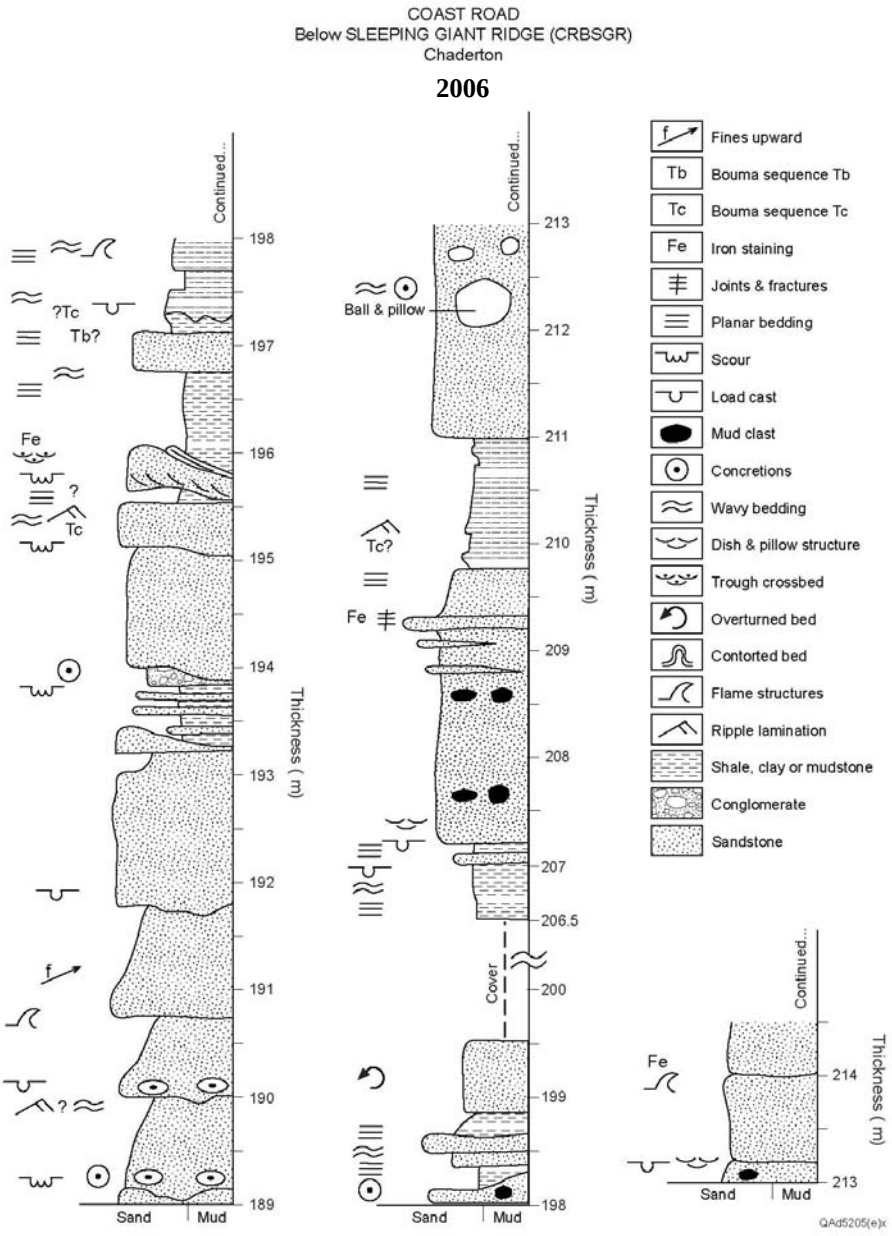

Figure A.14f: Coast Road Below Sleeping Giant Ridge Measured Section.

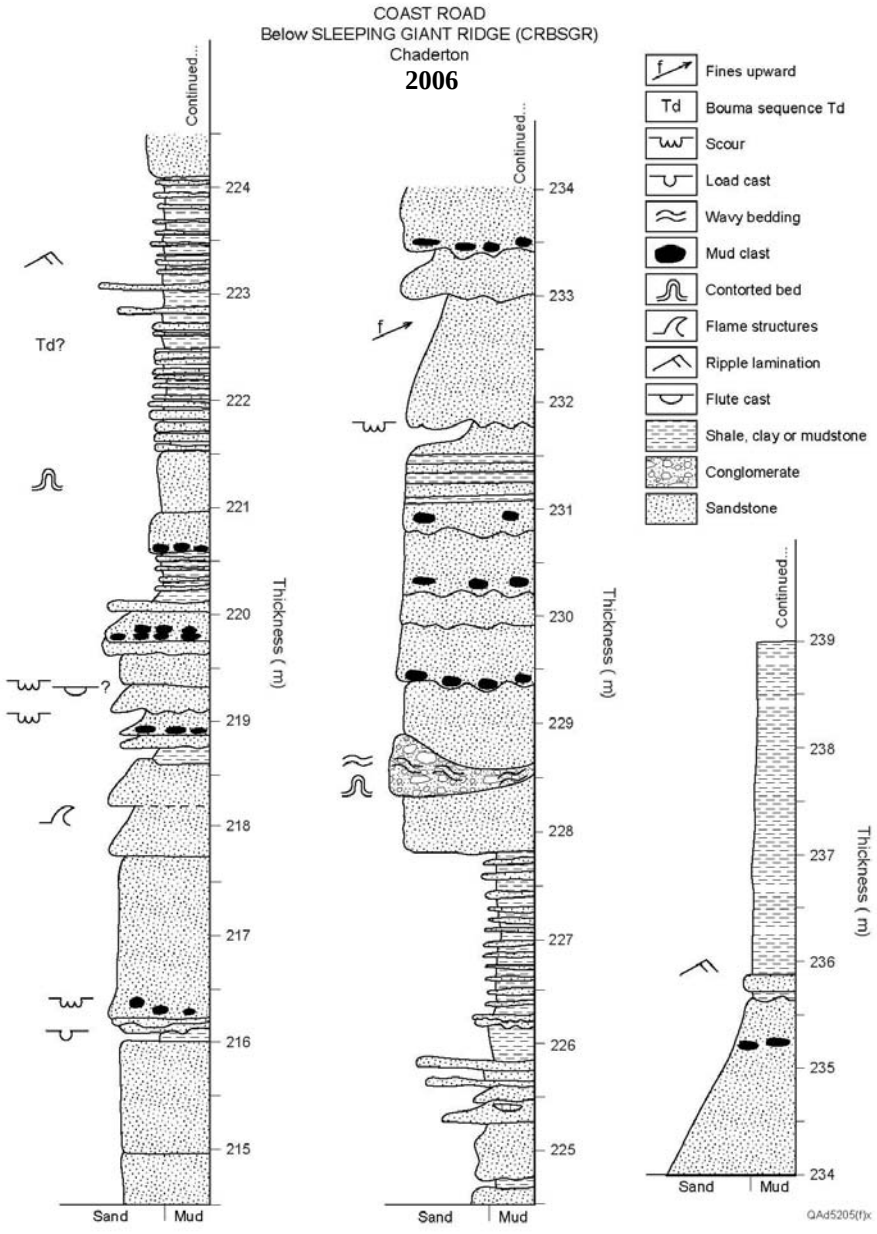

Figure A.14g: Coast Road Below Sleeping Giant Ridge Measured Section.

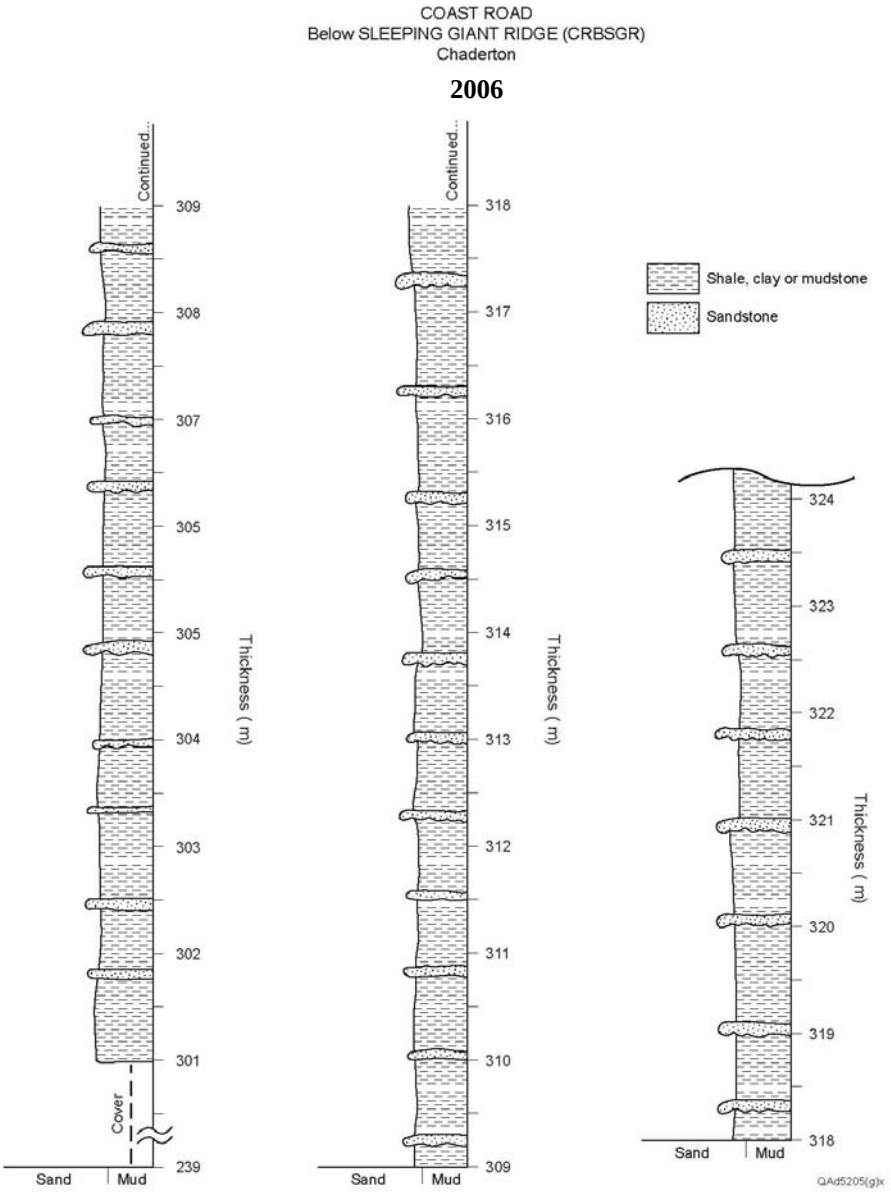

Figure A.14h: Coast Road Below Sleeping Giant Ridge Measured Section.

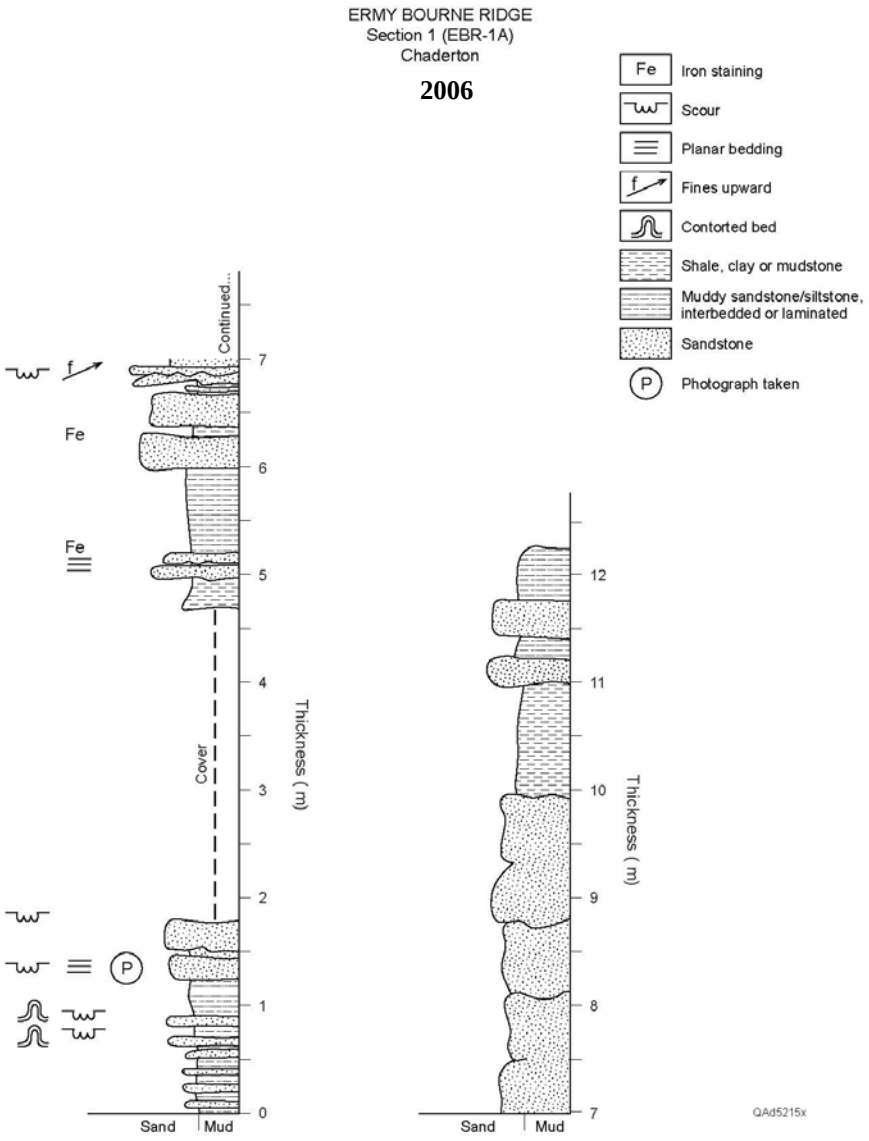

Figure A.15: Ermy Bourne Ridge Measured Section 1.

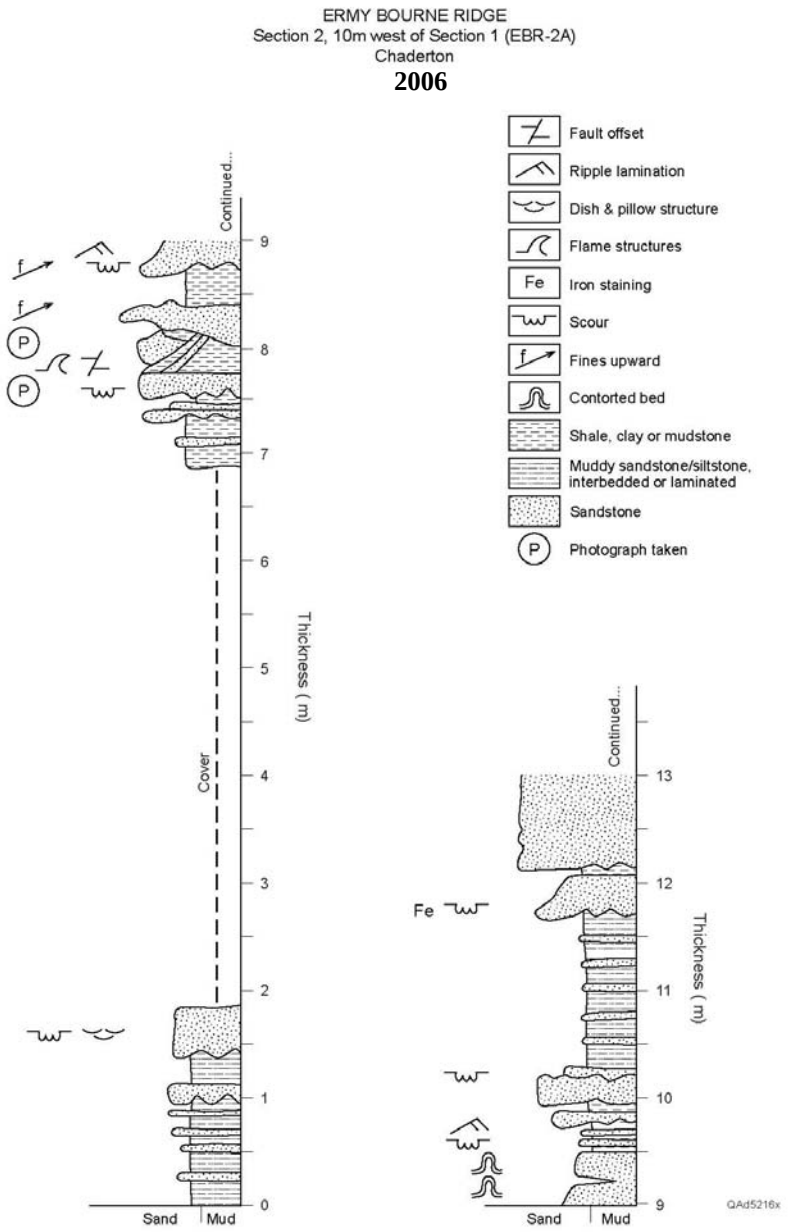

Figure A.16: Ermy Bourne Ridge Measured Section 1.

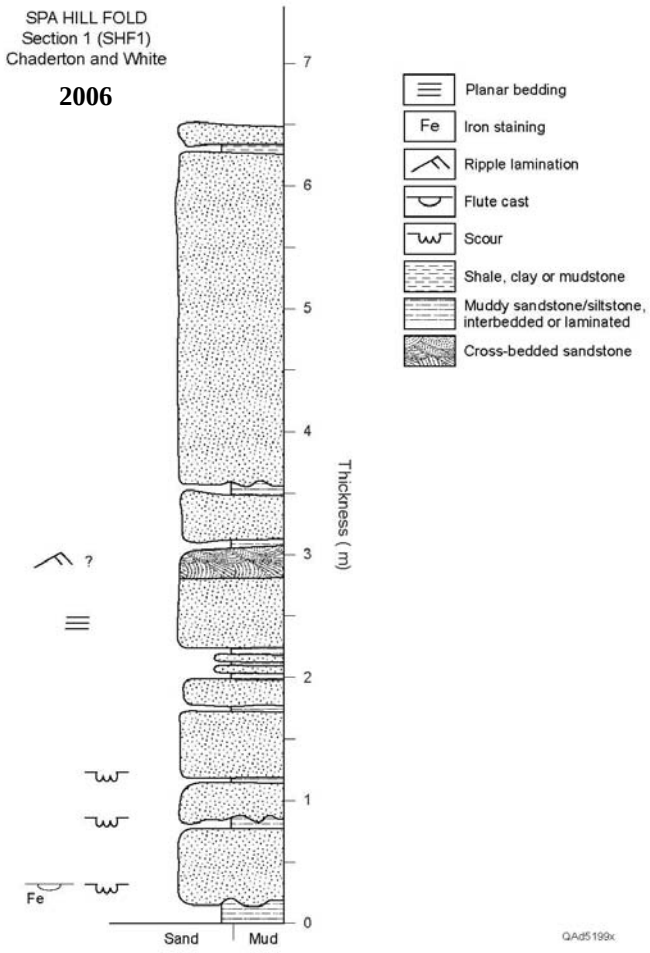

Figure A.17: Spa Hill Fold Measured Section 1.

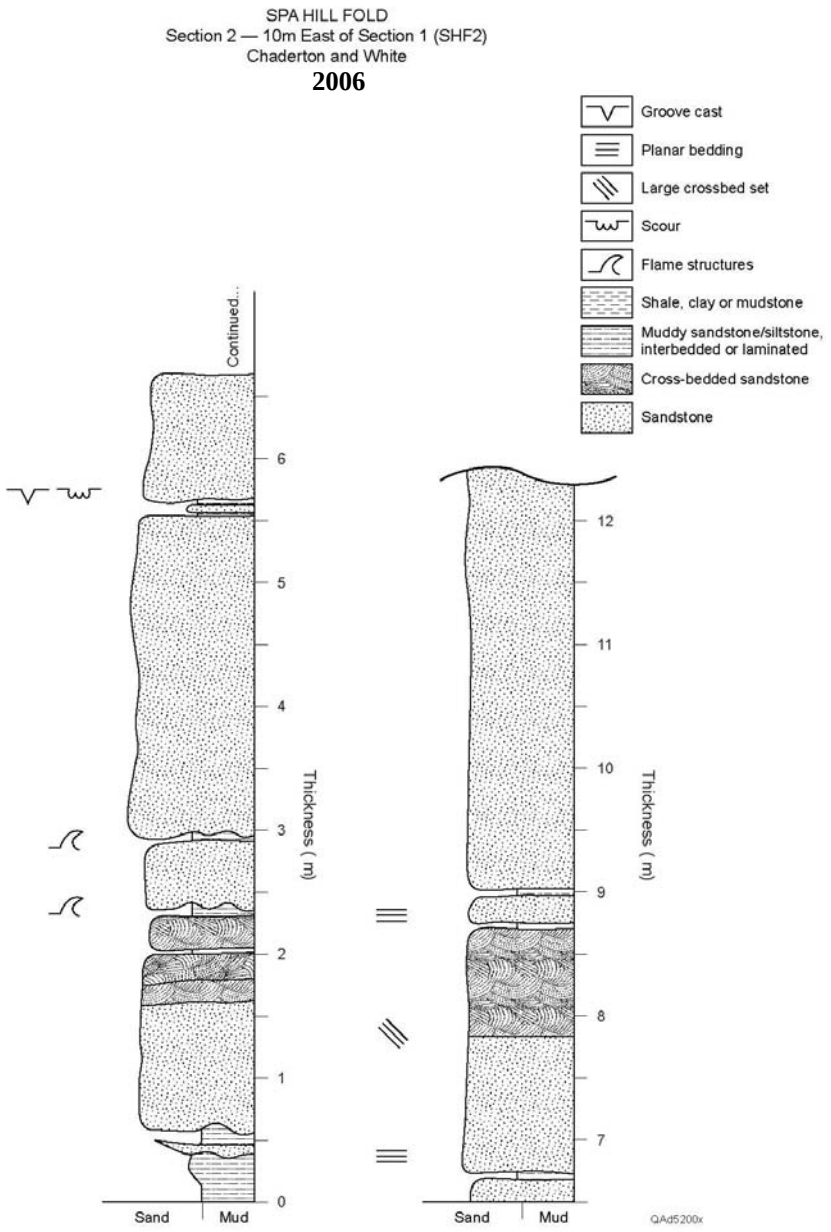

Figure A.18: Spa Hill Fold Measured Section 2.

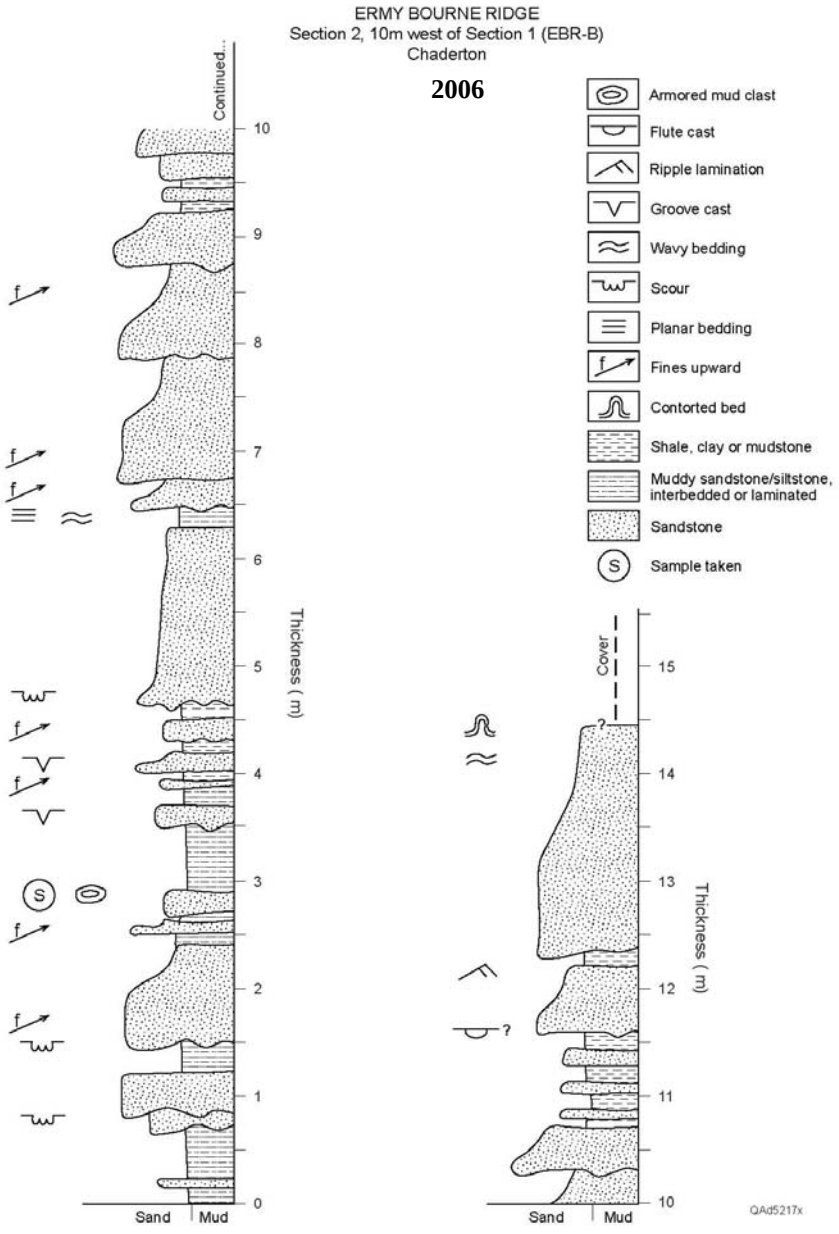

Figure A.19: Ermy Bourne Ridge Measured Section 1.

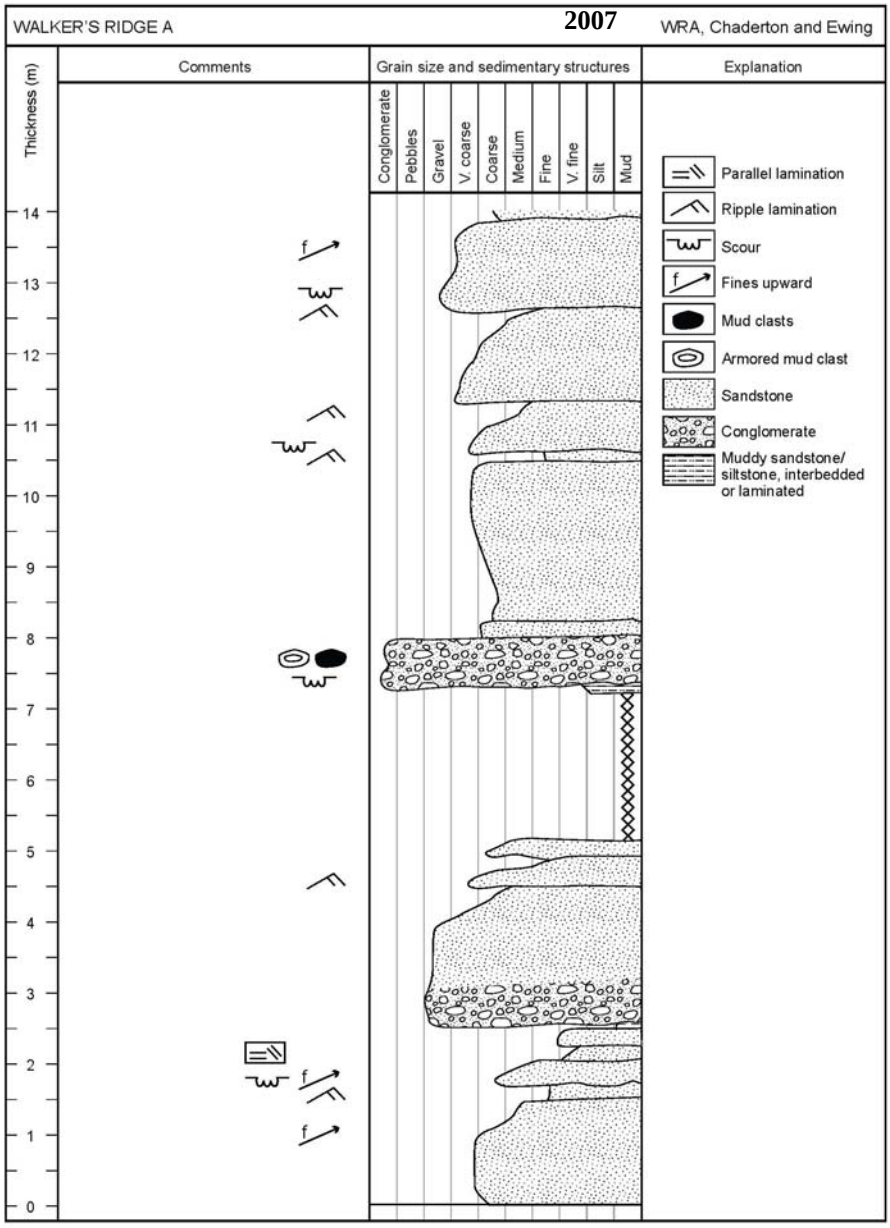

Figure A.20a: Walkers Ridge Measured Section A.

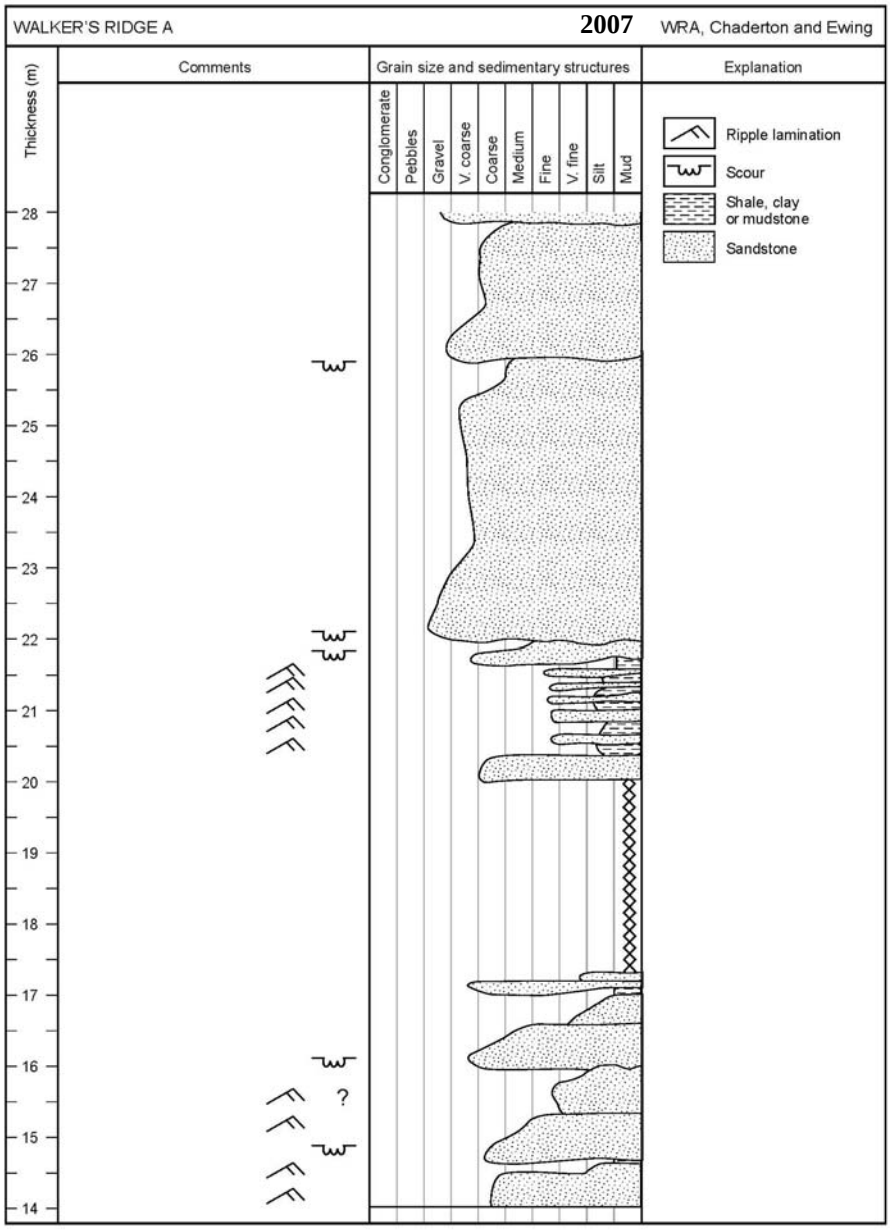

Figure A.20b: Walkers Ridge Measured Section A.

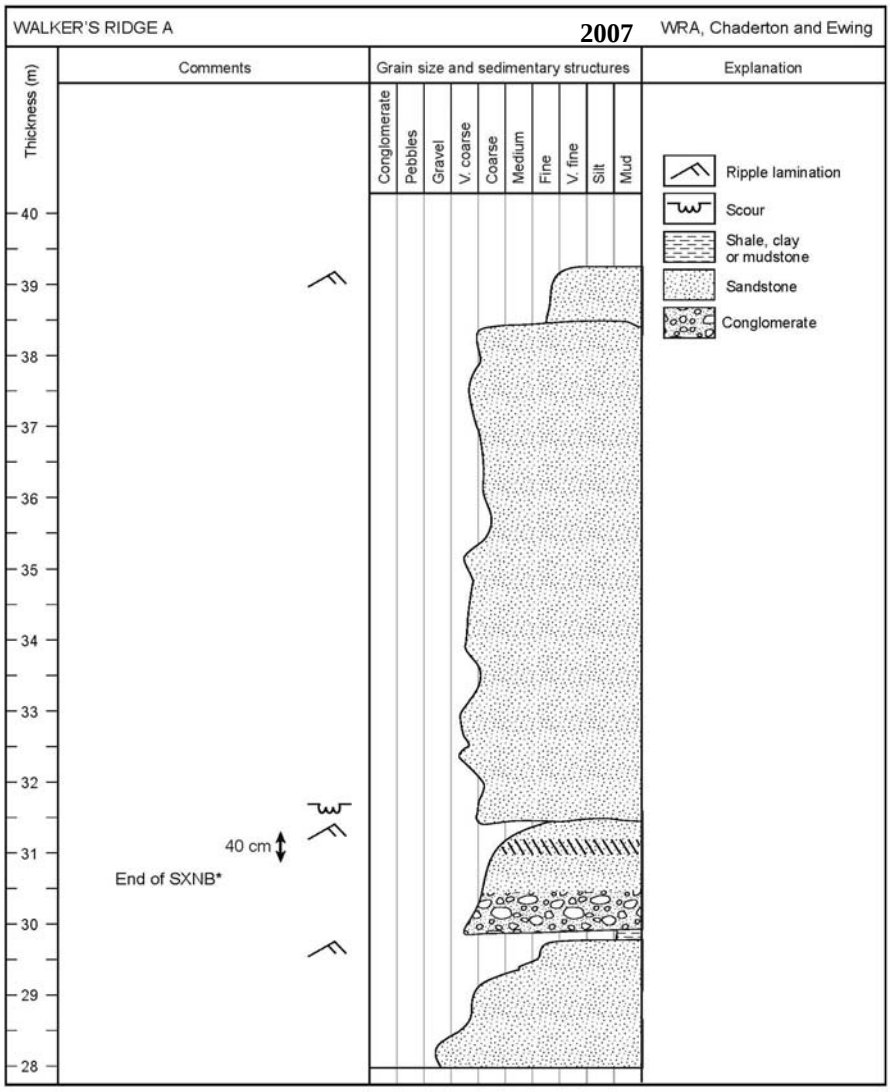

Figure A.20c: Walkers Ridge Measured Section A.

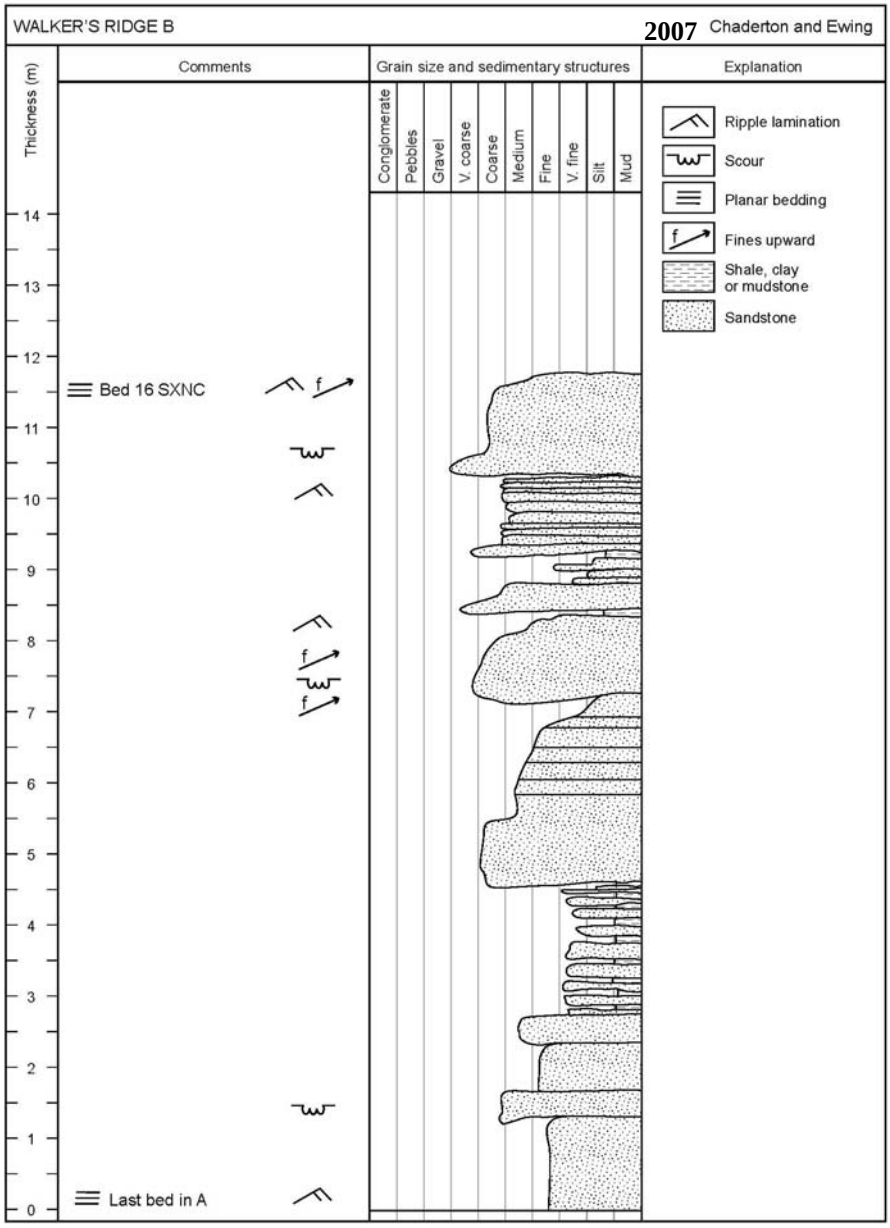

Figure A.21: Walkers Ridge Measured Section B.

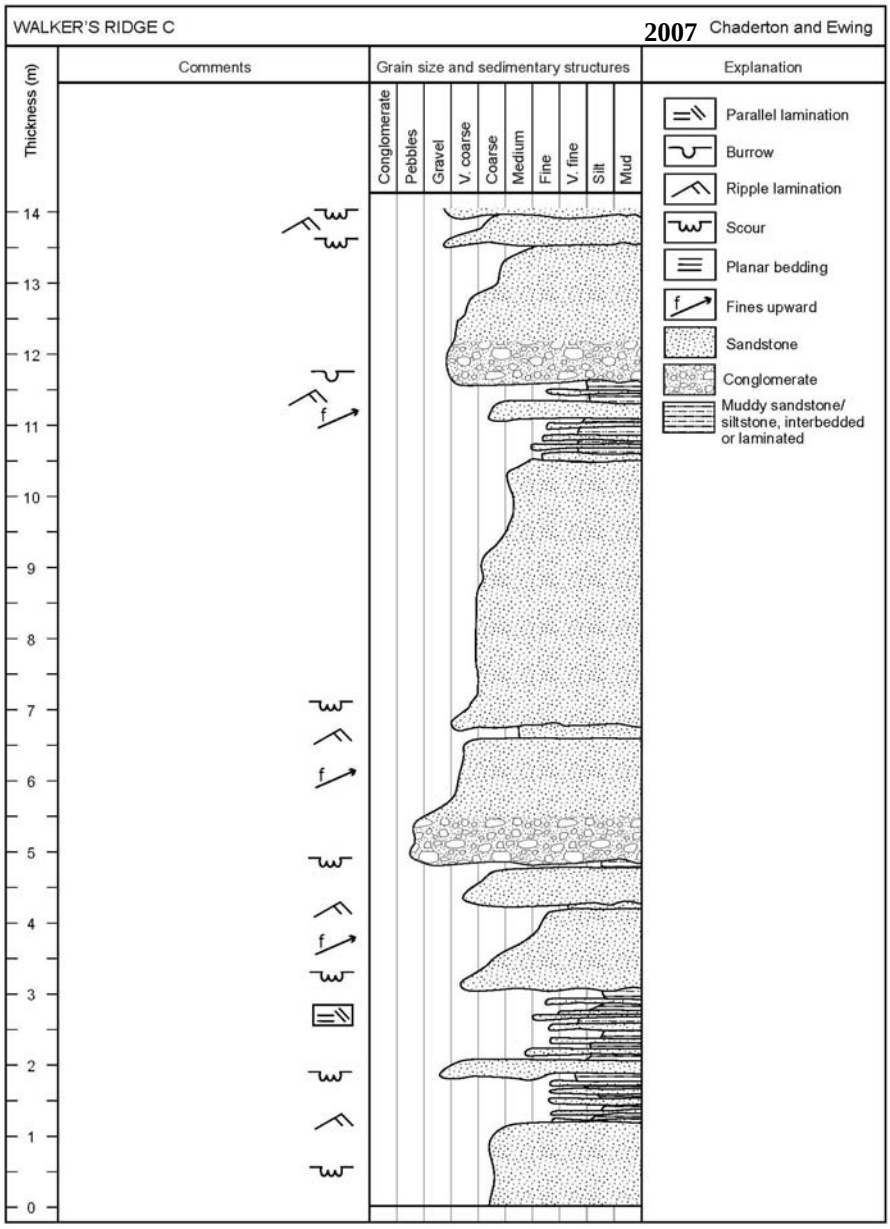

Figure A.22a: Walkers Ridge Measured Section C.

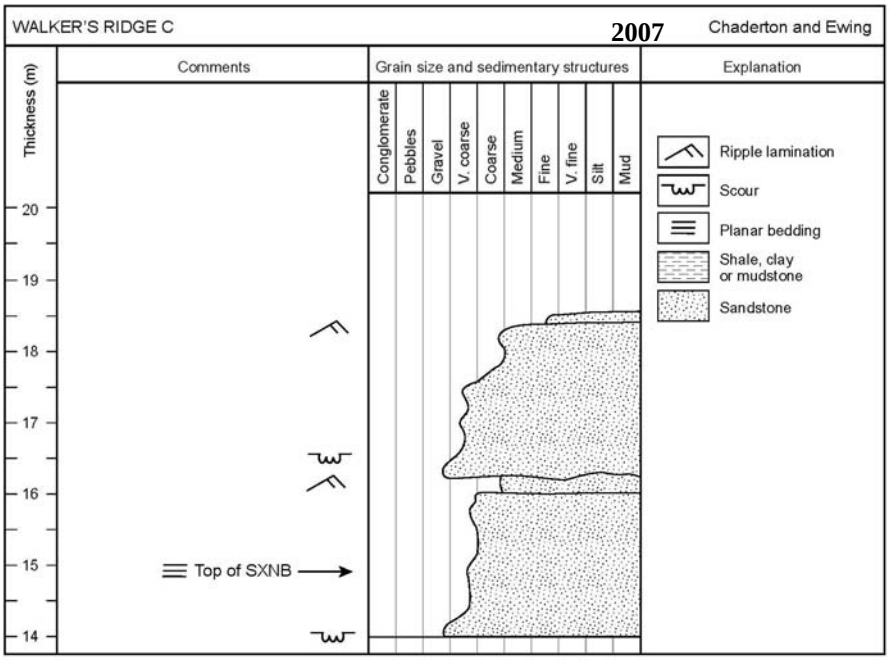

Figure A.22b: Walkers Ridge Measured Section C.

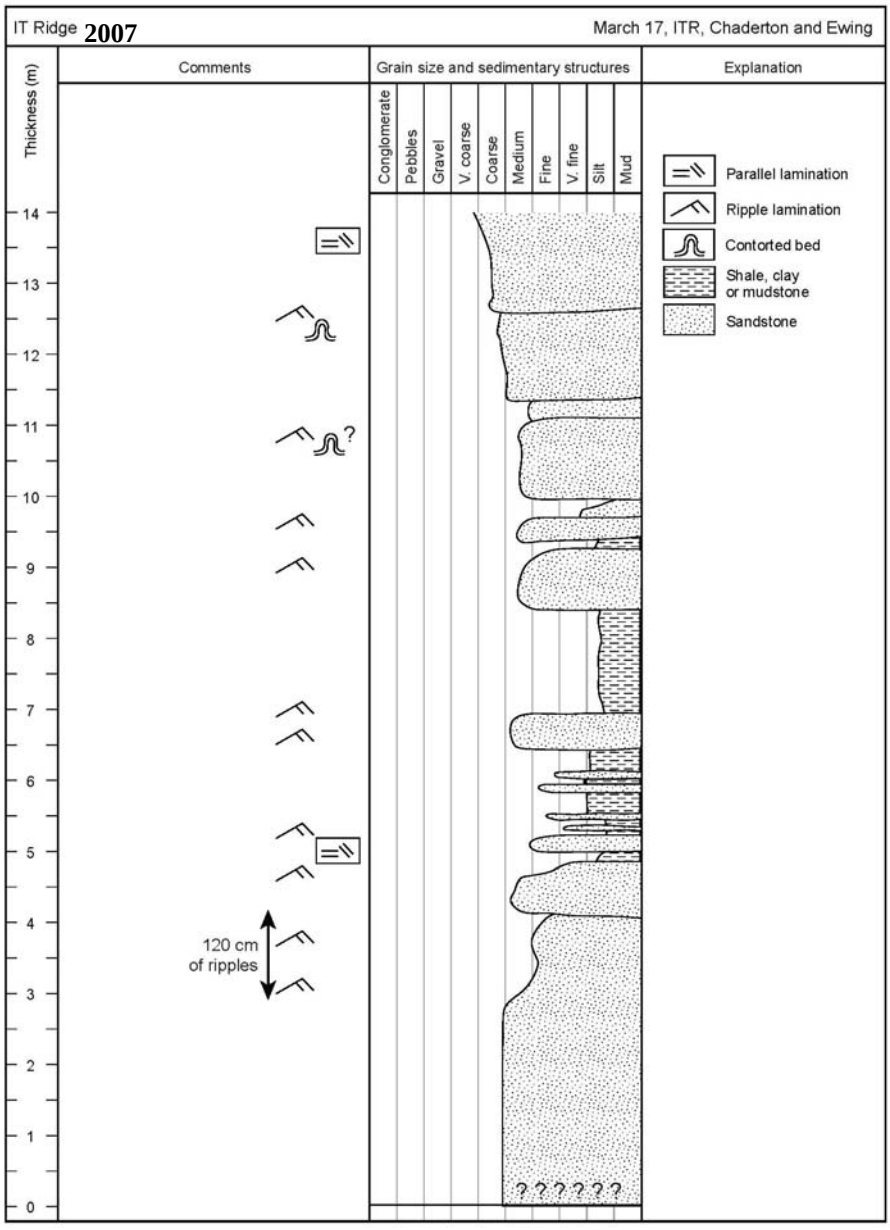

Figure A.23a: Inner Turner's Hall Ridge Measured Section.

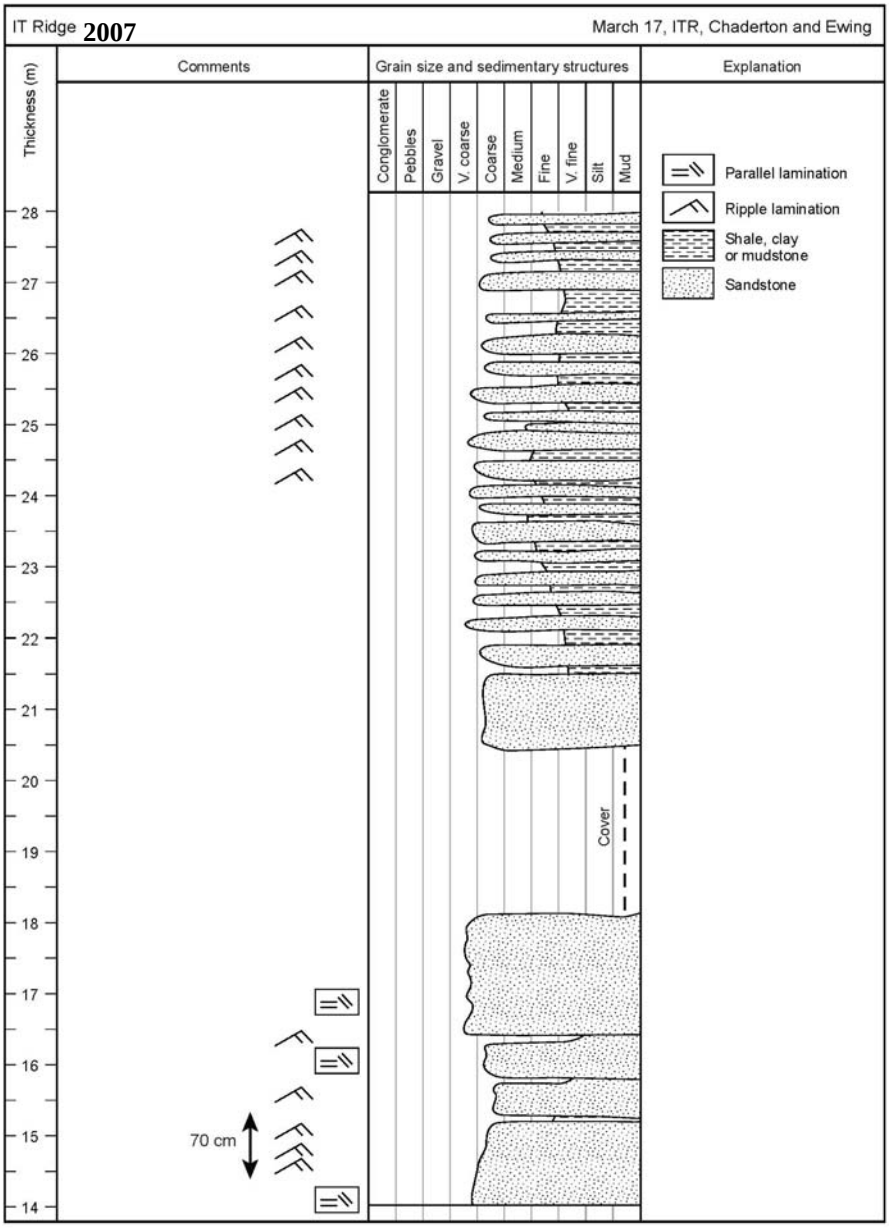

Figure A.23b: Inner Turner's Hall Ridge Measured Section.

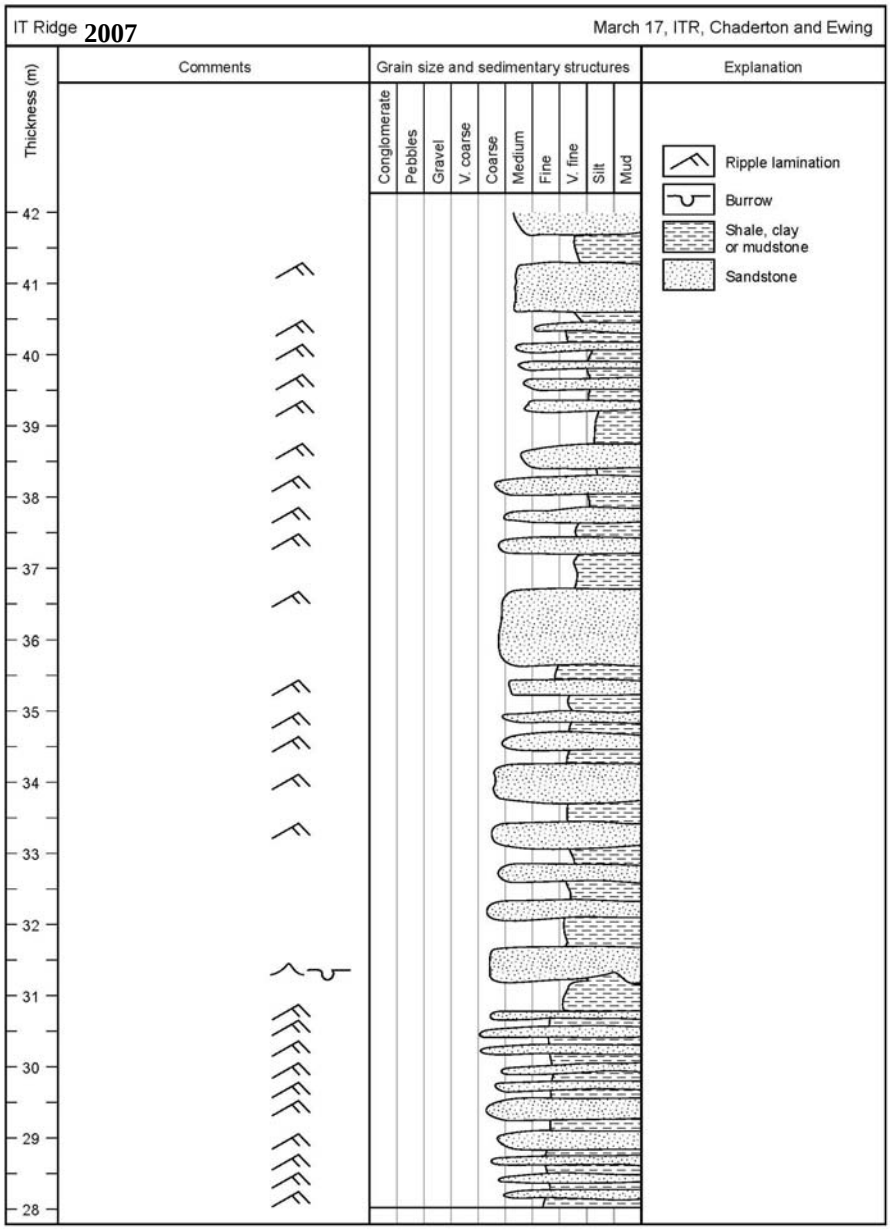

Figure A.23c: Inner Turner's Hall Ridge Measured Section.

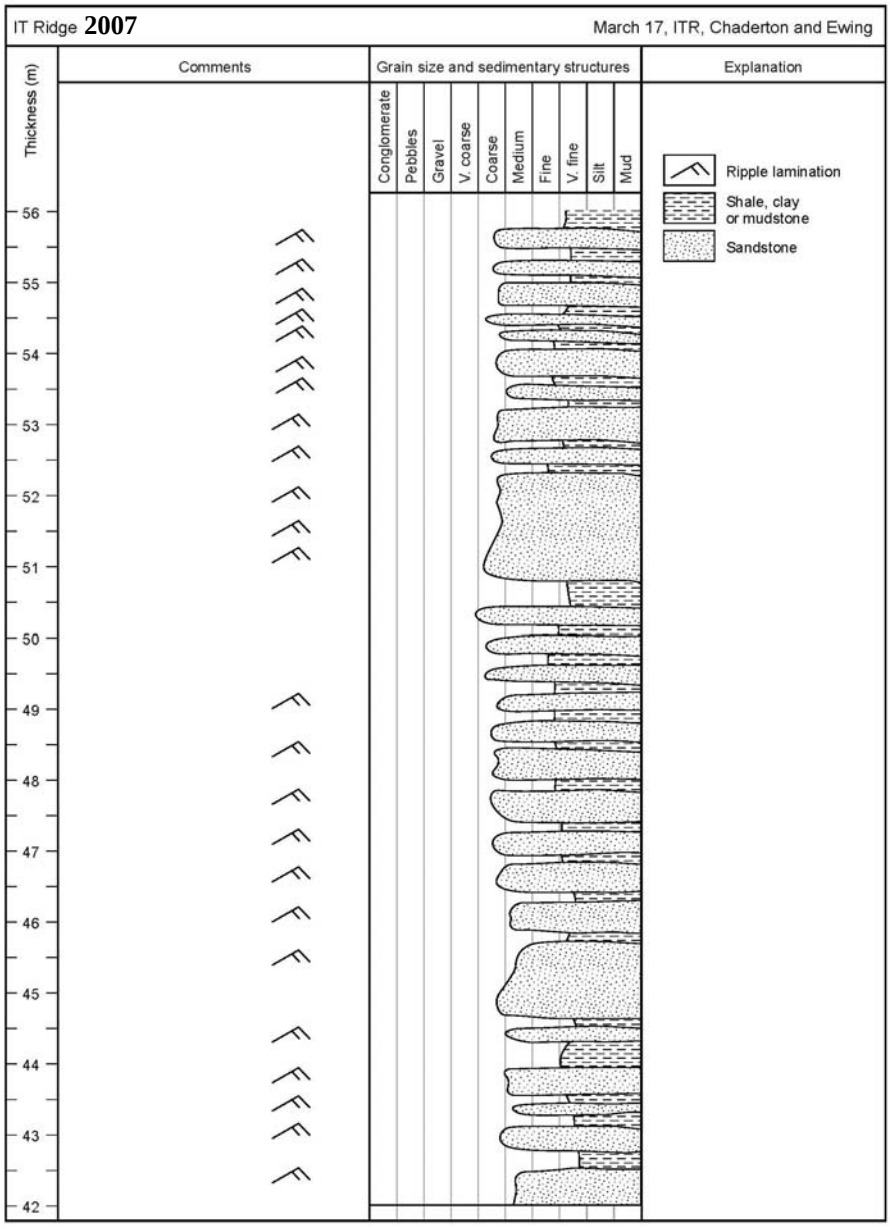

Figure A.23d: Inner Turner's Hall Ridge Measured Section.

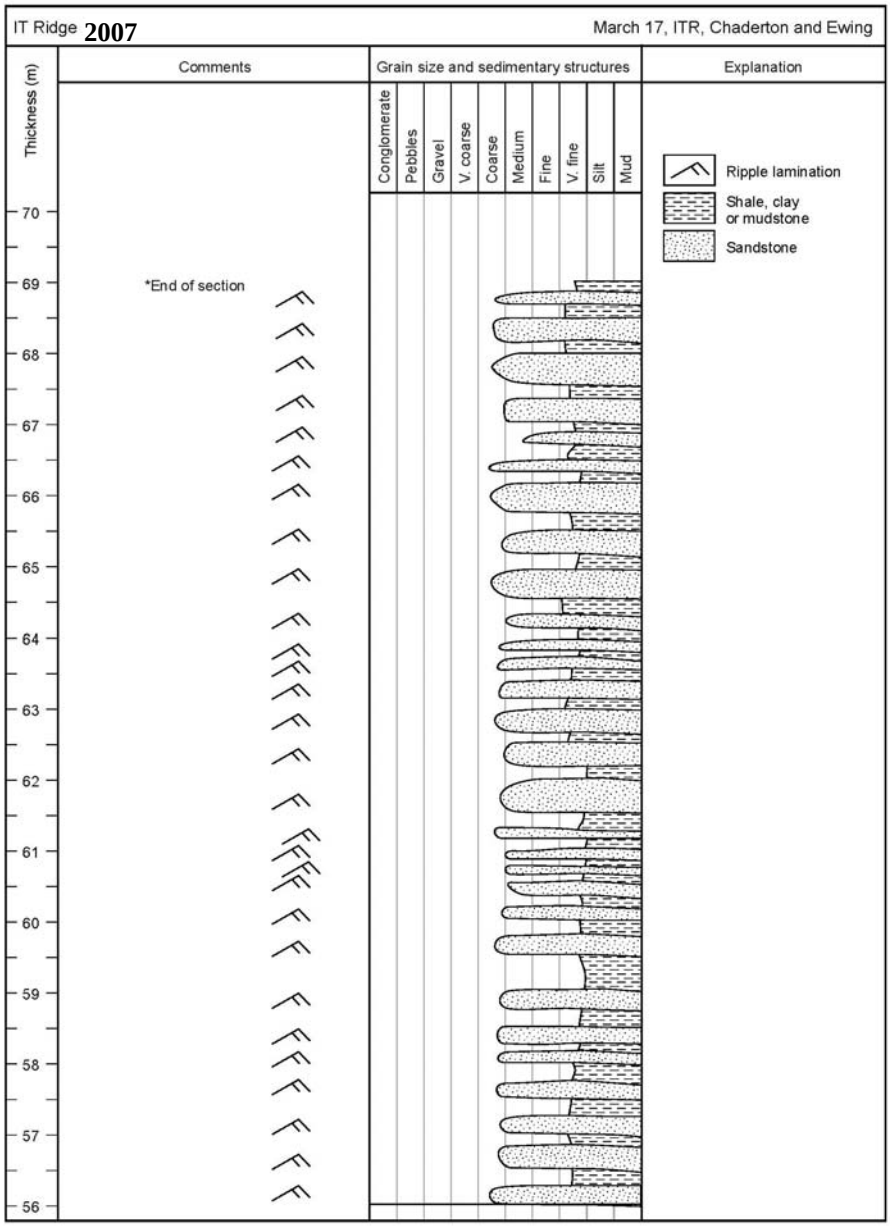

Figure A.23e: Inner Turner's Hall Ridge Measured Section.

Framework grains		Breedy's	CMRA	ITR9	ITR14	SGRF1C	SGRF9	SGRF11B	SGRF19C	WRA	WRB
	Polycrystalline	2	4	0	0	2	4	5	0	0	0
	Monocrystalline	7	30	19	22	40	31	30	2	15	4
	Factured Quartz grain	80	32	45	30	72	74	60	85	90	106
	Quartz with recycled quartz overgrowths	3	4	3	5	4	8	1	8	20	11
Quartz											
	K Feldspar (stained yellow) tartan twinning	6	10	10	16	7	8	7	4	6	4
	Ca- Plagioclase (stained pink/red) polysynthetic twinning	15	16	24	2		0	11	7	0	2
	Na-Plagioclase (doesn't take stain)									0	
Feldspar											
	Altered Volcanic Rock fragments- some pyrite, feldspars altered to clay	1	3	3				2			
	Chert			1		2		2			
	Argillaceous Rock fragments	1		1					1		
Rock Fragments											
	Muscovite	5	2	3	5	2	4	8	3		0
	Biotite	0		1	0	1	1				0
	Zircon	0		0	0	0	0				0
	Glauconite										
	Pyrite						1	2			
Accessory Minerals											
	Primary Intergranular	36	30	39	27	44	46	35	50	45	50
	Secondary Intragranular	11	2	8	4		12	0	4		2
	Secondary Moldic		1		3			2		1	
	Secondary Fractured Intragranular	12	7	10	7	5		5	21	10	15
Porosity*											
Authigenic Minerals											
	Quartz overgrowths										
	Kaolinite	5	10	5	4	1	0		5	3	
	Chlorite	1	11	4	5	4	1	7	1		
Pore Filling	Hematite	15	27	24	9	16	10	3	9	10	6
	Kaolinite		6		56			20			
	Chlorite		5		5						
Grain replacement											
Total		200	200	200	200	200	200	200	200	200	200

Table A.1: Table shows results of point counting of the ten samples selected for petrographic examination of the Scotland Formation. Oversized Plate (11x17) requires plotter or printer with tabloid printing.

Bibliography

ABREU, V., SULLIVAN, M., PIRMEZ, C., and MOHRIG, D., 2003, Lateral accretion packages (LAPs); an important reservoir element in deep water sinuous channels Turbidites; models and problems v. 20, p. 631-648.

ATKINS, J.E., and MCBRIDE, E.F., 1992, Porosity and packing of Holocene river, dune, and beach sands: AAPG Bulletin, v. 76, p. 339-355.

AYDIN, A., 1978, Small faults formed as deformation bands in sandstone Rock friction and earthquake prediction v. 116, p. 913-930.

AYDIN, A., BORJA, R.I., and EICHHUBL, P., 2006, Geological and mathematical framework for failure modes in granular rock Journal of Structural Geology v. 28, p. 83-98.

BAKER, J.C., HAVORD, P.J., MARTIN, K.R., and GHORI, K.A.R., 2000, Diagenesis and Petrophysics of the Early Permian Moogooloo Sandstone, Southern Carnarvon Basin, Western Australia: AAPG Bulletin, v. 84, p. 250-265.

BALDWIN, S.L., and HARRISON, T.M., 1986, Fission track evidence for the source of accreted sandstones, Barbados: Tectonics, v. 5, p. 457-468.

BARKER, L.H., and POOLE, E.G., 1980 The geology and mineral resource assessment of the Island of Barbados St. Michael Barbados Gov. Print. Off. .

BROWN, K., and WESTBROOK, G., 1987, The tectonic fabric of the Barbados Ridge accretionary complex: Marine and Petroleum Geology, v. 4, p. 71-81.

BRUHN, R.L., PARRY, W.T., and BUNDS, M.P., 2000, Tectonics, fluid migration, and fluid pressure in a deformed forearc basin, Cook Inlet, Alaska: GSA Bulletin, v. 112, p. 550-563.

CAMPION, K.M., SPRAGUE, A.R., MOHRIG, D., LOVELL, R.W., DRZEWIECKI, P.A., SULLIVAN, M.D., ARDILL, J.A., JENSEN, G.N., and SICKAFOOSE, D.K., 2003, Outcrop expression of confined channel complexes Bulletin of the South Texas Geological Society v. 44, p. 13-36.

CASHMAN, S., and CASHMAN, K., 2000, Cataclasis and deformation-band formation in unconsolidated marine terrace sand, Humboldt County, California: Geology, v. 28, p. 111-114.

CHADERTON, N., 2005, The Evolution of the Tobago Forearc Basin: Implications for Sedimentation and Hydrocarbon Prospectivity [unpublished Master of Sciences thesis]: The University of Texas at Austin, Austin, 113 p.

CLIFT, P.V., PAOLA, 2004, Controls on tectonic accretion versus erosion in subduction zones: implications for the origin and recycling of the continental crust: Review of Geophysics, v. 42, p. 31.

CLOUGH, J.G., BARKER, C.E., SCOTT, A.R., and ANONYMOUS, 2001, Opportunities for coal bed gas exploration in Alaska American Association of Petroleum Geologists 2001 annual meeting v. 2001, p. 37-38.

CRIMES, T.P., 1977, Trace fossils of an Eocene deep-sea sand fan, northern Spain Trace fossils 2 p. 71-90.
DEPTUCK, M.E., STEFFENS, G.S., BARTON, M., and PIRMEZ, C., 2003, Architecture and evolution of upper fan channel-belts on the Niger Delta slope and in the Arabian Sea Turbidites; models and problems v. 20, p. 649-676.
DICKINSON, W.R., 1979, Mesozoic forearc basin in central Oregon: Geology, v. 7, p. 166-170.
DITULLIO, L.D., and BYRNE, T., 1990, Deformation paths in the shallow levels of an accretionary prism; the Eocene Shimanto Belt of Southwest Japan: GSA Bulletin, v. 102, p. 1420-1438.
DOLAN, P., BURGGRAF, D., KHALID, S., FITZSIMMONS, R., AYDEMIR, E., SENNESETH, O., and LYNN, S., 2004, Challenges to exploration in frontier basins- the Barbados accretionary prism: AAPG International Conference.
DROZ, L., and BELLAICHE, G., 1985, Rhone deep-sea fan; morphostructure and growth pattern: AAPG Bulletin, v. 69, p. 460-479.
FOSSEN, H., SCHULTZ, R.A., SHIPTON, Z.K., and MAIR, K., 2007, Deformation bands in sandstone: a review: Journal of the Geological Society, v. 164, p. 755-769.
FOSSEN, H., and BALE, A., 2007, Deformation bands and their influence on fluid flow: AAPG Bulletin, v. 91, p. 1685-1700.
GORTNER, C.W., and LARUE, D.K., 1986, Hemipelagic rocks at Bissex Hill, Barbados; sedimentology, geochemistry, and depositional environment: Journal of Sedimentary Research, v. 56, p. 307-316.
HARDING, T.P., and LOWELL, J.D., 1979, Structural styles, their plate-tectonic habitats, and hydrocarbon traps in petroleum provinces: AAPG Bulletin, v. 63, p. 1016-1058.
HARDING, T.P., and TUMINAS, A.C., 1989, Structural interpretation of hydrocarbon traps sealed by basement normal block faults at stable flank of foredeep basins and at rift basins: AAPG Bulletin, v. 73, p. 812-840.
HARRIS, N.B., 1992, Burial diagenesis of Brent sandstones; a study of Statfjord, Hutton and Lyell fields Geology of the Brent Group v. 61, p. 351-375.
HILL, R.J., and SCHENK, C.J., 2005, Petroleum geochemistry of oil and gas from Barbados; implications for distribution of Cretaceous source rocks and regional petroleum prospectivity Marine and Petroleum Geology v. 22, p. 917-943
HOUGHTON, H.F., 1980, Refined techniques for staining plagioclase and alkali feldspars in thin section: Journal of Sedimentary Research, v. 50, p. 629-631.
HOWELL, D.G., and NORMARK, W.R., 1982, Submarine fans Sandstone depositional environments v. 31, p. 365-404.
HUYGHE, P., FOATA, M., DEVILLE, E., MASCLE, G., and GROUP, C.W., 2004, Channel profiles through the active thrust front of the southern Barbados prism: Geology, v. 32, p. 429-432.

IMPERATO, D.P., and NILSEN, T.H., 1990, Deep-sea-fan channel-levee complexes, Arbuckle Field, Sacramento Basin, California *in* Barwis, J.H., McPherson, J.G., and Studlick, J.R.J., eds., Sandstone petroleum reservoirs New York, NY Springer-Verlag p. 535-555.

JUKES-BROWNE, A.J., and HARRISON, M.A., 1891, The Geology of Barbados: Quarterly Journal of the Geological Society of London, v. 3, p. 197-243.

KASPER, D.C., 1985, Provenance of Paleogene terrigenous sandstones on Barbados: Stanford University, California, 104 p.

KASPER, D.C., and LARUE, D.K., 1986, Paleogeographic and tectonic implications of quartzose sandstones of Barbados: Tectonics, v. 5, p. 837-854.

LARUE, D.K., and SPEED, R.C., 1983, Quartzose turbidites of the accretionary complex of Barbados I: Chalk Mount succession: Sedimentary Petrology, v. 53, p. 1327-1352.

LARUE, D.K., 1985, Quartzose turbidites of the accretionary complex of Barbados II: variations in bedding style, facies and sequence: Sedimentary Geology, v. 42, p. 217-253.

LARUE, D.K., GORTNER, C.W., and TORRINI, R., 1987, Silica diagenesis in accreted Eocene siliceous rocks (Horizon A c) on Barbados: Journal of Sedimentary Research, v. 57, p. 1033-1039.

LOWE, D.R., 1982, Sediment gravity flows; II, Depositional models with special reference to the deposits of high-density turbidity currents, Journal of Sedimentary Petrology: United States, Society of Economic Paleontologists and Mineralogists : Tulsa, OK, United States, p. 279.

LOWE, D.R., 2004, Deep-Water Sandstones: Submarine Canyon to Basin Plain, Western California, AAPG Special Publication, Pacific Section American Association of Petroleum Geologists, p. 1-79.

MACPHERSON, B.A., 1978, Sedimentation and trapping mechanism in upper Miocene Stevens and older turbidite fans of southeastern San Joaquin Valley, California: AAPG Bulletin, v. 62, p. 2243-2274.

MAKOWITZ, A., and MILLIKEN, K.L., 2003, Quantification of Brittle Deformation in Burial Compaction, Frio and Mount Simon Formation Sandstones: Journal of Sedimentary Research, v. 73, p. 1007-1021.

MAKOWITZ, A., LANDER, R.H., and MILLIKEN, K.L., 2006, Diagenetic modeling to assess the relative timing of quartz cementation and brittle grain processes during compaction: AAPG Bulletin, v. 90, p. 873-885.

MCBRIDE, E.F., PICARD, M.D., and MILLIKEN, K.L., 2003, Calcite-Cemented Concretions in Cretaceous Sandstone, Wyoming and Utah, U.S.A.: Journal of Sedimentary Research, v. 73, p. 462-483.

MILLIKEN, K.L., MCBRIDE, E.F., and LAND, L.S., 1989, Numerical assessment of dissolution versus replacement in the subsurface destruction of detrital feldspars, Oligocene Frio Formation, South Texas: Journal of Sedimentary Research, v. 59, p. 740-757.

MONTGOMERY, S.L., BARKER, C.E., SEAMOUNT, D., DALLEGGE, T.A., and SWENSON, R.F., 2003, Coal bed methane, Cook Inlet, south-central Alaska: A potential giant gas resource: AAPG Bulletin, v. 87, p. 1-13.

MOORE, G.F., CURRAY, J.R., and EMMEL, F.J., 1982, Sedimentation in the Sunda Trench and forearc region Trench-Forearc geology; sedimentation and tectonics on modern and ancient active plate margins, conference v. 10, p. 245-258.

MOORE, J.C., BIJU-DUVAL, B., BERGEN, J.A.M., BLACKINTON, G., CLAYPOOL, G.E., COWAN, D.S., DAVIS, D.M., GUERRA, R.T., HEMLEBEN, C.H.J., MARLOW, M.S., PUDSEY, C.J., RENZ, G.W., TARDY, M., WILSON, D.S., WRIGHT, A.W., NATLAND, J.H., HYNDMAN, R.D., SALISBURY, M.H., BALLARD, A., BECKER, K., DENIS, J., HICKMAN, S.H., JACOBSON, R.S., LANGSETH, M.G., MATHEWS, M.A., MCGOWAN, D., NECHOROSHKOV, V.L., PONOMAREV, V.N., SVITEK, J.F., and WALLERSTEDT, R.L., 1984, Tectonic synthesis, Deep Sea Drilling Project Leg 78A; structural evolution of offscraped and underthrust sediment, northern Barbados Ridge complex Initial reports of the Deep Sea Drilling Project covering Leg 78A of the cruises of the drilling vessel Glomar Challenger, San Juan, Puerto Rico to San Juan, Puerto Rico, February-March 1981; and covering Leg 78B of the cruises of the drilling vessel Glomar Challenger, San Juan, Puerto Rico to Las Palmas, Grand Canary Island, March-April, 1981 v. 78A-78B, p. 601-621.

MOORE, J.C., 2001, Accretionary prisms at convergent plate boundaries, *in* Steele, J., Thorpe, S., and Turekian, K., eds., Encyclopedia of Ocean Sciences: London, Academic Press, p. 28-34.

MORRIS, J., VALENTINE, R., and HARRISON, T., 2002, 10Be imaging of sediment accretion and subduction along the northeast Japan and Costa Rica convergent margins: Geology, v. 30, p. 59-62.

MUTTI, E., and RICCI-LUCCHI, F., 1972, Le torbiditi dell'Appenino Settentrionale: introduzione all'analisi di facies.: Memoire Soc. Geologica Italiana.

MUTTI, E., 1977, Distinctive thin-bedded turbidite facies and related depositional environments in the Eocene Hecho Group (South-central Pyrenees, Spain) Sedimentology v. 24, p. 107-131.

MUTTI, E., 1977, Locations and Characteristics of Thin Bedded Turbidites in Passive Margin Setting Submarine Fans.

NGWENYA, B.T., ELPHICK, S.C., MAIN, I.G., and SHIMMIELD, G.B., 2000, Experimental constraints on the diagenetic self-sealing capacity of faults in high porosity rocks Earth and Planetary Science Letters v. 183, p. 187-199.

NORMARK, W.R., 1978, Fan Valleys, channels, and depositional lobes on modern submarine fans; characters for recognition of sandy turbidite environments: AAPG Bulletin, v. 62, p. 912-931.

NORMARK, W.R., PIPER, D.J.W., and HESS, G.R., 1979, Distributary channels, sand lobes, and mesotopography of Navy submarine fan, California Borderland, with applications to ancient fan sediments Sedimentology v. 26, p. 749-774.
NORMARK, W.R., 1989, Observed parameters for turbidity-current flow in channels, Reserve Fan, Lake Superior: Journal of Sedimentary Research, v. 59, p. 423-431.
OGILVIE, S.R., and GLOVER, P.W.J., 2001, The petrophysical properties of deformation bands in relation to their microstructure Earth and Planetary Science Letters v. 193, p. 129-142.
PAXTON, S.T., SZABO, J.O., AJDUKIEWICZ, J.M., and KLIMENTIDIS, R.E., 2002, Construction of an Intergranular Volume Compaction Curve for Evaluating and Predicting Compaction and Porosity Loss in Rigid-Grain Sandstone Reservoirs: AAPG Bulletin, v. 86, p. 2047-2067.
PEMBERTON, S.G., and MACEACHERN, J.A., 1995, The sequence stratigraphic significance of trace fossils; examples from the Cretaceous foreland basin of Alberta, Canada Sequence stratigraphy of foreland basin deposits; outcrop and subsurface examples from the Cretaceous of North America v. 64, p. 429-475.
PEREZ, O.J., BILHAM, R., BENDICK, R., VELANDIA, J.R., HERNANDEZ, N., MONCAYO, C., HOYER, M., and KOZUCH, M., 2001, Velocity field across the southern Caribbean plate boundary and estimates of Caribbean/South-American plate motion using GPS geodesy 1994-2000 Geophysical Research Letters v. 28, p. 2987-2990.
POOLE, E.G., and BARKER, L.H., 1980, The geology of the Scotland District of Barbados Transactions of the Caribbean Geological Conference = Memorias - Conferencia Geologica del Caribe v. 9, Vol. 2, p. 641-656.
PRYOR, W.A., 1973, Permeability-Porosity Patterns and Variations in Some Holocene Sand Bodies: AAPG Bulletin, v. 57, p. 162-189.
PUDSEY, C.J., 1982, Sedimentology and structure of the Scotland Group, Barbados, *in* Reading, H.G., ed., Special Publication - Geological Society of London: United Kingdom, Geological Society of London : London, United Kingdom, p. 291.
PUNCH, S., 2004, Provenance and Depositional Environment of Eocene Rocks in Trinidad and Barbados: University of Houston, Houston, 153 p.
READING, H.G., 1991, The classification of deep-sea depositional systems by sediment caliber and feeder system
10.1144/gsjgs.148.3.0427: Journal of the Geological Society, v. 148, p. 427-430.
RENTSCHLER, M.S., 1985, Structurally controlled Neogene sedimentation in the Vallecitos Syncline Geology of the Temblor Formation, western San Joaquin Basin, California v. 44, p. 87-96.
RICCI LUCCHI, F., and VALMORI, E., 1980, Basin-wide turbidites in a Miocene, over-supplied deep-sea plain; a geometrical analysis: Sedimentology, v. 27, p. 241-270.

RICHARDS, M., BOWMAN, M., and READING, H., 1998, Submarine-fan systems i: characterization and stratigraphic prediction: Marine and Petroleum Geology, v. 15, p. 689-717.

SAUNDERS, J., BERNOULLI, D., MULLER-MERZ, E., OBERHANSLI, H., PERCH-NIELSEN, K., RIEDEL, W.R., SANFILIPPO, A., and TORRINI JR., R., 1984, Stratigraphy of the Late Middle Eocene to Early Oligocene in the Bath Cliff Section, Barbados, West Indies: Micropaleontology, v. 30, p. 390-425.

SAUNDERS, J., BERNOULLI, D., and MARTIN-KAYE, P., 1985, Late Eocene deep-water clastics in Grenada , West Indies: Edogae Geol. Helv, v. 78, p. 469-485.

SCHUPPERS, J.D., 1993, Quantification of turbidite facies in a reservoir-analogous submarine-fan channel sand body, south-central Pyrenees, Spain The geological modeling of hydrocarbon reservoirs and outcrop analogues v. 15, p. 99-111.

SCHWARZ, E., and ARNOTT, R.W.C., 2007, Anatomy and Evolution of a Slope Channel-Complex Set (Neoproterozoic Isaac Formation, Windermere Supergroup, Southern Canadian Cordillera): Implications for Reservoir Characterization: Journal of Sedimentary Research, v. 77, p. 89-109.

SENN, A., 1940, Paleogene of Barbados and its bearing on history and structure of Antillean-Caribbean region, Bulletin of the American Association of Petroleum Geologists: United States, American Association of Petroleum Geologists : Tulsa, OK, United States, p. 1548.

SHIPLEY, T.H., MOORE, G.F., VOLPE, A.M., and ANONYMOUS, 1982, Sediment offscraping along the Middle America Trench American Geophysical Union; 1982 fall meeting v. 63, p. 1112.

SPEED, R.C., 1982, Barbados; architecture and implications for accretion, *in* Larue, D.K., ed., Journal of Geophysical Research: United States, American Geophysical Union : Washington, DC, United States, p. 3633.

SPEED, R.C., 1983, Structure of the accretionary complex of Barbados; I, Chalky Mount, Geological Society of America Bulletin: United States, Geological Society of America (GSA) : Boulder, CO, United States, p. 92.

SPEED, R., and R. TORRINI JR, E.A., 1989, Tectonic evolution of the Tobago Trough forearc basin: Journal of Geophysical Research, v. 94, p. 2913-2936.

SPEED, R., 1991, Buried accretionary prism drilled on Barbados, JOI/USSAC Newsletter: United States, Joint Oceanographic Institutions Inc. : Washington, DC, United States, p. 1.

SPEED, R., and AL, R.R.E., 1991, Evolution of the Southern Caribbean plate boundary, vicinity of Trinidad and Tobago [discussion and reply]: American Association of Petroleum Geologists, v. 75, p. 1789-1796.

SPEED, R., 1994, Barbados and the Lesser Antilles Forearc, *in* Donovan, S.K., and Jackson, T.A., eds., Caribbean Geology

An Introduction: Kingston, The University of the West Indies Publishers' Association.

SPEED, R.C., and CHENG, H., 2004, Evolution of Marine Terraces and Sea Level in the Last Interglacial, Cave Hill Barbados: GSA Bulletin, v. 116, p. 219-232.

SPRAGUE, A.R., SULLIVAN, M.D., CAMPION, K.M., JENSEN, G.N., GOULDING, F.J., GARFIELD, T.R., SICKAFOOSE, D.K., ROSSEN, C., JENNETTE, D.C., BEAUBOUEF, R.T., ABREU, V., ARDILL, J., PORTER, M.L., ZELT, F.B., and ANONYMOUS, 2002, The physical stratigraphy of deep-water strata; a hierarchical approach to the analysis of genetically related stratigraphic elements for improved reservoir prediction AAPG annual convention with SEPM v. 2002, p. 167.

TAYLOR, F.W., and MANN, P., 1991, Late Quaternary folding of coral reef terraces, Barbados: Geology, v. 29, p. 103-106.

TORRINI, R., and SPEED, R., 1989, Tectonic Wedging in the Forearc Basin-Accretionary Prism Transition, Lesser Antilles Forearc: Journal of Geophysical Research, v. 94, p. 10, 549 - 10, 584.

TRECHMANN, C.T., 1925, The Scotland beds of Barbados Geological Magazine v. 62, p. 481-504.

TRECHMANN, C.T., 1933, The uplift of Barbados Geological Magazine v. 70, p. 19-47.

TRECHMANN, C.T., 1937, The base and top of the coral-rock in Barbados Geological Magazine v. 74, p. 337-359.

VANNUCCHI, P., GALEOTTI, S., CLIFT, P.D., RANERO, C.R., and VON HUENE, R., 2004, Long-term subduction-erosion along the Guatemalan margin of the Middle America Trench: Geology, v. 32, p. 617-620.

VERMEESCH, P., MILLER, D.D., GRAHAM, S.A., DE GRAVE, J., and MCWILLIAMS, M.O., 2006, Multimethod detrital thermochronology of the Great Valley Group near New Idria, California: GSA Bulletin, v. 118, p. 210-218.

VON HUENE, R., and SCHOLL, D.W., 1991, Observations at convergent margins concerning sediment subduction, subduction erosion, and the growth of continental crust Reviews of Geophysics v. 29, p. 279-316.

WALDERHAUG, O., 1996, Kinetic modeling of quartz cementation and porosity loss in deeply buried sandstone reservoirs: AAPG Bulletin, v. 80, p. 731-745.

WALKER, R.G., 1978, Deep-water sandstone facies and ancient submarine fans; models for exploration for stratigraphic traps: AAPG Bulletin, v. 62, p. 932-966.

WEBB, G.W., 1981, Stevens and earlier Miocene turbidite sandstones, southern San Joaquin Valley, California: AAPG Bulletin, v. 65, p. 438-465.

WOOD, L.J., SULLIVAN, S., and MANN, P., 2004, Influence of mobile shales in the creation of successful hydrocarbon basins: concepts, applications, and case studies for the 21st century: 24th Annual GCSSEPM Foundation Bob F. Perkins Research Conference, p. 892–930.

WEBER, J.C., DIXON, T.H., DEMETS, C., AMBEH, W.B., JANSMA, P., MATTIOLI, G., SALEH, J., SELLA, G., BILHAM, R., PEREZ, O., PEREZ, O.J., BENDICK, R., VELANDIA, J.R., HERNANDEZ, N., MONCAYO, C., HOYER, M., and KOZUCH, M., 2001, GPS estimate of relative motion between the Caribbean and South American plates, and geologic implications for Trinidad and Venezuela Velocity field across the southern Caribbean plate boundary and estimates of Caribbean/South-American plate motion using GPS geodesy 1994-2000 Geophysical Research Letters v. 2928, p. 75-a-78 2987-2990.

WEIMER, P., 1990, Sequence stratigraphy, facies geometries, and depositional history of the Mississippi Fan, Gulf of Mexico: AAPG Bulletin, v. 74, p. 425-453.

WEIMER, P., 1995, Sequence stratigraphy of the Mississippi Fan (late Miocene-Pleistocene), northern deep Gulf of Mexico *in* Pickering, K.T., Hiscott, R.N., Kenyon, N.H., Ricci Lucchi, F., and Smith, R.D.A., eds., Atlas of deep water environments; architectural style in turbidite systems London Chapman and Hall p. 94-99.

WESTBROOK, G.K., 1973, Lesser Antilles Subduction Zone in the Vicinity of Barbados, *in* Bott, M.H.P., and Peacock, J.H., eds., Nature; Physical Science London: United Kingdom, Macmillan Journals : London, United Kingdom, p. 118.

WILKINSON, M., and HASZELDINE, R.S., 1996, Aluminium loss during sandstone diagenesis: Journal of the Geological Society, v. 153, p. 657-660.

WILKINSON, M., MILLIKEN, K.L., and HASZELDINE, R.S., 2001, Systematic destruction of K-feldspar in deeply buried rift and passive margin sandstones: Journal of the Geological Society, v. 158, p. 675-683.

WINN, R.D., and DOTT, R.H., 1979, Deep-water fan-channel conglomerates of Late Cretaceous age, southern Chile Sedimentology v. 26, p. 203-228.

WOOD, L.J., SULLIVAN, S., and MANN, P., 2004, Influence of mobile shales in the creation of successful hydrocarbon basins: concepts, applications, and case studies for the 21st century: 24th Annual GCSSEPM Foundation Bob F. Perkins Research Conference, p. 892–930.

WUELLNER, D.E., and JAMES, W.C., 1989, Braided and meandering submarine fan channel deposits, Tesnus Formation, Marathon Basin, West Texas Sedimentary Geology v. 62, p. 27-45.

Vita

Nysha Chaderton was born on the island of St Vincent. She attended secondary school at Harrison College on the island of Barbados. She was awarded a Bachelor of Science in Geology from the University of the West Indies, Mona, Jamaica campus in June of 2001. Nysha subsequently worked as a Petroleum Officer in the Barbados Government's Ministry of Energy.

Nysha entered the Jackson School of Geosciences, The University of Texas at Austin in the fall semester of 2003 and during her time there she worked as a Research Assistant with the Bureau of Economic Geology. She was awarded a Master of Science in Geological Sciences from The University of Texas at Austin in August 2005 and began pursuing her PhD at the same institution in September of 2005.

Nysha's publications and presentations include several posters at the American Geophysical Union, the American Association of Petroleum Geologists and a talk at the Geological Society of Trinidad and Tobago for which she received the Best Student Presentation award.

Email address : nchaderton@gmail.com

This dissertation was typed by Nysha Chaderton.